



The University of
Nottingham

UNITED KINGDOM • CHINA • MALAYSIA

**Characterisation and Development of Rubberised
Bitumen and Asphalt Mixture Based on
Performance-Related Requirements**

By

Ayad Tareq Subhy

Thesis submitted to the University of Nottingham for the
degree of Doctor of Philosophy

August 2016

To Afrak

Abstract

Incorporating recycled tyre rubber into flexible pavement applications by means of Recycled Tyre Rubber-Modified Bitumen RTR-MBs would solve a serious waste problem, save energy and materials, and enhance pavement life and performance. On the other hand, the excessive high-temperature viscosity of rubberised binders imposes handling difficulties during the mixing and compaction process. Therefore, producing rubberised binders with acceptable high-temperature viscosity, and equally having desirable mechanical properties that are truly reflected in asphalt mixtures, was the main aim of this study. Three different types of recycled tyre rubber, with two different base bitumens, were selected to produce different combinations of rubberised binders. The three different sources of recycled tyre rubber are; (1) normal ambiently produced tyre rubber (2) cryogenically produced tyre rubber that was pre-treated with Warm Mix Additive (Sasobit[®]) in order to reduce the high-temperature viscosity of rubberised binders and (3) normal ambiently produced recycled tyre rubber containing 20% devulcanised rubber. The two base bitumens were selected with large differences in their physical and rheological properties in order to identify the effect of the base bitumen on the interaction mechanism and the final rubberised bitumen properties; a hard base bitumen with a penetration of 40 dmm and a soft bitumen with a penetration of 200 dmm were, therefore, chosen.

The laboratory experimental design has been divided into three main parts in order to accomplish the main objectives of the study;

Part 1: Optimise the blending variables (temperature and time) based on the rheological characteristics of binders. This was carried out through low shear mixing by using the Brookfield Viscometer with a modified Dual Helical Impeller (DHI). The blending variables (temperature and time) were investigated based on their influence on measurements of the linear and nonlinear viscoelastic properties. The rheological measurements including dynamic mechanics analysis (DMA) and Multiple Stress Creep Recovery (MSCR) tests were conducted using the Dynamic Shear Rheometer (DSR).

Part 2: Manufacture the rubberised bitumens by using the Silverson L4RT High Shear Mixer based on the optimised blending variables that were identified from Part 1. The produced rubberised bitumens in addition to their base bitumens were characterised for their fatigue and rutting properties. Different test methods were used to evaluate the fatigue and rutting

resistance of binders. The fatigue testing involved the SHRP parameter, Time Sweep tests and the essential work of fracture using the double-edged notched tension (DENT) test. The dissipated energy approach was used to characterise the fatigue properties of binders. The effect of artificial ageing (short and long term ageing) was also investigated. The rutting testing involved the SHRP parameter, Shenoy Parameter, Zero Shear Viscosity, and non-recoverable compliance J_{nr} from the MSCR test.

Part 3: A typical stone mastic gradation (10mm) suitable for surface courses was selected from the British specification BS EN 13108-5/ PD 6691:2007 for designing rubberised bitumen mixtures (using the different rubberised bitumens from Part 2) in addition to the control mixture (without rubber). The fatigue and rutting properties of different mixtures were evaluated. The fatigue testing was carried out using the Indirect Tensile Fatigue Test in the Nottingham Asphalt Tester (NAT machine) equipment and SuperPave Indirect Tensile Test IDT using the INSTRON. The rutting was evaluated using the Repeated Load Axial Test (RLAT) in the NAT machine. Also, the mixture testing included evaluating the stiffness of mixtures and moisture susceptibility using the Indirect Tensile Stiffness Test (ITSM).

The results of this work have indicated that pre-treatment of the recycled rubber can significantly reduce the high-temperature viscosity; however, the fracture properties of binders are compromised, i.e. it makes the bituminous binders fragile and hence more susceptible to cracking. In general, the addition of rubber can produce bituminous materials with enhanced rutting and fatigue characteristics. This is especially evident for rubberised bitumen manufactured using very soft base bitumen (200 dmm penetration). The results of the RLAT have revealed that mixtures made using this binder were even more rutting resistant than mixtures made using the hard base bitumen H (40 dmm penetration). Such results suggest that rubberised bitumens produced with a very soft base bitumen can be a very effective option for pavements that are prone to both low temperature cracking and permanent deformation. All test methods and parameters, for binders and mixtures, have proven that the addition of rubber can improve the fatigue and rutting properties of materials.

Keywords: RTR-MBs, Performance-related Characteristics, Rheological Properties, Fatigue, Rutting

Acknowledgements

I would like to express my gratitude to almighty God, who made all things possible.

I owe my deepest gratitude to my supervisors Professor Gordon Airey and Dr Davide Lo Presti without their help and support this work would not have been possible. They were abundantly helpful and offered invaluable assistance, support and guidance. Their knowledge and experience in this field encouraged me to do my best. I would like to express my sincere thanks to Dr Nick Thom for reviewing my thesis and his valuable insights during the course of this research.

I would like to acknowledge and extend my sincere thanks to Dr James Grenfell, Nottingham Transportation Engineering Centre, for his assistance in setting up the laboratory testing machines. I also acknowledge the tremendous help and advice from Professor Jo Sias Daniel, University of New Hampshire, USA.

Special thanks also go to all technicians in the laboratory of the Nottingham Transportation Engineering Centre, Lawrence, Martyn, Jon Watson, Richard, Laura, Matthew, and Antony for providing necessary laboratory services and creating an efficient work environment.

My warm thanks are due to my friends and fellow researchers at Nottingham Transportation Engineering Centre (NTEC) with whom I shared my enjoyable moments and experiences.

I owe my loving thanks to my wife, Afrah, and my little kids, Ahmed, and, Jannah. They keep encouraging and supporting me. My loving thanks are due to my mother, her supplication and moral encouragement made things easier. Many thanks are due to my brothers, my sister and her family for their loving support.

Finally, my sincere thanks are due to the Ministry of Higher Education and Scientific Research / Republic of Iraq for awarding me a scholarship to study in the UK, their financial support is highly appreciated.

Declaration

The research described in this thesis was conducted at the Nottingham Transportation Engineering Centre, the University of Nottingham between March 2013 and August 2016. I declare that the work is my own and has not been submitted for a degree at another university.

Ayad Tareq Subhy

The University of Nottingham

Table of Contents

Abstract.....	i
Acknowledgements.....	iii
Declaration.....	iv
Table of Contents.....	v
List of Figures.....	ix
List of Tables.....	xii
Chapter 1 Introduction.....	1
1.1 Background.....	1
1.2 Problem Statement.....	3
1.3 Aim and Objectives.....	4
1.4 Research Methodology.....	5
1.5 Thesis Outline.....	8
Chapter 2 Literature Review.....	9
2.1 Introduction.....	9
2.2 Constituent Materials.....	10
2.2.1 Bitumen.....	10
2.2.2 Tyre Rubber.....	12
2.3 Recycled Tyre Rubber-Modified Bitumens (RTR-MBs).....	24
2.3.1 Incorporating Recycled Tyre Rubber into Bitumen and Mixtures.....	24
2.3.2 Bitumen-Rubber Interaction Process.....	29
2.3.3 Storage Stability of RTR-MBs.....	34
2.3.4 Artificial Ageing Effect on RTR-MBs.....	38
2.4 Performance-Based Binder Characterisation.....	40
2.4.1 Dynamic Shear Rheometer (DSR).....	41
2.4.2 Binder Fatigue Testing.....	52

2.4.3	Binder Rutting Testing.....	64
2.5	Asphalt Mixtures.....	71
2.5.1	Nottingham Asphalt Tester (NAT).....	73
2.5.2	SuperPave Indirect Tensile Test (IDT) and Energy Ratio ER.....	75
2.6	Summary.....	78
Chapter 3	Low Shear Development of RTR-MBs.....	80
3.1	Introduction.....	80
3.2	Materials and experimental programme.....	81
3.2.1	Materials.....	81
3.2.2	Rubberised bitumen manufacture.....	84
3.2.3	Rubber dissolution test.....	86
3.2.4	Dynamic Shear Rheometer DSR.....	87
3.3	Viscosity monitoring analysis.....	88
3.4	Rubber dissolution.....	92
3.5	Dynamic Mechanical Analysis (DMA).....	93
3.5.1	Master Curves.....	93
3.5.2	Black Diagrams.....	97
3.5.3	Temperature Susceptibility.....	100
3.6	Multiple Stress Creep and Recovery (MSCR).....	102
3.6.1	Non-recoverable compliance (J_{nr}).....	102
3.6.2	Percentage recovery.....	105
3.7	Summary and Conclusions.....	110
Chapter 4	RTR-MBs Manufactured Using High Shear Mixer.....	112
4.1	Introduction.....	112
4.2	Experimental Design.....	113
4.2.1	Materials.....	113
4.2.2	High Shear Blending.....	113

4.2.3	Testing Programme.....	115
4.3	High Shear Viscosity HSV.....	117
4.4	Multiple Stress Creep and Recovery (MSCR).....	119
4.5	Storage Stability of RTR-MBs.....	122
4.6	The effect of artificial ageing.....	126
4.7	Summary and conclusions.....	132
Chapter 5	RTR-MB Asphalt Mixtures	135
5.1	Introduction.....	135
5.2	Materials selection	136
5.2.1	Binders, selection and content	136
5.2.2	Aggregate.....	137
5.3	Specimen production.....	138
5.4	Volumetric properties of SMA mixtures.....	140
5.5	Indirect Tensile Stiffness Modulus (ITSM).....	143
5.6	Water damage susceptibility	145
5.7	Summary and Conclusions.....	148
Chapter 6	Fatigue Cracking in Binders and Mixtures	150
6.1	Introduction.....	150
6.2	Testing Programme	151
6.2.1	Binder Testing Protocol.....	151
6.2.2	Mixture Testing Protocol.....	153
6.3	Time Sweep Repeated Cyclic Load (TSRCL).....	156
6.3.1	Definition of fatigue failure	156
6.3.2	Traditional fatigue analysis.....	158
6.3.3	Cumulative dissipated energy.....	160
6.3.4	Ratio of Dissipated Energy Change (RDEC)	161
6.4	The Essential Work of Fracture and CTOD.....	167

6.5	Fatigue Properties of Asphalt Mixtures	174
6.5.1	ITFT Results	174
6.5.2	Superpave Indirect Tensile Test (IDT) Results	178
6.6	Summary and Conclusions.....	182
Chapter 7	Permanent Deformation in Binders and Mixtures	185
7.1	Introduction	185
7.2	Testing Programme	186
7.2.1	Binder Testing.....	186
7.2.2	Mixture Testing Using Repeated Load Axial Test	187
7.3	Rutting Resistance of Binders.....	188
7.4	Rutting Resistance of Mixtures	194
7.5	Rutting susceptibility: From binders to mixtures.....	198
7.5.1	Correlation between binder rutting parameters and RLAT	198
7.5.2	Establishing a more fundamental relationship between binders.....	201
7.6	Summary and Conclusions.....	203
Chapter 8	Conclusions and Recommendations	205
8.1	Conclusions	205
8.1.1	The Mechanical Characteristics of RTR-MBs.....	206
8.1.2	The Performance-Related Properties of RTR-MBs.....	207
8.1.3	The Relations between Different Test Binder Methods	208
8.2	Recommendations for Future Research	210
	References.....	212
	Appendix A - Specimen fabrication and testing procedure of the Superpave IDT Tests..	227
	Appendix B- Gap setting investigation.....	240
	Appendix C- Results.....	244

List of Figures

Figure 1.1: The main elements of research methodology.....	7
Figure 2.1: Schematic representation of (A) sol type and (B) gel type bitumen	12
Figure 2.2: Tyre structure (Lo Presti 2013)	14
Figure 2.3: The crosslink density effect on the main mechanical properties	16
Figure 2.4: Flow chart of the service life of tyres (.....	17
Figure 2.5: Extracting the steel structural skeleton from the tyre.....	18
Figure 2.6: Flow chart of a granulation process at ambient temperature	19
Figure 2.7: Simplified flow process diagram of the wet grinding technology	21
Figure 2.8: SEM images at 200 microns and 400x for rubber particles	22
Figure 2.9: Mechanism of cross-linking bond breakage reaction.....	23
Figure 2.10: Field schematic of dry process technology	25
Figure 2.11: Field schematic of the wet process technology	26
Figure 2.12: Progression of bitumen–rubber interaction at elevated temperature.....	30
Figure 2.13: The DSR testing configuration.....	41
Figure 2.14: Rheological behaviour of bitumen	44
Figure 2.15: Dynamic mechanical analysis representation	45
Figure 2.16: Strain sweep to determine linear region	47
Figure 2.17: Linear viscoelastic strain limits as a function of complex modulus	48
Figure 2.18: Time-temperature superposition principle	49
Figure 2.19: Construction of the master curve for $ G^* $	51
Figure 2.20: aT versus temperature plot	52
Figure 2.21: Typical RDEC plot versus load cycles.....	56
Figure 2.22: Identifying N_f (a) from the DER vs. number of load cycles	58
Figure 2.23: Schematic representation of inner and outer zone	59
Figure 2.24: Typical raw data from DENT test	60
Figure 2.25: DENT test moulds	61
Figure 2.26: Schematic sketch illustrated the relationship between w_t and length.....	62
Figure 2.27: Schematic sketch illustrated the influence of thickness	63
Figure 2.28: Comparison between the effectiveness of δ	66
Figure 2.29: Complex viscosity versus frequency	68
Figure 2.30: A typical one cycle of creep-recovery.....	70
Figure 2.31: A typical flexible pavement structure	72

Figure 2.32: Typical terms used to identify aggregate gradations.....	73
Figure 2.33: Testing arrangement in the NAT.....	74
Figure 2.34: Tensile strength versus tensile strain plot	77
Figure 3.1: SEM images for the different crumb rubber particles.....	83
Figure 3.2: The modified Dual Helical Impeller (DHI).....	85
Figure 3.3: The laboratory tools used for manufacturing RTR-MBs	86
Figure 3.4: #200 mesh (75 μ m) sieve used for rubber dissolution test.....	87
Figure 3.5: Viscosity progression over time for RTR-MBs produced using bitumen S	89
Figure 3.6: Viscosity progression over time for RTR-MBs produced using bitumen H.....	90
Figure 3.7: Rubber dissolution percentage	93
Figure 3.8: Master curves at 30 °C reference temperature	96
Figure 3.9: Master curves at 30 °C for RTR-MBs.....	97
Figure 3.10: Black diagram of RTR-MBs	99
Figure 3.11: Black diagram of RTR-MBs	100
Figure 3.12: TAN(δ) at 1Hz of RTR-MBs	101
Figure 3.13: TAN(δ) at 1Hz of RTR-MBs	102
Figure 3.14: J_{nr} of RTR-MBs produced using bitumen S	104
Figure 3.15: J_{nr} of RTR-MBs produced using bitumen H	105
Figure 3.16: Recovery of RTR-MBs produced using bitumen S	107
Figure 3.17: Recovery of RTR-MBs produced using bitumen H.....	108
Figure 3.18: The elastic response of RTR-MBs produced using bitumens S and H.....	109
Figure 4.1: Silverson L4RT High Shear Mixer	115
Figure 4.2: High-temperature viscosity development measured at 180°C	118
Figure 4.3 J_{nr} at 60°C of RTR-MBs collected at different blending time.....	120
Figure 4.4 Total accumulated strain of RTR-MBs	121
Figure 4.5 Recovery percentage of RTR-MBs	122
Figure 4.6: Master curves at 30 °C reference temperature	124
Figure 4.7: Master curves at 30 °C reference temperature	125
Figure 4.8: Master curves, at 30 °C reference temperature	125
Figure 4.9: Master curves, at 30 °C reference temperature	127
Figure 4.10: Master curves, at 30 °C reference temperature	128
Figure 4.11: Master curves, at 30 °C reference temperature	129
Figure 4.12: Master curves, at 30 °C reference temperature	130
Figure 4.13: The ageing indices for base bitumens S and its RTR-MBs.....	131

Figure 4.14: The ageing indices for base bitumens H and its RTR-MBs	132
Figure 5.1: The 10mm SMA gradations for control and RTR-MBs mixtures	138
Figure 5.2: (a) the mechanical mixer, and (b) steel roller.....	139
Figure 5.3: (a) gravimetric proportion and maximum densities	141
Figure 5.4: the measured air voids and bulk densities of the different mixtures	142
Figure 5.5: ITSM testing configuration in the NAT	143
Figure 5.6: ITSM results for the different mixtures.....	145
Figure 5.7: ITSM ratio for the mixtures after several water immersion cycles.....	147
Figure 5.8: ITS values for the conditioned and unconditioned specimens	148
Figure 6.1: DENT test moulds	153
Figure 6.2: ITFT testing configuration in NAT	154
Figure 6.3: The IDT configuration in the INSTRON	156
Figure 6.4: The failure points identified by different methods.....	158
Figure 6.5: Traditional fatigue curves “WÖHLER” for all binders	159
Figure 6.6: Total accumulative dissipated energy vs. N_f for all binders	161
Figure 6.7: RDEC evolution vs. the number of load cycles for H binder	162
Figure 6.8: Shape of dissipated energy vs. number of load cycles a	163
Figure 6.9: PV fatigue curves based on Equation 6.6 for H binder	163
Figure 6.10: Graphical illustration of determining PV	164
Figure 6.11: PV vs. N_f computed by the proposed approach	165
Figure 6.12: Comparison of different PV- N_f curves	166
Figure 6.13: Comparison of different PV- N_f curves of the current binders.....	167
Figure 6.14: The typical force-displacement curves for all unaged binders.....	168
Figure 6.15: Net section stress as a function of the ligament length	169
Figure 6.16: Determination of the essential and plastic works of fracture	170
Figure 6.17: The essential work of fracture w_e and CTOD values for unaged binders	171
Figure 6.18: The essential and plastic works of fracture analysis	172
Figure 6.19: The essential work of fracture, w_{ei} , and $CTOD_i$	172
Figure 6.20: The essential work of fracture, w_e , and CTOD	174
Figure 6.21: ITFT fatigue lives versus stress for control and RTR-MBs mixtures.....	175
Figure 6.22: ITFT fatigue lives versus strain.....	176
Figure 6.23: ITFT fatigue lives versus strain.....	176
Figure 6.24: The horizontal strain evolution.	177
Figure 6.25: Fatigue lives at $100 \mu\epsilon$ for the control and RTR-MBs asphalt mixtures.....	178

Figure 6.26: Creep compliance curves evolution with time for the different mixtures.....	179
Figure 6.27: Stress-Strain curve from the indirect tensile strength test.....	181
Figure 6.28: DCSE _f and DCSE _{min} for the different mixtures	182
Figure 6.29: ER for the different mixtures	182
Figure 7.1: RLAT testing configuration in NAT	188
Figure 7.2: SHRP rutting parameters for different binders	189
Figure 7.3: Shenoy rutting parameters for different binders	190
Figure 7.4: Complex viscosity of different binders tested at (a) 50°C and (b) 60°C.....	191
Figure 7.5: J _{nr} of binders at (a) 50°C and (b) 60°C.....	193
Figure 7.6: Recovery percentage of binders at (a) 50°C and (b) 60°C	194
Figure 7.7: RLAT results of different mixtures tested at 100kPa stress.....	195
Figure 7.8: RLAT results in terms of the minimum strain rate and total strain.....	197
Figure 7.9: One cycle results of MSCR test for binders S-N and H.....	197
Figure 7.10: Correlation between different rutting parameters	200
Figure 7.11: Correlation between J _{nr} @ 25.6 kPa stress	201
Figure 7.12: Correlation between J _{nr} obtained at different stress	203

List of Tables

Table 2.1: Effect of different temperatures on rubber	13
Table 2.2: Comparison of passenger car and truck tyres in the EU.....	14
Table 2.3: Comparison between the ambient and cryogenically ground rubbers.....	20
Table 2.4: Lists of the most common devulcanisation methods.....	23
Table 2.5: Available specifications for RTR-MBs	28
Table 3.1: The properties of base binders used in this study	82
Table 3.2: Crumb rubber particles gradation	83
Table 3.3: Crumb rubber particles properties	83
Table 3.4: Quantitative parameters associated with the interaction process	91
Table 3.5: The viscosity of RTR-MBs produced using bitumen S.....	91
Table 3.6 The MSCR properties of base bitumens.....	102
Table 4.1: The softening point of RTR-MBs after static storing at high temperature.....	123
Table 5.1: Aggregate, rubber and bitumen properties	137
Table 5.2: The main parameters associated with the production of SMA mixtures.....	139

Table 5.3: The complex modulus of the control binder and RTR-MBs	145
Table 5.4: The ITSM before and after successive cycles of water immersion	146
Table 6.1: Test conditions and parameters	152
Table 6.2: Calculated PV based on Equation 6.6 for H binder.....	163
Table 6.3: Fatigue equations versus resilient strain f.....	178
Table 6.4: The IDT results for the different mixtures.....	180
Table 7.1: The estimated binder strains under the RLAT conditions	202

Chapter 1 Introduction

1.1 Background

Approximately 300 million of scrap tyres are generated each year in Europe and around 30 million are produced in the UK alone (Rahman 2004, Lee, Amir Khanian et al. 2007). These scrap tyres impose a serious environmental problem because of their large size and they are a non-biodegradable waste. On the other hand, the use of ground rubber particles from recycled tyres in asphalt paving materials provides a solution to overcome environmental problems associated with hazardous landfill as well as having the potential to improve the mechanical properties of the pavement.

Although the modern use of involving recycled tyre rubber into flexible pavement applications started in the early 1960's, this initiative is not a new one and started over 170 years ago with the use of natural rubber (Heitzman 1992, Epps 1994). Charles McDonald, Materials Engineer for the City of Phoenix, Arizona, developed a highly elastic modified bitumen as a surface patching material by blending coarse rubber particles ($\sim 2.36\text{ mm}$) with bitumen for about an hour at high temperature. Another technology for including recycled tyre rubber was also introduced in the 1960's by Swedish companies through modifying the aggregate of asphalt mixtures (Epps 1994).

The introduction of ground rubber into road asphalt mixtures is, therefore, accomplished by two technologies known as the Wet process and Dry process. In the wet process, the ground rubber is blended with the bitumen at high temperature before introducing it into the

aggregate; while in the dry process, the recycled tyre rubber is added by replacing a small part of the aggregate in the asphalt mixture.

Although larger quantities of recycled tyre rubber are consumed in mixtures produced using the dry process and with minimal or no modification required in an asphalt plant, the inconsistency in field performance makes the dry process not widely used and increasingly it is being abandoned (Rahman 2004). On the other hand, the wet process is being paid more attention and extensive research has been carried out to develop technologies associated with producing improved binders that can sustain the highway stresses under different environmental conditions.

It should be mentioned here that different terms are found in the literature to describe the product of wet technology. However, the following terms (rubberised bitumen, rubberised binders, Recycled Tyre Rubber-Modified Bitumen (RTR-MBs)), in this work, will be used with a generic meaning that simply implies bitumen blending with tyre rubber particles at different processing levels, different rubber materials, and different modification levels. Also, the word ‘binder’ simply means neat bitumen or bitumen blended with rubber in this work.

Rubberised bitumen can also be produced using fine rubber particles and polymers (i.e. styrene–butadiene–styrene (SBS)) at a supplier’s terminal using elevated temperature and high shear stress to produce homogeneous binder with excellent storage stability and compatibility properties. This technology process is called Terminal-blend process. It was mainly developed to reduce the need for modifying the asphalt plant and also to have a better quality control compared to field blending practices.

The mechanical properties of rubberised bitumens are highly dependent on the interaction that happens between the rubber particles and bitumen. The interaction is traditionally considered to be a physical process with no chemical reaction. The main interaction mechanism is associated with swelling for rubber particles through the absorption of the lighter fractions available in the bitumen and rubber dispersion by the means of devulcanisation/depolymerisation (Heitzman 1992, Ghavibazoo and Abdelrahman 2012, Lo Presti 2013). The amount and rate of swelling and the dispersion of rubber particles can be regulated by changing the interaction parameters (temperature, time and mixing speed). The different tyre rubber particles (source, particles size, and grinding method), and the different

properties of bitumen, are also important variables that play a key role in determining the final mechanical properties of rubberised bitumens.

To that end, the development of performance properties of rubberised bitumens is required a better understanding the rubber-bitumen interaction and at the same time ascertain that the performance properties of binders are truly related to asphalt mixture and field pavement performance.

1.2 Problem Statement

The traffic density and axle loads are constantly increasing to the point that conventional bituminous materials cannot satisfactorily withstand them. In the UK alone, the vehicle miles increased by 13.5 billion for the period from 2010 to 2015 (Department for Transport Statistics 2016). This means that the accumulation of scrap tyres is also likely to increase. Thus, investigating enhanced materials by means of modifying the base bitumen using recycled tyre rubber is a significant need. Rubberized bitumen introduces itself as a solution to improve pavement performance and avoid hazardous landfill. However, widespread adoption of the rubberized bitumen option has been obstructed by many difficulties. The presence of insoluble particles has a detrimental effect on the homogeneity and storage stability. Also, the rubberised bitumens tend to have an excessively high value of High-Temperature Viscosity (HTV) which imposes handling difficulties, poor workability and pumpability, and also leads to increased energy consumption and emissions. In addition, the HTV of the rubberized bitumen reduces the possible hauling distance and the compaction temperature range.

There are a large number of variables associated with the manufacture of rubberised bitumen that determine the final product of RTR-MBs. Also, the variability of recycled tyre rubber sources and the variability of base bitumen, all make identifying guidance for general recipe formulation difficult to accomplish. If the material is not appropriately designed, produced and constructed, a counterproductive result could arise with pavement performance being inferior to conventional asphalt. An improved product development procedure is, therefore, required to develop superior rubberised binders.

Another important concern is the applicability of the current test methods whether they are appropriate to be used on rubberized bitumen. Many studies have suggested that current SHRP protocol test methods do not necessarily reflect the true binder performance related to mixture or pavement performance (Chen and Tsai 1999, Bahia, Hanson et al. 2001,

Planche, Anderson et al. 2004, Tsai, Monismith et al. 2005, Johnson, Bahia et al. 2007, Zhou, Mogawer et al. 2012). Furthermore, measuring the mechanical properties of bituminous materials under only small strains does not provide sufficient information to predict the performance of materials under the damaging circumstances that are normally accompanied by high strain levels and yielding. Thus, the resistance properties of materials under these circumstances should be considered in order to develop fundamental and more performance-related characterisations.

In this work, different test methods and parameters used for characterising the binders in terms of fatigue cracking and rutting will be adopted to understand the mechanical properties of rubberised binders and their asphalt mixtures. Also, a simple laboratory tool consisting of a standard Brookfield viscometer with a modified Dual Helical Impeller (DHI) stemming from previous research (Lo Presti 2011, Celauro, Celauro et al. 2012) was used to practically investigate the main parameters affected by the manufacture of RTR-MBs. Finally, the pre-treatment of recycled tyre rubber by Warm Mix Asphalt (WMA) additives (Fischer–Tropsch wax (Sasobit®)) and using partly devulcanised ground rubbers were used to obtain RTR-MBs with reduced HTV.

1.3 Aim and Objectives

The project involves a combination of the following aspects. Firstly, develop rubberised bitumen materials with the most desirable physical and rheological properties. Secondly, investigate and understand the effect of the main variables associated with RTR-MBs such as base bitumen, processing conditions, rubber type and pre-treatment of rubber particles on the rheological and performance-related characterisations. Thirdly, investigate and understand the effect of storage stability and artificial ageing on the rheological and mechanical properties of RTR-MBs. Finally, investigate and understand the relations between different binder test methods and asphalt mixture performance in order to evaluate appropriately the binder contribution to fatigue and rutting properties of asphalt mixtures. This work would contribute to improved understanding of the behaviour of rubberised binders and mixtures and aim to consider the rubberized bitumen option and put it into practice in the UK.

To achieve these aims, the following research objectives are identified:

- (1) Investigate the effect of processing conditions on the rheological properties of different rubberised binders tested under low and high strain levels

- (2) Investigate the feasibility of inclusion of WMA additive (Sasobit) in rubberised bitumen and its effect on the rheological and mechanical properties of the binders and asphalt mixtures
- (3) Investigate the effects of artificial ageing and storage stability on rheological properties of rubberised binders.
- (4) Characterise the fatigue and rutting resistance of the rubberised binders using different test methods and parameters
- (5) Investigate the mechanical and performance-related properties of rubberised asphalt mixtures
- (6) Identify and establish relations between the binder properties tested by different methods and their asphalt mixture performance.

1.4 Research Methodology

In order to achieve the overall objectives and aims of the research, the methodology primarily involves an extensive laboratory investigation into rubberised binders and base bitumen in addition to their asphalt mixtures. The rubberised binders were blended using two different base bitumens and three different rubber types. The two base bitumens were selected with large differences in their physical and rheological properties. The first bitumen is very soft and has a penetration of 200 dmm and a softening point of 37°C and the second bitumen is relatively hard and has a penetration of 40 dmm and a softening point of 51.4°C. The three different sources of recycled tyre rubber used were labelled as N, D and SE. The normal straight rubber N is recycled rubber, derived from discarded truck and passenger car tyres by ambient grinding. D and SE are both non-standard crumb rubbers chosen to pursue a reduction in high-temperature viscosity. The partly vulcanised rubber D is a recycled from truck and passenger car tyres, also by ambient grinding, but contains 20% vulcanised rubber. The last one SE consists of 100% recycled truck tyres which by nature have a relatively high content of natural rubber. SE is pre-treated with special oil and FT-wax component. The asphalt mixtures for both control and rubberised binders were produced using one type of aggregate and a typical stone mastic asphalt gradation (10mm) suitable for surface courses.

The effects of blending variables are firstly evaluated and then optimised by producing different combinations of rubberized bitumens using a Brookfield Rotational Viscometer at low shear rate. At this stage, the investigation and optimisation study are based on

characterising the rheological properties using HTV, Dynamic Mechanical Analysis (DMA) and Multiple Stress Creep and Recovery (MSCR).

The next stage is to manufacture rubberized bitumens using a Silverson L4RT High Shear mixer. The storage stability is assessed using the toothpaste test, investigating the rheological properties of binders extracted from the top and bottom of the toothpaste. The effects of artificial ageing on the rheological properties of RTR-MBs are also evaluated using the thin film oven test (TFOT) and pressure ageing vessel (PAV) test to simulate short-term ageing and long-term ageing, respectively.

The mechanical and rheological properties of materials at different in-service temperatures are evaluated. Dynamic Shear Rheometer DSR is used for intermediate and high in-service temperatures to characterise the fatigue and rutting resistance of binders. Additionally, the fracture mechanics-based failure properties are evaluated using the double-edge-notched tension test DENT. The asphalt mixtures using different rubberised binders in addition to the control are produced using one type of aggregate and a gradation selected from the British specification BS EN 13108-5/ PD 6691:2007. The mechanical properties of the asphalt mixtures are characterised by their stiffness, moisture sensitivity, fatigue cracking resistance, permanent deformation resistance and fracture properties. The flow chart below, Figure 1.1, illustrates the main elements of the research methodology.

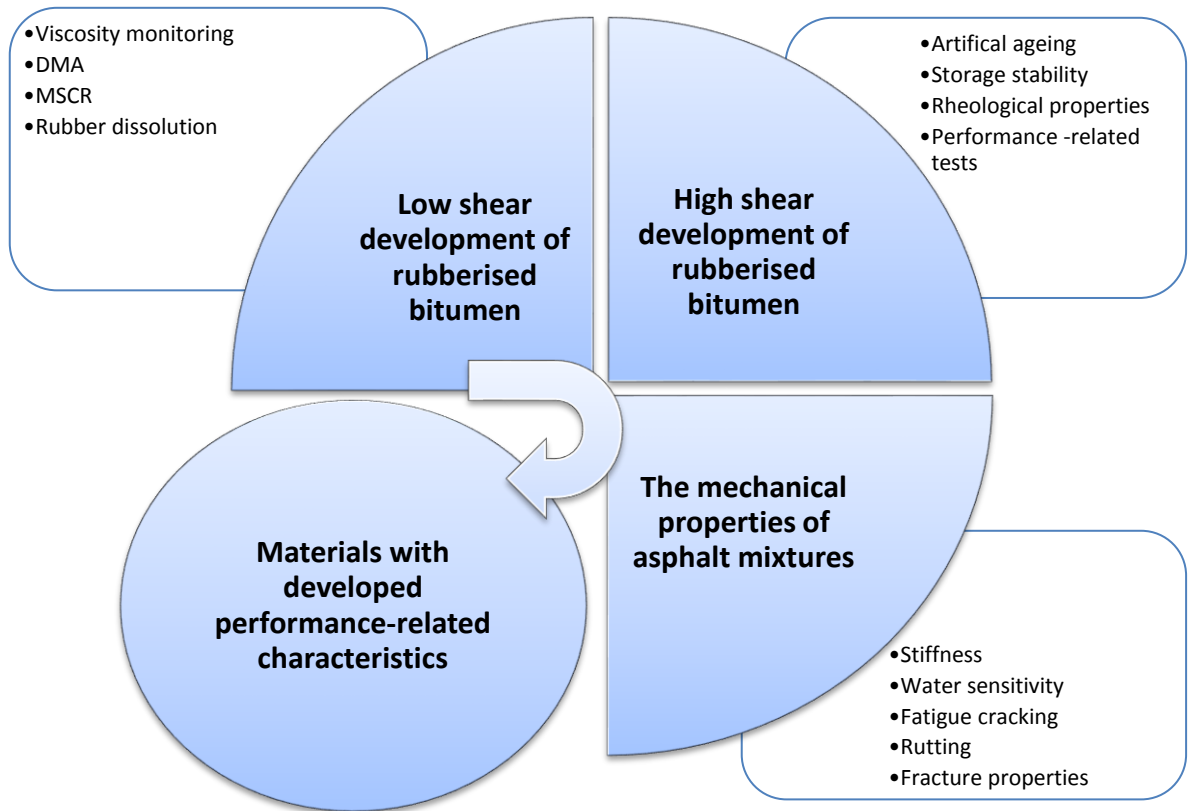


Figure 1.1: The main elements of research methodology

1.5 Thesis Outline

Chapter	Description
Chapter 1	An overview and general background information about the technology of rubberised bitumens. This chapter also includes the problem statement, and aims and objectives in addition to the methodology.
Chapter 2	This chapter provides an overview, background and basis for understanding the main elements associated with the constituent materials of rubberised binders and rubber-bitumen interaction. It also presents the fundamental tests and parameters that are used for characterising the mechanical properties of binders and mixtures.
Chapter 3	This chapter investigates the effect of curing temperature and mixing time on the mechanical properties of rubberised bitumen by utilising a simple laboratory tool consisting of a standard Brookfield viscometer with a modified Dual Helical Impeller (DHI).
Chapter 4	In this chapter, the manufacture of RTR-MBs using Silverson L4RT High Shear Mixer is described. This chapter also investigates the effect of blending time on the rheological properties tested over a wide range of stresses. The storage stability of materials and artificial ageing are also evaluated by means of rheological properties.
Chapter 5	A brief description of materials and the mixture design method associated with manufacturing HMA samples is presented. This chapter also investigates the mixture's volumetric properties, stiffness and moisture susceptibility.
Chapter 6	The fatigue properties of the different binders in addition to their asphalt mixtures are investigated in this chapter using different testing methods. This chapter also provides a review and critical evaluation of different approaches used to define fatigue failure to assess accurately the fatigue damage resistance.
Chapter 7	The deformation of different binders using SHRP rutting parameter, Shenoy rutting parameter, ZSV and MSCR tests are investigated. The rutting resistance of asphalt mixtures is also investigated using the Repeated Load Axial Test (RLAT).
Chapter 8	In this chapter, the main conclusions and recommendations for future research are introduced.

Chapter 2 Literature Review

2.1 Introduction

This chapter provides an overview, background and basis for understanding the main elements associated with rubber-bitumen interaction in addition to the fundamental testing and parameters for characterising the mechanical properties of binders and mixtures. The literature review begins by addressing the constituent materials of bitumen and tyre rubber with an emphasis on the tyre properties as a modifier for bitumen. The details about the techniques used to incorporate recycled tyre rubber into bituminous materials, the nature of the interaction and changes between the rubber and bitumen, the storage stability, and the effect of ageing, are described in the next section. The testing methods and parameters that have been used for characterising fatigue and rutting for the binders are presented and discussed in the fourth section. The literature review covers different approaches used to evaluate the fatigue and rutting of bituminous binders. The use of the dissipated energy approach and the essential work of fracture (EWF), for characterising the fatigue properties of binders, are described and reviewed in detail. The parameters and testing methods associated with evaluating the rutting of binders, including, SHRP parameter, Shenoy Rutting Parameter, Zero Shear Viscosity and Multiple Stress Creep and Recovery, are also described. This section also includes descriptions pertaining to the fundamentals of using the Dynamic Shear Rheometer (DSR) as a testing device for measuring the rheology of materials. The last section focuses on addressing the testing methods that deal with characterising the mechanical properties of asphalt mixtures, such as Indirect Tensile

Stiffness Modulus (ITSM), Indirect Tensile Fatigue Test (ITFT), Repeated Load Axial Test (RLAT) and SuperPave Indirect Tensile Test (IDT).

2.2 Constituent Materials

2.2.1 Bitumen

Bitumen is a complex material of organic molecules obtained by a series of distillation processes of crude oil. It is also found as a natural material. Bitumen has unique engineering properties such as adhesion properties, it is highly waterproof and durable, highly resistant to the actions of most acids, alkalis, and salts and it has a great versatility. Moreover, the viscoelastic properties of bitumen help to accommodate the expansion and contraction strains with day-night temperature variation, making it suitable to be used in highway application. Hydrocarbons are the main components of bitumen with minor amounts of other functional groups like oxygen, nitrogen and sulphur (Romberg, Nesmith et al. 1959). As bitumen is derived from the distillation of crude oil where properties differ from region to region, this makes the exact breakdown of hydrocarbon groups of bitumen not an easy process. However, elementary analysis of bitumen extracted from a variety of crude sources has shown that most of them contain Carbon: 82-88%, Hydrogen: 8-11%, sulphur: 0-6%, Oxygen: 0-1.5%, Nitrogen: 0-1% (Rahman 2004). Generally, the chemical components of bitumen are discerned into four broad classes of molecule as shown in Figure 2.1 (Read and Whiteoak 2003):

- Asphaltenes
- Resins
- Aromatics
- Saturates

The resins, aromatics and saturates are also assembled in one group called maltenes. They perform as a dispersion medium or peptisers for the asphaltenes, and their proportion to asphaltenes determines whether the bitumen is SOL type or GEL type. The SOL type bitumen generally has sufficient maltenes, hence, the asphaltenes are well dispersed or dissolved in the oily medium. GEL type bitumen, on the other hand, has gelatinous (GEL) structure because of a lack of resins and aromatics, so the asphaltenes form large agglomerations or continuous networks, because they are not fully peptized in the medium (Read and Whiteoak 2003). A definition of each group is given below:

- **Asphaltenes:** they are black or brown amorphous (without shape) solids and have the highest molecular weight and polarity within the medium. Their molecular weight ranges from 1,000 to 100,000 and they tend to agglomerate together to form micelles with a molecular weight between 20,000 and 1,000,000. Asphaltenes content within the bitumen usually ranges from 5% to 25%. Generally, the asphaltenes determine the stiffness and acidity of the bitumen. The higher the asphaltenes content the harder the bitumen with lower penetration, higher softening point and higher viscosity, which is suitable for hotter climates. However, the performance of asphaltenes changes with temperature, gel structure of the micelles has a tendency to break down on heating but it reforms on cooling.
- **Resins:** They are also black or brown solid or semi-solid high molecular weight and very polar in nature. The molecular weight ranges from 500 to 50,000 and their polarity makes the resins very adhesive. Resins act as co-solvent agents or peptisers for the asphaltenes along with their oxidation inhibitor character (Read and Whiteoak 2003). Their proportion to asphaltenes determines the proportion of (SOL) or (GEL) type bitumen. If there are adequate resins a solution (SOL) structure bitumen occurs, whereas a reduction forms a gelatinous (GEL) structure in the bitumen. The volatilization and oxidation of resins results in hardening of the bitumen due to conversion of resins into more chemically polar molecules or asphaltenes. Finally, resins serve as stabilisers in the bitumen which keep holding the bitumen components together.
- **Aromatics:** they are black or brown in colour and have low molecular weight, ranging from 300 to 20,000. They might be present in bitumen as both polar (low polarity) and non-polar oily fluid. The polar aromatics are generally more viscous and darker while non-polar aromatics are yellow to orange and less viscous. They serve as a solvent for both asphaltenes and resins and are considered as a plasticiser of bitumen. They represent the major proportion of the bitumen (40-65%) and help in protecting the oils from oxidation during the ageing process (Read and Whiteoak 2003).
- **Saturates:** they are straw or white in colour with a molecular weight range from 300 to 1500. They are non-polar viscous oils that give fluidity to the system. They form between 5-20% of the bitumen; bitumen with more saturates is generally softer and is more able to reform broken bonds (Thom 2008). Most of the waxy components of bitumen are present in the Saturates.

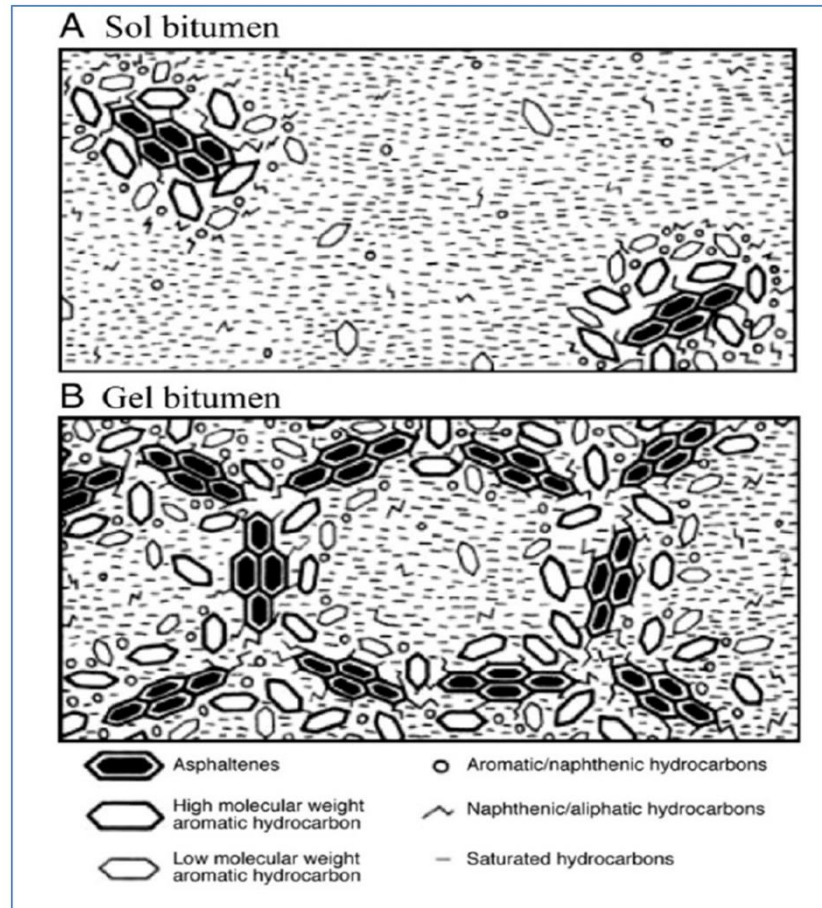


Figure 2.1: Schematic representation of (A) sol type and (B) gel type bitumen (Read and Whiteoak 2003)

2.2.2 Tyre Rubber

Vehicle Tyre Structure

The vehicle tyre is made up of three main materials; elastomeric (rubber) compound, fabric and steel. The fabric and steel form the structural skeleton of the tyre with the rubber forming the “flesh” of the tyre in the tread, sidewall, apexes, liner and shoulder wedge, as seen in Figure 2.2 (Lo Presti 2013). The elastomeric (rubber) compound of a vehicle tyre is mainly composed of natural rubber, synthetic rubber, carbon black, sulphur and other chemical components. Natural rubber is found in a tree called *Hevea-braziliensis* as a milky colloidal suspension or latex. It is a long straight-chain isoprene hydrocarbon polymer that has a physical appearance and a spongy or flocculent nature. Natural rubber is sticky in nature and its physical properties change with temperature; at low temperature becomes stiff and brittle whereas at high temperatures above 100°C it becomes flexible, soft and transparent; the effect of temperature can be found in Table 2.1 (Rahman 2004). Synthetic rubbers are made from petroleum products and other minerals and produced in two main stages: first the

production of monomers (long molecules consisting of many small units), then polymerisation to form a rubber (Rahman 2004). The properties of rubber are mainly controlled by the chemical nature of the long polymer chains from which the molecules are arranged.

Generally, the same tyre rubber properties and tyre compositions are produced worldwide. The main ingredients of the tyre are rubber, carbon black, metal and textile along with some percentage of additives. The general tyre compositions in cars and truck tyres in the EU are summarised in Table 2.2 (Shulman 2000). However, the percentage of natural rubber to synthetic rubber in truck or bus tyres is typically much more than in cars; in truck or bus tyres the percentage of natural rubber to synthetic is about 65% but in car tyres it is only 35% (Rahman 2004).

Rubber properties have been developed to be resistant to mould, mildew, heat and humidity, to retard bacterial development, resist sunlight, ultraviolet rays, some oils, many solvents, acids and other chemicals. Other physical characteristics include their non-biodegradability, non-toxicity, weight, shape and elasticity. However, some of these characteristics which are beneficial during on road service life could be detrimental after the end of their intended use and can create problems for collection, storage and dumping (Rahman 2004, Lo Presti 2013).

Table 2.1: Effect of different temperatures on rubber (Rahman 2004)

Temperature	Appearance
-10°C	Brittle and opaque
+20 °C	Soft, resilient and translucent
+50 °C	Plastic and sticky
120 °C-160 °C	Vulcanised when agents e.g., sulphur are added
~182 °C	Break down as in the masticator
200 °C	Decomposes

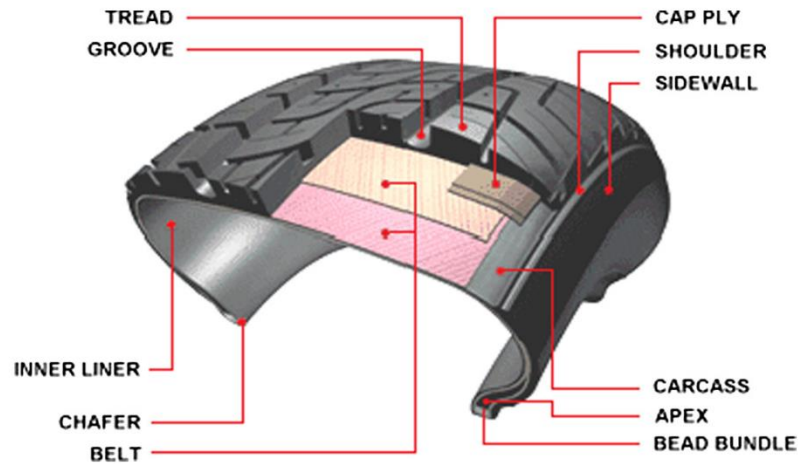


Figure 2.2: Tyre structure (Lo Presti 2013)

Table 2.2: Comparison of passenger car and truck tyres in the EU (Shulman 2000)

Material constituents	Passenger car %	Truck/Buses %
Rubber/Elastomers	48%	45%
Carbon Black	22%	22%
Metal	15%	25%
Textile	5%	--
Zinc oxide	1%	2%
Sulphur	1%	1%
Additives	8%	5%

Rubber Processing

Rubber is defined according to ASTM D 6814-02 as a natural or synthetic elastomer that can be chemically cross-linked/vulcanised to enhance its useful properties. Cross-linked rubbers or elastomers are three-dimensional molecular networks, with the long molecules held together by chemical bonds. They absorb solvents and swell but they do not dissolve unless very high temperatures are used. Additionally, they cannot be reprocessed simply by heating (Hamed 1992). To produce material with superior durability and elasticity, raw rubber needs to be vulcanised and compounded to meet the end use requirements. During the vulcanization or curing, the rubber chains are chemically linked together by the aid of sulphur to form a network; by this means, the materials are changed from a viscous liquid to a tough elastic solid. There are two types of vulcanisation process: hot (mould cured) and cold (pre-cure system). The hot process is used for the majority of rubber goods, including tyres. Hot vulcanisation (mould cured) is accomplished by heating the raw rubber with sulphur to a temperature between 120°C and 160°C. The soft rubber is transformed by the

hot process into a hard, durable, usable stage material, with improved strength and elasticity, and improved temperature susceptibility. On the other hand, cold vulcanization is used to produce soft, thin rubber products such as surgical gloves or sheeting (Rahman 2004).

Rubber compounding or formulation is a term for the process of adding various chemical additives to the raw rubber materials such as base polymer, cross-linking agent, accelerator for the cross-linking reaction, reinforcing filler (carbon black; mineral), processing aids (softeners, plasticizers, lubricants), diluents (organic materials, extending oils), colouring materials (organic or inorganic), specific additives (blowing agent; fibrous materials) in order to enhance their properties (Hamed 1992, Rahman 2004, Gent 2012). Compounding is essential to incorporate the ingredients and ancillary substances that are necessary for vulcanisation and to adjust the hardness and modulus of the vulcanised product to meet the end requirement. It should be mentioned that some of the ingredients still remain when the vehicle tyres are recycled at the end of their life. For example, the stabilisers which provide the resistance to cracking and degrading of the tyre can also prolong the life of roads, and make the tyres useful for sports and safety surfaces; the pigments and black carbon that are added to the rubber during the processing of the tyres can also contribute to darkening the colour of the pavement and improve the contrast for roads that are modified by the recycled tyre rubber (Rahman 2004).

The rubber performance is highly controlled by the selection of appropriate additives and fillers during the vulcanising and compounding process. In terms of vehicle tyre rubber, they consist mainly of hydrocarbon elastomers. These include styrene-butadiene rubber (SBR), butadiene rubber (BR), and polyisoprene rubber – both natural (NR) and synthetic (IR). In addition, these “diene” rubbers contain substantial chemical unsaturation in their backbones, causing them to be rather prone to attack by oxygen, and especially by ozone. Also, they are readily swollen by hydrocarbon fluids (Hamed 1992). Finally, the mechanical performance of an elastomer depends highly on its crosslink density as schematically shown in Figure 2.3 (Hamed 1992, Rahman 2004). As can be seen from Figure 2.3, there is no optimum crosslink density that can meet all the maximum values for the three properties. However, there is a constant increase in the stiffness as the crosslink density increases, while other fracture characteristics such as the tear strength and the tensile strength do not necessarily reach a maximum at same crosslink density level. When modifying bitumen by recycled tyre rubber, the crosslink density of rubber can have a significant effect on the resultant mechanical properties of RTR-MBs. Also, the crosslink density of rubber could be altered during

manufacturing RTR-MBs depending on the processing conditions (temperature and time). This is the main reason why there should be an appropriate investigation to optimise the processing conditions in order to allow binders to be produced with the most desirable mechanical properties, and the next two chapters (Chapter 3 and Chapter 4) will be dedicated to manufacturing and developing RTR-MBs with desirable mechanical properties.

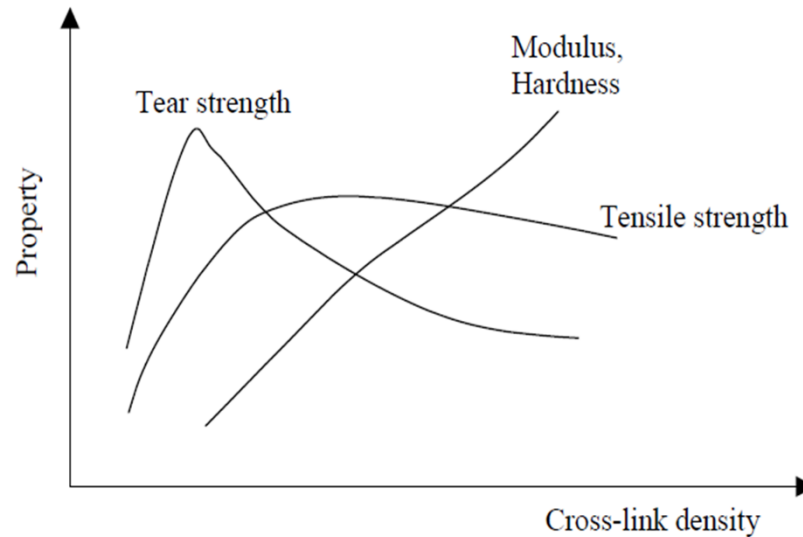


Figure 2.3: The crosslink density effect on the main mechanical properties of rubber (Rahman 2004)

Transforming the Vehicle Tyres into a Bitumen Modifier

The brief life cycle of a tyre is illustrated in Figure 2.4; the main stages of the tyre life cycle include extraction, production, consumption, collection of used tyres and waste management (Lo Presti 2013). When tyres are no longer suitable for use on vehicles because of wear and severe damage, these tyres are discarded and/or consigned to another use, such as scrap tyres in civil engineering applications. End of life tyres are considered one of the most challenging sources of waste because of their large volume and they are non-biodegradable. After the scrap tyres are collected, some of them are disposed to landfill, stockpiles or illegal dumps and others are recovered to be used in different applications such as energy fuel (the heating value of scrap tyres ranging from 28000kJ/kg to 35000 kJ/kg, equivalent to the good quality coal (Rahman 2004); therefore, it is used widely as an alternative to fossil fuels), or chemical processing such as pyrolysis, thrombolysis and gasification (Lo Presti 2013). Also, some of these tyres are assigned for granulate recovery which involves tyre slitting, shredding and chipping processes to produce tyre shreds or chips that can be used for a variety of civil engineering projects.

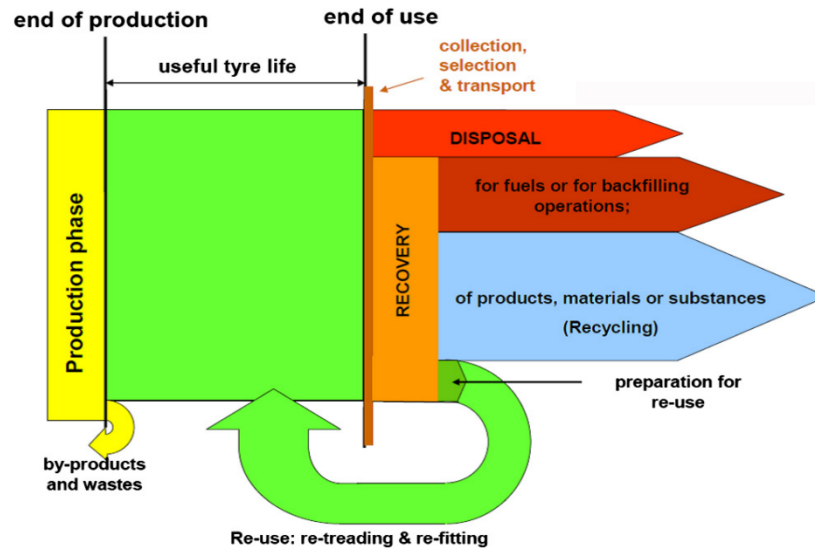


Figure 2.4: Flow chart of the service life of tyres (Lo Presti 2013)

In the first stage of granulated tyre recovery, the steel structural skeleton is extracted from the whole tyre, and it is directly fed into the shredding process, as shown in Figure 2.5 (JLLC 2008). In the shredding process, the tyres are cut into small pieces by using large cutting machinery. The physical appearance of shreds is basically that of flat, irregularly shaped tyre chunks with jagged edges that may or may not contain protruding sharp pieces of metal, which are parts of the steel plates or beads (Rahman 2004). This process produces shreds with different sizes that vary with the condition and type of the processing equipment and could range from 460 mm to 25 mm, with most particles within the 100 mm to 200 mm range. Their loose densities also vary in relation to the size of the shreds and they range from 390 kg/m³ to 535 kg/m³. The average compacted density ranges from 650 kg/m³ to 840 kg/m³ (Shulman 2000, Rahman 2004).

The next stage is to produce tyre chips by further chopping the shreds to produce finer and more uniformly sized chips ranging from 76 mm to 13 mm. The chips are sometimes used in civil engineering construction as a partial replacement for aggregate. Their loose density ranges from 320 kg/m³ to 490 kg/m³ while the compacted density ranges from 570 kg/m³ to 730 kg/m³.

The chips can also be reduced in size to produce ground rubber particles which have particle sizes from 9.5 mm to 0.85 mm.

Finally, these chips are further reduced in size to form particulate or crumb known as Crumb Rubber Modifier (CRM). CRM should be clean and free of fabric, steel and other

contaminants to produce highly consistent rubber material suitable for RTR-MBs. The specific gravity of the crumb rubber varies from 1.10 to 1.20 and the size ranges from 1.2 mm to 0.42 mm with some particles as fine as 0.075 mm (Rahman 2004).

CRM is produced by the reduction in size of tyre shreds or chips using different reduction techniques; however, ambient and cryogenic grinding are the two main methods used to produce CRM. A brief description of the two methods, in addition to other methods that are less common, is presented in the next section.

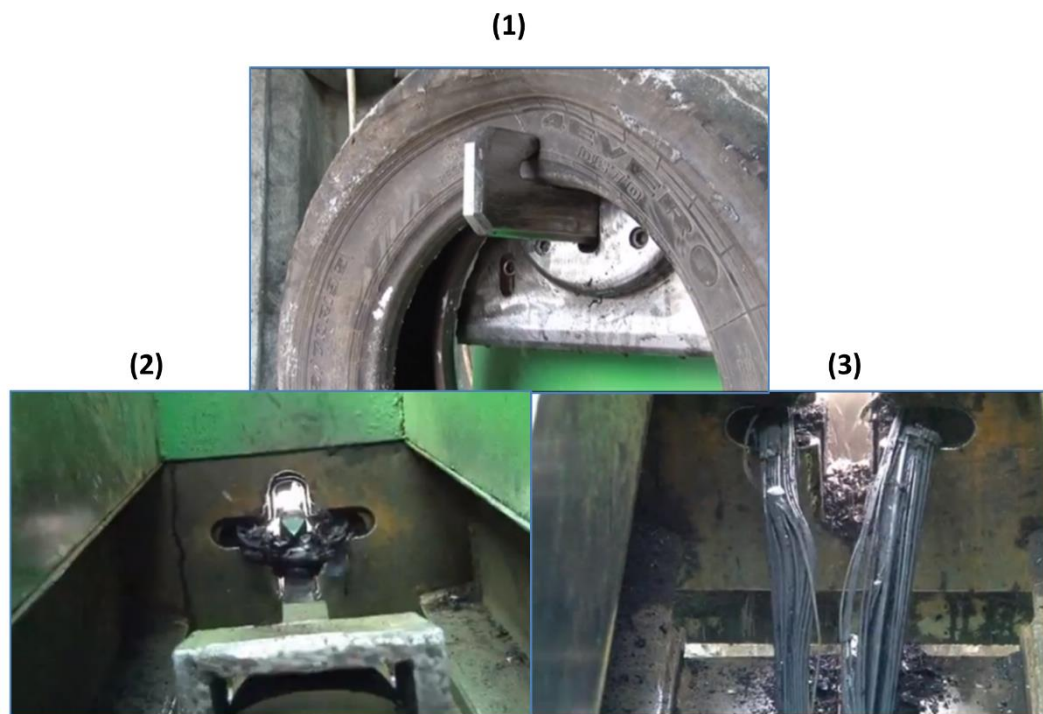


Figure 2.5: Extracting the steel structural skeleton from the tyre (JLLC 2008)

1. Ambient Grinding

In the ambient process, the tyre shreds or chips are processed mechanically at or above normal room temperature to produce finer rubber crumbs. The machinery that is generally used for fine grinding in ambient plants consists of; granulators, high-speed rotary mills, extruders or screw presses and cracker mills. The secondary granulators and high-speed rotary mills reduce further the rubber size by means of a cutting and shearing action. The particles are controlled through screens into different particle sizes. Figure 2.6 shows a schematic granulation process at ambient temperature.

The metallic material is removed using a magnetic separator while fibres and extraneous material are removed using a combination of shaking screens and air sifters to produce fairly

clean material. The process produces materials with an irregular jagged particle shape, rough in texture. Additionally, the rubber particles produced in the cracker mill process are typically long and narrow in shape with a high surface area (Rahman 2004). The torn particles from ambient grinding also have a large surface area which is beneficial to promote interaction between the rubber and bitumen.

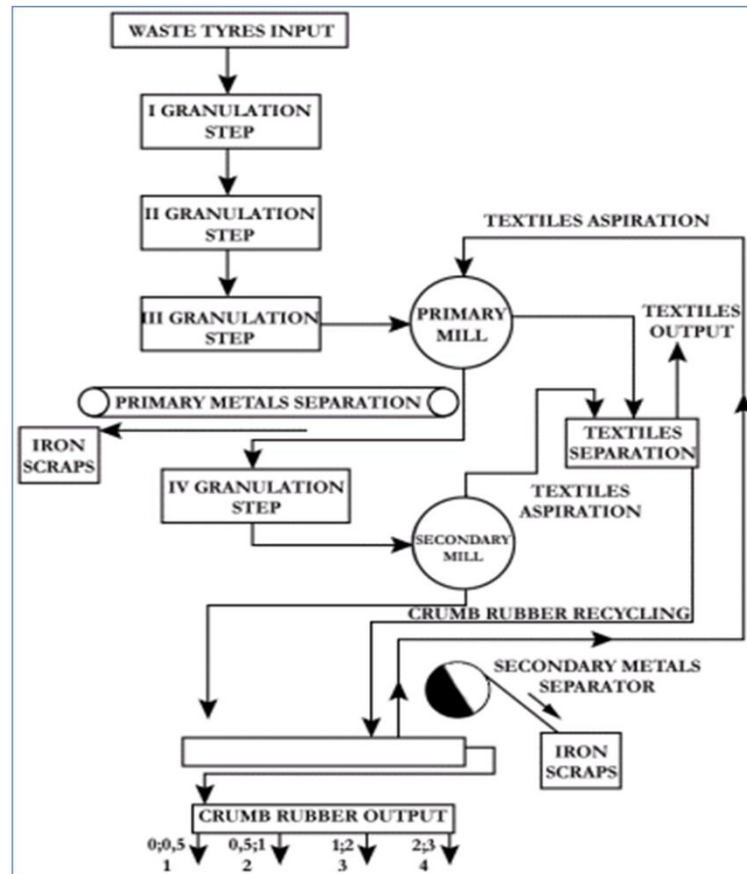


Figure 2.6: Flow chart of a granulation process at ambient temperature (TUT 2013)

2. Cryogenic Grinding

The reduction in size is accomplished here through freezing the tyre chips to a temperature below $-80\text{ }^{\circ}\text{C}$ before crushing them using a hammer mill. The rubber chips are chilled by using liquid nitrogen in a tunnel-style chamber or immersed in a “bath” of liquid nitrogen to reduce the temperature (typically between $-87\text{ }^{\circ}\text{C}$ to $-198\text{ }^{\circ}\text{C}$) (Peralta 2009, Lo Presti 2013). Below the glass transition temperature, the rubber behaves almost as brittle as glass, and thus less energy and fewer pieces of machinery are required to shatter the rubber chips into fine particles. The resulting rubber particles have fairly smooth fracture surfaces, homogeneously cut pieces, shiny and clean. However, the interaction between rubber and base bitumen are generally enhanced by using rubber particles with rough and large surface areas, less specific

gravity, finer particles and porous rubber; therefore, the use of CRM from the cryogenic process in bituminous mixtures is not always encouraged (Lo Presti 2013)

As in the ambient process, the steel, fibres and other extraneous materials, are separated from the rubber by using magnets and air aspiration or shaking screens. Removing the steel and fibres is more controlled and the materials are produced with almost zero steel and fibre content due to the clean breaks between fibre, steel and rubber (Rahman 2004). Very small granules with negligible steel or textile contamination can be obtained through cryogenic technology. A general comparison between the physical properties of rubber particles obtained by the ambient and cryogenic processes is presented in Table 2.3.

Table 2.3: Comparison between the ambient and cryogenically ground rubbers (CWC 1998)

Physical Property	Ambient Ground	Cryogenic Ground
Specific gravity	Same	Same
Particle shape	Irregular	Regular
Fiber content	0.5%	Nil
Steel content	0.1%	Nil
Cost	Comparable	Comparable

3. Wet-Grinding Processes

In addition to the conventional ambient and cryogenic processes, there are other wet-grinding processes to produce fine and super-fine grades of rubber particles. In the wet-grinding process, the milling of fine rubber particles is further reduced in size within a liquid medium, normally water (Memon 2011). The first stage processing is the same as ambient, but in this process, the water is added to form water/rubber slurry, and then milling is applied by narrowly spaced grinding stones in order to produce fine or superfine particles down to 80-500 mesh (CLEMSON-UNIVERSITY 2013). Water is important to reduce the loss of rubber “dust”, move material through the system and to prevent the particles from overheating (CLEMSON-UNIVERSITY 2013). Figure 2.7 shows the main elements of the Wet-Grinding process.

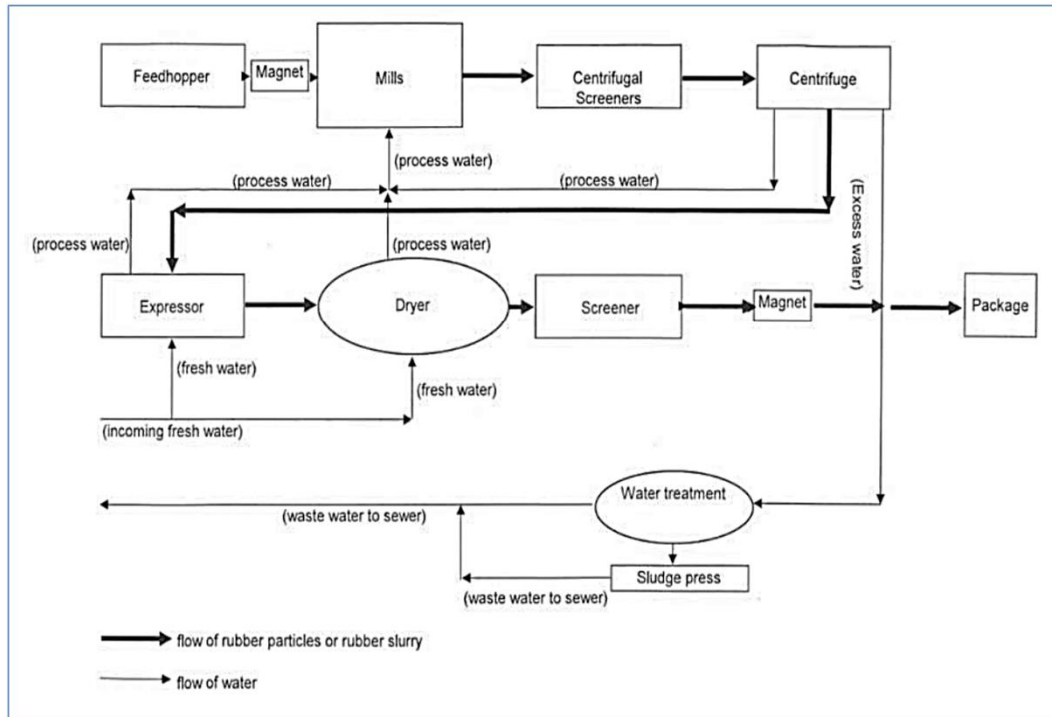


Figure 2.7: Simplified flow process diagram of the wet grinding technology (CLEMSON-UNIVERSITY 2013)

4. Hydro Jet Process

The reduction in the size of rubber granulates is accomplished by the help of pressurised water jets. Water jets are applied at very high operating pressure (around 55,000 psi) rotating in high-speed arrays producing clean, wire-free rubber crumbs that have a wide range of applications in re-manufacturing or as filler in adhesives and sealants. This product is very attractive for bitumen modification due to the high level of roughness of the resulting rubber crumbs (Lo Presti 2013). Figure 2.8 shows SEM analysis taken at 400x magnification with a working distance of 200 μm for a) crumb rubber produced by the ambient process b) cryogenic and c) by the hydro-jet process.

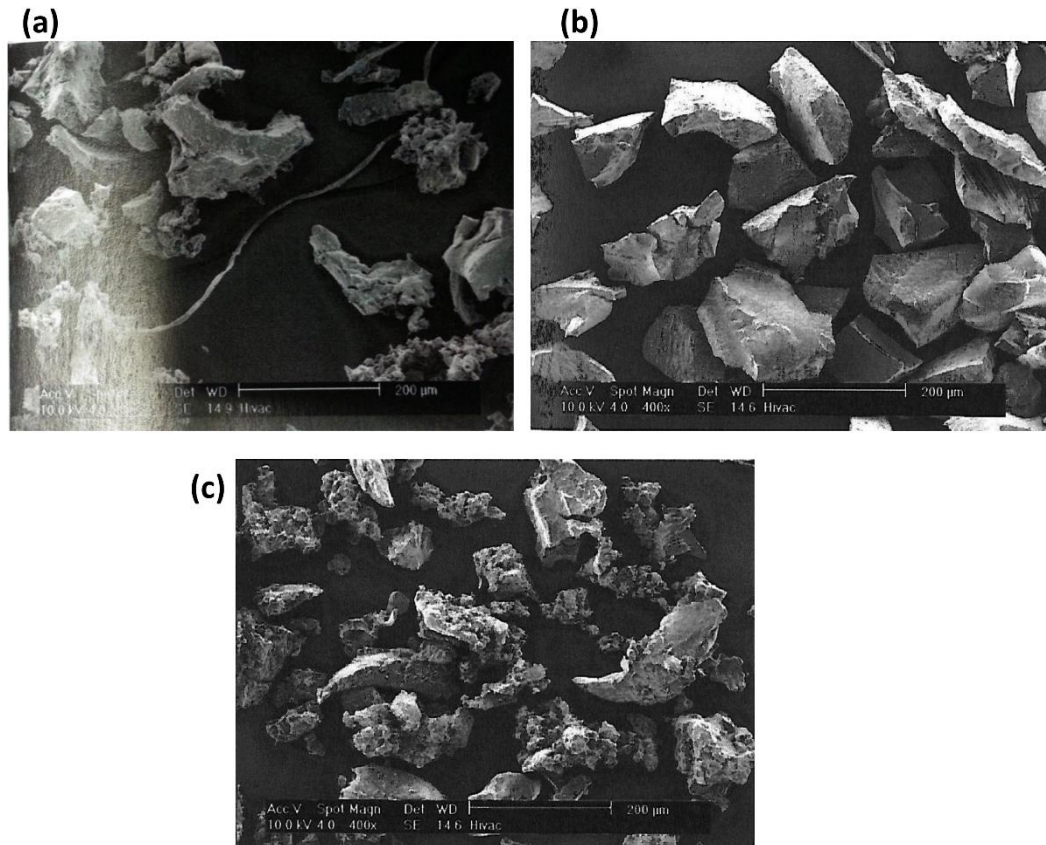


Figure 2.8: SEM images at 200 microns and 400x for rubber particles processed by a) ambient b) cryogenic and c) hydro-jet (Memon 2011)

Devulcanisation of Tyre Rubber

Devulcanisation is defined according to ASTM D 6814-02 as the process of breaking down chemical crosslinks of cured rubber. In chemical terms, devulcanisation means returning rubber from its thermoset, elastic state back to a plastic, mouldable state by the cleavage of cross-linking sulphur bonds in vulcanised rubber without cleavage of the polymer chain bonds (Reschner 2008, TUT 2013). The sulphur bonds in the molecular structure of rubber particles are broken by exposing the vulcanised rubber to either elevated temperatures for an extended period of time or to intense mechanical work. The most common devulcanisation methods are listed in Table 2.4 (Reschner 2008).

Figure 2.9 shows the stages of the devulcanisation reaction; the polysulphide and disulphide bonds are converted to monosulphide bonds by heat, and then the monosulphide bond is broken by the addition of shear stress, and finally recycled uncured rubber is obtained (TUT 2013).

Table 2.4: Lists of the most common devulcanisation methods (Reschner 2008)

Devulcanization Method	Description
Thermal Reclaim Process	Rubber is exposed to elevated temperatures over an extended period of time in order to break the sulfur bonds as well as the polymer back bone. This process was first patented by H. L. Hall in 1858, but is rarely used today due to environmental concerns and relatively severe degradation of the material.
Mechanical Devulcanization	Vulcanized rubber is exposed to intense mechanical work (mastication) in order to selectively break the sulfur bonds in the polymer matrix. The machines used are two roll mills, high shear mixers and extruders. Mechanical devulcanization method leads to good results and may be economically viable in the near future.
Devulcanization with Ultrasound	Technically speaking, this is a special form of mechanical devulcanization. First research results on this subject are encouraging.
Bacterial Devulcanization	Fine rubber powder is exposed to an aqueous suspension with bacteria that consume sulfur and sulfur compounds, e.g., thilbacillus, rodococcus und sulfolobus. Technically viable, but questionable economics due to the complexity of the process.

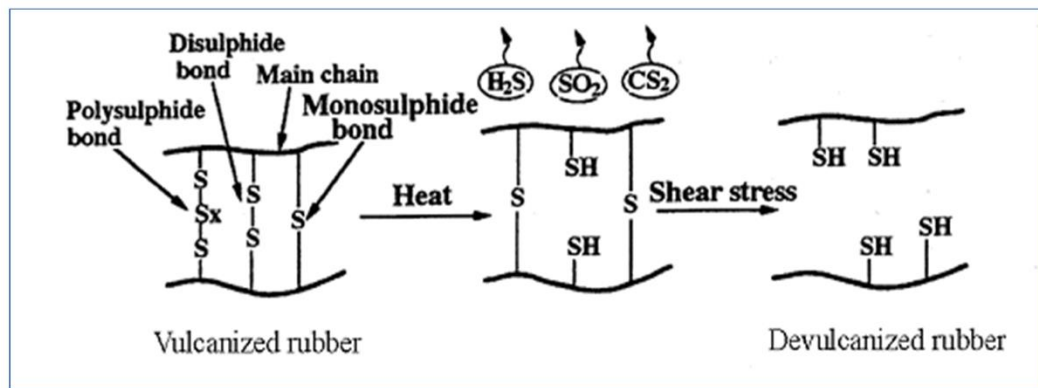


Figure 2.9: Mechanism of cross-linking bond breakage reaction (TUT 2013)

It should be mentioned that if the thermal devulcanisation is too intensive, this could break both sulphur bonds in the polymer matrix and the polymer chains of the rubber leading to a significant decrease in physical properties (Reschner 2008). Also, it is not easy to achieve total devulcanisation without causing chemical transition such as depolymerisation, thermal destruction and oxidation, all of which processes can lead to deterioration in the properties of the recovered elastomers. Thus, it is important to consider experimentally the optimum devulcanisation process that makes possible devulcanised products with desirable properties.

Incorporating the devulcanised crumb rubber into bitumen can enhance the physical properties of binder and improve the hot storage stability. Breaking the sulphur bonds of devulcanised rubber makes the rubber particles more compatible with the base binder and can provide a stable bituminous composition. Moreover, the treated devulcanised crumb rubber particles can be completely digested into bitumen resulting in a stable bituminous

binder during the hot storage period. Also, the carbon black that results from digesting rubber particles would disperse into the bituminous phase rather than precipitate by means of sedimentation (Liang 1999, Xiao-qing, Can-hui et al. 2009, Dong, Li et al. 2011).

2.3 Recycled Tyre Rubber-Modified Bitumens (RTR-MBs)

2.3.1 Incorporating Recycled Tyre Rubber into Bitumen and Mixtures

The environmental problems and health hazards of discarded automobile tyres are well recognised around the world. A huge amount of scrap tyres are generated every year across the world, many of them are illegally disposed or stockpiled. Many countries have prompted strategic regulation for management of scrap tyres to minimise the illegal disposal and reduce the environmental hazards of these tyres. One option of tyre recycling is “thermal recycling” by which the discarded tyres are incinerated as a fuel supplement. However, the use of scrap tyre rubber in applications that are beneficial to society is a sensible choice from an environmental and economic point of view. Thus, using recycled tyre rubber as a modifying agent for bitumen would significantly alleviate the environmental problems and open a large market for scrap tyres because a large quantity of recycled tyres can be used in the pavement industry. Additionally, this approach has been broadly recognised to improve the performance characteristics of asphalt pavements and has increased service life in comparison to conventional asphalt. The recycled rubber has been incorporated into asphalt mixtures by two distinct processes known as “dry process” and “wet process”:

Dry Process

In this technology, the recycled crumb rubber is added to the aggregate before blending with the bitumen. Typically, coarser crumb rubber particles up to 9.5mm are used to replace a small portion of fine aggregate, Figure 2.10. The percentage of crumb rubber usually used is from 1 to 3% of total weight of the mixture, or, roughly as 15 to 35% by the weight of the binder. The grading of aggregate is modified by replacement of one or two aggregate gradations with crumb rubber particles. The degree of interaction between the binder and crumb rubber is influenced by many factors such as the grading, size of crumb rubber, mixing temperature, mixing time and the specific area of rubber particles. Generally, using coarser crumb rubber with less specific surface area results in very slight interaction, and has no significant effect on the properties of the bitumen in comparison to the wet process (Rahman 2004).

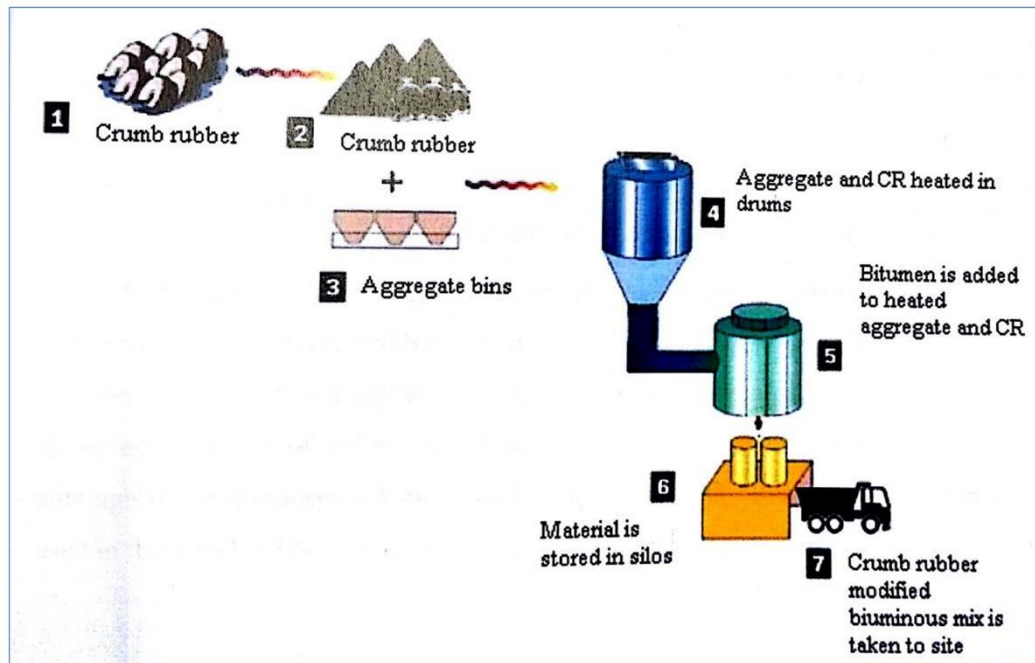


Figure 2.10: Field schematic of dry process technology (Memon 2011)

There are two common types of dry process technology used in the industry; PlusRide and the Generic dry process. PlusRide was developed in the United States in the late 1960's by modifying a gap-graded mixture; the modification is achieved by replacement of up to 3% of aggregate by a coarse granulated crumb rubber. The interaction between crumb rubber and bitumen is kept at a minimum level so the rubber particles maintain their physical and elastic properties within the asphalt mixture which are important to modify the stability of a gap-graded mixture (Rahman 2004).

The generic dry process, also known as the "TAK" system, on the other hand, was developed in the late 1980's by modifying dense-graded and gap-graded mixtures (Takallou and Hicks 1988). Both coarse and fine rubber are added to the dense graded mixture by a percentage up to 3% of total mixture mass. The philosophy behind the Generic dry process is to allow a greater binder modification by the fine rubber, while the coarse particles act as a flexible replacement to the aggregate that improves the elastic properties of the mixture.

Although larger quantities of scrap tyres are consumed in mixtures produced using the dry process and minimal or no modification is required in an asphalt plant, the dry process is not widely used and increasingly is being abandoned. Inconsistency in field performance of pavements made with the dry process is the main reason for this (Emery 1995, Rahman 2004).

Wet Process

In this process and according to McDonald's technique, the crumb rubber is blended with the bitumen for a period of time (45 to 60 min) at elevated temperature $\sim 160^{\circ}\text{C}$, and the rubber particles are swollen by absorbing the light frictions of the bitumen. Figure 2.11 shows a schematic of production of rubberised bitumen in the field by means of the wet process. The interaction between crumb rubber and bitumen leads to an increase in the viscosity of the matrix and imparts enhancement to the engineering characteristics of the product.

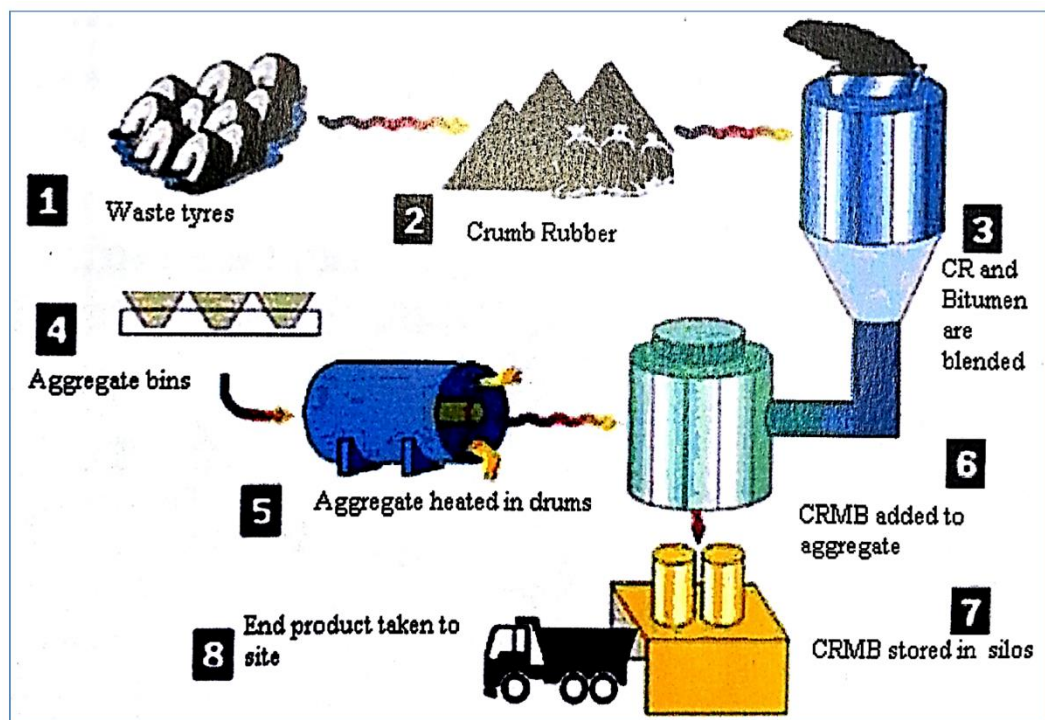


Figure 2.11: Field schematic of the wet process technology (Memon 2011)

The definition of recycled tyre rubber modified bitumen RTR-MB according to ASTM D8 is “a blend of bitumen and crumb rubber and certain additives, where the crumb rubber is at least 15% by the mass of total blend. The mixture has been sufficiently reacted to cause swelling of the crumb rubber particles”. Moreover, a number of RTR-MB specifications have been introduced to specify each of the crumb rubbers used as a modifier (content and properties), the base binder and the final product. The most commonly used specifications are ASTM D6114, CalTrans Bitumen Rubber User Guide, SABITA Manuel 19, VicRoads and APRG Report No. 19 and Austroads User Guide; a comparison between them is presented in Table 2.5 (Memon 2011).

However, the properties of RTR-MBs vary significantly with the interaction process, and the extent of this interaction also depends on a number of variables such as blending temperature, blending time, type and amount of mechanical mixing, crumb rubber type, size, content and specific surface area of the crumb rubber, extender oil and the type of bitumen. Therefore, it is not always possible to define a generic type of RTR-MB for a very specific product.

The main shortcomings of RTR-MBs are the phase separation and the construction challenges due to the high viscosity of the binder. Because of these limitations, many researchers have investigated producing a product with extended storage or shelf life characteristics by adopting much severer curing conditions and fine rubber particles (Zanzotto and Kennepohl 1996, Billiter, Chun et al. 1997, Billiter, Davison et al. 1997, Glover, Davison et al. 2000, Attia and Abdelrahman 2009). But, the key issue is still how to produce material with no minimal phase segregation problems and at the same time maintaining an acceptable level of modification.

RTR-MBs have been successfully used in hot bituminous mixture applications (gap and open graded hot mixes), chip seals or spray applications, and asphalt rubber stress absorbing membrane interlayers (SAMI-R). RTR-MBs applied to wearing course and base course mixtures have shown improved rutting resistance when tested by the full-scale field accelerated loading (ALF) (Mohammad, Huang et al. 2000). In addition, the improvement when using the wet process has been evident in both laboratory and field performance. Many studies have shown that both low-temperature properties and high-temperature properties of asphalt mixtures are improved by the incorporation of RTR-MBs (Glover, Davison et al. 2000, Wong and Wong 2007, Lee, Akisetty et al. 2008). Finally, asphalt-rubber pavement could be considered a more cost-effective option than a conventional pavement when the long-term performance is taken into account (Jung, Kaloush et al. 2002).

Table 2.5: Available specifications for RTR-MBs (Memon 2011)

Properties	ASTM Specification (D6114 2002)			Caltrans Specification (CalTrans 2002)	Austroads Specification (AP-T41/06 2006)	Sabita Specification (2003)
	Type- I	Type- II	Type- III			
Binder Specifications						
Apparent Viscosity (cP)	1500-5000	1500-5000	1500-5000	1500-4000 @ 190 °C	Not specified	2000-5000 @ 190 °C
Penetration @ 25°C	25-75	25-75	25-75	25-70	Not specified	≥ 70
Softening Point °C	≥ 57.2	≥ 54.4	≥ 51.7	52-74	≥ 55	≥ 62
Resilience @ 25°C	≥ 25	≥ 20	≥ 10	≥ 18	Not specified	13-40
Flash Point °C	≥ 232.2	≥ 232.2	≥ 232.2	Not specified	Not specified	Not specified
Crumb Rubber Specification						
Passing Sieve Size (mm)	2.36	2.36	2.36	2	2.36	1.18
Specific gravity	1.15±0.05	1.15±0.05	1.15±0.05	1.15±0.05	Not specified	Not specified
Relative Density	Not specified	Not specified	Not specified	Not specified	Not specified	1.10-1.25
Presence of metal (%)	0.01	0.01	0.01	0.01	Not specified	0.1
Presence of fibre (%)	0.5	0.5	0.5	0.5	Not specified	Not specified
Blending Protocol						
Rubber content (%)	≥ 15	≥ 15	≥ 15	18-22	15-30	20-25
Extender oil (%)	Not specified	Not specified	Not specified	2.5-6	Not specified	3
Blending Speed (rpm)	Not specified	Not specified	Not specified	Not specified	Not specified	3000
Blending Temperature (°C)	177	177	177	190-220	180-200	170-210
Blending Time (min)	Not specified	Not specified	Not specified	45	120	45

2.3.2 Bitumen-Rubber Interaction Process

Bitumen and rubber interact together at high temperature, resulting in adjustment of the physical properties of both binder and rubber; therefore, the nature of the interaction process between bitumen and crumb rubber should be carefully understood in order to clarify the change in the resulting binder properties. Basically, the interaction process between rubber particles and bitumen can be divided into two simultaneous mechanisms; the swelling phenomenon and devulcanisation /depolymerisation.

Crumb rubber is a composite of vulcanised natural and synthetic rubber with permanently cross-linked three-dimensional molecular networks by an intermediate group or atom such as sulphur (Flory and Rehner Jr 1943, Rahman 2004). The rubber particles are first swollen by absorbing the aromatic oil available in the bitumen to a degree depending on the type of bitumen and the structure of the polymer. The reaction is not considered a chemical reaction rather the absorption of aromatic oils from the bitumen into the polymer chains (Heitzman 1992). This can lead to an increase in the rubber particle size and at the same time a reduction in the oily fraction forming a gel-like matrix. That could lead to an increase in the viscosity of the matrix up to a factor of 10 (Heitzman 1992). Increasing the dimensions of the rubber particles results in a consequent reduction in the inter-particle distance; this happens while maintaining the same shape of the cross-linked network which is important to keep the elastic properties of rubber within the matrix.

Devulcanisation means the cleavage of cross-linking sulphur–sulphur or carbon–sulphur bonds that are formed by the vulcanization process during tyre production. On the other hand, depolymerisation means the cleavage of polymer chain bonds. Devulcanisation and depolymerisation cause a reduction in the molecular weight of the rubber and they are sometimes considered a chemical reaction (Abdelrahman and Carpenter 1999). Devulcanisation/depolymerisation occur at high processing conditions (prolonged interaction time and high temperature). When the swelling has reached an equilibrium state but the process continues at extremely high temperature for a long time, the rubber particles start melting and dispersing into the liquid phase of bitumen corresponding to a gradual reduction in the modification level. A full depolymerisation can occur if the interaction is maintained at the very high temperature for a long time; at these conditions, the rubber starts releasing its polymer compounds back into the binder and most of the modified properties vanish (Abdelrahman 2006).

The reduction in the modification starts firstly by a decrease in material stiffness (G^* value), while the elastic properties (phase angle δ) continue to be modified up to a point, and then start losing the effect of modification due to increased destruction of the binder networking (Abdelrahman and Carpenter 1999). The swelling phenomenon, devulcanisation /depolymerisation and the changes that occur in the rubber particles and matrix are shown in Figure 2.12.

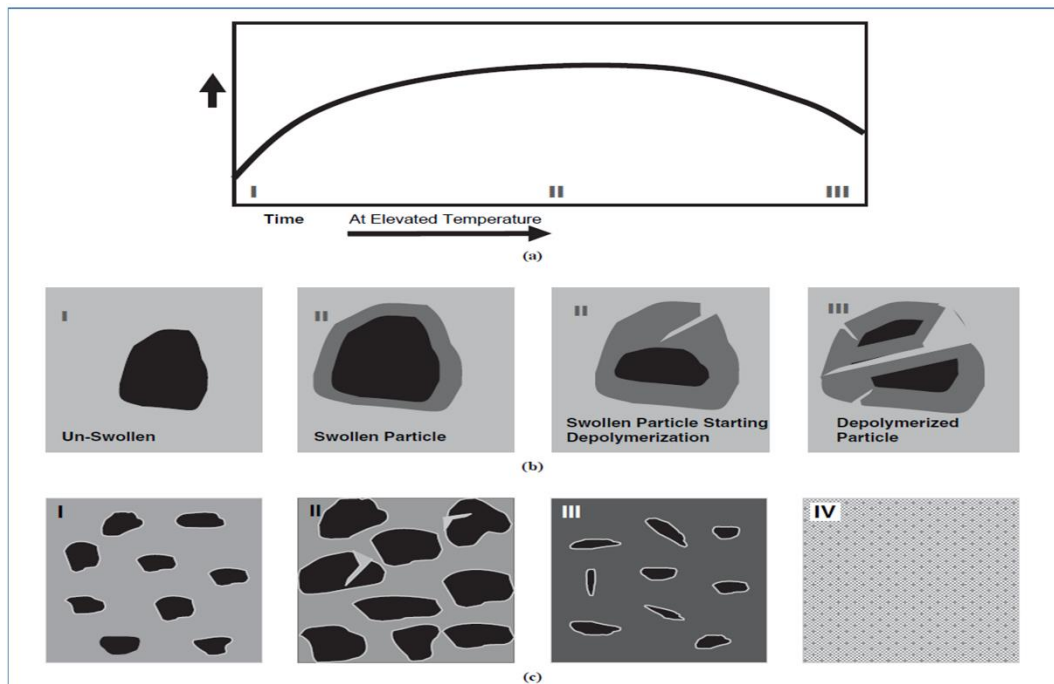


Figure 2.12: Progression of bitumen–rubber interaction at elevated temperature: (a) change in binder viscosity over time, (b) change in particle size over time, and (c) change in binder matrix over time (Abdelrahman 2006)

Therefore, the development of rubberized bitumen properties depends mainly on the nature of the interaction process between rubber and bitumen and the latter depends largely on the curing variables and the type of material.

The Effects of the Processing Conditions

The processing variables (temperature, time and the applied shear stress) have a significant effect on the rubberized bitumen. The swelling rate and swelling extent of crumb rubber are significantly influenced by the interaction of temperature and time. As the temperature increases, the rate of swelling increases but the extent of swelling decreases (Green and Tolonen 1977, Abdelrahman 2006). Elevated temperatures lead to more rapid mass transfer and chemical reaction rates and can reduce the cross-link density of the rubber making the solvent diffuse into the rubber network more readily.

The maximum volume of swelling also increases with increasing temperature because the cross-link density is reduced and the rubber becomes more stretchable. Thus, less force for the solvent molecules is needed to penetrate the polymer network. In addition, if the temperature is maintained at a high level and for sufficient time, the rubber starts being digested into the binder and breaking the cross-linking network by means of devulcanisation and depolymerisation. The rate of dissolution/dispersion of rubber particles into the bitumen is considerably increased by employing a very high temperature $\sim 260^{\circ}\text{C}$. This results in a drastic reduction in the elastic properties of binders due to the faster rates of breaking crosslink bonds (Glover, Davison et al. 2000, Navarro, Partal et al. 2007, Attia and Abdelrahman 2009).

The effect of interaction time varies significantly with the other two processing conditions (temperature and applied shear). As a general trend, the time needed for achieving a desired swelling state and/or digestion state is significantly reduced by increasing the processing temperature and mixing speed. However, if the interaction temperature is not high enough to break up the chemically cross-linked network, the rubber would not dissolve in the binder even if an extremely prolonged time is used.

Many studies have demonstrated that the processing device and impeller geometry have minimal effect on the rheological properties of the rubberised bitumen (Navarro, Partal et al. 2007, Memon 2011, González, Martínez-Boza et al. 2012). However, Attia and Abdelrahman have demonstrated that high shear speed is important to better disperse the rubber particles in the binder matrix in order to improve the storage stability (Attia and Abdelrahman 2009).

Generally, optimisation of curing variables for rubberised bitumen can be divided into two general approaches; the first approach is by adopting relatively low to moderate curing conditions. The resultant product is normally a highly viscous gel-like product due to the maximum swelling volume of the rubber particles. The optimisation process is normally accomplished by monitoring the high-temperature viscosity versus processing time and then identifying the time at which the viscosity reaches its highest value. Although the viscosity is an important property especially for handling the materials, it cannot be solely used to predict the in-service performance of the binder within the bituminous mixture. Moreover, the high viscosity and the heterogeneity of this product are the main drawbacks that in some cases could lead to detrimental effects on the compaction process and storage stability.

The second approach is by adopting a high curing condition to allow a partial digestion of crumb rubber. Making use of more intensive curing conditions leads to a less heterogeneous matrix, lowering the bulk viscosity, especially in the compaction range. The viscosity of binders produced using high-cure conditions is substantially lower than binders produced using the lower cure conditions. Also, the ageing and storage stability properties of binders produced using high-cure conditions are favourably modified (Billiter, Davison et al. 1997). Under high-cure conditions, the rubber releases its polymeric compounds into the base bitumen resulting in higher modification for the liquid phase of binder (the extracted residue) than the bulk matrix (bitumen plus rubber), and this modification is considered more stable than the bulk matrix modifications (Attia and Abdelrahman 2009). Therefore, selecting the optimum curing variables should be based on a careful assessment of the rheological properties, high-temperature viscosity, ageing effect and storage stability.

The processing temperature is the main blending variable that controls swelling rate, swelling extent, and the type and state of the released polymeric components from the rubber particles. All these parameters determine the properties of the resultant rubberised binder. The shearing mixing speed plays an accelerating role in the swelling and dispersion process that helps reducing agglomeration of rubber particles and hence improving the storage stability. The required mixing time to reach the desirable properties depends mainly on curing temperature and applied shearing.

The Effects of the Material Characteristics

The physical and chemical properties of the base binder and crumb rubber have a direct effect on the nature of the interaction process, and thus, on the resultant RTR-MB properties. Base bitumen composition, penetration, source and chemical characteristics have a significant influence on the mechanical properties of the final blend. It has been demonstrated that during the early stages of interaction, soft base bitumen (lower viscosity) diffuses into the rubber at higher penetration rate. However, the total amount of solvent that diffuses into the rubber depends mainly upon the chemical nature of the rubber; the greater the cross-link density the lower the maximum volume of swelling (Rahman 2004).

The interaction between rubber particles and the base binder is usually reported as a physical changing of the material without chemical reaction (Heitzman 1992), and the increase in viscosity is accounted for by particle swelling, the reduction in the inter-particle distance, and the stiffening of the bitumen by reducing the oily fractions. However, other researchers

have raised basic questions as to why the interaction is a function of bitumen type if it is mainly a diffusion phenomenon, suggesting that the increase in viscosity cannot be attributed solely to the physical changes in material (Bahia and Davies 1994). Thus, the effects of adding the rubber have been separated into two main parts; interaction effect (IE) or liquid phase modification and particle effect (PE) (Abdelrahman and Carpenter 1999, Putman and Amirkhani 2006, Ghavibazoo and Abdelrahman 2013). The liquid phase modification refers to the polymeric components of rubber that dissolve into the binder while the particle effect refers to the presence of undissolved rubber and the dispersed carbon black as fillers in the matrix.

It has been validated that bitumen acidity can improve the rheological properties of rubberised bitumen and that it has an effect on the dissolution process (Leite, Constantino et al. 2001). Also, bitumen with higher aromatic content is more compatible with rubber particles and can better devulcanise the rubber during the interaction process while bitumen with higher molecular weight fractions or asphaltenes can better depolymerise the rubber (Billiter, Davison et al. 1997). The effect of bitumen source has been reported by some studies to have minimal to no effect on the interaction process (Hanson and Duncan 1995, Leite, Constantino et al. 2001). Other studies, however, showed that bitumen source plays an important role in the interaction process (Putman and Amirkhani 2006). A general conclusion about bitumen source cannot be made because of other overlapping effects. For example, if the particle rubber is very fine, it could be dissolved and depolymerised very easily into any bitumen regardless of the bitumen source.

The size of rubber particles has a controlling effect on the interaction mechanism and the properties of the final material. Finer rubber particles have an increased specific surface area and hence interact very quickly with the binder (swell faster and depolymerise faster) and modify more effectively the liquid phase than coarser rubber particles do (Leite, Constantino et al. 2001, Abdelrahman 2006). Also, using fine rubber particles can result in reducing the high-temperature viscosity which is preferable for the mixing and compaction process.

The production process of crumb rubber has an effect on the surface texture and the specific surface area of particles. Rubber particles produced by the ambient process have generally rough surface texture and larger specific surface area than rubber particles produced by the cryogenic process. Therefore, ambiently produced rubber particles interact more effectively with the bitumen than cryogenically produced rubber particles. Lee, Akisetty et al. (2008)

have demonstrated that rubberized bitumen produced using ambient rubber particles showed a better resistance to low temperature cracking and they were less susceptible to rutting at high pavement temperatures than those produced using cryogenic rubber particles.

Rubber content is a major factor that defines the degree of modification. Generally, the higher the rubber content, the stiffer the resultant product at a high temperature and the more flexible at low temperature. Thus, both high and low-temperature susceptibility are improved by increasing the rubber content. However, many studies have suggested that rubber content exceeding 25% of binder mass can lead to counterproductive and detrimental effects on the pumpability and compaction process (Celauro, Celauro et al. 2012, Wang, You et al. 2012). In addition, Wang, You et al. (2012) have shown that increasing the rubber content from 20% to 25% has resulted in minor influences on high-temperature viscosity and low-temperature stiffness. This is also in agreement with a study conducted by Celauro, Celauro et al. (2012) which indicated that there were no appreciable rheological improvements when rubber content changed from 21% to 24%. Celauro, Celauro et al. (2012) have also suggested that 21% rubber content should be a fundamental datum, and the base bitumen cannot be modified with more than this limit without adding extender oil.

2.3.3 Storage Stability of RTR-MBs

The phase separation between rubber particles and the base bitumen during the hot storage period is considered one of the main drawbacks of RTR-MBs. The lack of compatibility between rubber and binder leads to phase separation between the two through the settling of rubber particles to the bottom of the transport tanker or the storage tank. This could result in having material at the top of the tanker with inferior mechanical properties and material at the bottom with detrimental high viscosity due to the high percentage of settled rubber particles. Thus, continuous circulation through mechanical agitation must be applied during the transportation to obtain an acceptable level of homogeneity. Nevertheless, this cannot ensure that phase separation is completely overcome and this would also lead to an increase in the overall cost of the RTR-MBs. Therefore, developing RTR-MBs with improved storage stability could result in a significant cost reduction and increase the adoption of rubberized bitumen in the bitumen industry.

Mechanism of Phase Separation

The differences in the physical properties, and more particularly the differences in the specific gravity between the rubber particles and the base bitumen have a direct effect on

phase separation. The mechanism of phase separation is considered as mechanical/hydrodynamic behaviour for non-dissolved crumb rubber suspended in a low viscosity medium rather than as colloidal activity (Navarro, Partal et al. 2004). The sedimentation velocity of these particles determines the degree of storage stability of the product over time. Such a stable system that has a very low settling velocity and hence the phase separation would not be noticeable after prolonged storage time. The sedimentation process of non-dissolved rubber particles under high-temperature storage can be regulated by Stokes' regime as the particles settle at very slow velocity and thus, the Reynolds number is low (Navarro, Partal et al. 2004, Galooyak, Dabir et al. 2010).

$$V = \frac{2(\rho_0 - \rho_1)gr^2}{9\eta} \quad \text{Equation 2.1}$$

Where: V is the falling velocity of particles, ρ_0 and ρ_1 are density of bitumen and rubber particles, respectively; g is gravitational acceleration, r is mean the radius of particles, and finally η is the viscosity of the bitumen.

Under these conditions, the separation rate is mainly governed by the size of rubber particles, the shape of the particles, storage conditions, and the nature of the modification process. Fine rubber particles tend to settle very slowly as the falling velocity is significantly reduced by decreasing the particle radius; therefore, more stable product can be produced by using very fine rubber particles. Also, after the interaction process, the density of swollen polymer particles could be reduced to a degree less than the density of base bitumen, thus floating the rubber particles to the top of the storage container. This phenomenon was reported by some studies (Pérez-Lepe, Martínez-Boza et al. 2007, Ghaly 2008, Galooyak, Dabir et al. 2010). The shape of rubber particles also has an effect on the settlement mechanism; non-spherical particles tend to orientate their main axis in the movement direction; thus, particles with lower projected diameter would settle faster because the falling velocity is inversely proportional to the diameter of the projected area (Navarro, Partal et al. 2004). Moreover, increasing the rubber content could also reduce the sedimentation velocity and hence improve the storage stability of RTR-MBs. This can be explained by the increased bulk viscosity of the system, increased inter-particle interactions and collisions that all significantly hinder the sedimentation velocity (Navarro, Partal et al. 2004, Navarro, Partal et al. 2005).

Techniques Used to Improve the Storage Stability

Phase segregation between rubber particles and base bitumen can be minimised by selecting high cure conditions that result in dissolving most of the rubber into the liquid phase of bitumen (Glover, Davison et al. 2000). However, this can weaken the level of modification such as the temperature susceptibility and elasticity obtained when the rubber particles are not severely devulcanised /depolymerised and still in the swollen state (Lo Presti 2013).

Improving the storage stability and compatibility while maintaining an acceptable level of performance properties has been investigated by many researchers. Zanzotto and Kennepohl (1996) produced rubberized bitumen capable of lasting for two days during hot storage without a significant phase separation. This was achieved by partially depolymerising the vulcanised rubber matrix into lower molecular weight molecules through the use of heat and shear.

Memon (2011) treated the rubber particles by a carbenium ion-generating material such as hydrogen peroxide to create carboxylic sites on the surface of rubber particles in order to enhance the interaction with the functional groups of bitumen and thus enhance the settling properties of RTR-MBs while maintaining improved rheological properties. Memon (1999) activated the surface of rubber particles to improve the storage stability and the rheological properties of RTR-MBs through boiling the rubber in water at temperatures between 85 °C and 90 °C for about five minutes to form a slurry. After the excess oils and chemicals are released from rubber particles to the slurry, the heavier rubber particles are removed and the slurry is then dried. The improvements in storage stability through activating the rubber by hot water were also confirmed by Shatanawi, Biro et al. (2009).

Adding chemical stabilisation substances is also considered to reduce the settlement and keep the rubber particles dispersed in the binder (Memon 2011). Activating the rubber by blending with polymeric compatibilizer to be more compatible with bitumen has also improved the storage stability (Cheng, Shen et al. 2011). Breaking the three-dimensional network of vulcanised rubber by means of using devulcanised rubber, can also result in improving the dispersion and interfacial adhesion of rubber particles and bitumen (Liang 1999, Xiao-qing, Can-hui et al. 2009).

Characterising the Storage Stability

Measuring or evaluating the storage stability of modified bitumen is usually conducted by placing the binder vertically in a tube (common names are Cigar tube and Toothpaste tube),

sealing, and conditioning in the oven at 180°C for 72 hours. The test is described in detail in BS EN 13399:2010. The difference in softening point or needle penetration between the top and bottom of the tube is normally determined as an indication of the degree of phase separation. However, many storage stability indices have been suggested to evaluate the storage stability of RTR-MBs. These parameters are normally based on measuring fundamental rheological characteristics such as G^* , δ and ZSV. Abdelrahman (2006) has suggested the following separation index:

$$SI (\%) = \left[\frac{(G^*/\sin\delta)_{max} - (G^*/\sin\delta)_{avg}}{(G^*/\sin\delta)_{avg}} \right] \times 100 \quad \text{Equation 2.2}$$

Where: SI represents the separation index, G^* = shear modulus (measured in the DSR test), δ = phase angle (measured in the DSR test), $(G^*/\sin\delta)_{max}$ = higher value of either the top or the bottom portion of the tube, and $(G^*/\sin\delta)_{Avg}$ = average value of the two portions.

Also, Navarro, Partal et al. (2004) defined the storage stability index as the ratio between the value of the elastic modulus at 0.1 rad/s and 50°C, at a given distance from the bottom of the settling tube, to the value of the same parameter calculated on a fresh sample (not stored).

Furthermore, Pérez-Lepe, Martínez-Boza et al. (2007) calculated the instability index as follows:

$$I_I = \left[\frac{ZSV_{max} - ZSV_{fresh}}{ZSV_{fresh}} \right] \quad \text{Equation 2.3}$$

Where: I_I is the instability index, ZSV_{fresh} is the zero shear viscosity, at 75 °C for the fresh binder (not stored), and ZSV_{max} is higher value of zero shear viscosity at 75°C of either the top or the bottom portion of the tube. It should be mentioned that ZSV is a reliable parameter to detect the phase segregation as it is very sensitive to the higher molecular weight fraction that could settle down to the bottom of the storage tube.

Finally, the Texas Department of Transportation (TxDOT) specified that modified binder that meets their storage stability requirements should have a difference between the softening points of the top and bottom samples of 4 percent or less, based on the average of the top and bottom softening points as shown below (Glover, Davison et al. 2000):

$$\frac{SP_{bot} - SP_{top}}{(SP_{bot} + SP_{top})/2} < 0.04 \quad \text{Equation 2.4}$$

Where: SP_{bot} and SP_{top} are the ring and ball softening point temperature at the bottom and the top of the tube, respectively.

2.3.4 Artificial Ageing Effect on RTR-MBs

Durable bituminous pavement is expected to provide an acceptable serviceability over a prolonged period of time. The main elements that affect the durability of asphalt pavement are ageing and moisture damage (Airey 2003). The ageing can solidify the binders and make them less ductile. This can reduce the ability of the pavement to accommodate the stresses from low-temperature contraction and expansion, and/or, heavy traffic loads, and that leads to deteriorating performance of the pavement and increases the cost of maintenance for pavements. The ageing also affects the cohesive properties of binders and the adhesion between the binder and aggregate interface. Ageing of asphalt pavement is generally related to hardening of the binder due to volatilization and oxidation of the light components which convert into more chemically polar molecules or asphaltenes. The oxidation and volatilization of light oil occur under elevated temperatures during mixture production in hot mixture plant (short-term ageing), and this oxidation continues after placing the asphalt materials in the pavement (long-term ageing). Additional elements that could contribute to ageing include molecular structuring over time (steric hardening) and actinic light (primarily ultraviolet radiation, particularly in arid conditions) (Airey 2003).

Generally, the laboratory tests used to simulate the hardening development of bitumen in an accelerated way are the rolling thin film oven test (RTFOT) or thin film oven test (TFOT), for short-term ageing; and pressure ageing vessel (PAV), for long-term ageing. The short-term ageing of bitumen happens at a rapid rate (called initial-jump phenomenon) corresponding to the presence of sulfoxide materials and increasing carbonyl content, and that results in viscosity growth and oxidative hardening (Liu, Ferry et al. 1998). The hardening rate (the increase in the viscosity during ageing) after the initial-jump phenomenon is held constant and it is considered a characteristic of material for a given oxidation condition where less hardening growth per unit carbonyl growth is preferred (Liu, Ferry et al. 1998, Ruan, Davison et al. 2003). Hardening susceptibility (HS) is defined as the ratio of viscosity growth to carbonyl growth and it is a constant regardless of the ageing temperature, for unmodified bitumens (Chippis, Davison et al. 2001). However, for binders modified with rubbers, it has been found that the HS varies with ageing temperature due to the presence of rubber particles that absorb more oxygen at higher temperatures than at lower

temperatures (Chipps, Davison et al. 2001). Also, the interaction between the base bitumen and the rubber particles could continue during the artificial ageing. Therefore, the mechanism of ageing for rubberised bitumen is more complex than for neat bitumen. Although, the oxidative ageing of RTR-MBs is not completely understood, the measured physical properties after artificial ageing show improvement in ageing resistance for RTR-MBs in comparison to the neat bitumens (Glover, Davison et al. 2000).

The changes in the rheological properties of RTR-MBs after artificial ageing have been investigated by many research groups (Huang 2008, Ghavibazoo and Abdelrahman 2014, Wang, Wang et al. 2015, Al-Mansob, Ismail et al. 2016). The relative degree of change in the rheological properties of RTR-MBs has been shown to vary depending on ageing conditions, rubber content, rubber particle size and the source of base bitumen. Huang (2008) investigated the effect of long-term oxidative ageing for modified binders manufactured using different rubber content and different bitumen type. The relationship between the shear susceptibility of viscosity (SSV) and the shear susceptibility of phase angle (SSD) was used to evaluate the ageing resistance of the different binders. The results from this research indicated that the addition of a lower rubber percentage (5% by bitumen mass), to a bitumen, has high sulphur and high asphaltene content, resulted in a higher phase angle at the same oxidation viscosity which could translate into better long-term fatigue performance. On the other hand, the addition of higher rubber concentration (20% by bitumen mass) showed improved low-temperature properties (higher m-value and low stiffness) after oxidative ageing in comparison to 10% rubber concentration and 0% rubber concentration (Ghavibazoo and Abdelrahman 2014). The effects of artificial ageing on binders modified by epoxidised natural rubber have been studied by means of dynamic mechanical analysis (Al-Mansob, Ismail et al. 2016). These analyses have shown that the artificial ageing increased the viscous behaviour for the epoxidised natural rubber modified binders compared to the base bitumen behaviour, showing an increase in the elastic components with ageing. The increase in the viscous behaviour, within the polymer dominant areas (high temperatures and low frequencies), after ageing, has been attributed to a dissolution of the rubber network structure and a reduction in the size of rubber particles (Al-Mansob, Ismail et al. 2016). This increase is considered to be beneficial for the long-term durability of flexible pavements. Increasing the rubber dissolution into the liquid phase of bitumen has also been shown to enhance the ageing characteristics of binders by lowering the hardening and carbonyl formation rates (Glover, Davison et al. 2000).

It is postulated that the improvements in the oxidative ageing through the addition of rubber are attributed to the following causes. Firstly, the presence of rubber can decrease the hardening rate of binders by providing some sort of oxidation shielding (Chipps, Davison et al. 2001). Secondly, some of the rubber compounds, such as carbon black, have antioxidant characteristics that can improve the ageing resistance of RTR-MBs when they are released and dispersed into the bitumen during binder production or during artificial ageing (Lo Presti 2013, Wang, Wang et al. 2015). In addition, the absorption of the light fraction and oils by rubber particles protects these fractions from being more susceptible to oxidative ageing (Wang, Wang et al. 2015). Finally, there is some dissolution/dispersion of rubber particles occurring during ageing and that leads to reducing the bulk viscosity of binders, and hence, retards the hardening rate.

2.4 Performance-Based Binder Characterisation

The improvements obtained from developing modified binders should be reflected by fundamental testing parameters. It is essential to characterise the binders based on testing methods and parameters that can reliably measure their contribution to resist external damage within the asphalt mixtures. The mechanical properties of bitumen for low, intermediate to high-temperature conditions, have traditionally been characterised using empirical methods. For example, Fraass breaking point, capillary viscosity, and softening point have been used to identify the low, intermediate and high in-service temperature properties, respectively. However, the empirical nature of those tests has resulted in many cases in failure to establish a good correlation between these conventional, empirical binder properties and asphalt mixture or pavement performance. In addition, these tests do not provide sufficient information about the physical and rheological properties for modified bitumens, especially for rubberised binders, because of their complex response to stress degree and rate which cannot be assessed using these empirical tests. Therefore, using more fundamental engineering properties for characterising the bituminous binders has increasingly been needed to reliably predict pavement performance (Airey and Brown 1998, Chen and Tsai 1999, Airey 2002, Planche, Anderson et al. 2004, Tsai and Monismith 2005, Zhou, Mogawer et al. 2012, Paliukaite, Verigin et al. 2015). The dynamic shear rheometer (DSR) is usually used to characterise fundamentally the viscous and elastic properties of binders at high and intermediate service temperatures. Characterising the fracture properties, by means of essential work of fracture, has also been shown to be a promising approach for characterising the bituminous binders (Andriescu, Hesp et al. 2004).

A detailed description of the main elements associated with the DSR is presented in the next section. Also, the most common and fundamental test methods for characterising the fatigue and rutting properties of binders, are introduced in the subsequent sections.

2.4.1 Dynamic Shear Rheometer (DSR)

The dynamic shear rheometer is used to measure the viscoelastic response (stiffness, viscosity, phase angle) of materials when subjected to a given load state (degree and rate), and a given temperature. The load can be applied in a sinusoidal (oscillatory) mode, or in a creep and recovery mode. The sinusoidal load is normally applied under strain-controlled loading in which a small strain within the linear viscoelastic range is used and the resulting stress is measured. On the other hand, in the creep and recovery mode, a stress-controlled load is normally applied and the resulting strain is measured. The principal measurements taken by the DSR are the torque (T) and angular rotation (θ). The other mechanical properties are computed based on these measurements. Figure 2.13 shows schematically the main configuration of DSR testing. It can be seen that a sinusoidal load or creep load is applied to a sample of bitumen sandwiched between two parallel disks, and the amplitude of the transmitted torque and angular rotation of the sample, are measured.

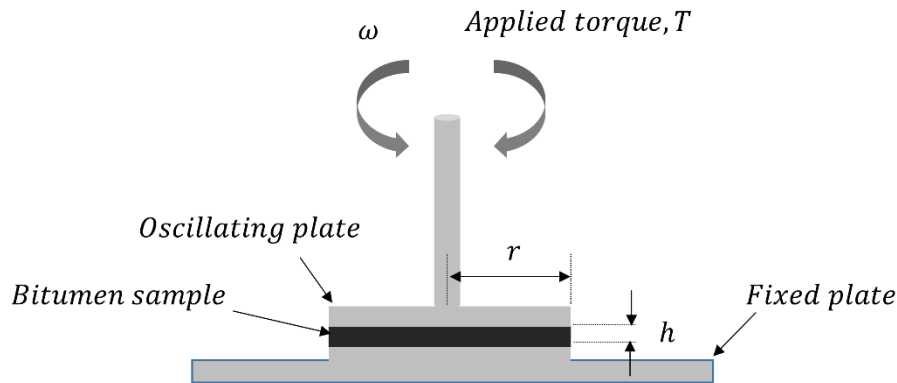


Figure 2.13: The DSR testing configuration

The stress and strain are calculated based on the measured torque and angular rotation as follows:

$$\sigma = \frac{2T}{\pi r^3}$$

Equation 2.5

Where:

σ = maximum shear stress (N/ mm²)

T = torque (N.m)

r = radius of the parallel disks (mm)

$$\gamma = \frac{\theta r}{h}$$

Equation 2.6

Where:

γ = shear strain

θ = deflection angle (radians)

h = gap between parallel discs (mm)

The absolute complex modulus, G^* , can be calculated from the following formula:

$$G^* = \frac{\sigma_{max}}{\gamma_{max}}$$

Equation 2.7

It can be seen, from equations 2.5 and 2.6, that the magnitudes of the shear stress and strain are strongly dependent on the geometric properties of the oscillating plate, i.e. radius of the parallel plates and gap between the upper and the lower parallel plates. Therefore, various parallel plate sizes are used in the DSR testing depending on the expected stiffness of materials, to comply with the compliance of the device. Generally, the size of the plate that should be selected to test the sample decreases as the expected stiffness of the sample increases. Plates with smaller radius are normally used at lower testing temperatures while larger radius is used at higher testing temperatures to reliably measure the viscoelastic properties of the bitumen. A number of different parallel plate geometries are used in DSR testing to measure a wide range of bitumen stiffness. However, the following different plate sizes are suggested by SHRP-A-369 (Anderson, Christensen et al. 1994).

- Use 8-mm parallel plates with a 2-mm gap, for temperature range 0°C to 40°C, when $0.1 \text{ MPa} < G^* < 30 \text{ MPa}$
- Use 25-mm parallel plates with a 1-mm gap, for temperature range 40°C to 80°C, when $1.0 \text{ kPa} < G^* < 100 \text{ kPa}$.
- Use 40-mm parallel plates, for temperatures $> 80^\circ\text{C}$, when $G^* < 1 \text{ kPa}$

It should be mentioned that using 1 mm gap for some modified binders that contain undissolved particles, such as rubberised binders, could give unreliable measurements because of the large volume of these particles. Thus, a larger gap size can be used when testing those binders (Subhy, Lo Presti et al. 2015). As a rough practical rule, the gap setting should be set at least 3 times higher than the maximum dimension of any particle in the matrix (Lo Presti 2011).

Dynamic Mechanical Analysis (DMA)

The rheological properties of unmodified bitumen vary with the applied load rate and temperature, at temperatures below 60°C, and vary with a temperature above 60°C, as

illustrated in Figure 2.14 (Airey 1997). In addition, the rheological properties of rubberised binders are even more complicated where their mechanical properties vary with both temperature and shear rate at a temperature above 60°C. Therefore, the materials need to be characterised over a wide range of temperatures and loading times in order to predict their performance. In terms of DMA, a sinusoidal strain or stress controlled load, within the linear viscoelastic range, is applied to a sample of bitumen, in the DSR, sandwiched between two parallel discs with a loading frequency, ω ($\frac{rad}{ses}$).

The sinusoidally varying strain can be represented as in Equation 2.8 (Airey 1997).

$$\gamma_t = \gamma_o \sin \omega t \quad \text{Equation 2.8}$$

Where:

γ_t = dynamic oscillating shear strain

γ_o = peak shear strain

ω = angular frequency (rad/sec)= $2 \pi f$, where f is the frequency Hz

t = the time (seconds)

The stress response is also sinusoidal but is out of phase by, δ , as represented in equation 2.9.

$$\sigma_t = \sigma_o \sin(\omega t - \delta) \quad \text{Equation 2.9}$$

Where:

σ_t = dynamic oscillating shear stress, Pa

σ_o = peak stress, Pa

δ = phase angle, degrees

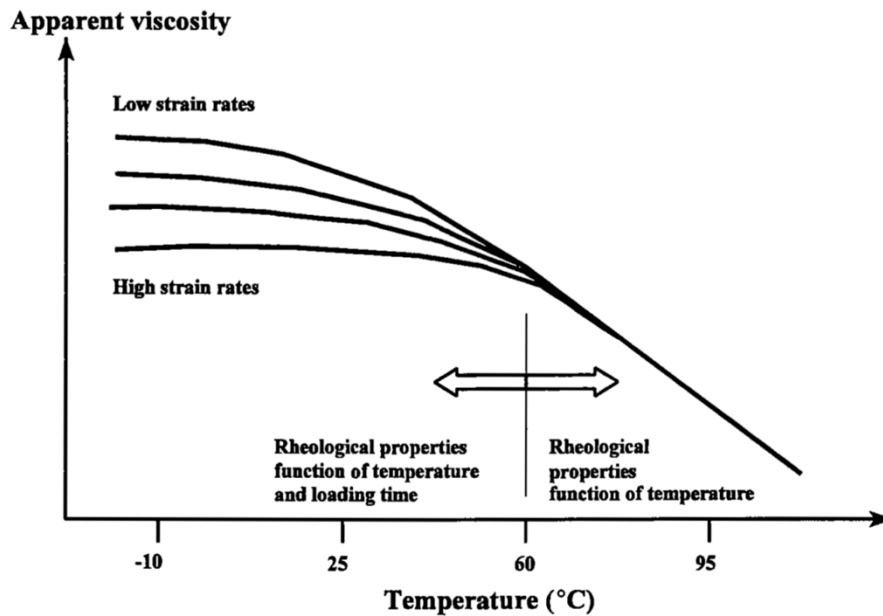


Figure 2.14: Rheological behaviour of bitumen (Airey 1997)

The phase angle, δ , is the phase or lag difference between the sinusoidal stress and strain, and it gives an indication of the viscoelasticity state of materials. For example, materials with 0° phase angle, are considered to be purely elastic materials, where both the strain and stress waveforms are in the same phase, as can be seen in Figure 2.15 (a); the deformation in this case is fully and immediately recovered after releasing the load if the load is below the yielding limit. On the other hand, materials with 90° phase angle, are considered to be purely viscous materials, as can be seen in Figure 2.15 (c), and these materials approach ideal liquid behaviour. For phase angles between 0° and 90° , the materials are considered to be viscoelastic and are characterised by two components namely, storage component and loss component, as can be seen in Figure 2.15 (b). In this case, the material's response to the applied strain becomes highly dependent on loading time and temperature with a large amount of delayed elasticity (Airey 1997).

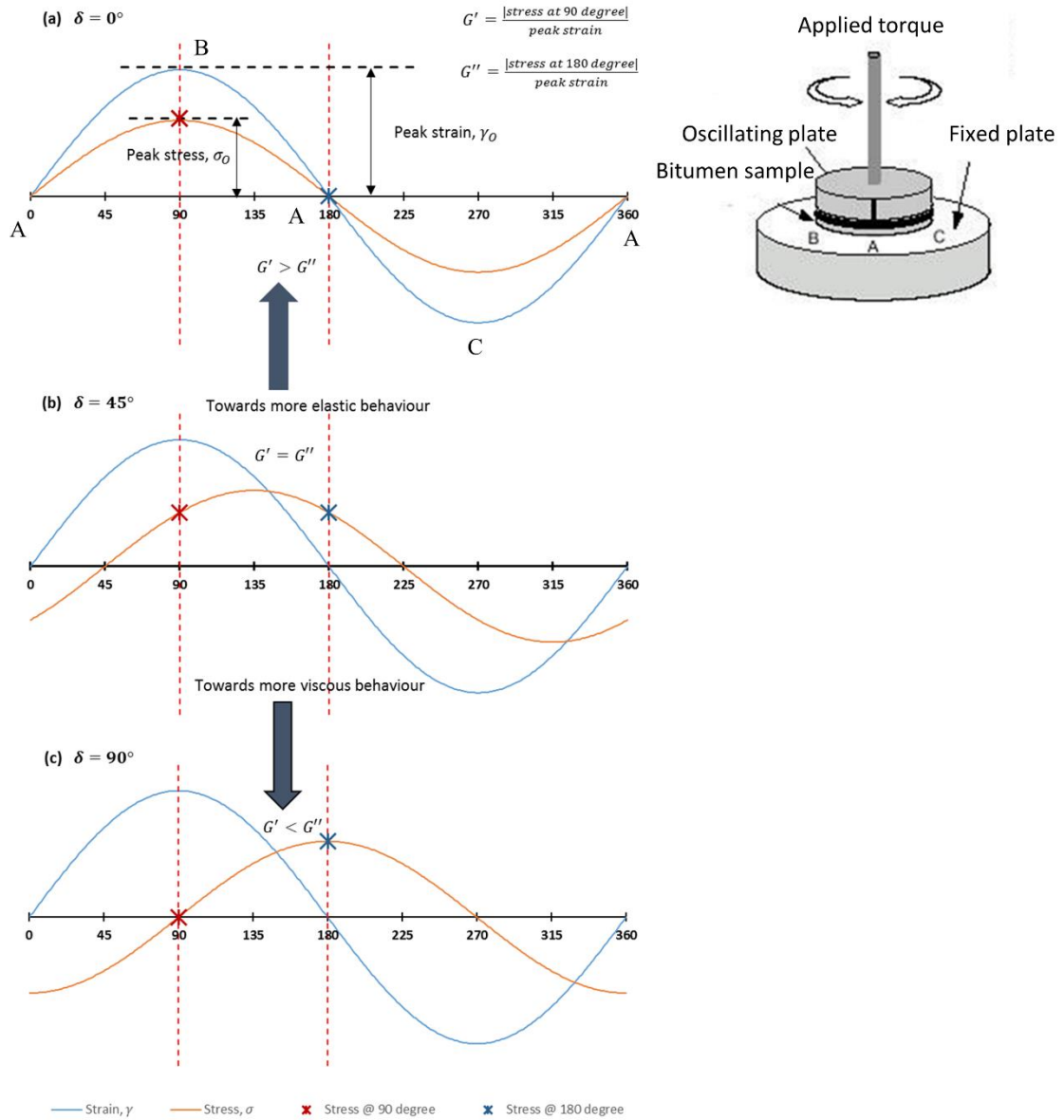


Figure 2.15: Dynamic mechanical analysis representation

The resulting dynamic test outputs, for the stress and strain sinusoidal waveforms, are shown in Figure 2.15 for the different viscoelastic states. The ratio of the resulting stress to the applied strain at any time is called the complex shear modulus, G^* , defined by:

$$G_t = \frac{\sigma_t}{\gamma_t} = \left(\frac{\sigma_0}{\gamma_0} \right) \cos \delta + i \left(\frac{\sigma_0}{\gamma_0} \right) \sin \delta \quad \text{Equation 2.10}$$

The term $\left(\frac{\sigma_0}{\gamma_0} \right)$ (the ratio of the peak stress to the peak strain) is called the norm of the complex modulus, $|G^*|$, Pa.

Equation 2.10 can also be written as:

$$\mathbf{G}_t = \mathbf{G}' + i \mathbf{G}'' \quad \text{Equation 2.11}$$

Where:

G' = the storage modulus, and G'' is the loss modulus

The storage modulus equals the stress that is in phase with the strain divided by the strain, as described in the following equation:

$$\mathbf{G}' = |\mathbf{G}^*| \cos \delta \quad \text{Equation 2.12}$$

The storage modulus reflects the amount of energy that is stored and released elastically, including immediate and delayed elasticity, in each oscillation and is therefore also called the elastic component of the complex modulus (Airey 1997).

The (shear) loss modulus is the out-of-phase component or the imaginary part of the complex modulus. The loss modulus equals the stress 90° out of phase with the strain divided by the strain, as described in the following equation:

$$\mathbf{G}'' = |\mathbf{G}^*| \sin \delta \quad \text{Equation 2.13}$$

The loss modulus is also referred to as the viscous modulus or the viscous component of the complex modulus (Airey 1997).

The magnitude of the norm of the complex modulus, $|\mathbf{G}^*|$ can be calculated as the square root of the sum of the squares of the storage modulus and loss modulus as follows:

$$|\mathbf{G}^*| = \sqrt{(\mathbf{G}')^2 + (\mathbf{G}'')^2} \quad \text{Equation 2.14}$$

The ratio of the viscous component of the complex modulus to the elastic component of the complex modulus is known as the tangent of the phase angle and also as the loss tangent:

$$\tan \delta = \frac{\mathbf{G}''}{\mathbf{G}'}, \text{ thus } \delta = \tan^{-1} \frac{\mathbf{G}''}{\mathbf{G}'} \quad \text{Equation 2.15}$$

At low temperatures and high loading frequencies, the phase angle, δ , approaches 0°, the bituminous materials tend to behave like solid materials, and the storage modulus dominates over the loss modulus, as can be seen in Figure 2.15 (a). On the other hand, at high temperatures and low loading frequencies, the phase angle, δ , approaches 90°, the bituminous materials tend to behave like liquids, and the loss modulus dominates over the storage modulus, as can be seen in Figure 2.15 (c).

The dynamic viscoelastic response of the materials described above must be within the linear range during the DSR testing so that the stiffness of materials is not influenced by the magnitude of the applied strain or load, but is only influenced by temperature and loading time. The linear viscoelastic region is identified using strain sweep tests as the point where the complex modulus decreases to 95% of its maximum value, as seen Figure 2.16, according to SHRP. This region varies with the measured stiffness of binders, the strain limit increases with a decrease in stiffness of the materials. Therefore, small strain boundaries must be used at low temperatures and increased at high temperatures. According to the SHRP research, the linear viscoelastic stress and strain limits, for neat bitumens, has been found to be a function of complex modulus according to the following notations:

$$\gamma = \frac{12.0}{(G^*)^{0.29}} \quad \text{Equation 2.16}$$

$$\sigma = 0.12 (G^*)^{0.71} \quad \text{Equation 2.17}$$

Where γ is the shear strain, σ the shear stress, Pa, and G^* is the complex shear modulus, Pa. Figure 2.17 shows the linearity strain limits plotted as a function of complex modulus, determined according to the 95% SHRP definition, for different neat and polymer modified bitumens tested at different temperatures and loading frequencies (Airey and Rahimzadeh 2004). It can be seen from this figure that using a 1 percent strain level is assured to be within the LVE limits at a wide range of temperatures and loading frequencies.

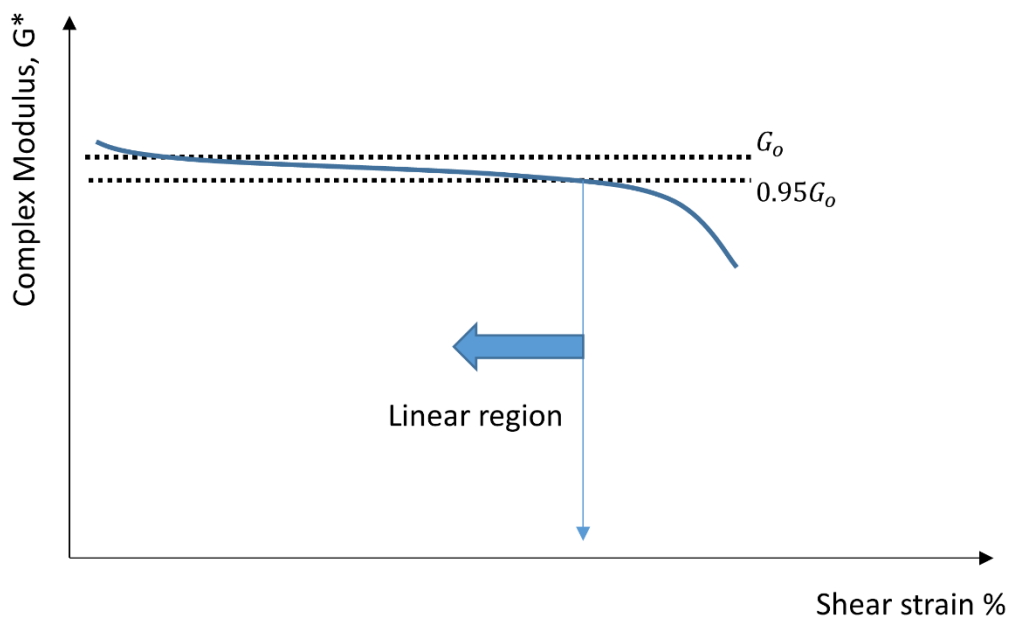


Figure 2.16: Strain sweep to determine linear region

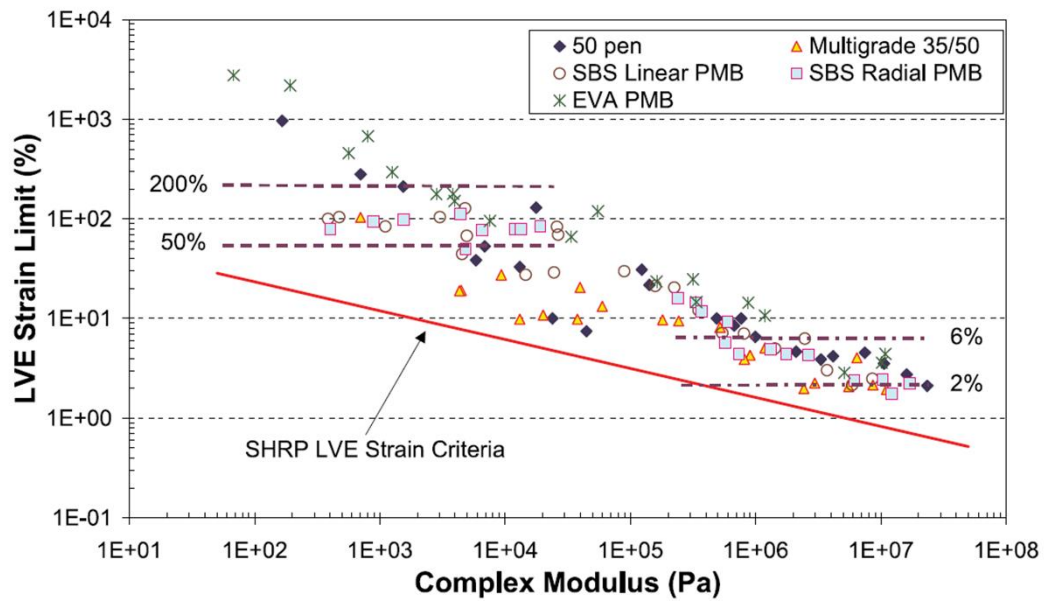


Figure 2.17: Linear viscoelastic strain limits as a function of complex modulus (Airey and Rahimzadeh 2004)

Time-Temperature Superposition Principle (TTSP)

The TTSP is mainly used to represent the rheological properties of bituminous materials over a wide range of frequencies that exceed the compliance limit of the DSR. Studies conducted investigating the viscoelastic properties of binders have found that there is an interrelationship between temperature and loading time. The viscous response of bitumen is strongly dependent on temperature, while negligible effect for temperature is associated with the elastic behaviour; therefore, the influence of temperature and frequency can be separated using the time-temperature superposition principle (Airey 1997). The viscoelastic behaviour of binders at a given temperature over a defined range of loading times can be equivalent to the behaviour tested at different temperatures, through multiplying the loading times by a shift factor. Therefore, the viscoelastic measurements, i.e. complex modulus, G^* , and phase angle δ , tested at different temperatures, can be shifted to a reference temperature to produce a continuous curve at a reduced frequency or time scale, known as a master curve. This principle is also known as the time-temperature superposition principle or the method of reduced variables (Anderson, Christensen et al. 1991, Airey 1997). Binders where their viscoelastic response over a range of temperatures and frequencies can be reduced to a smooth master curve, are termed thermo-rheologically simple (Airey 1997). An example of the concept of applying the time-temperature superposition principle on a thermo-rheologically simple material, is shown graphically in Figure 2.18.

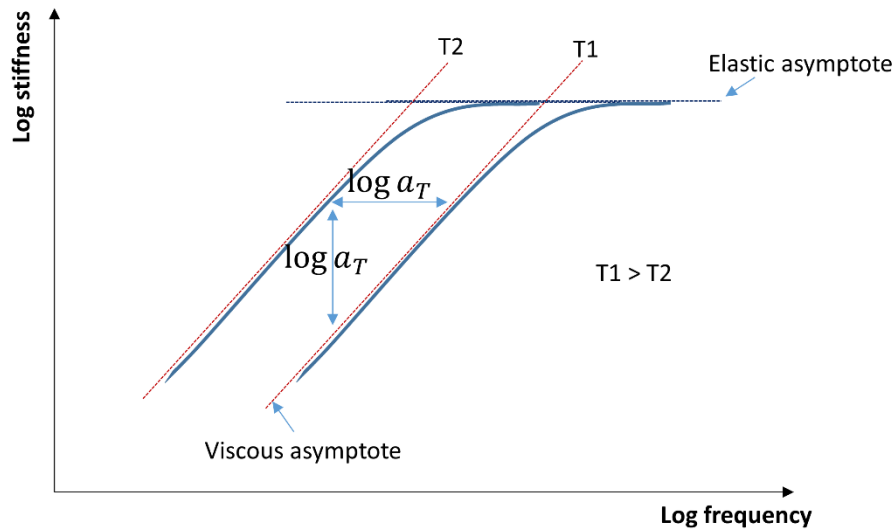


Figure 2.18: Time-temperature superposition principle (Airey 1997)

Stiffness modulus of bitumen can approach a horizontal asymptote at low temperatures and at very high frequencies, as can be seen in Figure 2.18. The elastic modulus of this asymptote is called the glassy modulus, G_g , and it is approximately independent of temperature and loading time. On the other hand, the stiffness modulus at high temperatures and low frequencies approaches viscous flow asymptotes with a unit slope, and these are separated depending on temperature. The binder is considered as thermo-rheologically simple when a change in temperature causes the modulus curve to shift together with its asymptotes over the same distance $\log a_T$ (Airey 1997). Thermo-rheologically simple behaviour is found in almost all unmodified bitumens; however, some types of modification and a high wax content bitumens can alter significantly the behaviour of binders and make their viscoelastic behaviour more complex.

A master curve is constructed for a selected reference temperature by shifting other curves horizontally without changing the shape to coincide with the reference curve and forming a single curve. Figure 2.19 describes manually the shifting process in order to combine the curves into a smooth and continuous master curve. The horizontal shift factor, a_T , determined at each temperature is plotted versus temperature in conjunction with a master curve construction, as can be seen in Figure 2.20. This curve provides a quick evaluation of the effect of temperature on viscoelastic properties of material. The Williams, Landel and Ferry equation, or WLF equation, has been widely used to describe the relationship between a_T and temperature.

The WLF is:

$$\log a_T = -\frac{c_1(T-T_r)}{c_2+(T-T_r)} \quad \text{Equation 2.18}$$

Where:

a_T = shift factor at temperature T, T is temperature, T_r is the reference temperature, C_1 and C_2 are taken as constants.

The WLF equation requires three constants to be determined namely C_1 , C_2 and T_r . The constants C_1 and C_2 can be calculated from the slope and intercept of the linear formula of the WLF equation (Airey 1997):

$$-\frac{(T-T_r)}{\log a_T} = \frac{c_2}{c_1} + \frac{1}{c_1} (T - T_r) \quad \text{Equation 2.19}$$

The constant coefficients C_1 and C_2 with the shift factors for each temperature can be solved simultaneously using a non-linear least squares fitting with the aid of the Solver function in a MS Excel Spreadsheet.

The extended frequency scale used in a master curve is referred to as the reduced frequency scale and defined as:

$$f_r = f \cdot a_T \quad \text{Equation 2.20}$$

Where:

f_r = reduced frequency, Hz

f = original loading frequency, Hz

a_T = shift factor

The viscoelastic measurements such as complex modulus, G^* , the storage modulus, G' , the loss modulus, G'' and phase angle, δ , can all be shifted to obtain a master curve using the time-temperature superposition principle as (Airey 1997):

$$V(f, T) = V(f \cdot a_T, T_r) \quad \text{Equation 2.21}$$

Where:

V = viscoelastic measurements, i.e. G^* , G' , G'' or δ

f = original loading frequency, Hz

T = Temperature, °C

a_T = shift factor

T_r = reference temperature, °C

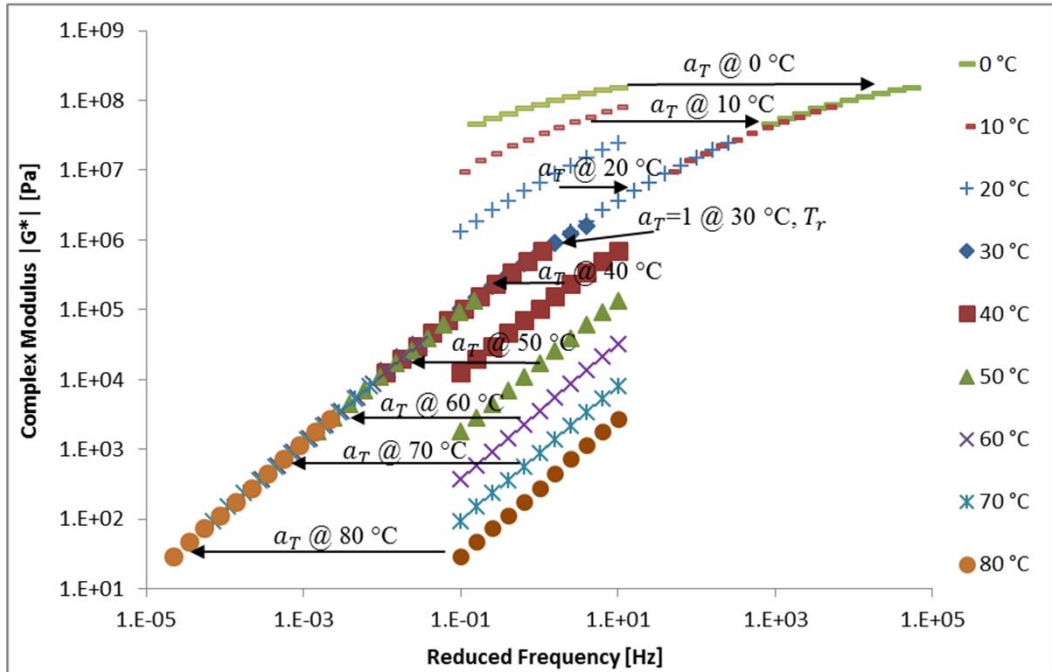


Figure 2.19: Construction of the master curve for $|G^*|$

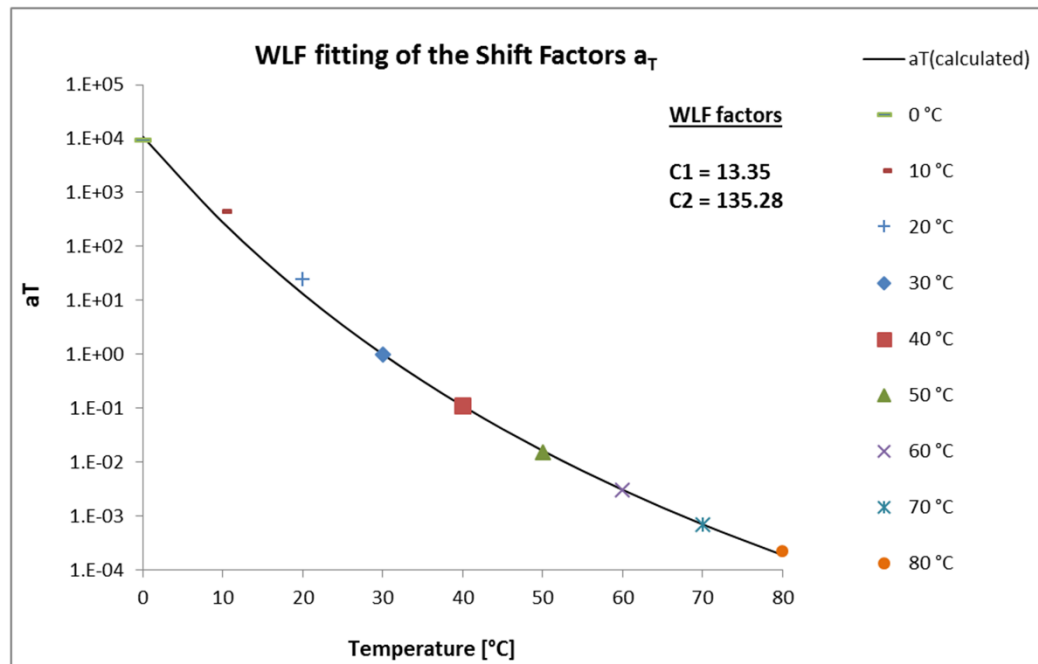


Figure 2.20: a_T versus temperature plot

2.4.2 Binder Fatigue Testing

Bitumen is a viscoelastic, thermoplastic, complex material that behaves differently with temperature and loading time. It is purely viscous at high temperatures and/or under slow moving loads; at those conditions, the materials become prone to permanent deformation (rutting). It is also totally elastic and eventually brittle at low temperatures and/or high rapid loads and subsequently the materials become apron to the low-temperature cracking. However, within 10 to 35 °C in-service pavement temperatures, where the pavement is subjected to a considerable part of its repetitive traffic loads, within those temperatures, the main mode of distress is fatigue cracking. The asphalt pavement is comparatively harder and more elastic at these temperatures and the excessive repetitive stress loads are dissipated through crack initiation and eventually propagation.

It is well recognised that fatigue resistance of hot-mix asphalt (HMA) mixtures is significantly related to the properties of their bituminous binders. Fatigue cracking usually starts and propagates within the binder or the mastic. Therefore, characterising the fatigue resistance of binders and improving this property by means of modification have been a topic of intensive studies for many years. The SHRP fatigue parameter ($G^* \sin \delta$) is widely used to characterise and control the fatigue property of binders within intermediate temperatures. Smaller ($G^* \sin \delta$) is desirable as the dissipated energy per loading cycle is reduced. Lower modulus G^* can better dissipate the work energy without developing large stresses, while

lower δ (more elastic) helps the binders to regain their original shape with minimum dissipated energy.

However, many studies have suggested that the current SHRP fatigue parameter does not necessarily reflect the true binder contribution related to mixture or pavement performance (Chen and Tsai 1999, Bahia, Hanson et al. 2001, Planche, Anderson et al. 2004, Tsai, Monismith et al. 2005, Johnson, Bahia et al. 2007, Zhou, Mogawer et al. 2012). The reasons behind the poor binder-mixture correlation for the SHRP fatigue parameter are mainly attributed to (1) the fact that measuring G^* and δ under relatively small strain within the linear viscoelastic region does not represent the actual variety of strains or stresses that place in binder films of pavements; (2) the resistance properties under damaging conditions are not considered; (3) the theoretical derivation behind the SHRP parameter is not clearly understood (Chen and Tsai 1999, Johnson and Bahia 2010).

Consequently, many different approaches have been investigated to develop a more fundamental and related performance-based characterisation (Planche, Anderson et al. 2004, Shen, Airey et al. 2006, Zhou, Mogawer et al. 2012). Time sweep repeated cyclic loading (TSRCL) tests using the DSR have been successfully used to evaluate the fatigue properties of binders (Anderson, Hir et al. 2001, Bahia, Hanson et al. 2001, Planche, Anderson et al. 2004). Applying the dissipated energy approach to analysing the fatigue data of TSRCL tests has been shown to provide more fundamental material properties and an intrinsic fatigue law (Bahia, Hanson et al. 2001, Shen and Carpenter 2005, Shen, Airey et al. 2006).

Moreover, another accelerated fatigue test named the linear amplitude sweep (LAS) test has been recently proposed by (Johnson and Bahia 2010, Hintz, Velasquez et al. 2011). The method was developed based on using viscoelastic continuum damage (VECD) and fundamentally linked to the TSRCL test (Johnson and Bahia 2010). The test is clearly performance related and can be conducted in short period of time; however, the fatigue life equation is derived after several complex mathematical formulations and statistical fitting. Additionally, the conceptual assumption of evaluating the material integrity under accumulated damage, which is based on the reduction in $G^* \sin \delta$, can be negated by a non-linear decrease.

Fatigue behaviour of binders has also been evaluated based on the delayed elastic response of binders tested empirically using a ductility test machine or fundamentally by the multiple stress creep recovery (MSCR) test using the DSR (Zhou, Mogawer et al. 2012).

It is believed that the main drawback of the SHRP fatigue parameter is because it neglects the damaging circumstances that would take place in the pavement during the fracture process (Andriescu, Hesp et al. 2004, Paliukaite, Verigin et al. 2015). These damaging conditions are normally accompanied by high strain levels and yielding in binder films in the nonlinear viscoelastic range. Thus, the resistance properties of materials under these circumstances should be considered in order to develop fundamental and more performance-based characterisations. In response to that, researchers at Queen's University proposed the double-edged notched tension (DENT) test which is based on the concept of essential work of fracture (EWF) of materials in a ductile state (Andriescu, Hesp et al. 2004). The binder ranking based on this method showed a strong correlation with observed fatigue cracking in the accelerated loading facility (ALF) and exactly the same ranking as the push-pull asphalt mix fatigue test (Gibson, Qi et al. 2010, Zhou, Mogawer et al. 2012).

More details about the dissipated energy approach and the concept of essential work of fracture (EWF) are presented in the next sections.

Dissipated energy approach

Several research studies have supported the use of the dissipated energy approach for fatigue damage analysis. This approach enables an independent fatigue law to be derived regardless of loading mode, frequency, rest periods and temperature (Van Dijk and Visser 1977, Ghuzlan and Carpenter 2000, Shen, Airey et al. 2006). When viscoelastic materials are subjected to cyclic loading, they generate different paths for the loading and unloading cycles leading to hysteresis loops. The dissipated energy per cycle is computed as the area within the hysteresis loop and calculated by the following equation:

$$w_i = \pi \sigma_i \varepsilon_i \sin \delta_i \quad \text{Equation 2.22}$$

Where w_i = the dissipated energy at cycle i ; σ_i , ε_i , δ_i = the stress amplitude, strain amplitude and phase angle at cycle i , respectively. It can be seen that this approach contains the main viscoelastic parameters (stress, strain and phase angle) and thus monitoring the variation in these parameters during the fatigue evolution allows an intrinsic fatigue law to be derived. The early studies of applying the dissipated energy approach to characterise fatigue cracking in asphalt mixtures were introduced by Van Dijk and his colleagues (Van Dijk, Moreaud et al. 1972, Van Dijk 1975, Van Dijk and Visser 1977). They showed that the relation between accumulated dissipated energy (W_{fat}) at failure and number of cycles N_f to failure depends solely on material properties and it is constant irrespective of the mode of

loading, frequency and temperature. The accumulated dissipated energy after n cycles can be calculated as:

$$W_n = \sum_{i=0}^n w_i \quad \text{Equation 2.23}$$

The relationship between cumulative dissipated energy and the number of load cycles to failure was found to be a power law relation as follows:

$$W_{fat} = A \cdot N_{fat}^z \quad \text{Equation 2.24}$$

Where W_{fat} = total dissipated energy until failure due to fatigue cracking, N_{fat} = number of loading cycles to fatigue; and A and z = material constants. The main concern with this approach is that the sum of dissipated energy computed using Eq.1 includes energies that are not responsible for fatigue damage such as recoverable viscoelastic energy and heat energy. Therefore, Ghuzlan and Carpenter (2000) proposed the use of the Dissipated Energy Ratio (DER) to study the fatigue behaviour. The DER or the Ratio of Dissipated Energy Change (RDEC) approach was then developed by Carpenter and Shen (2006) who emphasised the fact that damage will only be generated when there is a difference in dissipated energy between consecutive cycles. RDEC is expressed as:

$$\text{For controlled stress mode: } RDEC_i = \frac{(w_i - w_j)}{w_i \cdot (i - j)} \quad \text{Equation 2.25}$$

$$\text{For controlled strain mode: } RDEC_i = \frac{(w_j - w_i)}{w_i \cdot (i - j)} \quad \text{Equation 2.26}$$

Where $RDEC_i$ = ratio of dissipated energy change value at cycle i ; w_i and w_j = dissipated energies at cycles i and j ; and i, j = loading cycle, $i > j$. The subtraction, in the numerator of Eq. 2.25 and Eq. 2.26, between consecutive cycles is believed to eliminate energies like viscoelastic damping, plastic deformation energy and thermal energies that are not causing damage while keeping the relative amount of incremental damage coming from each additional load cycle (Shen, Airey et al. 2006, Bhasin, Castelo Branco et al. 2009, Shen, Chiu et al. 2010). As previously depicted by Ghuzlan and Carpenter (2000) and Shen, Chiu et al. (2010), three distinct phases can be identified when the RDEC is plotted versus the number of cycles, as shown in Figure 2.21.

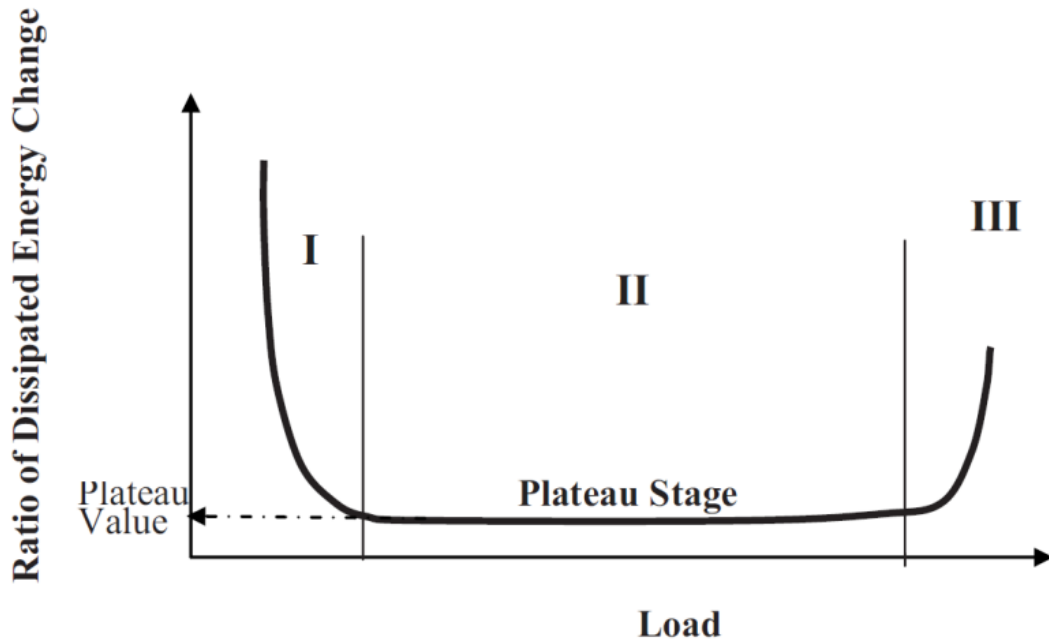


Figure 2.21: Typical RDEC plot versus load cycles (Shen, Chiu et al. 2010)

Phase I is defined by a rapid decrease of the RDEC. The decrease is considered to be not only caused by fatigue damage but includes molecular reorientation and other reversible phenomena such as thixotropy. Phase II reflects the internal damage characteristic of materials and is defined by a plateau of steady-state micro-crack development. The change in the dissipated energy is almost constant with a relatively constant percentage of input energy being transformed into damage. Phase III is defined by a rapid increase in RDEC and thus indicates a sign of fatigue failure. Carpenter and Shen (2006) proposed that the RDEC value at Phase II or the plateau value (PV) is insensitive to the mode of loading. Several studies showed that PV can provide a unique relationship with the number of loading cycles to failure for different mixtures, loading modes and loading levels (Shen and Carpenter 2005, Carpenter and Shen 2006, Shen, Airey et al. 2006, Shen, Chiu et al. 2010).

The relationship between PV and the number of load cycles to failure was found to be a power law relation as follows (Ghuzlan and Carpenter 2000):

$$PV = C \cdot N_{fat}^d \quad \text{Equation 2.27}$$

Where c and d = regression constants; and N_{fat} = number of load cycles to failure.

Definition of fatigue failure

Under repeated cyclic loading, the fatigue life should correspond to the transition point between crack initiation and crack propagation. Several approaches have been adopted to correctly identify the fatigue failure point (Bonnetti, Nam et al. 2002, Lundstrom, Di Benedetto et al. 2004, Tapsoba, Sauzéat et al. 2012). The classical approach of a 50% decrease in the initial stiffness is the most commonly used approach to identify fatigue failure in bituminous materials. However, many studies have shown that this criterion may not always be appropriate for analysing fatigue properties (Bahia, Hanson et al. 2001, Lundstrom, Di Benedetto et al. 2004, Tapsoba, Sauzéat et al. 2012). In addition, the different stress/strain loading modes do not always produce a unique intrinsic fatigue law if this arbitrary definition is applied. Therefore, it is important to find other approaches that are not arbitrary but can define fatigue failure based on a more fundamental analysis. The Dissipated Energy Ratio (DER) concept proposed by Pronk and Hopman (1991) was shown to provide a reasonable criterion for defining the fatigue failure of bituminous mixtures.

$$DER = \frac{\sum_{l=1}^n W_l}{W_n} \quad \text{Equation 2.28}$$

Where, W_l = dissipated energy per cycle, W_n = dissipated energy at cycle n. The plotting of the relationship between DER and number of cycles in the stress-controlled mode provides a distinctive way to evaluate the stage of fatigue damage at which the material undergoes a transition from crack initiation to crack propagation. Figure 2.22 shows the evolution between DER and loading cycles, where during the first portion there is negligible damage of the materials and $DER = n$, i.e. the dissipated energy is almost equal for consecutive cycles. As the relative difference in dissipated energy between consecutive cycles becomes significant, DER starts deviating from the equality line which is interpreted as crack initiation. The fatigue failure N_f point in Figure 2.22a is defined by the sudden change in DER which can be related to the point of transition from crack initiation to crack propagation. This change is considered to be highly material specific and independent of the mode of loading (Bahia, Hanson et al. 2001, Bonnetti, Nam et al. 2002). Under strain controlled testing the N_f is defined by the intersection of two tangents as shown in Figure 2.22b.

Another fatigue failure criterion was evaluated from the evolution of phase angle versus complex modulus (Black diagram), see Figure 2.22c. Di Benedetto et al. (2004) demonstrated that using the Black diagram during fatigue evolution is a promising approach

to defining the stages of fatigue development. The change in the process evolution of the Black diagram in Figure 2.22 gives a definitive limit between crack initiation and crack propagation. The N_f value can be defined from the value of the phase angle at the intersection of two straight lines. These lines are used to linearize the evolution of phase angle for each period; N_f corresponding to the defined phase angle is then determined.

In terms of continuum damage mechanics, fatigue damage commences with homogeneous global damage which is distributed in the body of the material. The microstructural state of the material during this stage is reflected by a steady change in the stress-strain relationships (stiffness modulus, phase angle, dissipated energy...etc.). On the other hand, a rapid change in the mechanical properties of materials happens corresponding to the occurrence of coalescence and unstable propagation of cracking by means of molecular rupture and molecular scission leading to structural failure. Thus, unlike the phenomenological approach of 50% decrease in the initial stiffness, the DER and the Black diagram can be considered a mechanistic-based approach as they account for the evolution of damage mechanics based on monitoring the main viscoelastic measurements (G^* and phase angle) throughout the fatigue process.

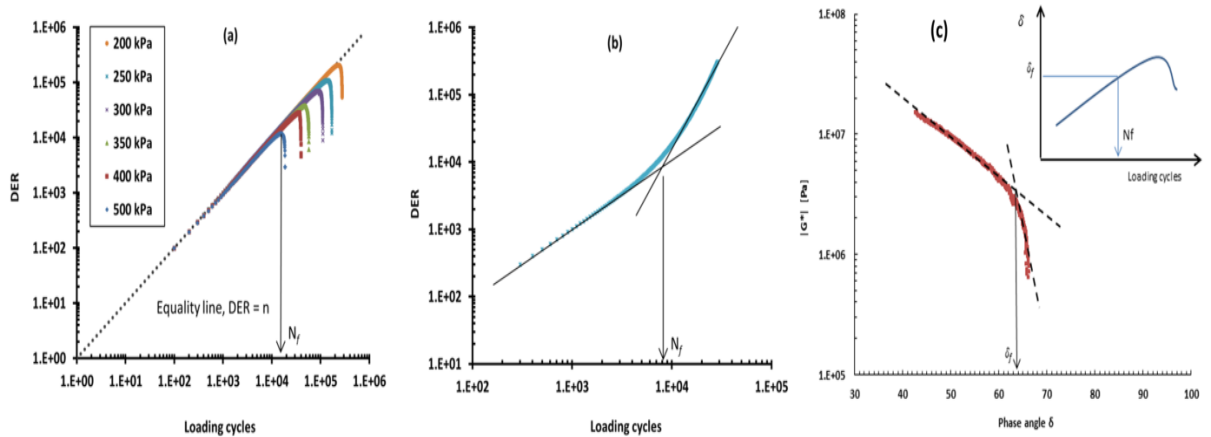


Figure 2.22: Identifying N_f (a) from the DER vs. number of load cycles under controlled stress loading conditions, (b) from the DER vs. number of load cycles under controlled strain loading conditions and (c) from the evolution of phase angle versus complex modulus (Black diagram)

Essential work of fracture (EWF) method

The EWF concept has been increasingly used to determine the fracture toughness in polymers. Yet, there are only a few studies that have used this test on bituminous materials. Andriescu, Hesp et al. (2004) successfully applied this test on bituminous binders. They

found that no correlation exists between fracture properties and the SHRP fatigue parameter. That means binders with desirable fatigue properties, according to $(G^* \sin \delta)$, do not necessarily have good fracture properties and vice versa. Therefore, it is important to characterise the fracture behaviour of materials for a proper material selection.

According to the EWF test when a notched ductile specimen (binder or bituminous mixture) is being loaded the total energy required for fracturing consists of two separate parts: an essential work (W_e) takes place in the inner process zone of the progressing crack, and nonessential or plastic work (W_p) performed in the outer plastic zone (Wu and Mai 1996), see Figure 2.23. The essential work (W_e) is the energy dissipated in the fracture region that is needed to create two new fracture surfaces and it is considered a constant material property (Wu and Mai 1996). The nonessential or plastic work is the energy dissipated in ductility, plasticity, and tearing. The essential work of fracture is proportional to the ligament cross-sectional area ($L \times B$), whereas, the plastic work is related to the plastic zone volume ($L^2 \times B$) multiplied by β .

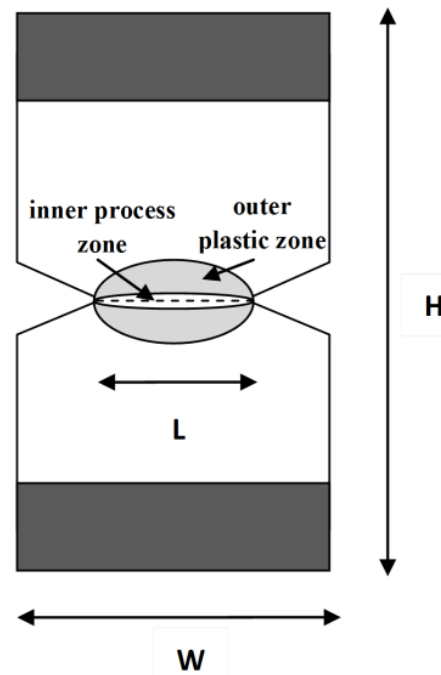


Figure 2.23: Schematic representation of inner and outer zone for a typical DENT specimen

The total work of fracture (W_T) is expressed mathematically by the following simple relationship:

$$W_T = w_e \cdot l \cdot B + \beta \cdot w_p \cdot l^2 \cdot B \quad \text{Equation 2.29}$$

The above equation can be written in specific terms by dividing both sides by ligament cross-sectional area ($L \times B$) as follows:

$$w_t = \frac{W_T}{L \cdot B} = w_e + \beta \cdot w_p \cdot l \quad \text{Equation 2.30}$$

Where: W_T is the total work of fracture in a DENT test as provided by the area under the force-displacement curve (J), as can be seen Figure 2.24, w_t is the total specific work of fracture (J/m^2), l is the ligament length (m), B is the sample thickness (m), β is a geometrical constant which depends on the shape of the plastic zone, w_e is the specific essential work of fracture (J/m^2), and w_p is the specific plastic work of fracture (J/m^3) (Wu and Mai 1996, Andriescu, Hesp et al. 2004).

The test is performed on similar specimens with different ligament lengths (5, 10, and 15 mm) as shown in Figure 2.25, the total work of fracture W_T is obtained by measuring the area under the force-displacement curve (J). The total specific work of fracture is then calculated by dividing the latter by ligament cross-sectional area ($L \times B$).

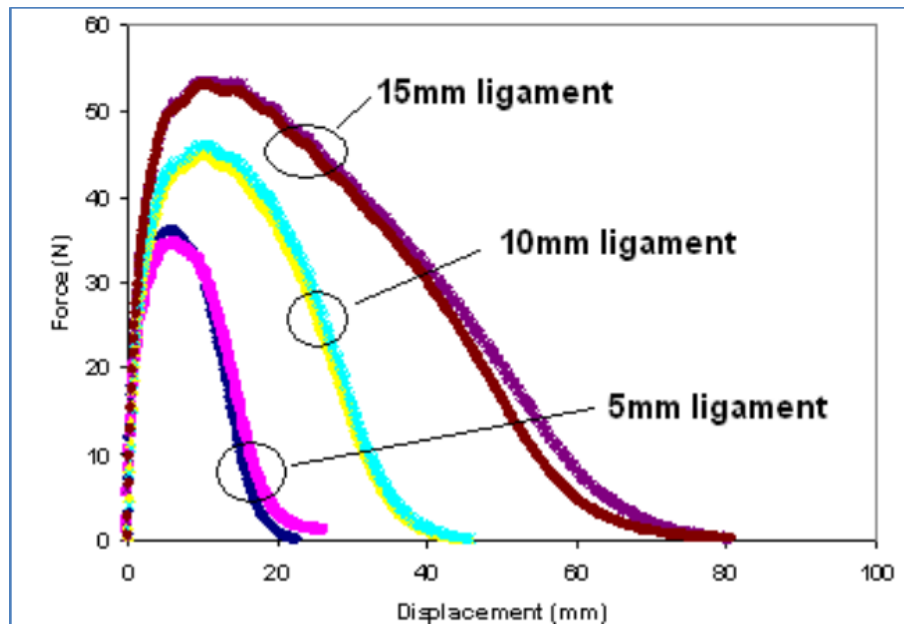


Figure 2.24: Typical raw data from DENT test (Nelson Gibson, M. Emin Kutay et al. 2012)

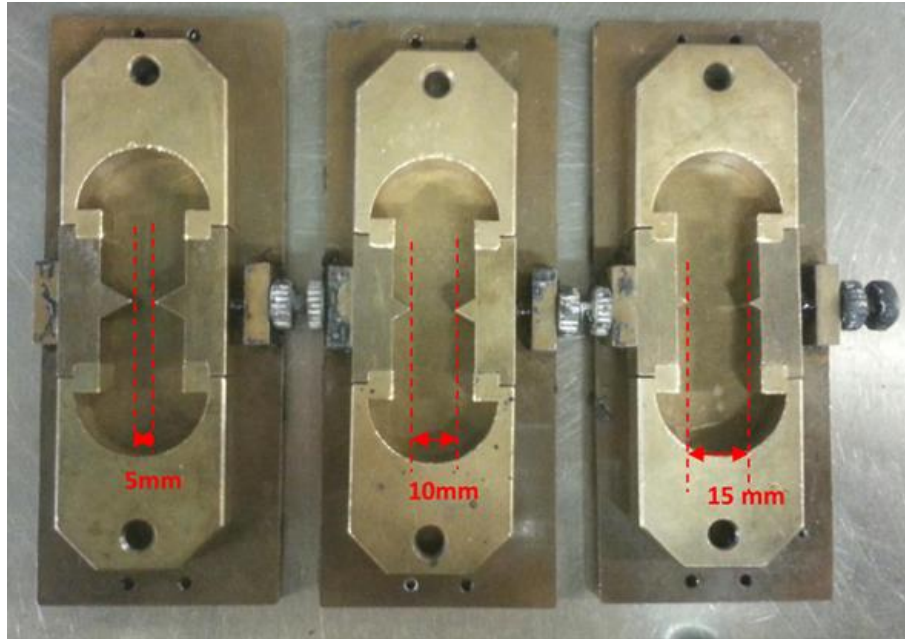


Figure 2.25: DENT test moulds

By plotting the w_t versus the ligament length l and using a linear fitting procedure a straight line results as shown in Figure 2.26. The intercept of the line represents the specific essential work (w_e) and it is attained by extrapolation to zero ligament, and the slope is the geometry constant times the plastic work of fracture βw_p . The references in the literature that deal with EWF suggest many assumptions and conditions that need to be met in order to have an intrinsic material property (Andriescu, Hesp et al. 2004, Martinez, Gamez-Perez et al. 2009, Bárány, Czigány et al. 2010). These recommendations, conditions and assumptions are as follows:

- (1) The ligament must be fully yielded before cracking initiates.
- (2) Load–displacement (L–d) diagrams should be self-similar in appearance for all ligament lengths, verifying a common geometry of fracture.
- (3) The sample must be yielded under truly a plane stress state of tension.

Generally, the first two requirements are easily fulfilled; however, the third assumption is not always attained. Pure plane stress prevails over plane strain in thin sections (small thickness to ligament ratio) and its influence gradually decreases as the ligament length reduces for a given thickness. The influence of thickness on the fracture toughness is illustrated diagrammatically in Figure 2.27 (Hashemi 1993). It can be seen from Figure 2.27 that when the thickness reaches a certain value B_c , pure plane strain conditions are thought to take place and the fracture toughness becomes independent of thickness. Also, there is an

optimum thickness, B_o , at which the plane stress conditions are met. In the transition zone between B_o and B_c , the fracture toughness is at plane-stress/plane-strain (mixed mode). The thickness boundaries B_o and B_c may be estimated as follows:

$$B_o = \frac{K_{Ic}^2}{3\pi\sigma_y^2} \quad \text{Equation 2.31}$$

$$B_c = 2.5 \left(\frac{K_{c1}}{\sigma_y} \right)^2 \quad \text{Equation 2.32}$$

Where K_{c1} is the fracture toughness, and σ_y is the tensile yield stress of the material. The influence of plane stress or plane strain condition mode on EWF can be seen in Figure 2.27.

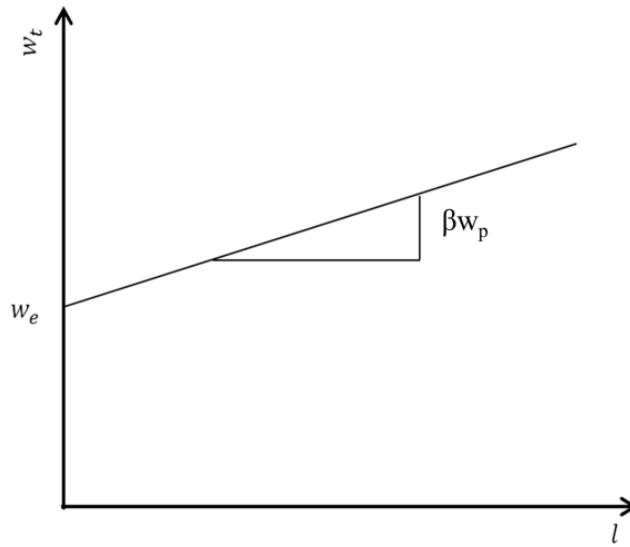


Figure 2.26: Schematic sketch illustrating the relationship between w_t and ligament length l (Wu and Mai 1996)

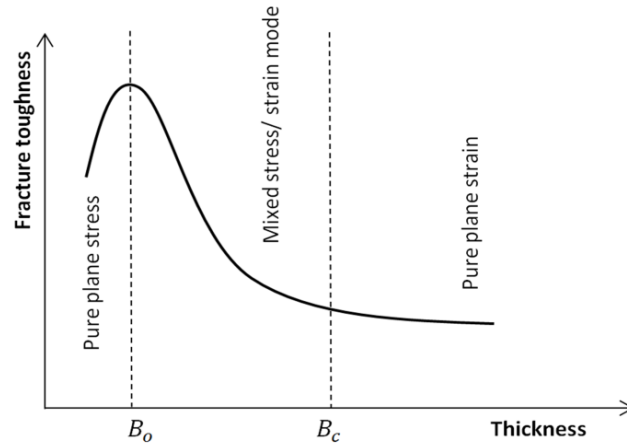


Figure 2.27: Schematic sketch illustrating the influence of thickness on the fracture toughness (Hashemi 1993)

To examine the plane stress or strain conditions, the Hill criterion can be applied (Hill 1952). According to that when a plot is made between the net section stress (maximum load divided by ligament cross section), σ_n , versus ligament length, L , a horizontal line should appear with $\sigma_n = 1.15 \sigma_y$, where σ_y is the yield stress of the material. However, these conditions are not normally met in the case of bituminous binders. Bituminous materials are not as tough as polymers or metals, and having very thin samples to maintain plane stress is not achievable from a practical point of view. Therefore, the w_e from mixed plane stress/ plane strain is normally deduced in the case of bituminous binders. It should be noted that the plane strain value of w_e is also considered a valuable material property that is independent of sample geometry (Wu and Mai 1996, Andriescu, Hesp et al. 2004).

The specific work of fracture in Eq. 2.29 represents the energy required for full ligament yielding preceding the necking and tearing. However, research groups that deal with fracture of polymers have introduced the concept of energy partitioning by splitting the total energy of the load-displacement curves in the two energies (Bárány, Czigány et al. 2010):

- (1) the specific work of fracture required for yielding (w_y) and
- (2) the specific work of fracture required for necking plus tearing (w_{n+t})

It is believed that the load drop at full ligament yielding in the load-displacement curve corresponds to a clear transition of the process between crack initiation and the onset of crack propagation (Karger-Kocsis and Ferrer-Balas 2001, Barany, Ronkay et al. 2005). The mathematical terms of Eq. 2.29 after applying the partitioning concept becomes as follows:

$$\begin{aligned} \mathbf{w}_t &= \mathbf{w}_{t(\text{yielding})} + \mathbf{w}_{t(\text{necking+tearing})} \\ &= (\mathbf{w}_{ey} + \beta_y \cdot \mathbf{w}_{py} \cdot l) + (\mathbf{w}_{en} + \beta_n \cdot \mathbf{w}_{pn} \cdot l) \end{aligned} \quad \text{Equation 2.33}$$

Researchers on polymers have shown that the energy partitioning presented above may be a good technique to overcome problems related to plane stress/ plane strain conditions and also to have more information about crack initiation and propagation fracture parameters (Karger-Kocsis and Ferrer-Balas 2001, Bárány, Czigány et al. 2010). It is interesting to consider applying the partitioning concept to bituminous binders. Therefore, the yield-related essential w_{ey} will also be used in this study to have a more reliable parameter which should be independent of the stress state of the ligament.

Finally, an approximation of the critical crack opening displacement CTOD can also be defined from the ratio of w_e over the net section stress. It is believed that a sufficient and complete yielding in the ligament section takes place at the smallest ligament, thus CTOD is approximated as $\delta t = w_e / \sigma_{net}$ (Hashemi 1993). CTOD gives an indication about the strain tolerance of the binder in the presence of a crack and a high degree of stress concentration during the ductile regime. It is a useful parameter, and has a very good correlation with the fatigue property where binders with large CTOD can resist fatigue cracking better. It was also successfully used to rank the fatigue performance of binders at different temperatures and rates of loading that cover the ductile state, and it is highly recommended by many researchers for performance grading of both binders and mixtures (Andriescu, Hesp et al. 2004, Andriescu and Hesp 2009, Nelson Gibson, M. Emin Kutay et al. 2012, Zhou, Mogawer et al. 2012).

2.4.3 Binder Rutting Testing

Accumulation of permanent deformation in a flexible pavement occurs at high in-service temperatures and/or under slow moving loads. The densification and shear viscous flow are the main mechanisms that are associated with rutting at varying degrees (Collop, Cebon et al. 1995, Tayfur, Ozen et al. 2007). Densification can be controlled and minimised by the mix volumetric properties while the shear plastic deformation is related to the viscoelastic properties of binders and the bonding interaction between bitumen and aggregate. It is well recognised that the viscous component of binder dominates the rheological response at high temperatures and extended loading time and it is, therefore, solely responsible for the non-recoverable deformation (Anderson, Christensen et al. 1991).

Many high temperature parameters and test methods have been developed to characterise the rutting resistance of binders (D'Angelo, Kluttz et al. 2007, D'Angelo 2009, Gibson, Qi et al. 2011, Nelson Gibson, M. Emin Kutay et al. 2012). The following test methods and parameters are the most frequently used to predict the high-temperature performance of binders.

Superpave high-temperature parameter ($G^*/\sin \delta$)

The current Superpave high-temperature binder parameter is specified such that the binder after ageing in the RTFOT must be greater than 2.2 kPa and 1kPa for unaged binder at the maximum 7-day average pavement design temperature (Kennedy, Huber et al. 1994). This parameter is derived from the definition of the loss compliance ($J'' = \sin\delta/G^*$) (Shenoy 2001). It is, therefore, important to select binder with reduced (J'') to minimise the irrecoverable strains (γ_{irr}) where:

$$\gamma_{irr} = \sigma_o \sin \delta / G^* \quad \text{Equation 2.34}$$

There have been considerable criticisms of the Superpave parameter ($G^*/\sin\delta$) because of the lack of correlation with asphalt mixture or pavement performance (Shenoy 2001, D'Angelo, Kluttz et al. 2007, D'Angelo 2009). Also, the lower contribution of the elasticity parameter, δ , underestimates the benefits that are obtained by elastomeric modifiers. Moreover, the parameter is derived by testing binders within the linear viscoelastic region at a fixed temperature and frequency. It is measured at ($\omega=10$ rad/s) and at this frequency the delayed elasticity cannot be neglected (De Visscher and Vanelstraete 2004). Consequently, many test methods or refinements to the existing Superpave parameter have been proposed to develop a parameter that is more sensitive and related to pavement performance (Shenoy 2001, D'Angelo 2009).

Shenoy rutting parameter

Shenoy (2001) proposed ($G^*/(1-(1/\tan\delta \sin\delta))$) as a refinement to ($G^*/\sin\delta$). The parameter was derived through a semi-empirical approach. It represents the inverse of the non-recoverable compliance and is derived by linking the strain response in the creep experiment with the complex modulus G^* from oscillatory shear experiments at a matched timescale. This parameter is more sensitive to phase angle than the Superpave parameter as shown in Figure 2.28; therefore, it better explains the changes in elastic properties when adding the polymeric modifier. It should be noted that the term ($1-(1/\tan\delta \sin\delta)$) becomes zero when δ is equal to or lower than 52 degrees; therefore, the parameter is not applicable at values of δ

below 52 degrees. However, the parameter is for characterising the high temperature properties at which δ tends to be higher than 52 degrees. Also, if it happens that δ gets lower than 52 degrees, the parameter, $G^*/(\sin\delta)^9$, can be used to give a very close approximation based on the best-fit curve to $G^*/(1-(1/\tan\delta \sin\delta))$ (Shenoy 2001). The temperature at which $G^*/(1-(1/\tan\delta \sin\delta))$ is greater than (50 Pa) for RTFO aged binders at $\omega=0.25$ rad/s, has been specified as the high specification temperature T_{HS} ($^{\circ}\text{C}$) (Shenoy 2003).

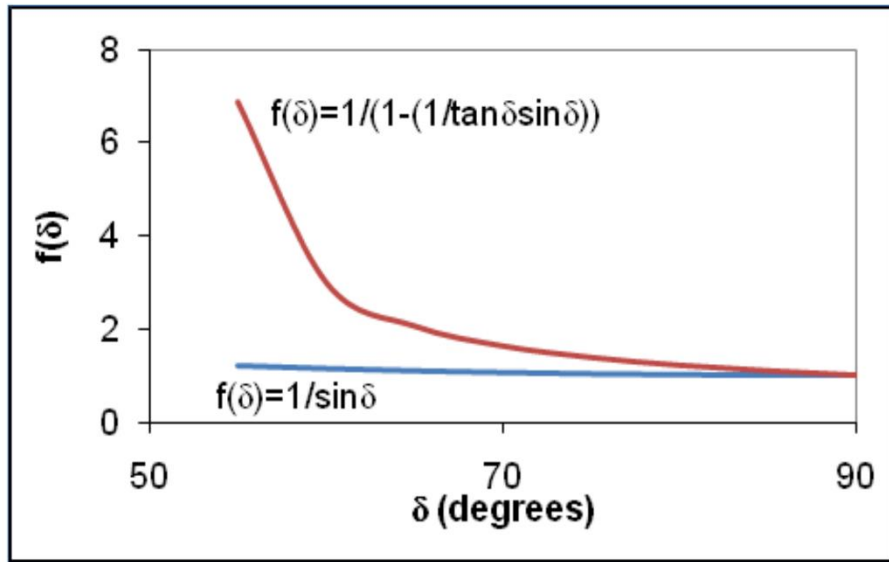


Figure 2.28: Comparison between the effectiveness of δ on both Shenoy rutting parameter and Superpave rutting parameter

Zero Shear Viscosity ZSV

Zero shear viscosity is defined as a measure of viscosity at a steady state flow when the shear rate approaches zero, and it is a physical property of the material that is independent of shear rates and stress. The ZSV concept is based on the fact that the purely dissipative viscous component is solely responsible for the non-recoverable deformation (Airey 2004). Zero shear viscosity is strongly related to rutting resistance of bituminous materials and many researchers have proven a strong correlation to rutting performance in mixtures or field pavement (Phillips and Robertus 1996, Morea, Agnusdei et al. 2011). The ZSV is highly influenced by the higher molecular weight fraction and binder stiffness, and thus, it can reliably predict the rutting resistance of binders under slow-moving load (Morea, Agnusdei et al. 2011).

Even though ZSV is an intrinsic property of bitumen, a 'true' value of ZSV may never be achieved particularly for highly modified bitumen. Several factors undermine obtaining a

reliable measurement for ZSV; amongst them are, the extrapolation and approximations that are made to calculate the ZSV, the different test methods and experiments used, and the fact that a steady state flow is not readily reached for some highly elastomer modified bitumens.

Generally, ZSV can be identified from three test methods; single creep tests, creep and recovery and oscillation tests (De Visscher and Vanelstraete 2004). The oscillation test has been considered in this study.

Utilising a cyclic oscillatory test in the low-frequency domain has been suggested by many researchers to evaluate ZSV (Sybilski 1996, Anderson, Le Hir et al. 2002, De Visscher and Vanelstraete 2004, Morea, Agnusdei et al. 2011). In this method, a frequency sweep test within the linear viscoelastic regime at a specific high test temperature is used to determine the ZSV (Morea, Agnusdei et al. 2010).

At low frequencies and relatively high temperatures binders tend to behave like Newtonian fluids in which the complex viscosity becomes independent of the applied shear rate or frequency. Additionally, the contribution of the delayed elasticity or recovered deformation is minimised and tends to zero as frequency approaches zero, hence, the total dissipated energy reflects only the viscous component or permanent deformation. Therefore, ZSV calculated from an oscillation test at low frequency is considered a reliable candidate indicator and it better characterises binders than the SHRP parameter $G^*/\sin \delta$ at 10 rad/s, because the latter does not distinguish between the effects of recovered and non-recovered strain on the total dissipated energy (De Visscher and Vanelstraete 2004).

ZSV can be defined as the ratio between the complex modulus G^* or loss modulus and the radial frequency as the frequency approaches zero (Sybilski 1996, Anderson, Le Hir et al. 2002).

$$\omega \rightarrow 0 \Rightarrow \eta^* \text{ or } ZSV \rightarrow \frac{G^*}{\omega} \text{ or } \frac{G''}{\omega} \quad \text{Equation 2.35}$$

In the case of neat binder, the effect of the delayed elasticity is substantially diminished at low frequencies and high temperatures, and a plateau is evident when a curve is plotted of complex viscosity versus frequency. Thus, ZSV can be readily identified by the asymptote. However, for highly modified bitumen such as high content crumb rubber modified bitumens or cross-linked polymer bitumens, such a plateau is not always developed as shown in Figure 2.29.

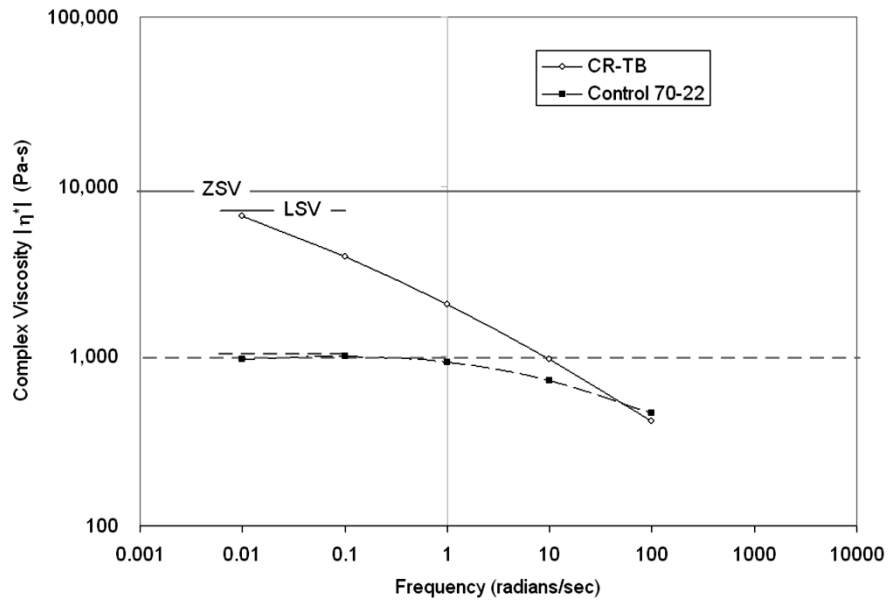


Figure 2.29: Complex viscosity versus frequency (Gibson, Qi et al. 2012)

Since it is not possible to measure directly the complex viscosity at very low frequencies due to the limitations of DSR resolution, mathematical models are usually used to fit the data and extrapolate the complex viscosity to very low or zero frequency (De Visscher and Vanelstraete 2004). The flow curve of pseudoplastic fluids can be adequately fitted by using a four parameter Cross model as follows (Sybilski 1996, Anderson, Le Hir et al. 2002):

$$\eta^* = \frac{\eta_0 - \eta_\infty}{1 + (K\omega)^m} + \eta_\infty \quad \text{Equation 2.36}$$

Where η^* is complex viscosity, η_0 is zero shear viscosity (first Newtonian region viscosity), η_∞ is infinite shear viscosity in the second Newtonian region viscosity (viscosity at infinite frequency), ω is frequency (rad/s), K and m , are constants.

The Cross model can also be simplified to three parameters as shown in Eq. 2.36 because the infinite viscosity η_∞ is too small in comparison to complex viscosity η^* and zero shear viscosity η_0 ; therefore, it can be neglected (Anderson, Le Hir et al. 2002):

$$\eta^* = \frac{\eta_0}{1 + (K\omega)^m} \quad \text{Equation 2.37}$$

It should be mentioned that some modified bitumens experience very high complex viscosity gradients at low frequencies, the ZSV values become unreliable from the rheological point of view (Morea, Agnusdei et al. 2011). Thus, low shear LSV viscosity is sometimes suggested to solve this problem. It was also shown that complex viscosity measured at 0.001

and 0.01 Hz give as a good correlation with mixture rutting performance as those measured at 0.0001 Hz (Morea, Agnusdei et al. 2011).

Multiple Stress Creep and Recovery (MSCR)

It is well recognised that the nonrecovered deformation of binders has a significant influence on pavement rutting performance. The multiple stress creep-recovery (MSCR) test, which is based on binder creep and recovery characterisation, was firstly developed by the NCHRP 9-10 research program (Bahia, Hanson et al. 2001) and then extended by (Dongré, D'Angelo et al. 2003). The validity of the test to characterise binders at high-temperature has been ascertained by many researchers, and it does better than Superpave parameter $G^*/\sin\delta$ in rating binders to their mixtures or pavement rutting resistance (D'Angelo, Dongre et al. 2006, Tabatabaee and Tabatabaee 2010, Wasage, Stastna et al. 2011, Nelson Gibson, M. Emin Kutay et al. 2012, Zoorob, Castro-Gomes et al. 2012).

The MSCR test consists of applying repeated creep recovery of shear stress for a short duration of 1s and then removing the stress for 9s to allow the material to recover, this is repeated for 10 cycles using different stress levels. The creep stress levels start at 25 Pa and end at 25600 Pa by doubling the stress each time. The test is usually performed on RTFO aged samples to simulate the ageing during mixing and lay-down. The test is conducted on samples between two parallel plates of 25mm diameter using the dynamic shear rheometer (DSR) equipment and described in detail in the ASTM D7405-08 or AASHTO TP 70-12 standards. In the new test protocol, two levels of shear stress are used 100 Pa and 3200 Pa, 10 repeated cycles of 1s creep and 9s recovery are applied at each stress level with no time lag between cycles. A typical one cycle of creep-recovery is shown in Figure 2.30; the parameters retrieved from MSCR test are:

$$\text{Recovery \% at 100 Pa or 3200 Pa} = \frac{1}{10} \left\{ \sum_{i=1}^{10} \frac{Y(r)i}{Y(t)i} \right\} * 100 \quad \text{Equation 2.38}$$

$$J_{nr \text{ at } 100 \text{ Pa}} \left(\frac{1}{\text{KPa}} \right) = \frac{1}{10} \left\{ \sum_{i=1}^{10} \frac{Y(nr)i}{0.1} \right\} \quad \text{Equation 2.39}$$

$$J_{nr \text{ at } 3200 \text{ Pa}} \left(\frac{1}{\text{KPa}} \right) = \frac{1}{10} \left\{ \sum_{i=1}^{10} \frac{Y(nr)i}{3.2} \right\} \quad \text{Equation 2.40}$$

$$\text{Difference in recovery } R_{diff. \%} = \left\{ \frac{R_{at 100 \text{ Pa}} - R_{at 3200 \text{ Pa}}}{R_{at 100 \text{ Pa}}} \right\} * 100 \quad \text{Equation 2.41}$$

$$\text{Difference in non – recoverable compliance } J_{nr(diff.) \%} = \left\{ \frac{J_{nr \text{ at } 3200 \text{ Pa}} - J_{nr \text{ at } 100 \text{ Pa}}}{J_{nr \text{ at } 100 \text{ Pa}}} \right\} * 100 \quad \text{Equation 2.42}$$

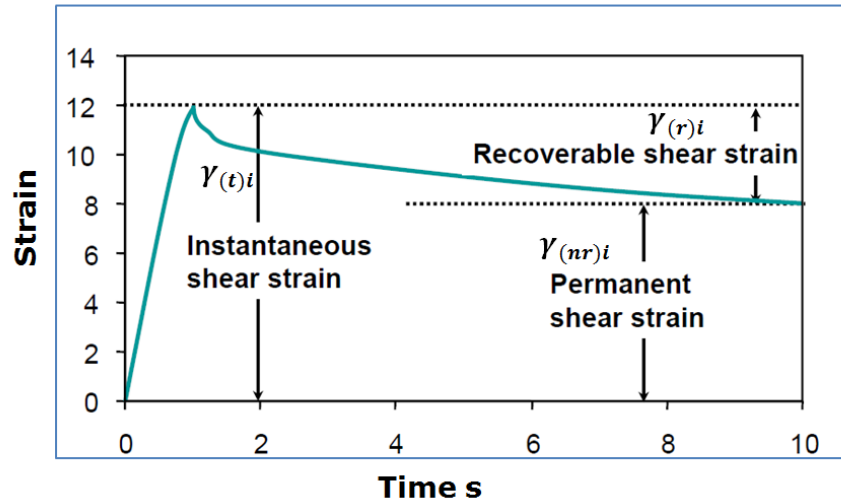


Figure 2.30: A typical one cycle of creep-recovery

Where: Recovery % is average recovery of the 10 cycles tested at 100 Pa or 3200 Pa, $\gamma_{(r)i}$ is the recovered strain from the end of the 9 second recovery portion, $\gamma_{(nr)i}$ is the non-recovered strain from the end of the 9 second recovery portion, $\gamma_{(t)i}$ is the creep strain at the end of the 1 second of creep portion and J_{nr} is average non-recoverable compliance of cycles tested at 100 Pa or 3200 Pa.

The non-recoverable creep compliance, J_{nr} , is strongly recommended as an alternative to the current SHRP parameter $G^*/\sin \delta$ (D'Angelo, Kluttz et al. 2007). The J_{nr} has the ability to predict the improvement imparted by modification and it is suitable for specification to both neat and modified bitumen (D'Angelo 2009). Measuring the J_{nr} of binders at high stresses that are not within the linear viscoelastic region is potentially better to capture the rutting behaviour in mixtures because the strains in binder films on aggregate surfaces can be several hundred times greater than the strain in the mixture.

The J_{nr} is very sensitive to both temperature and stress level, and the stress dependency is more apparent with polymer modified bitumen. For some highly polymer modified bitumens, the 9s recovery may not be sufficient to get the elastic strain portion fully recovered. In that case, the residue of delayed elastic strain would add to the viscous component resulting in decreasing both the peak strain value and its irrecoverable strain value in every subsequent cycle (Shenoy 2001).

It is crucial to define the stress level that should be used to rank the binders in term of their rutting resistance. Literature suggests that the stress level is defined by conducting MSCR at

multiple stress conditions and then select the most appropriate stress level that relates most to mixtures and field performance (D'Angelo 2009, Wasage, Stastna et al. 2011, Zoorob, Castro-Gomes et al. 2012). Additionally, the delayed elastic properties of cross-linked elastomers should be taken into consideration and it should be ensured that all elastic strain is fully recovered during the 9s. Otherwise, an extended recovery time should be considered.

2.5 Asphalt Mixtures

An asphalt mixture is a composite material consisting of aggregate and bitumen. The aggregate particles form the skeleton matrix that is cemented together by the bitumen. Asphalt mixtures are the main materials used to construct the bituminous layers of flexible pavements, as shown in Figure 2.31. The bituminous layer of a flexible pavement comprises surfacing, binder course and base. The base layer is the main structural part of a flexible pavement that acts as a load-bearing layer. The main role of binder course is to spread the traffic load into the base layer and also to provide a smooth layer for constructing the thin surfacing. The surfacing layer should provide adequate skid resistance, water-resistance and a comfortable vehicle ride.

The materials selection and designing process for asphalt mixtures should guarantee the following mechanical properties (Rahman 2004); (1) high elastic stiffness to ensure load spreading ability (2) high fatigue resistance to prevent the initiation and propagation of cracks (3) high permanent deformation resistance to prevent surface rutting. There are different aggregate gradations used in asphalt mixture production to accommodate the different requirements of designing the flexible pavement, i.e. the location of the bituminous layer in the pavement structure, repetition of traffic, traffic axle loads, and other environmental conditions. The asphalt mix design is, therefore, essential to define an optimum material blend that meets the requirements and specifications of pavement construction. Three types of aggregate gradation are generally associated with Hot Mix Asphalt (HMA):

- Dense or well-graded mixes: this is the most common gradation used in HMA. The gradation is optimised to give the densest particle packing which in turn provides maximum density and stability. The maximum density gradation curve is widely determined based on Fuller's curve using the following equation (Roberts, Kandhal et al. 1991):

$$P = 100 \left(\frac{d}{D} \right)^n \quad \text{Equation 2.43}$$

Where P is the total percent passing or finer than the sieve, d is the size of the sieve being considered, D is the maximum size of the aggregate to be used, and n is an exponent constant. The maximum density for an aggregate can be obtained when $n=0.5$, however, a 0.45 exponent is normally used in the specification (Roberts, Kandhal et al. 1991).

- Open-graded mixes: this type of gradation contains only a small percentage of fine particles where the gradation curve is almost vertical in the mid-size range; and flat in the small size range. This results in having mixes with more air voids and relatively lower binder content. The high air voids content between the coarse aggregate allows additives such as rubber and fibres to be used with this kind of gradation.
- Gap-graded mixes: hot rolled asphalt HRA and stone mastic asphalt SMA are examples of this type of gradation. It is widely used in Britain on heavily trafficked roads and motorways. Stone mastic asphalt (SMA) is well known for its stability and durability. It comprises essentially a coarse aggregate skeleton filled with a high content of bitumen/filler mortar. The stone-to-stone aggregate skeleton of coarse aggregate provides excellent rutting resistance while the bitumen/filler mortar provides high fatigue resistance and a durable HMA mixture. The gradation contains a small or missing percentage of aggregate particles in the mid-size range. The different gradations used in HMA can be depicted in Figure 2.32.

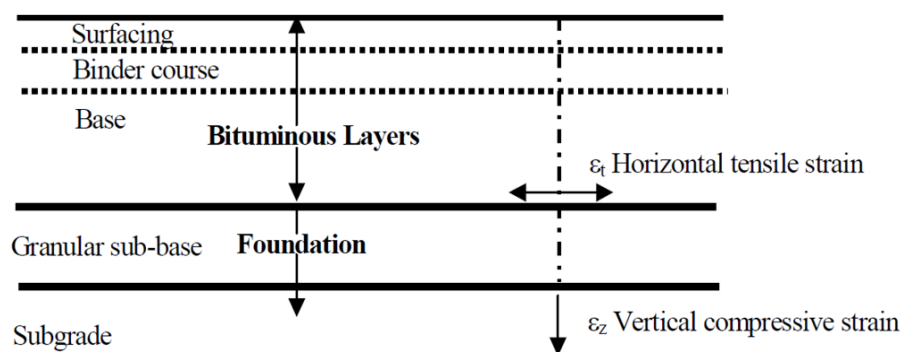


Figure 2.31: A typical flexible pavement structure

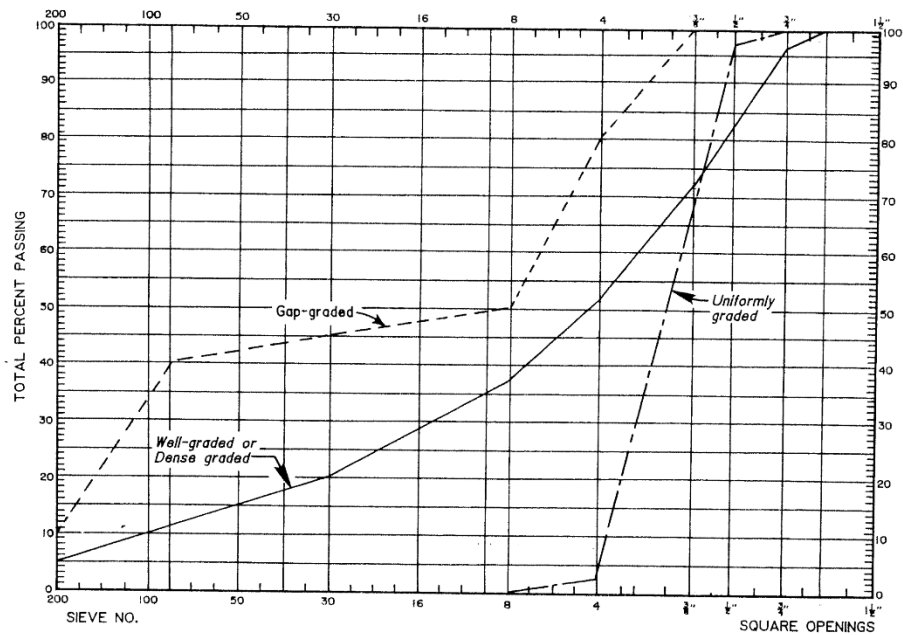


Figure 2.32: Typical terms used to identify aggregate gradations (Roberts, Kandhal et al. 1991)

2.5.1 Nottingham Asphalt Tester (NAT)

The Nottingham Asphalt Tester (NAT) is widely used in the UK and across the world for measuring and assessing the mechanical properties of asphalt mixtures. Asphaltic specimens can be tested in the indirect tensile mode for stiffness and fatigue, or in the repeated load axial testing mode for rutting testing (Rahman 2004). Figure 2.33 shows the three different testing configuration that are used in NAT.

The main parts of the NAT machine are; a test frame located in a temperature control cabinet, data acquisition and control unit, a servo-pneumatic unit in conjunction with the data acquisition and control unit, and a low-friction actuator to apply repeatable stress variations controlled by a high precision pneumatic valve.

The pulsating load is controlled through a voltage/pressure (V/P) converter and a solenoid valve. This is achieved using a Windows software by introducing a pre-determined pressure into a reservoir of the pneumatic unit, and by switching the solenoid valve, a load is applied to the specimen. The load is then measured using a load cell, and the V/P converter is adjusted to reach the designed load or deformation.

For specimens tested in the indirect tensile mode, a pulsating load is applied vertically across the diameter of the cylindrical specimen and the horizontal deformation is measured using

two linear variable differential transformers, LVDTs, as shown in Figure 2.33. The LVDTs are placed diametrically opposite each other by a rigid frame clamped to the test specimen.

One of the most common uses of the NAT machine is to measure the Indirect Tensile Stiffness Modulus of asphaltic samples. The test is conducted on specimens with dimensions of 100 ± 2 mm diameter and 40 ± 2 mm thickness, by applying an impulse load diametrically on a specimen, as shown in Figure 2.33a, to induce a small horizontal strain. The test is carried out under the standard specification BS EN 12697-26, 2004.

The NAT machine also provides a simple method for evaluating the fatigue properties of asphalt mixtures by means of the Indirect Tensile Fatigue Test (ITFT), Figure 2.33b. The test can be conducted on cylindrical specimens manufactured in the laboratory or cored from the pavement in the field. The ITFT has been proven to be able to distinguish between mixtures containing different binders (type and content) based on the stiffness and the number of cycles to failure (Rahman 2004). The test and fatigue analysis can be carried out in accordance with EN 12697-24:2012 (E) and EN 12697-24: 2012 standards; the details about the differences between the two methods are presented in Chapter 6.

The susceptibility of asphaltic materials to rutting can also be evaluated in the NAT machine using the Repeated Load Axial Test (RLAT). In the RLAT, a load pulse is applied vertically to the specimen, as seen in Figure 2.33c, and the accumulated permanent strain is monitored by two vertical LVDTs fixed on top of the upper platen. The test is conducted according to BS DD 226. The testing setting and parameters are introduced in Chapter 7.

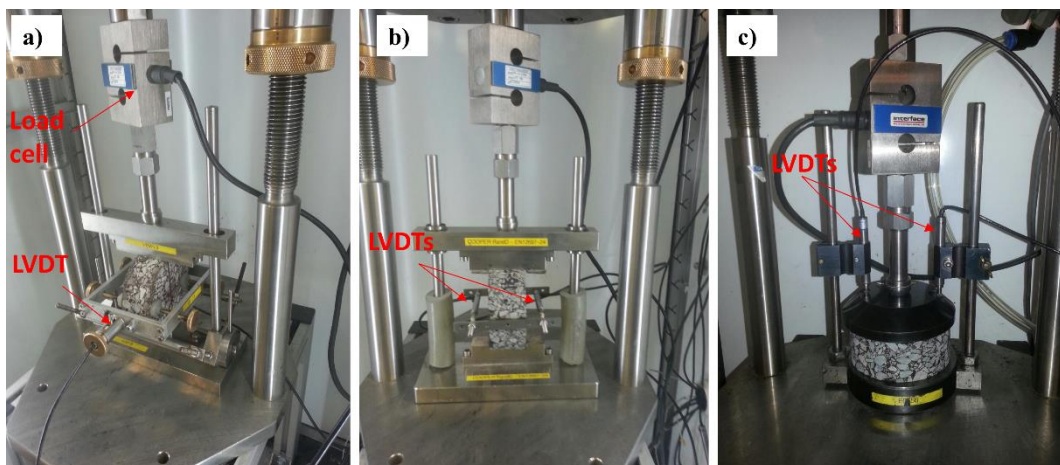


Figure 2.33: Testing arrangement in the NAT; a) ITSM testing configuration b) ITFT testing configuration and c) RLAT testing configuration

2.5.2 SuperPave Indirect Tensile Test (IDT) and Energy Ratio ER

The tensile testing of Superpave IDT includes the resilient modulus, creep, and indirect tensile strength tests, which have been shown to give a coherent interpretation of the fracture behaviour of asphalt mixtures. The details about specimen preparation, test settings, and connections can be found in Chapter 6 and Appendix A.

Fracture analysis approaches are considered more fundamental and have the ability to accurately predict pavement performance (Roque, Birgisson et al. 2004). Fracture energy-based criteria have been used to evaluate the fatigue cracking and low-temperature performance of materials. The University of Florida developed a viscoelastic fracture mechanics model to predict and control the crack initiation and crack propagation in an asphalt pavement (Roque, Birgisson et al. 2004). They introduced the ER which is based on the fact that each asphalt mixture has the ability to resist the initiation of a crack if its fundamental dissipated creep strain energy threshold $DCSE_f$ is larger than its minimum dissipated creep strain energy $DCSE_{min}$. Therefore, asphalt mixtures with larger ER values (1.0 and higher) should resist better the development and propagation of fatigue cracking in comparison to asphalt mixtures with lower ER. They analysed and evaluated data from 22 field test sections in Florida and found that the minimum dissipated creep strain energy $DCSE_{min}$ required so such pavement would not exhibit top-down cracking was a function of the power law parameters (D1 and m-value) obtained from the creep test. It is also dependent on the mixture tensile strength and level of average tensile stress to which the mixture will be subjected. The pavement structural characteristics also play a key role in determining the level of the stress and its distribution.

The following steps are required to determine the ER parameter (Roque and Buttlar 1992, Roque, Birgisson et al. 2004):

1. Calculate the resilient modulus as follows:

$$M_R = \frac{P}{\varepsilon_x \cdot t \cdot D \cdot C_{CMPL}} \quad \text{Equation 2.44}$$

where,

M_R = resilient modulus;

P = maximum load;

ε_x = horizontal strain;

t = thickness of specimen;

D = diameter of specimen;

C_{CMPL} = nondimensional creep compliance factor,

$$C_{CMPL} = 0.6354 \left(\frac{X}{Y}\right)^{-1} - 0.332 \quad \text{Equation 2.45}$$

(X/Y) = ratio of horizontal to vertical deformation.

2. Calculate the tensile strength as follows:

$$S_t = \frac{2*P}{\pi*t*D} (C_{SX}) \quad \text{Equation 2.46}$$

Where,

S_t = indirect tensile strength;

P = maximum load;

C_{SX} = horizontal stress correction factor;

$$C_{SX} = 0.948 - 0.01114 \left(\frac{t}{D}\right) - 0.2693 (v) + 1.436 \left(\frac{t}{D}\right)(v);$$

$$v = \text{Poisson's ratio, } v = -0.10 + 1.480 \left(\frac{X}{Y}\right)^2 - 0.778 \left(\frac{t}{D}\right)^2 \left(\frac{X}{Y}\right)^2;$$

and t, D, and $\left(\frac{X}{Y}\right)$ are the same as described above.

3. Calculate the $DCSE_f$ as follows:

From the tensile strength test, a typical stress-strain response of the mixture is obtained as shown in Figure 2.34. The total fracture energy until failure FE_f is determined as the area under the stress-strain curve. The $DCSE_f$ is then determined by subtracting the elastic energy at fracture EE from the total fracture energy limit FE_f , which can be expressed as follows:

$$DCSE_f = FE_f - \frac{S_t^2}{2.M_R} \quad \text{Equation 2.47}$$

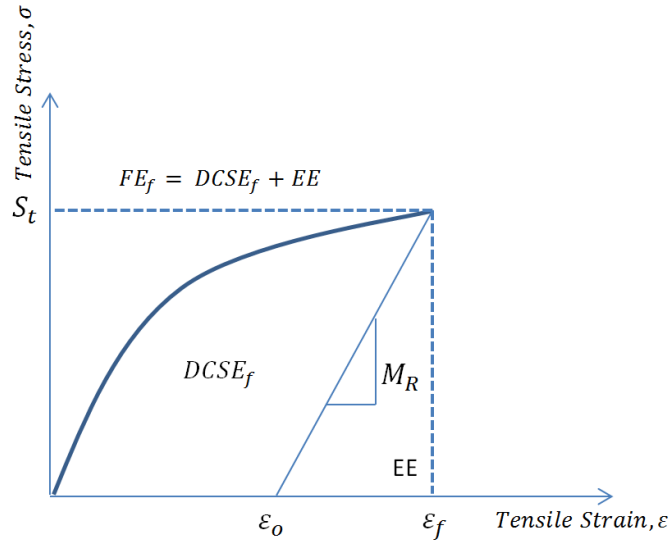


Figure 2.34: Tensile strength versus tensile strain plot

4. Calculate the creep compliance $D(t)$ at time t from the creep test as follows:

$$D(t) = \frac{\epsilon_x \cdot t \cdot D \cdot C_{CMPL}}{P} \quad \text{Equation 2.48}$$

The power function parameters (D_1 and m) are then obtained by fitting the $D(t)$ data using the following power function:

$$D(t) = D_o + D_1 t^m$$

5. Calculate the $DCSE_{min}$ as follows:

$$DCSE_{min} = \frac{m^{2.98} \cdot D_1}{A} \quad \text{Equation 2.49}$$

where the parameter A was determined as follows:

$$A = 0.0299 \sigma_t^{-3.10} (6.36 - S_t) + 2.46 \times 10^{-8}$$

Where σ_t = the applied tensile stress and S_t = the tensile strength. It can be seen that the parameter A in $DCSE_{min}$ requires information about pavement structural characteristics reflected in σ_t and mixture tensile strength. However, this study has investigated in the laboratory the properties of different asphalt mixtures; therefore it was assumed that the different mixtures are subjected to the same level of stress. Thus, σ_t is assumed to be constant, a value of 300 kPa is given as the average tensile stress for all studied mixtures.

6. Finally, the energy ratio parameter ER is defined as follows:

$$ER = \frac{DCSE_f}{DCSE_{min}} \quad \text{Equation 2.50}$$

The ER was designed as a dimensionless parameter to evaluate the cracking performance of different asphalt mixtures. Field test sections and laboratory testing showed that the ER parameter can reliably predict and control top-down cracking performance of pavements (Roque, Birgisson et al. 2004, Shu, Huang et al. 2008, Timm, Sholar et al. 2009, Zou, Roque et al. 2013) .

2.6 Summary

The literature review has provided a background and basis to study the constituent materials of rubberised binders and address the main physical changes associated with the manufacture of RTR-MBs. The most fundamental testing and parameters for characterising the mechanical properties of binders and mixtures have also been discussed in this chapter.

The literature review has shown that there could be significant differences in the chemical and physical properties between different bitumens depending on the source and distillation processes. Also, the main ingredients of crumb rubber modifiers that determine their physical properties vary from one manufacturer to another. On the other hand, the mechanism and the degree of swelling and/or dissolution of crumb rubber during the rubber-bitumen interaction play a key role in adjusting the final mechanical properties of rubberised binders. Since the swelling and dissolution extent depends on the source of materials and blending conditions, it is important to regulate and control these variables to develop high-performance materials. The next chapter will be devoted to studying rubber interaction mechanisms and develop the binders accordingly.

This chapter has also addressed in detail the problem of storage stability for RTR-MBs. The mechanism of phase separation, techniques used to reduce the separation, and the methods used to measure the extent of separation, have also been explained in this chapter. The problem of phase separation seems to be an unavoidable issue in rubberised binders, and the techniques used to overcome this problem were only able to reduce the degree of separation but were not able to eliminate it. The effect of oxidative ageing on both neat and rubberised binders has been explored. The presence of rubber particles makes the ageing mechanism of rubberised binders more complicated than that of neat bitumens. The artificial ageing can cause breakdown to rubber particles which leads to altering the mechanical properties by reducing the bulk viscosity of binders, and hence, lowering the hardening rates. The thin film oven test (TFOT) and pressure ageing vessel (PAV), have been chosen and will be used as accelerating laboratory ageing methods in Chapter 4.

Various test methods and parameters used to characterise the fatigue and rutting properties of binders, have been described in detail in this chapter, and will be applied in the next chapters. The Dynamic Shear Rheometer (DSR) is widely used to measure fundamentally the viscoelastic response of binders at various loading rates and temperatures. Most of the fatigue and rutting testing methods for binders, adopted in this work, are accomplished using the DSR. The literature review has revealed that using only a single binder property cannot adequately describe the true binder contribution related to asphalt mixture or pavement performance. Bituminous binders and especially rubberised ones have a complex behaviour depending on stress degree and rate. Therefore, it is important to evaluate the materials using different test methods that involve various strain ranges to assert a realistic performance for the developed materials which is one of the main objectives of this work.

Finally, the last section of this chapter has been devoted to asphalt mixtures. The Nottingham Asphalt Tester (NAT) and SuperPave Indirect Tensile Test (IDT), which will be used in the next chapters, have been described. These tests are widely used for characterising the mechanical properties of asphalt mixtures.

Chapter 3 Low Shear Development of RTR-MBs

3.1 Introduction

Bitumen and rubber particles interact together under different processing conditions resulting in adjusting of the physical properties of both binder and rubber and hence the rubberised bitumen. The nature of the interaction process between bitumen and crumb rubber should be carefully studied to clarify the change of final product. Therefore, the effect of curing temperature and time on the mechanical properties of rubberised bitumen are extensively studied in this chapter in order to develop superior rubber modified binders.

Rubberised bitumen is currently manufactured by means of a number of different bitumen–rubber interaction mechanisms. The interaction mechanism is traditionally considered to be a physical process with rubber particles being swollen by absorbing the lighter fractions (oily compounds) available in the bitumen into the bulk of these particles with no chemical reaction (Heitzman 1992, Ghavibazoo and Abdelrahman 2013, Lo Presti 2013). The swelling mechanism and rubber dispersion are mainly controlled by temperature, time and rubber particle size (Attia and Abdelrahman 2009). The optimisation process of manufacturing RTR-MBs is normally done by monitoring the high-temperature viscosity which indicates the state of swelling over time, and then identifying the time at which the viscosity reaches its highest (peak) value. Although viscosity is an important property especially in terms of binder pumpability, mixture workability and compaction, it cannot be solely used to predict the in-service performance of the binder within the asphalt mixture.

Specifying a generic recipe for the interaction variables of rubberised bitumen is almost impossible as the performance trend associated with these variables is not always clear due to the overlapping effects that include the base binder (physical and chemical properties), and crumb rubber type, size, content and surface texture. All these factors play a key role in controlling the resultant product. Navarro and his co-workers (Navarro, Partal et al. 2007) demonstrated that a processing temperature of 210°C is the optimum temperature for RTR-MBs in terms of their rheological properties and storage stability. They also stated that processing device and impeller geometry have almost negligible influence at this temperature. Furthermore, Ragab and his colleagues (Ragab, Abdelrahman et al. 2013) suggested that a combination of a very high mixing speed of 50 Hz and moderate temperature of 190°C gave the best improvements in complex modulus $|G^*|$ and phase angle (δ) and provided improved cross-linking by forming a 3D network structure within the binder matrix. However, these studies investigating the processing conditions were only based on characterising the materials within the linear viscoelastic region LVE. The effect of processing conditions on nonlinear viscoelastic properties has not been addressed yet.

In this chapter, the manufacture of RTR-MBs has been carried out by utilising a simple laboratory tool consisting of a standard Brookfield viscometer with a modified Dual Helical Impeller (DHI). This configuration allows the practical investigation of a large number of variables associated with the manufacture of RTR-MBs while measuring viscosity in real-time. This part of the study also aims to understand the effects of processing conditions on the rheological properties of RTR-MBs produced using two different base binders and different rubbers. The blending variables (temperature and time) are investigated based on their influence on measurements of the linear and nonlinear viscoelastic properties of the RTR-MBs.

3.2 Materials and experimental programme

3.2.1 Materials

Two straight-run bituminous binders were used in this study, labelled H for “hard” and S for “soft”. Binder H has a penetration of 40 dmm and a softening point of 51.4°C, whereas binder S has a penetration of 200 dmm and a softening point of 37°C. Other physical and rheological properties are presented in Table 3.1. The two binders were selected with large differences in their physical and rheological properties in order to identify the effect of the base binder on the interaction mechanism and the final RTR-MBs. In addition to binder H being

considerably harder than binder S, it also has an asphaltenes content that is almost four times higher than binder S (15.2% compared to 4.2%). Therefore, higher maltenes (light fractions) are available in bitumen S compared to H.

Table 3.1: The properties of base binders used in this study

Ageing states	Index	Binder “S”	Binder “H”
Unaged binder	Penetration @25 °C, 0.1mm	200	40
	Softening point °C	37.0	51.4
	Rotational viscosity, Pa.s		
	@135 °C	0.192	0.474
	@160 °C	0.065	0.170
	@180 °C	0.025	0.075
	@200 °C	0.012	0.032
Asphaltenes content		4.2%	15.2%
	G* /sinδ @ 60 °C & 1.59Hz, kPa	0.615	1.95
RTFOT aged residue	G* /sinδ @ 60 °C & 1.59Hz, kPa	1.256	7.70
RTFOT + PAV aged residue	G* .sinδ @ 20 °C & 1.59Hz, kPa	1050	10027

Three different sources of recycled tyre rubber were used, labelled as N, D and SE. The normal straight rubber N is a recycled rubber, derived from discarded truck and passenger car tyres by ambient grinding supplied by J. Allcock & Sons Ltd (England). D and SE are both non-standard crumb rubbers chosen to pursue a reduction in high-temperature viscosity. The partly vulcanised rubber D is recycled from truck and passenger car tyres also by ambient grinding but contains 20% devulcanised rubber supplied by RUBBER PRODUCTS, Riga, Latvia. The devulcanisation was based on mechanochemical processes in which the sulphur crosslinks in the polymer chain were uncoupled, but its chemical composition was not changed. The last one SE consists of 100% recycled truck tyres which by nature have a relatively high content of natural rubber. SE is pre-treated with special oil and FT-wax component. The SE was supplied by STORIMPEX AsphaltTec GmbH. Table 3.2 shows the percent passing gradation of rubber particles, and Figure 3.1 shows SEM images taken at different magnifications. SEM images show that crumb rubber produced by ambient grinding (N and D) has very irregular shapes and rougher surface area which are desirable for rubber-bitumen interaction and hence give better physical properties. Generally, cryogenically ground rubbers have smooth fractured surfaces with angular corners. However, the SEM images of SE show that the pre-treatment process has resulted in rougher texture surface in comparison to SEM images found in other references (Shen and Amirhanian 2005, Thives, Pais et al. 2013). The main properties of the different RTRs used in this study are shown in Table 3.3.

Table 3.2: Crumb rubber particles gradation

Sieve size (mm)	Percentage passing (%)		
	N	D	SE
1.18	100	100	100
0.6	97.1	62.2	99.2
0.3	7.7	25.0	5.5
0.212	1.9	11.3	0.8
0.15	0.6	4.5	0.2
0.075	0	0	0

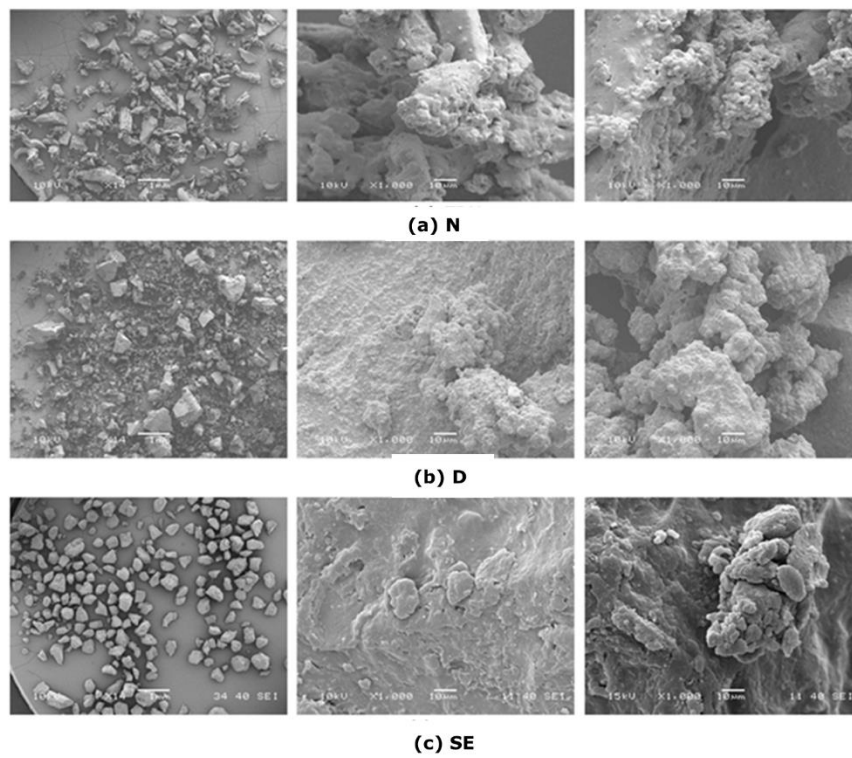


Figure 3.1: SEM images for the different crumb rubber particles

Table 3.3: Crumb rubber particles properties

Recycled Tyre Rubber RTR	Density (g/cm ³)	Grinding method	Source	Average diameter (mm)	Remarks
N	1.21	Ambient	Trucks and cars	0.30	A straight standard one
D	1.22	Ambient	Trucks and cars	0.30	Partially devulcanized
SE	1.19	Cryogenic	100% Trucks	0.30	Pre-treated with Sasobit®

3.2.2 Rubberised bitumen manufacture

A simple laboratory tool consisting of a standard Brookfield viscometer with a modified Dual Helical Impeller (DHI) shown in Figure 3.2 and Figure 3.3 were used to manufacture rubberised bitumen. This configuration allows the practical investigation of a large number of variables associated with the manufacture of rubberised bitumen while measuring viscosity in real-time. The Brookfield viscometer with DHI has a number of benefits including the precise control of mixing and testing temperature, continuous monitoring of viscosity, and the need for small quantities (10 to 15 g) of material (Celauro, Celauro et al. 2012, Lo Presti and Airey 2013, Lo Presti, Fecarotti et al. 2014). Also, it has the ability to keep the rubber uniformly distributed within the blend by creating a convective-like flow, see Figure 3.2 (Lo Presti, Fecarotti et al. 2014). The RTR-MBs were blended at different temperatures (160, 180, and 200°C) and different mixing times (60 and 140 min). The RTR-MBs produced using crumb rubber N at a processing temperature of 200°C and at the time required to reach the maximum viscosity were also characterised. The rubber percentage mass was kept constant for all RTR-MB combinations, being 18% by bitumen weight which is equal to 15.25% by weight of the total blend. This concentration was chosen based on previous studies (Celauro, Celauro et al. 2012, Wang, You et al. 2012, Lo Presti and Airey 2013) which showed that increasing the CRM content from 20% to 25% (by weight of bitumen) results in only minor changes in high temperature viscosity and low temperature stiffness. The processing conditions and rubber concentration were selected to match the commonly used specifications; ASTM D6114, CalTrans Bitumen Rubber User Guide, SABITA Manuel 19, VicRoads and APRG Report No. 19 and Austroads User Guide and previous literature (Memon 2011). Temperatures exceed 200°C were excluded due to unpleasant odours and possible hazardous fumes. The following protocol was used for each blend:

- (1) About 200g of neat bitumen (contained in a tin) was heated at 160°C in the oven for 45 minutes. The fluid test sample was then stirred and 10g of bitumen transferred into separate Brookfield viscometer tubes. The sample tubes were then placed in a sealed container to protect them against any unwanted oxidation and then left to cool down to room temperature.
- (2) Each of the sample tubes was then placed into the preheated temperature control Chamber of the Brookfield viscometer (preheated to the selected mixing

- temperature) and given 15 minutes to obtain equilibrium temperature throughout the sample.
- (3) The designed rubber quantity (1.8g to achieve the 18% rubber content by weight of bitumen) was gradually added while manually stirring the blend with a thin spatula. All the rubber was fed into the sample viscometer tube within 5 minutes.
 - (4) After that, the preheated DHI was lowered into the blend of bitumen and rubber and rotated at a constant speed of 100 rpm. Viscosity was constantly monitored throughout the mixing time. The mixing time was taken as the time from when the impeller started rotating.
 - (5) Once the designed blending time was reached, the sample container was taken out of the temperature control unit and the RTR-MB poured directly into a 10 ml vial. The vial was left to cool down to room temperature before being sealed and stored in a cold store at 5°C for future DSR testing. All rubberised binder combinations were produced using these identical conditions in order to eliminate any unwanted side effects.
 - (6) The different RTR-MBs were labelled in such a way to give information about the processing conditions and materials. For example, the code of “S-N-180-60” means, soft bitumen S blended with normal tyre rubber “N” at processing temperature of “180” °C and mixing time of “60” minutes.
 - (7) At least two replicates of each RTR-MB blend were produced and the average values are reported.

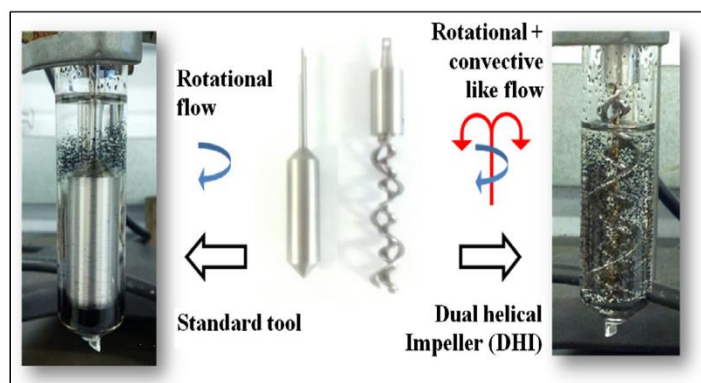


Figure 3.2: The modified Dual Helical Impeller (DHI)(Lo Presti, Fecarotti et al. 2014)

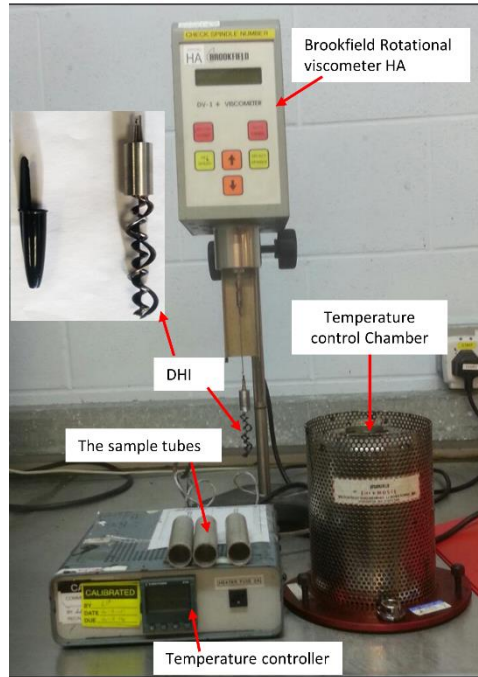


Figure 3.3: The laboratory tools used for manufacturing RTR-MBs

3.2.3 Rubber dissolution test

A gravimetric procedure was used to determine the CRM particles that dissolved into the bitumen at the different processing conditions. As all CRM particles are larger than $75\mu\text{m}$, they can be extracted using a #200 mesh ($75\mu\text{m}$) sieve, as seen in Figure 3.4. Using a #200 sieve ($75\mu\text{m}$) to determine the dissolution state of CRM particles has been proved to be a good method with high repeatability (Ghavibazoo and Abdelrahman 2013). The assumption is that particles less than $75\mu\text{m}$ can be considered to be dissolved in the bitumen rather than present in the bitumen as solid intrusions. The details of the procedure are as follows:

- (1) Approximately 3g of RTR-MB was transferred into an Erlenmeyer flask and the mass of the sample determined to the nearest 1 mg.
- (2) About 100ml of toluene was then added to the flask with continuous agitation until most lumps disappeared and the flask was then placed into a steam bath for 30 minutes.
- (3) The solution was then strained through a pre-weighed #200 ($75\mu\text{m}$) mesh and the retained insoluble rubber particles were washed with extra toluene until the filtrate flow was substantially colourless.
- (4) The #200 mesh was then heated in an oven at 110°C for 30 minutes, removed from the oven and placed in a desiccator for 30 minutes and the mass determined to the

nearest 0.1mg. The drying and weighing were repeated until constant mass was attained.

- (5) The rubber that did not dissolve into the bitumen (rubber particles $> 75 \mu\text{m}$) was calculated by taking the difference in mass between the final (containing insoluble rubber particles) and initial (clean) #200 mesh. The percent of rubber dissolution was then determined based on the initial rubber content.
- (6) Three replicates were made for each blend.



Figure 3.4: #200 mesh (75 μm) sieve used for rubber dissolution test

3.2.4 Dynamic Shear Rheometer DSR

The dynamic mechanical analysis (DMA) of the RTR-MBs was undertaken by means of a Kinexus Model Dynamic Shear Rheometer (DSR) supplied by Malvern Instruments Ltd. The RTR-MBs' samples were tested under the following settings with at least two replicates:

- Oscillatory sweep frequency (0.1 – 10 Hz)
- Strain control mode within the LVE region (less than 1% strain), amplitude sweep strain controlled tests were done to check the LVE region
- Multiple temperatures (30°C - 80°C at 10°C intervals)
- Parallel plate geometry 25mm diameter and 2mm gap to minimise the effect of rubber particles on the viscoelastic measurements [An investigation was done to check the effect of using different gaps and using 2mm gap was proved to give repeatable and reliable results for RTR-MBs, see Appendix B. The gap between parallel plates for the base bitumens is 1 mm]
- All tests were conducted on unaged samples.

In addition to the oscillatory DMA tests, the Multiple Stress Creep Recovery (MSCR) test was also conducted on the RTR-MBs using a Malvern DSR CVO Model. The test consists

of applying repeated creep-recovery cycles with 1-second applied creep shear stress followed by 9 seconds recovery period. At least two replicates were tested for each of the RMR-MBs. The test methodology follows the standard ASTM D 7405 procedure but instead of only using two shear stresses (0.1 kPa and 3.2 kPa), multiple stress levels are used to examine the stress sensitivity and nonlinearity of RTR-MBs. The following sequence was used for the MSCR test:

- Isothermal temperature of 60°C
- Seven stress levels were used (100, 400, 1600, 3200, 6400, 12800 and 25600 Pa). The sequence was designed so that there were no rest periods when changing in stress level
- Applying 10 cycles at each stress level
- Plate geometry was 25mm diameter parallel plates and 2mm gap for RTR-MBs and 1mm for the base bitumens
- All tests were conducted on unaged samples.

3.3 Viscosity monitoring analysis

Monitoring the viscosity of rubberised binders constantly as a function of processing time and the temperature is very beneficial in order to understand the actual physical change throughout the processing (production) of rubberised binders. The increase in viscosity due to adding rubber is attributed to the following factors; firstly rubber particles act as filler-modifier in the binder, secondly the swelling of rubber particles results in a reduction in the inter-particle distance, and finally stiffening of the binder occurs by reducing the oily fractions in the bitumen (absorbed by the rubber particles). Figures 3.5 and 3.6 show the viscosity progression over time for both base binders S and H, respectively; when interacting with the rubber at different temperatures. The viscosity readings from the Brookfield viscometer were recorded every 5 minutes for the first 60 minutes and then every 10 minutes for the next 80 minutes. The viscosity values for the base bitumen (binders S and H) at the three processing temperatures (values given in Table 3.1) have also been included in the plots at a time of -5 minutes which corresponds to the 5 minutes period required to manually add the rubber particles to the blend.

The results in Figures 3.5 and 3.6 show that all the RTR-MBs followed the same trend in terms of viscosity profile regardless of the type of base binder. Generally, RTR-MBs produced with non-standard pre-treated rubbers D and SE have a much lower viscosity in

comparison to binders produced with N, and that is observed for both base bitumens. The significant reduction in viscosity for rubberised bitumen produced using SE can be attributed to the special oil and FT-wax activation in addition to the grinding method. FT-wax has the ability to liquefy and significantly reduce the blending viscosity beyond its melting point (Jamshidi, Hamzah et al. 2013). This is important for pumpability and to ensure that the binder can be practically mixed and compacted with aggregate. It also seems that RTR-MBs produced with D and SE did not exhibit a significant change in viscosity during mixing at the three mixing temperatures. In contrast, the effect of mixing time and temperature is very clear on viscosity development for binders produced with the standard crumb rubber N. Therefore, the following analysis will be focusing on materials produced with N crumb rubber.

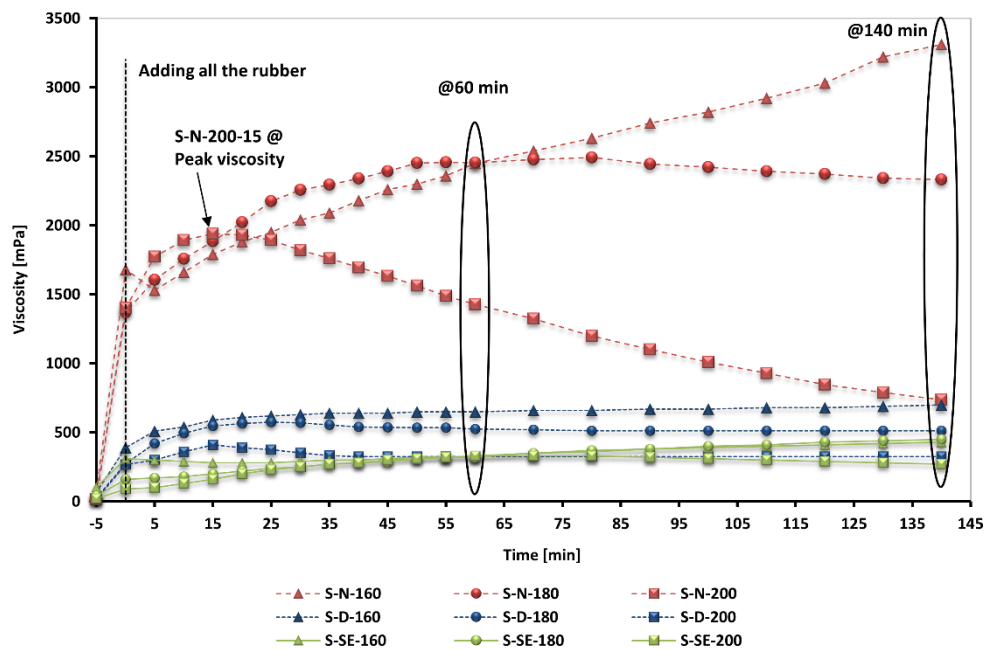


Figure 3.5: Viscosity progression over time for RTR-MBs produced using bitumen S

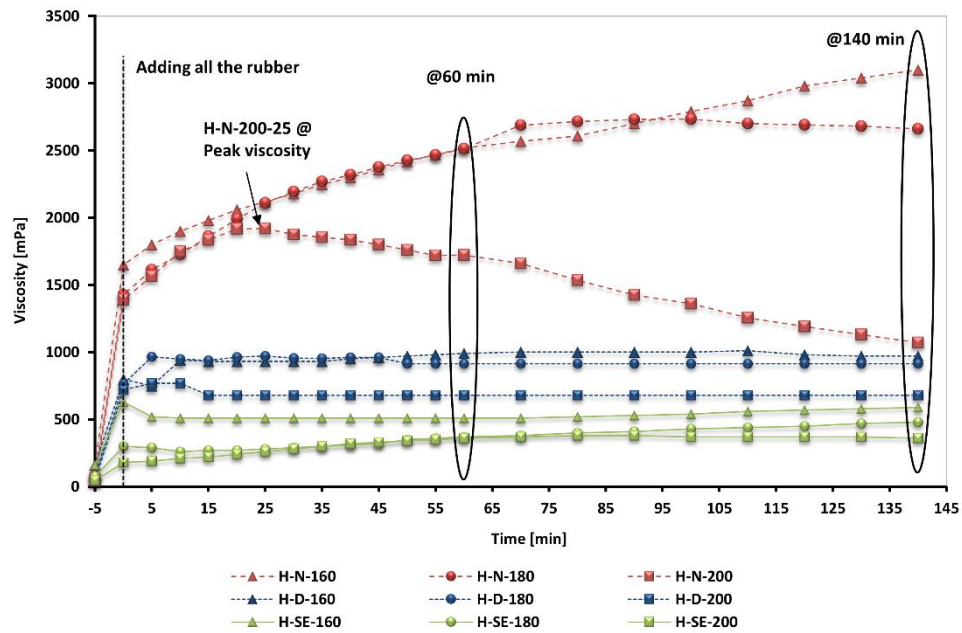


Figure 3.6: Viscosity progression over time for RTR-MBs produced using bitumen H

Three parameters corresponding to the swelling rate (increasing viscosity with time), swelling extent (time to reach maximum viscosity) and dispersion/dissolution rate (decreasing viscosity with time) are quantitatively evaluated from the viscosity progression displayed by each binder in Figures 3.5 and 3.6 and are listed in Table 3.4. The swelling rate is defined here as the rate of viscosity gain with respect to time and determined by taking the arithmetic average of tangents ($\partial v/\partial \tau$) of the viscosity progression curves (Figures 3.5 and 3.6) from the point of adding all the rubber up to the peak viscosity. The dissolution rate represents the decrease in viscosity with respect to the time and is derived by taking the slope of viscosity progression curves after reaching the peak viscosity. The results show that as the temperature increases, the rate of swelling increases (36 mPa.s/min for S-N-200 compared to 14 mPa.s/min for S-N-160) but the extent of swelling decreases (Green and Tolonen 1977, Abdelrahman 2006). In addition, the RTR-MBs processed with binder S swelled and devulcanised at a faster rate than those produced with binder H. This was more pronounced at 200°C where the swelling rate for binder S was almost double that for binder H and the time needed to reach the peak viscosity was 15 minutes compared to 25 minutes. The explanation for this is that the softer base binder (lower viscosity) with higher aromatic content has a higher rate of penetration (diffusion) into the rubber particles. The time needed to achieve a desirable swelling state and/or digestion state is significantly regulated by the processing temperature. However, production at 160°C appeared to be too low to have a significant effect on the digestion state of the rubber particles regardless of the base bitumen.

Therefore, the viscosity progression of binders produced at 160° was at a constant increase during the entire 140 min of mixing.

Table 3.4: Quantitative parameters associated with the interaction process

Code	Swelling rate (mPa.s/min)	Swelling extent (min)	Dissolution rate (mPa.s/min)	Peak viscosity mPa.s	Final viscosity mPa.s @140min
S18TR-N-160°	14	----	----	3310	3310
S18TR-N-180°	17	80	2.7	2492	2331
S18TR-N-200°	36	15	9.6	1940	737
H18TR-N-160°	12	----	----	3100	3100
H18TR-N-180°	16	90	1.8	2730	2660
H18TR-N-200°	21	25	7.4	1920	1070

The viscosity of all rubberised binders, blended using bitumen S and crumb rubber N at the end of the mixing time (140 minutes) for each mixing temperature, was measured at three temperatures (160, 180 and 200°C) in order to evaluate the influence of a constant test temperature on the final viscosity of the rubberised binders as shown in Table 3.5. The viscosity results in Table 3.5 show that binders produced at 180°C and 200°C have a lower viscosity than those produced at 160°C due to the devulcanisation and depolymerisation of the rubber particles at these higher processing temperatures.

Table 3.5: The viscosity of RTR-MBs produced using bitumen S measured at different temperatures using the modified impeller (Dual Helical Impeller DHI)

Test temperature	Rotational viscosity (mPa.s)		
	S18TR-N-160-140	S18TR-N-180-140	S18TR-N-200-140
160 °C	3220	2950	1810
180 °C	2520	2270	1190
200 °C	1940	1480	740

The effect of the devulcanisation and depolymerisation of the rubber particles on the overall viscosity of rubberised binders can be explained qualitatively by applying the equation derived by Einstein for the viscosity of a dilute suspension of rigid spheres (Glover, Davison et al. 2000):

$$\eta = \eta_{(s)} (1 + \eta' \cdot \phi) \tag{Equation 3.1}$$

Where η is the bulk viscosity of the matrix, $\eta_{(s)}$ is the viscosity of the solvent, η' is the intrinsic viscosity. η' is empirically linked to the particle properties such as size, shape and rigidity and also particle interaction with the interstitial fluid, and ϕ is the volume fraction

of the spheres. It should be mentioned that the Einstein equation is able to accordingly represent suspensions with low concentrations where the distance between particles is much bigger than the filler radius, while the Frankel equation is able to predict the viscosity behaviour of suspensions with high concentrations (Hesami, Jelagin et al. 2012).

For rubber particles processed at 200°C, there is a reduction in rubber particle size as will be demonstrated by the dissolution test results. This leads to a lowering of the effective volume fraction ϕ and therefore a decrease in the matrix viscosity η . Although, the liquid phase viscosity $\eta(s)$ would definitely increase due to the polymeric components (<75 μ m) being released from the rubber particles and becoming dissolved in the base binder, their relative effect is very small compared to the particulate effect. Support for this conclusion can be found in work undertaken by Thodesen and his co-workers (Thodesen, Shatanawi et al. 2009) which revealed that the effect of rubber particles on viscosity, when considered as an inert filler, is 12 times greater than the effect of rubber dissolved in the base bitumen (rubber-bitumen interaction).

Although, increasing the binder viscosity at high in-service temperature is favourable to improve rutting resistance, high viscosity at mixing and compaction temperatures imposes large difficulties in the production of asphalt mixtures. Controlling the volumetric properties of these asphalt mixtures becomes extremely challenging resulting in high air voids, or to counter this, excessively high mixing temperatures are required which could cause emission problems and further harden the bitumen. The reduced viscosity of RTR-MBs processed at (200°C-140min) could be beneficial at mixing and compaction temperatures; however, the lower degree of modification of the final product would be a concern in the final asphalt mixture.

Many researchers have demonstrated that the optimum blending time to give the most desirable material (good rutting resistance) is the time at which the viscosity reaches its peak (Kandhal 1992, Memon 2011, Celauro, Celauro et al. 2012, Lo Presti and Airey 2013). However, in the following sections of this Chapter, a more detailed rheological assessment of the final RTR-MBs will be undertaken to prove or disprove this assumption.

3.4 Rubber dissolution

Figure 3.7 shows the average crumb rubber dissolution results for the six processing combinations of 3 temperatures and 2 mixing times and for both base binders S and H. The range bars represent the maximum and minimum values for the replicates. It can be seen that

rubber dissolved into the bitumen is strongly dependent on the processing conditions. As the processing temperature increases, the dissolution percent of rubber particles increases. A similar trend can also be found with increasing processing time. The effect of time on the dissolution increased with an increase in mixing temperature. For example, increasing the processing time from 60 to 140 minutes at 200°C led to a considerable amount of rubber being dissolved for binders produced using crumb rubber N. The difference between the effect of the three types of crumb rubber on the dissolution percentages is apparent for both base binders. Generally, the rubberised bitumen produced using SE had the greatest dissolution percent almost at all processing conditions except 200°C-140min. The results also show that softer bitumen S is somewhat better at dissolving the rubber than stiffer bitumen H due to its higher rate of diffusion into rubber. However, at higher processing conditions (200°C-140min), the effect of base binder on dissolution percentage was significantly reduced as the influence of temperature and extended processing time (reduced cross-link density of the rubber) is far greater than the effect of the base binders.

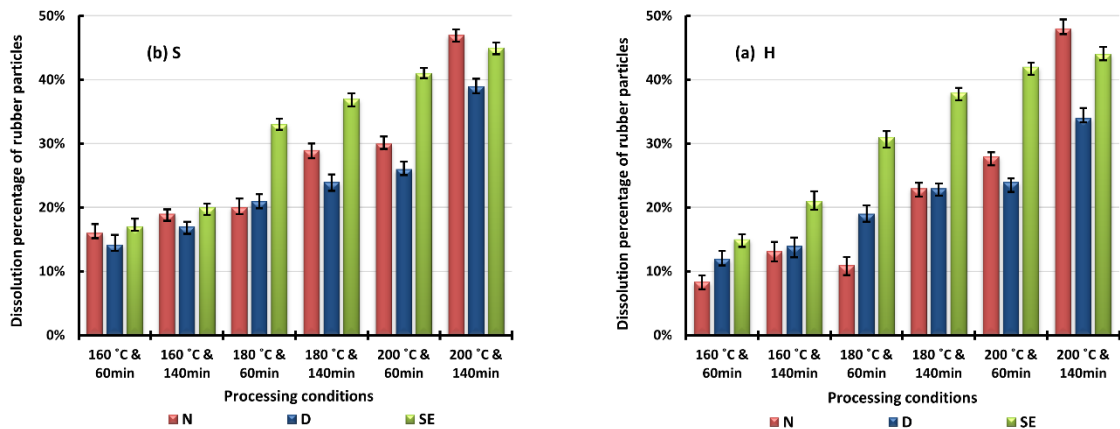


Figure 3.7: Rubber dissolution percentage (a) crumb rubber interacting with bitumen S and (b) crumb rubber interacting with bitumen H

3.5 Dynamic Mechanical Analysis (DMA)

3.5.1 Master Curves

It is important to evaluate the rheology and viscoelastic properties of the final RTR-MBs under different loading times and temperatures. This has been achieved by means of DMA to define the stress-strain-time-temperature response of the binders. Master curves of complex modulus $|G^*|$ at a reference temperature of 30°C were produced for the RTR-MBs using the Time-Temperature Superposition Principle (TTSP) and William, Landel and Ferry (WLF) equation. Figure 3.8 shows the master curves for the RTR-MBs produced using

binder S while Figure 3.9 shows the data for binder H. For brevity, the binder H-SE was not tested for DMA and MSCR tests as the results of viscosity showed that the processing conditions did not alter significantly the properties of binders produced using rubber SE.

It is clear from Figures 3.8 and 3.9 that the processing (mixing) conditions have influenced the final properties of the RTR-MBs. The master curves show that rubber modification has resulted in a significant increase in the complex modulus at low frequencies (equivalent to high-temperature response) and consequently the RTR-MBs can be expected to have enhanced rutting behaviour. This increased stiffness can be attributed to the prevalence of the rubber (polymer) network formation which is stiffer and more elastic than the viscous phase of the base binders (Airey, Singleton et al. 2002, Navarro, Partal et al. 2005). The rubber modification is less effective within the base bitumen dominant areas (low temperatures and high frequencies) and the curves tend to coincide at high frequencies, particularly for the RTR-MBs processed with H bitumen. However, Figure 3.8 (c) shows that the modification of SE with soft bitumen S at high frequencies was very clear and significant in comparison to other rubber types. The increase in the complex modulus for S-SE blends within the base bitumen dominant areas can be due to the effect of FT-wax. The FT-wax forms a crystal lattice structure in the modified binder at temperatures lower than its melting point and stiffens the modified binder (increasing the viscosity) at low and intermediate temperatures (Jamshidi, Hamzah et al. 2013).

In terms of the effect of production conditions, it can be observed that RTR-MBs produced using crumb rubber N were more sensitive to the processing conditions than others produced using D and SE crumb rubbers. Also, for binders produced using D and SE crumb rubbers, the effect of varying processing conditions on the viscoelastic properties followed different trends from binders produced using the standard crumb rubber N. Increasing the processing conditions to (200°C-140min) led to a substantial reduction in complex modulus within the rubber dominant areas (high temperatures and low frequencies) for binders produced with crumb rubber N. Meanwhile a different trend seen for binders produced using D and SE, i.e. the complex modulus was increased when the processing conditions increased to 200°C-140min. The reduction in complex modulus is believed to be due to the partial degradation of the polymer network by means of depolymerisation and devulcanisation (Abdelrahman and Carpenter 1999, Attia and Abdelrahman 2009). Additionally, the lighter components which were absorbed by the rubber during the swelling process might have been released back into the liquid phase of the bitumen during the depolymerisation/devulcanisation

process and further decreased the complex modulus (Abdelrahman and Carpenter 1999). On the other hand, the higher processing conditions caused oxidative age hardening of base bitumen and increased complex modulus for binders produced using D and SE crumb rubbers, but this effect was not as dominant as the depolymerisation and devulcanisation in the case of crumb rubber N. These binders can be considered to be over processed. However, these processing (mixing) conditions have reduced the complex modulus at low temperatures and high frequencies relative to the other conditions which may be desirable for fatigue and low temperature cracking resistance.

The results also show that the RTR-MBs processed at 160°C and 60 minutes have lower complex modulus demonstrating a lower degree of swelling (under processed). There are no significant differences for the other processing (mixing) conditions in terms of the $|G^*|$ master curves.

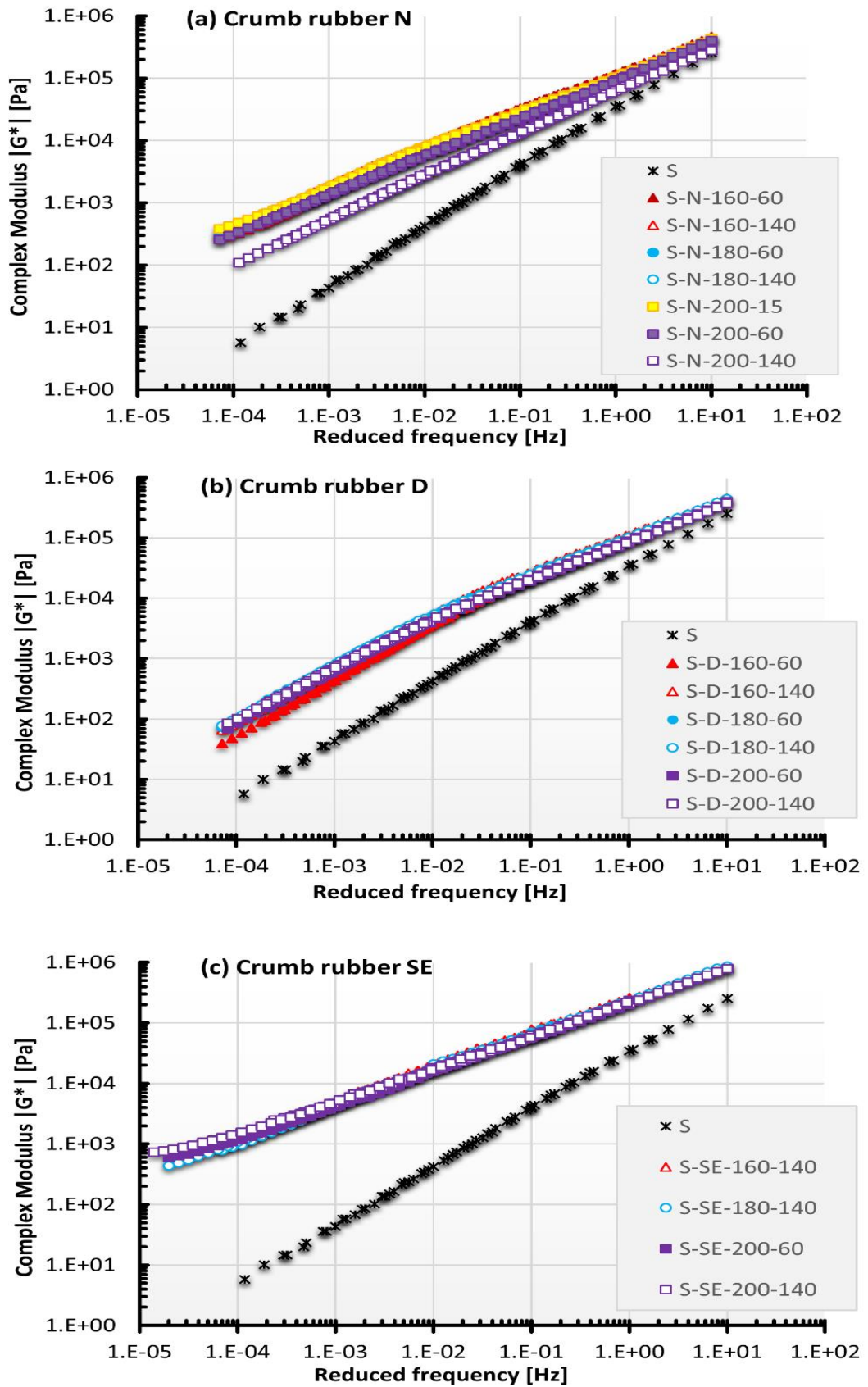


Figure 3.8: Master curves at 30 °C reference temperature for RTR-MBs produced using bitumen S blended with different crumb rubbers and at different processing conditions

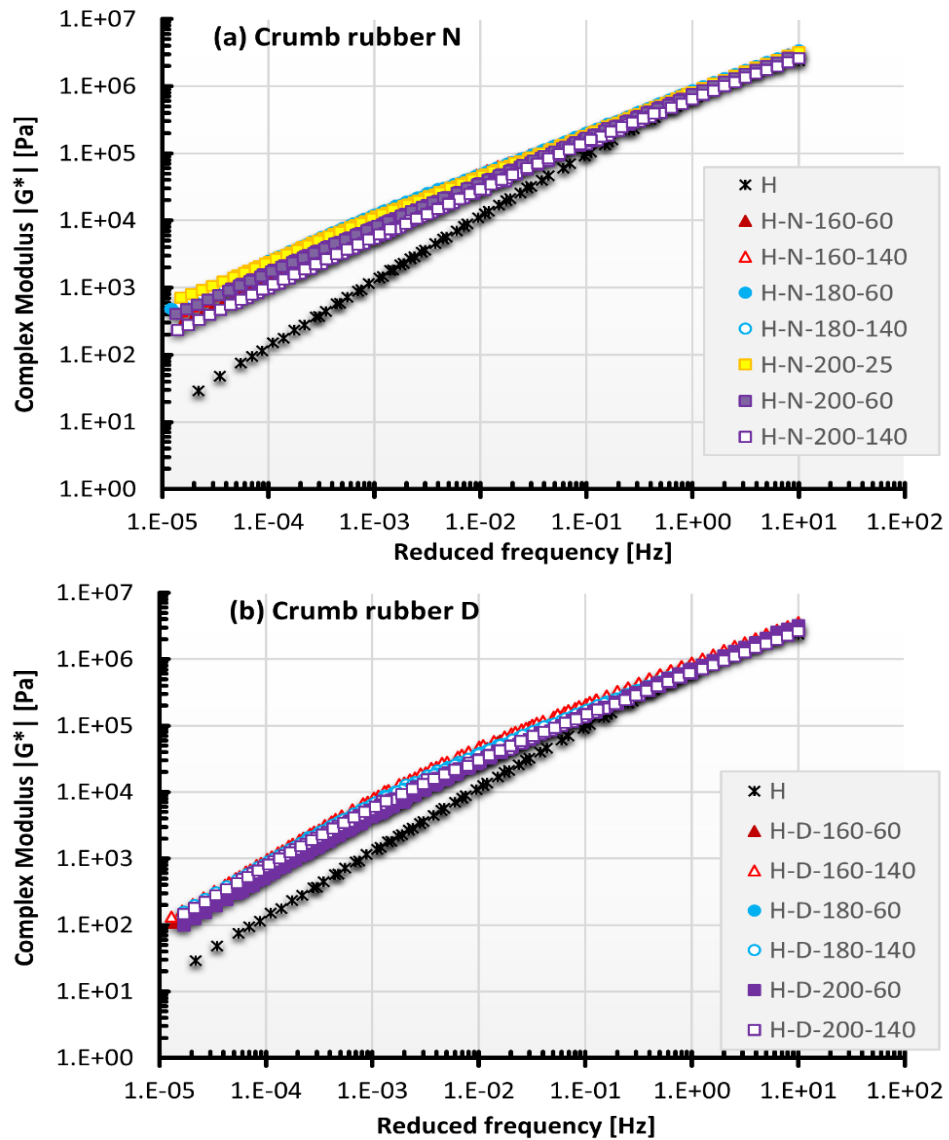


Figure 3.9: Master curves at 30 °C for RTR-MBs produced using bitumen H blended with different crumb rubbers and at different processing conditions

3.5.2 Black Diagrams

Black diagrams can be used to show the relation between stiffness and viscoelasticity of materials without the need to apply shift factors to the raw data as required for master curves (Airey 2002). Therefore, the presence of the polymer structure within the RTR-MBs and their thermo-rheological properties can be conveniently distinguished in one plot. Figures 3.10 and 3.11 show a clear shift for the RTR-MBs to lower phase angles (improved elastic response) and slightly higher complex modulus compared to the base bitumens. The increased complex modulus with decreased phase angle at higher temperatures can be attributed to the addition of rubber particles and the establishment of a rubber (polymer) rich phase. The complexity and the different patterns of RTR-MBs Black curves demonstrate the

sensitivity of phase angle measurements to the microstructural modifications and chemical structure that have been imparted by the addition of rubber.

Each rubberised bitumen produced with each type of crumb rubber has its own distinctive plot. For example, RTR-MBs produced using crumb rubber N and H binder formed a typical 3-shape curve, while with S binder formed an incomplete 3-shape. For RTR-MBs produced using SE crumb rubber, the black diagrams tend to be scattered and discontinuous, providing clear evidence of FT-wax presence and the formation of a lattice structure in the modified bitumen. The modification level of rubberised bitumens produced using D crumb rubber was not significant within the polymer rich phase as seen by their black diagrams (higher phase angle measurements in comparison to others), demonstrating inferior viscoelastic properties.

The Black curves of RTR-MBs produced using the straight crumb rubber N show a significant change in shape when higher processing conditions (200°C-140min) are used. They become less curved and shift to higher phase angles. This suggests that processing at higher temperatures and extended times results in a certain amount of rubber being dissolved/dispersed into the base bitumen (as shown in the dissolution tests) leading to the production of a more compatible material that has a smoother transition from solid-like to liquid-like behaviour. The results of S-N and H-N RTR-MBs also show that at blending times corresponding to the maximum swelling extent (200°C-15min and 200°C-25min) they have the lowest phase angles within the rubber dominant areas (high temperatures and low frequencies). On the other hand, the Black curves associated with RTR-MBs S-N and H-N produced at low processing conditions (160°C-60min) are more complex and also have higher phase angles. The higher phase angles of these products in comparison to other conditions can be attributed to the higher amount of light fractions still within the bitumen as the undissolved rubber particles were not completely swelled.

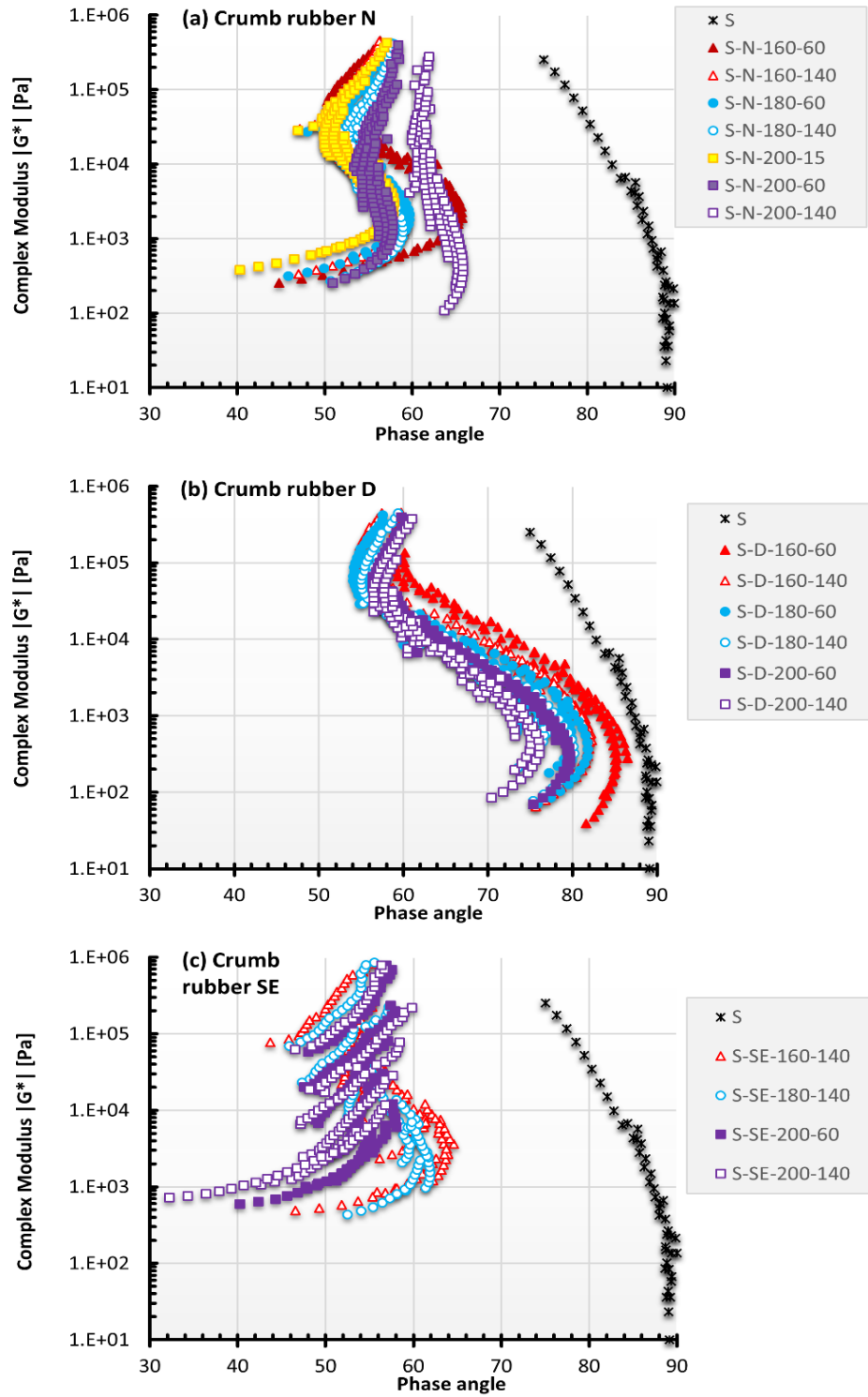


Figure 3.10: Black diagram of RTR-MBs produced using bitumen S blended with different crumb rubbers and at different processing conditions

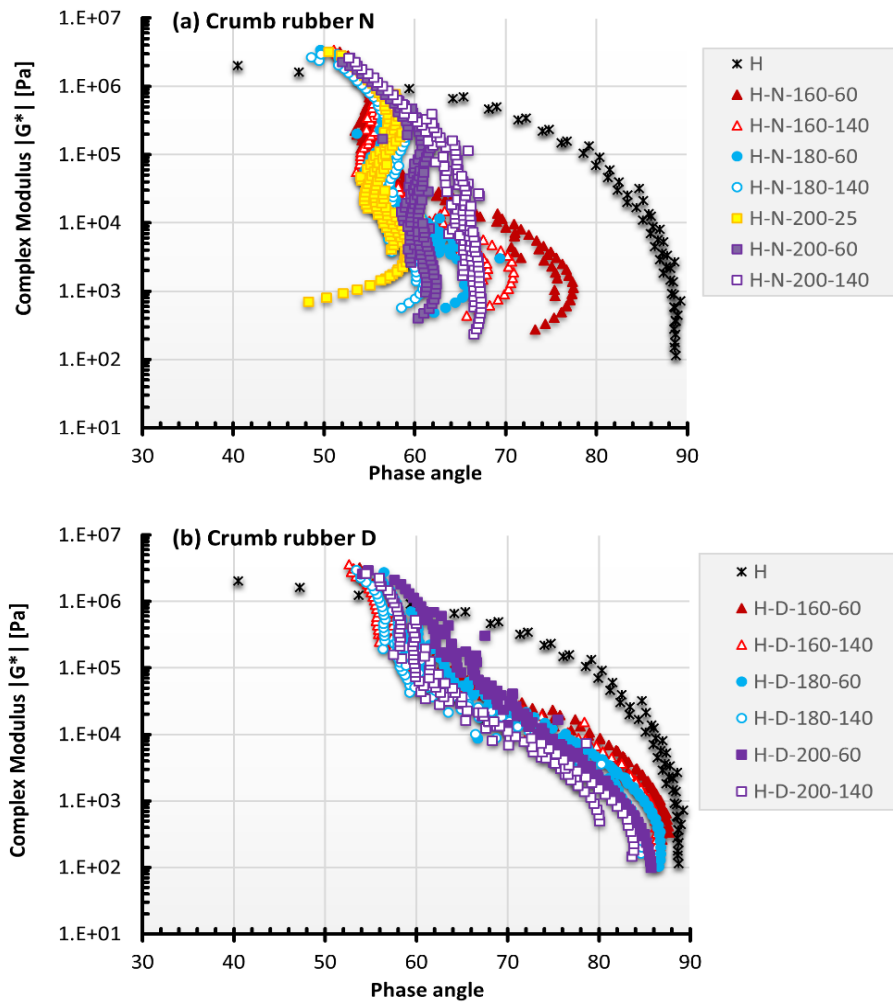


Figure 3.11: Black diagram of RTR-MBs produced using bitumen H blended with different crumb rubbers and at different processing conditions

3.5.3 Temperature Susceptibility

The evolution of the loss tangent with temperature is also used here to examine the effects of processing conditions on temperature susceptibility of RTR-MBs. An extended plateau region or flattening of the $\tan\delta$ curves over a wide range of intermediate temperatures is desirable for better temperature susceptibility (González, Munoz et al. 2006, Nejad, Aghajani et al. 2012). A reduction in temperature susceptibility is important to produce a material that is able to resist rutting at high temperatures while maintaining good fatigue cracking resistance (González, Munoz et al. 2006).

Previous analyses showed that altering the processing conditions has a significant effect on the viscoelastic properties of RTR-MBs produced using crumb rubber N. Therefore, this section will only present the results of materials produced using crumb rubber N. Figures 3.12 and 3.13 show the $\tan\delta$ values over a range of temperatures between 30 and 80°C at a

constant frequency of 1Hz. The range bars represent the maximum and minimum of values of $\tan\delta$ for different replicates.

It can be seen that processing conditions of (180°C-140min), (200°C-60min) and (200°C-15, 25min) have produced materials with the lowest temperature susceptibility as indicated by their flat curves. Although higher processing (200°C-140min) resulted in comparatively higher $\tan\delta$ values, these binders still demonstrated good temperature resistance properties as shown by the low slope of their $\tan\delta$ versus temperature relationship. The RTR-MBs produced at the low-temperature processing condition of 160°C showed the largest change in $\tan\delta$ over the range of temperatures and therefore the poorest temperature susceptibility. Even though the base binder H is stiffer and more elastic than S, the RTR-MBs produced using the soft bitumen S generally had lower $\tan\delta$ values than RTR-MBs produced using the hard bitumen H. This can be attributed to the difference in swelling and dissolution mechanisms of rubber with the S binder being more compatible with the crumb rubber particles and the modification being more dominant.

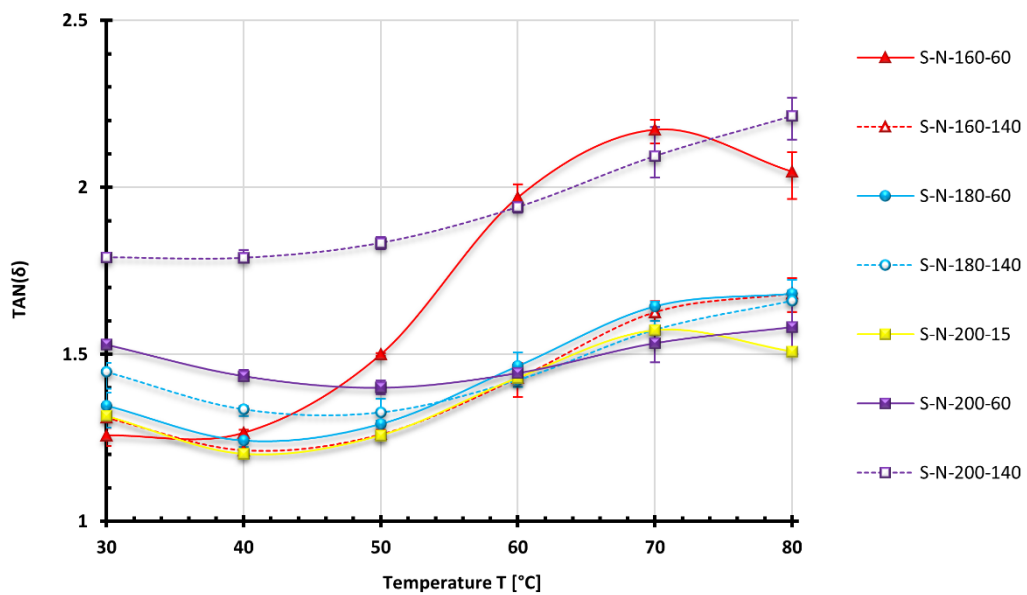


Figure 3.12: $TAN(\delta)$ at 1Hz of RTR-MBs produced using bitumen S and crumb rubber N

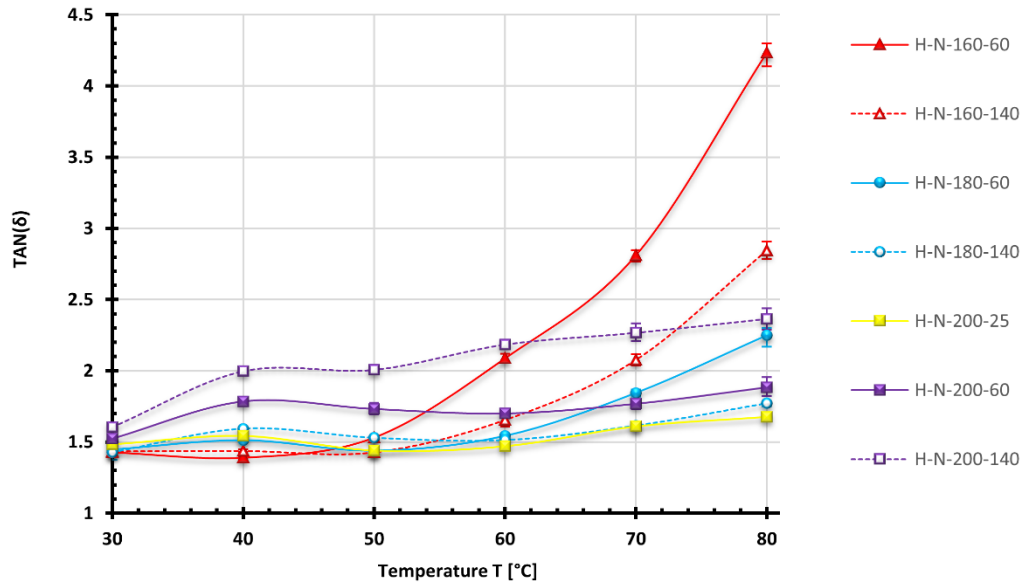


Figure 3.13: TAN(δ) at 1Hz of RTR-MBs produced using bitumen H and crumb rubber N

3.6 Multiple Stress Creep and Recovery (MSCR)

The testing and analyses of the previous section (3.5) have dealt with the properties of materials within a linear viscoelastic region. The MSCR test was conducted in order to understand more about the behaviour of materials at high stresses that are outside the linear viscoelastic region. The performance of base bitumens (H and S) is given in Table 6.3 in terms of J_{nr} and recovery percentage. It was not possible to test the soft base bitumen S at 60°C as it tended to fail when the stress increases above 3.2kPa.

Table 3.6 The MSCR properties of base bitumens

Stress level [kPa]	S @ 50°C		H@ 60°C	
	J_{nr} [1/kPa]	Recovery %	J_{nr} [1/kPa]	Recovery %
0.1	2.25102	5.136461	1.24968	5.206206
0.4	2.26278	4.306556	1.253655	4.420258
1.6	2.3307	2.745458	1.269188	3.46615
3.2	2.4198	1.528114	1.297313	2.363053
6.4	2.550375	0.896821	1.332666	1.33996
12.8	2.718984	0.451503	1.380094	0.814969
25.6	6.337781	0	1.736906	0.358032

3.6.1 Non-recoverable compliance (J_{nr})

J_{nr} has the ability to predict the improvement that is brought by modification, it is also more sensitive to the stress dependency of modified binders making it suitable for specification purposes for both neat and modified bitumen (D'Angelo 2009, Tabatabaee and Tabatabaee 2010). Figures 3.14 and 3.15 show the results of J_{nr} (average value for the 10 creep and

recovery cycles) over a wide range of stresses between 100 Pa and 25,600 Pa at a test temperature of 60°C. The results clearly highlight the significance of stress dependency in RTR-MBs being more apparent in materials processed using the crumb rubber SE. The RTR-MBs processed using the hard bitumen H were less dependent on the stress with values of J_{nr} being relatively stable up to a stress level of approximately 1.60 kPa after which there is evidence of an inflection point in the material response and the presence of non-linearity at the higher stress levels.

The J_{nr} also captured the effects of processing conditions. The materials produced using crumb rubber N at processing conditions of (180°C-140min), (200°C-15min) and (200°C-25min) all performed very well as indicated by their low J_{nr} values. Good results were also seen for rubberised bitumens with the soft bitumen S and crumb rubber N at (180°C-60min) and (160°C-140min). The higher J_{nr} values of the S-N and H-N binders produced at high processing conditions (200°C-140min) indicated that these conditions lead to breaking some of the cross-linking rubber (polymer) network by means of devulcanisation and depolymerisation. At the other extreme, higher J_{nr} values at low processing conditions of (160°C-60min) of the same materials suggest incomplete interaction (insufficient swelling) between rubber particles and base binder. The results of J_{nr} for materials produced using crumb rubber D showed a different trend where the J_{nr} was decreased at high processing conditions (200°C-140min).

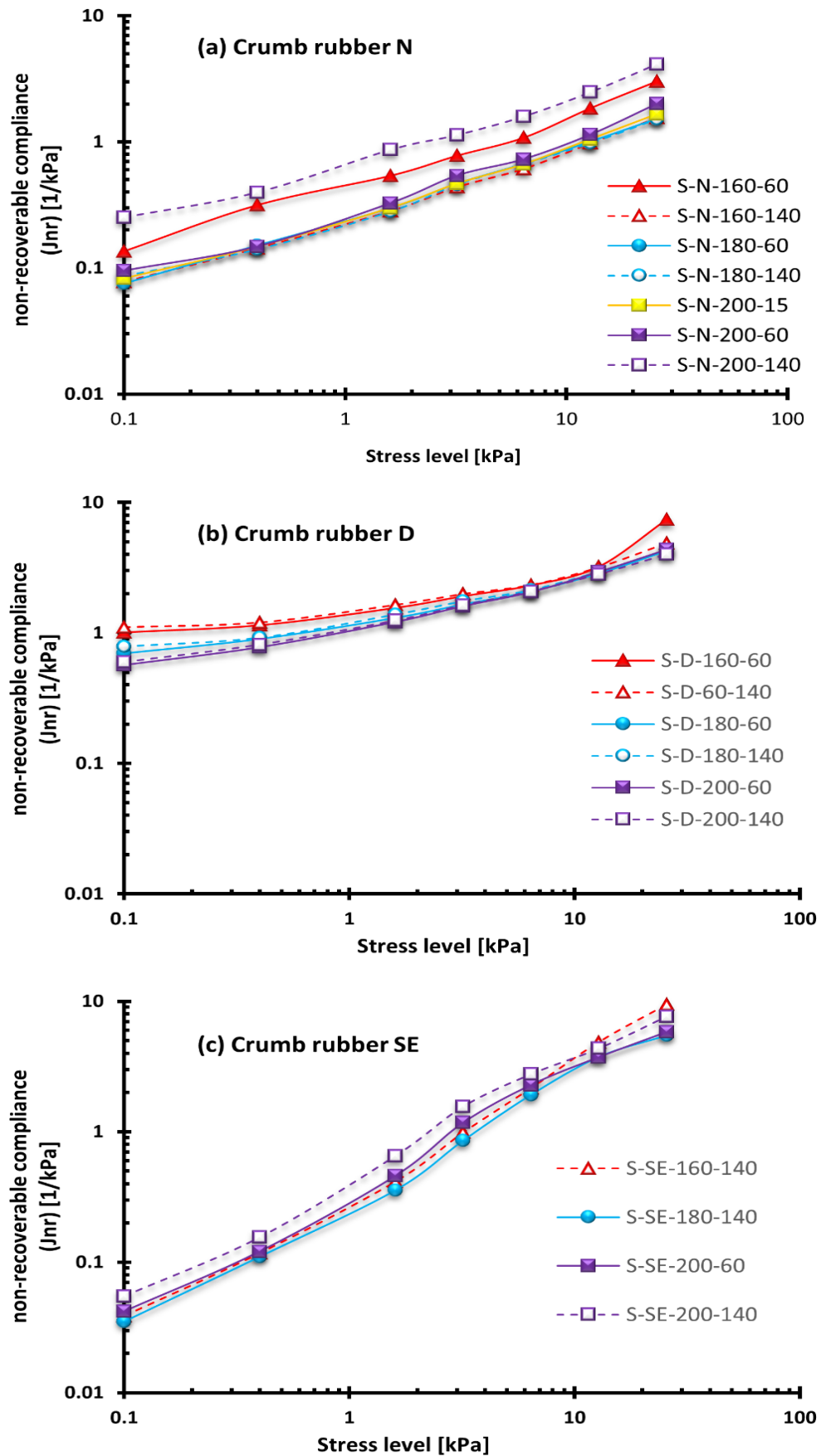


Figure 3.14: J_{nr} of RTR-MBs produced using bitumen S

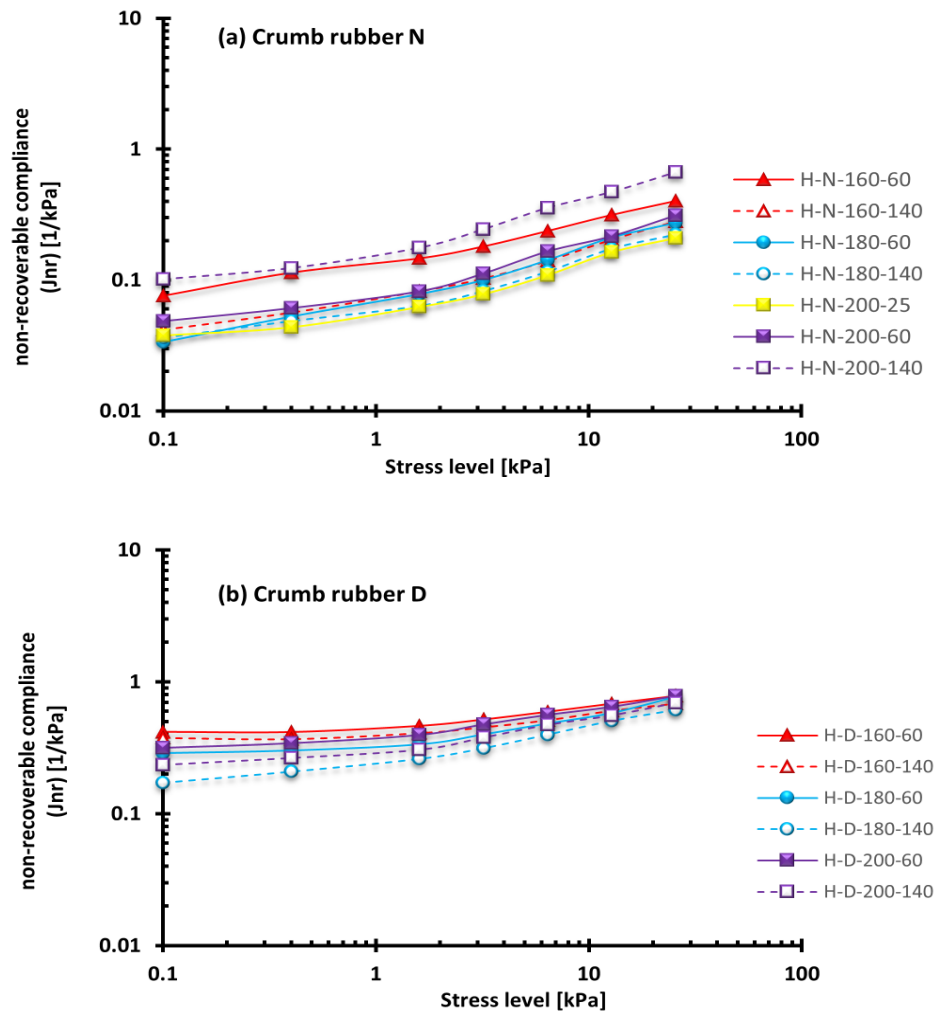


Figure 3.15: J_{nr} of RTR-MBs produced using bitumen H

3.6.2 Percentage recovery

Providing information about elastic recovery in addition to the non-recoverable compliance, stress sensitivity and non-linearity behaviour of modified bitumens is another advantage of performing the MSCR test. The average percentage recovery of 10 cycles at three stress levels (0.1, 3.2 and 6.4 kPa) is presented in Figures 3.16 and 17 with the error bars denoting the standard deviation of the 10 cycles. It can be seen that materials produced with crumb rubber N maintained excellent recovery response over the wide range of stresses. On the other hand, poor recovery results were associated with RTR-MBs produced using crumb rubbers D and SE. Although the materials produced using crumb rubber SE showed superior recovery percentage at small stress (0.1 kPa), their recovery diminished considerably at higher stresses.

The results show that materials produced using crumb rubber N processed at (180°C-140min) and (200°C-60min) had the highest elastic response compared to the other binders

produced at other conditions. Additionally, these conditions maintained a high elastic recovery across all the stress levels. For RTR-MBs produced using crumb rubber D, processing at 200°C with the base bitumen S gave the best recovery while with the base bitumen H processing at (180°C-140min) gave the highest recovery. It can be seen that as the stress level increased, the relative difference in recovery response of different materials became more significant.

In terms of the effect of the base binder, the different processing conditions modified the binders in the same trend with the only difference being that RTR-MBs produced using soft bitumen failed to maintain high elastic response at higher stresses compared to the H bitumen. A limit of 15% reduction in the percentage of recovery from 0.1 to 3.2 kPa is considered acceptable for modified bitumen that has a good elastomeric response (Morea, Marcozzi et al. 2012). Thus, only binders processed using bitumen H and crumb rubber N at (180°C-140min) and (200°C-60min) fulfilled the 15% maximum specification which could be translated into a better rutting resistance. The results also highlight that characterising the material within only the linear viscoelastic region is not enough for an appropriate material ranking. Figure 3.18 is used by AASHTO TP 70-13 as an indicator of the presence of an acceptable elastomeric polymer. The average percentage recovery at 3.2 kPa, versus the average non-recoverable creep compliance at 3.2 kPa was plotted on the graph. All the RTR-MBs produced using crumb rubber N fell above the line indicating an acceptable elastomeric polymer except those produced at (160°C-60min). On the other hand, all binders produced using crumb rubber D or SE failed to fulfil the AASHTO TP 70-13 requirements.

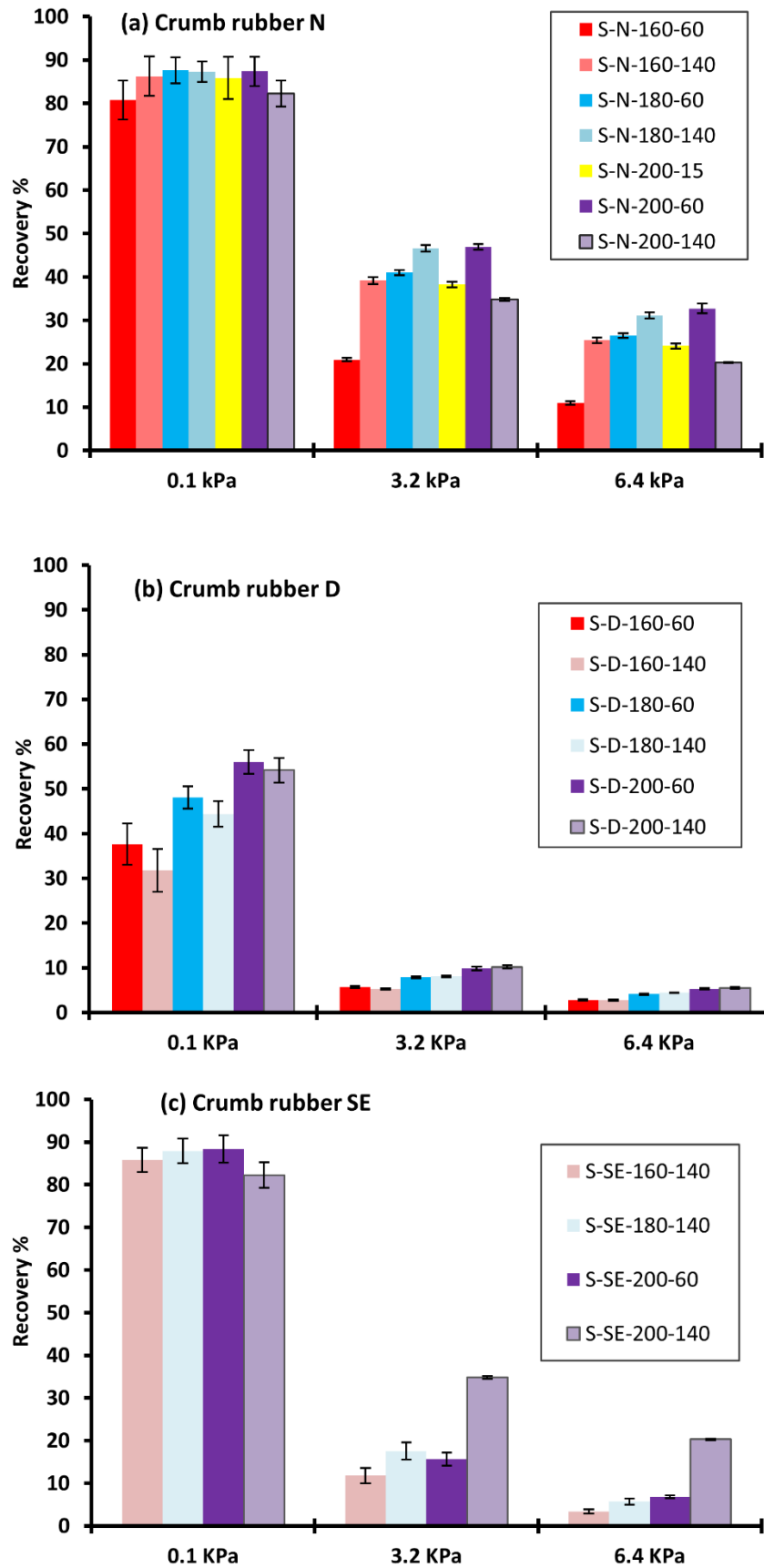


Figure 3.16: Recovery of RTR-MBs produced using bitumen S

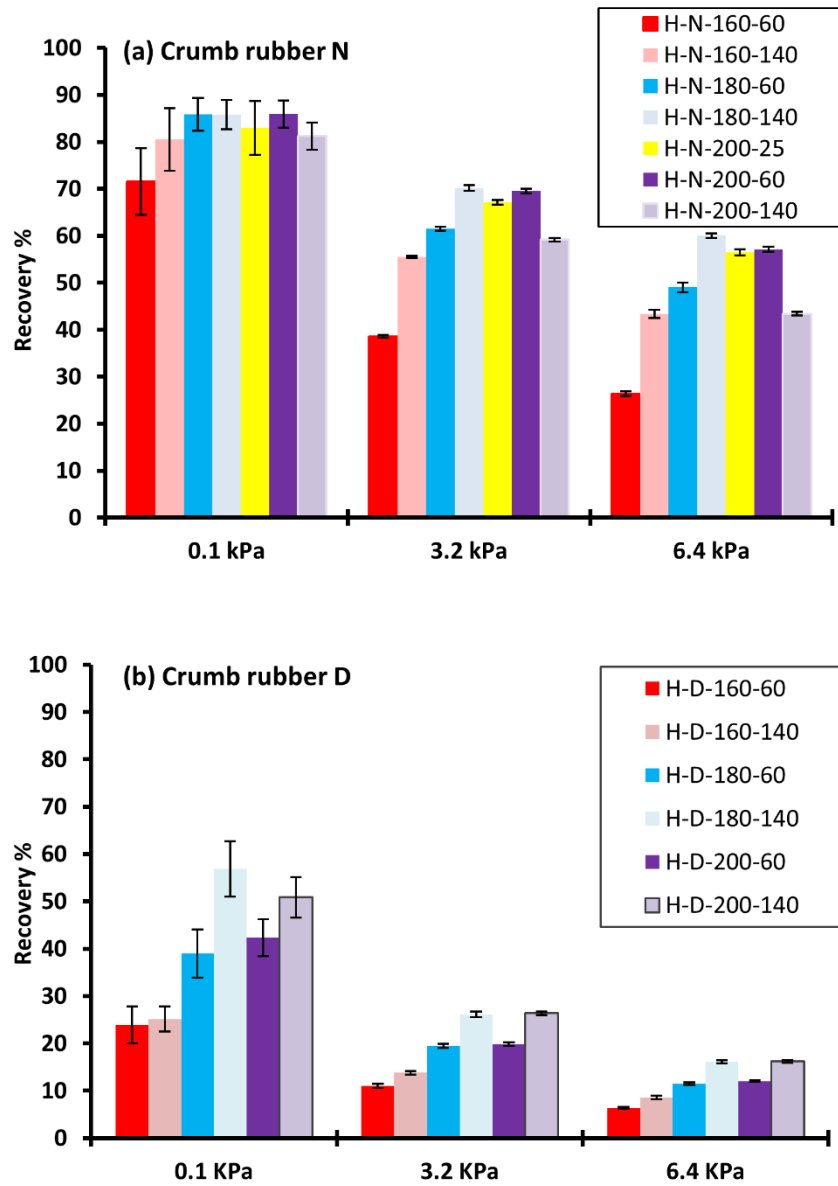


Figure 3.17: Recovery of RTR-MBs produced using bitumen H

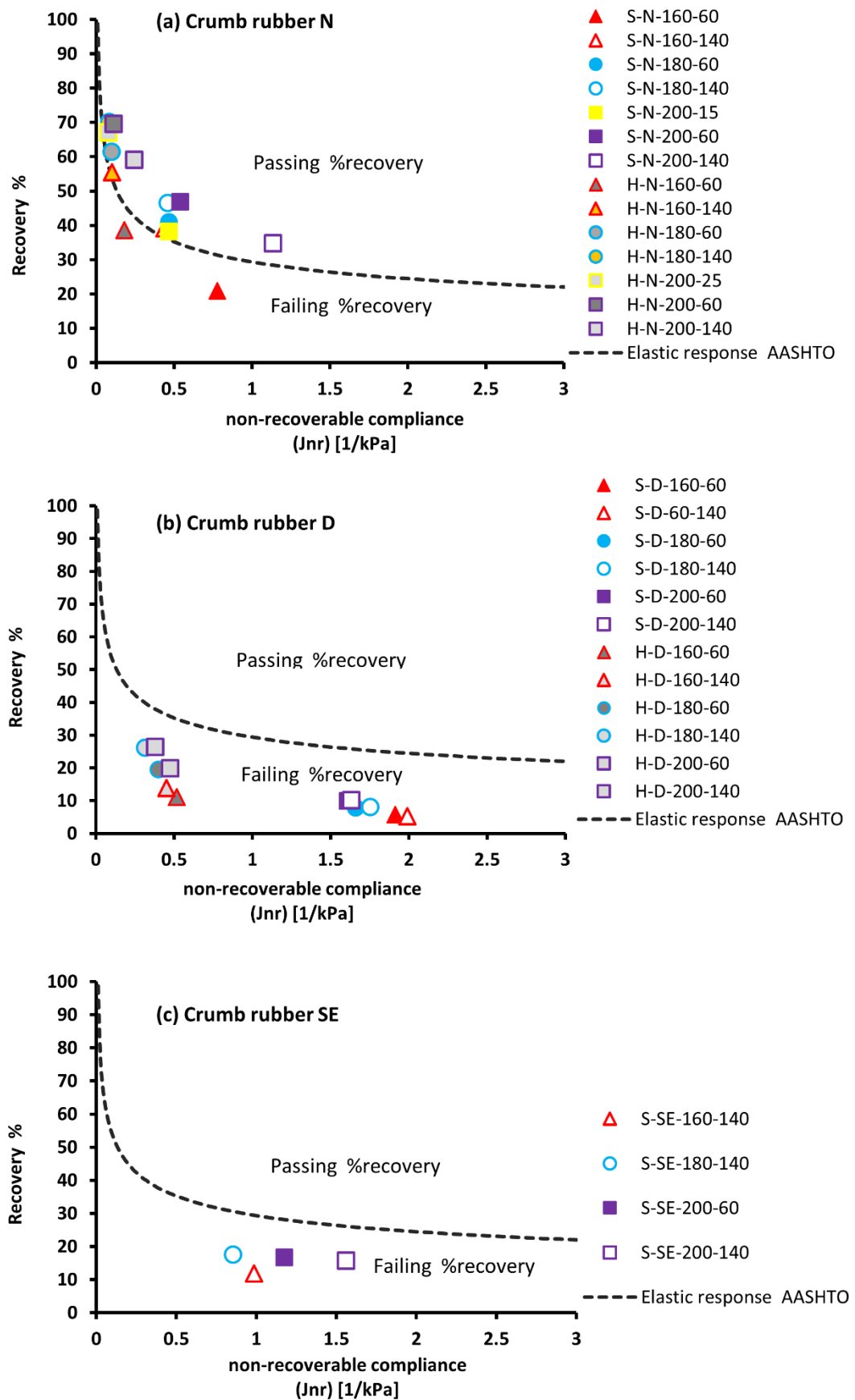


Figure 3.18: The elastic response of RTR-MBs produced using bitumens S and H

3.7 Summary and Conclusions

RTR-MBs were successfully produced in the laboratory by using the Brookfield rotational viscometer and a modified impeller (Dual Helical Impeller (DHI)) that allowed a reliable control of the blending temperature as well as keeping the rubber particles evenly dispersed throughout the production process. Three mixing temperatures (160°C, 180°C and 200°C) and two mixing times (60 and 140 minutes) were used to produce the different binders which all consisted of 18% CRM by bitumen mass. Two additional mixing times (15 and 25 minutes) were also included at 200°C as these times were associated with the peak viscosities for RTR-MBs produced using crumb rubber N. The rheological properties of the final product were determined by means of standard Dynamic Mechanical Analysis (DMA) oscillatory and Multiple Stress Creep Recovery (MSCR) testing using a dynamic shear rheometer (DSR). The main conclusions that could be drawn based on the laboratory investigations in this Chapter are:

- (1) The tools used to produce RTR-MBs give an excellent opportunity to effectively investigate the many variables associated with the manufacturing of RTR-MBs using minimum material consumption for laboratory needs
- (2) The RTR-MBs' properties are largely dependent on their manufacturing conditions; therefore, carefully assessing these variables is essential to develop better materials. Based on the findings of this study, processing the RTR-MBs at low temperature ~160°C was not appropriate for developing high-performance binders. On the other hand, processing conditions of (180°C-140min), (200°C-15, and 25min) and (200°C-60min) gave the most desirable properties for RTR-MBs manufactured using crumb rubber N. The results of crumb rubber D indicated that these materials should be processed at high temperature, i.e. 200°C.
- (3) Selecting higher mixing temperature (200°C) can significantly reduce the time needed to reach the maximum swelling extent for binders produced using crumb rubber N. This also develops superior rheological properties and potential saving in energy consumption
- (4) The results also highlight that selecting materials based only on the linear viscoelastic region properties is not sufficient and in some cases might be misleading. Therefore, characterising the non-linear behaviour in addition to linear is essential for an appropriate materials selection.

- (5) Optimising the blending variables based only on the highest viscosity does not always guarantee the best performance materials. Using rheological testing within and outside the LVE region has helped increase understanding of the material and hence optimise effectively the processing conditions.
- (6) The RTR-MBs produced using crumb rubber D showed the poorest elastic network within the bitumen compared to N and SE, as seen by their increased phase angle.

Chapter 4 RTR-MBs Manufactured Using High Shear Mixer

4.1 Introduction

The amounts of RTR-MBs produced in chapter 3 were only adequate for DSR testing. Therefore, the Silverson L4RT High Shear Mixer was used to produce RTR-MBs at a larger scale for future testing. The results from the previous chapter, for evaluating the effect of blending conditions on rheological properties of RTR-MBs, demonstrated that blending at low temperature ($\sim 160^{\circ}\text{C}$) did not promote sufficient swelling between rubber and base bitumen. Hence, inferior mechanical properties were associated with RTR-MBs blended at 160°C . At the other extreme, utilising very high mixing temperature ($\sim 200^{\circ}\text{C}$) resulted to some extent in breaking the polymeric network of rubber. In addition, there is an increasing concern about the effects of processing materials at high temperature on worker health and safety. Thus, the optimum mixing temperature was selected to be 180°C . It should be mentioned that because the applied shear energy in the High Shear Mixer is different from that in the low shear Brookfield Viscometer, the mixing time needs to be evaluated and then optimised in order to produce RTR-MBs with desirable mechanical properties. Many studies have been conducted to investigate the effect of blending device, i.e. shear rate and impeller geometry on the physical properties of the blend (Navarro, Partal et al. 2007, Memon 2011, González, Martínez-Boza et al. 2012). Navarro, Partal et al. (2007) stated that processing device and impeller geometry have a negligible effect on the physical properties of rubberised bitumen. González, Martínez-Boza et al. (2012) also showed that the gap between

rotor and stator of the blending device seemed to hold little influence on the swelling/digestion state of crumb rubber. Meanwhile Memon (2011) made recommendations about accelerating the interaction process between rubber and base bitumen through utilising a High Shear Mixer. Despite the fact that there are many studies devoted to the effects of blending variables on the properties of RTR-MBs, all those studies focused on only the viscosity as a benchmark criterion to evaluate the modified binders and a few considered the rheological properties within only the linear viscoelastic region LVE. None of these studies have considered characterising the materials at higher stresses under the nonlinear viscoelastic range. Consequently, with the aim of optimising the blending time for formulating RTR-MBs with desirable mechanical properties, this chapter focuses on the influence of blending time on the J_{nr} and recovery percent tested over a wide range of stresses. This chapter also investigates the storage stability of materials by evaluating their softening point and rheological properties before and after being stored at high temperature. The chapter also looks at the effects of artificial ageing on rheological properties of RTR-MBs.

4.2 Experimental Design

4.2.1 Materials

The materials used in Chapter 3 are also used in this chapter. Two base bitumen binders labelled H and S are used, their properties are presented in Chapter 3 (Table 3.1). Also, the three different sources of crumb rubber modifiers (CRM) used in the previous chapter, labelled as N, D and SE are also used in this chapter.

4.2.2 High Shear Blending

The recycled tyre rubber modified bitumen (RTR-MB) was manufactured by using the Silverson L4RT High Shear Mixer shown in Figure 4.1 as a blending device. High shear mixers have been utilised by many researchers and verified to produce RTR-MBs with superior properties (Huang 2008, Huang and Pauli 2008, Shen, Amirkhanian et al. 2009, Memon 2011, Celauro, Celauro et al. 2012). The rubber concentration of 15.25% by weight of total blend was kept the same as in Chapter 3 for all blends. Each blend of RTR-MB was produced in the laboratory according to the following protocol:

- (1) About 2000g of base bitumen heated was at 180°C in the oven until it was liquefied enough to pour

- (2) The designed mass of base bitumen was then weighed out into a clean tin and placed back into an oven at a temperature of 180°C for about 30 to 45 min
- (3) Whilst the bitumen was heating up the hotplate (located together with the High Shear Mixer in a fume extraction cabinet) was switched on and the mixer head lowered down so that it was positioned slightly above the hotplate to absorb heat
- (4) After that, the bitumen in the tin was taken out from the oven, placed on the hot plate and the shear mixer head fully submerged into the sample
- (5) The shear mixer was turned on and the speed set to the maximum allowable without causing the bitumen to expel out from the tin
- (6) The required amount of CRM (weighed out with respect to the amount of bitumen) was then slowly added into the sample. The temperature of the blend was regularly checked using a hand temperature probe to ensure the blend was mixing at the designed temperature $180\pm 5^{\circ}\text{C}$
- (7) In order to optimise the blending time, samples were collected at different times (5, 15, 30, 60, 100, and 140 minutes). Samples were labelled as in Chapter 3



Figure 4.1: Silverson L4RT High Shear Mixer

4.2.3 Testing Programme

High-Temperature Viscosity (HTV)

The viscosity of binder at high temperatures is important for pumpability and to ensure that the binder can be practically mixed and compacted with aggregate. Also, it gives very beneficial information about the actual physical change between CRM and bitumen during the blending. The Brookfield Rotational Viscometer HA with a standard spindle (SC-27) were used to measure the (HTV) of different combinations of RTR-MBs at 180°C and at a rotation speed of 100 rpm.

Multiple Stress Creep Recovery (MSCR)

Samples of different RTR-MBs collected at blending times of 30, 60, 100 and 140 min were characterised using the MSCR test under the following settings using a Malvern DSR CVO Model.

- Isothermal temperature of 60°C

- Seven stress levels were used (100, 400, 1600, 3200, 6400, 12800 and 25600 Pa).
- Applying 10 cycles at each stress level
- Plate geometry was 25mm diameter parallel plates and 2mm gap

Storage stability

The storage stability test was carried out on RTR-MBs produced at the optimum blending time. This was done by placing vertically the RTR-MBs in a tube (the common name is Toothpaste tube), sealed, and conditioning in the oven at 180°C. The standard conditioning time of the test is 72 hours. However, the phase separation between CRM and base bitumen occurs very quickly. Therefore, the materials in this study were removed after 6 and 24 hours of being conditioned in the oven. The samples in the toothpaste tubes were cooled down to room temperature and then placed in a refrigerating chamber, for 30 min at - 20 °C. After that, the frozen specimens were cut into three equal parts using a heated knife, the two ends (top and bottom) were kept for future testing. The difference in softening point and rheological properties between the top and bottom of the specimen were measured to give an indication about the degree of phase separation. In the softening point test, two steel balls (weight 3.5 g) are placed on two bitumen samples contained in metal rings. Then, they are placed in a water bath (bitumen with softening point 80°C or below) or in glycerol (bitumen with a softening point greater than 80°C) and the bath temperature is raised at a constant rate (5°C/min). The softening point is defined as the equi-viscous temperature measurement when the bitumen softens enough and eventually deforms slowly to allow the steel balls enveloped in bitumen to fall a distance of 25 mm into the bottom plate. The test method is described in BS 2000 Part 58, 1983, IP 58/83 and ASTM D36. In addition to the softening point test, the materials from the top and bottom of the toothpaste tubes were also characterised by means of DMA using a Malvern DSR CVO Model. The DMA testing protocol was conducted under the following settings:

- Oscillatory sweep frequency 0.1 – 10 Hz
- Strain control mode within the LVE region (less than 1% strain)
- Multiple temperatures (30°C – 80°C at 10°C intervals)
- Parallel plate geometry 25mm diameter and 2mm gap

Artificial ageing

The effects of artificial ageing on the rheological properties of RTR-MBs were evaluated using the thin film oven test (TFOT) and pressure ageing vessel (PAV) test to simulate the short-term ageing and long-term ageing, respectively. The ageing tests were conducted on only the RTR-MBs produced at the optimum blending time. In the TFOT, the materials were poured into stainless steel pans, the materials in these pans formed in a film thickness of approximately 3.2mm. The binders in the pans were then placed on a rotating shelf in an oven at 163°C for 5 hours. In the PAV test, the residue from the TFOT (contained in the pans) was transferred into a pre-heated vessel pressurised with air to 2.1 MPa for 20 hours at a temperature of 90°C. The aged residues after TFOT and TFOT plus PAV were tested by means of the DMA under the same testing protocol mentioned earlier. The testing temperatures were extended here to include 0°C – 30°C at 10°C intervals using 8mm parallel plate geometry and 2mm gap.

4.3 High Shear Viscosity HSV

The high-temperature viscosities were measured to investigate the swelling/digestion state of the blend as a function of blending time. Figure 4.2 shows the viscosity development measured at 180°C for different crumb rubbers interacted with different base bitumens. The findings in Figure 4.2 clearly indicate that the type of crumb rubber has a significant effect on the trend and magnitude of the high-temperature viscosity. It is clear that the pre-treatment of crumb rubbers (D and SE) has resulted in a significant reduction in the high-temperature viscosity compared to the binders produced using a standard crumb rubber N. Also, the viscosity development of binders blended with crumb rubber D and SE (Figure 4.2 b and c) did not follow a consistent trend and did not go through significant changes in viscosity with respect to the blending time. Therefore, it is not possible to identify the swelling/digestion state of these materials based on only the high-temperature viscosity. In the case of binders produced using crumb rubber N, there is a defined trend, where the viscosity measurements firstly fluctuate, followed by a consistent increase until they reached a peak point, and finally decreased. It can be seen from Figure 4.2a that the time needed to reach the peak viscosity was 60 min for RTR-MB producing using the soft bitumen S while this was achieved after 100 min of blending with the hard bitumen H. These results suggest that softer bitumens interact more with rubber than harder bitumens as the softer bitumens have higher aromatic content, and hence a higher rate of diffusion into the rubber particles. After reaching the peak viscosity, both S-N and H-N could have undergone some

depolymerisation/devulcanisation as indicated by decreasing viscosity with time. Generally, the findings in Figures 4.2 indicate that materials produced using crumb rubber N reached a complete swelling state. On the other hand, for materials produced using crumb rubbers D and SE, there was no clear evidence to reveal that complete swelling occurred.

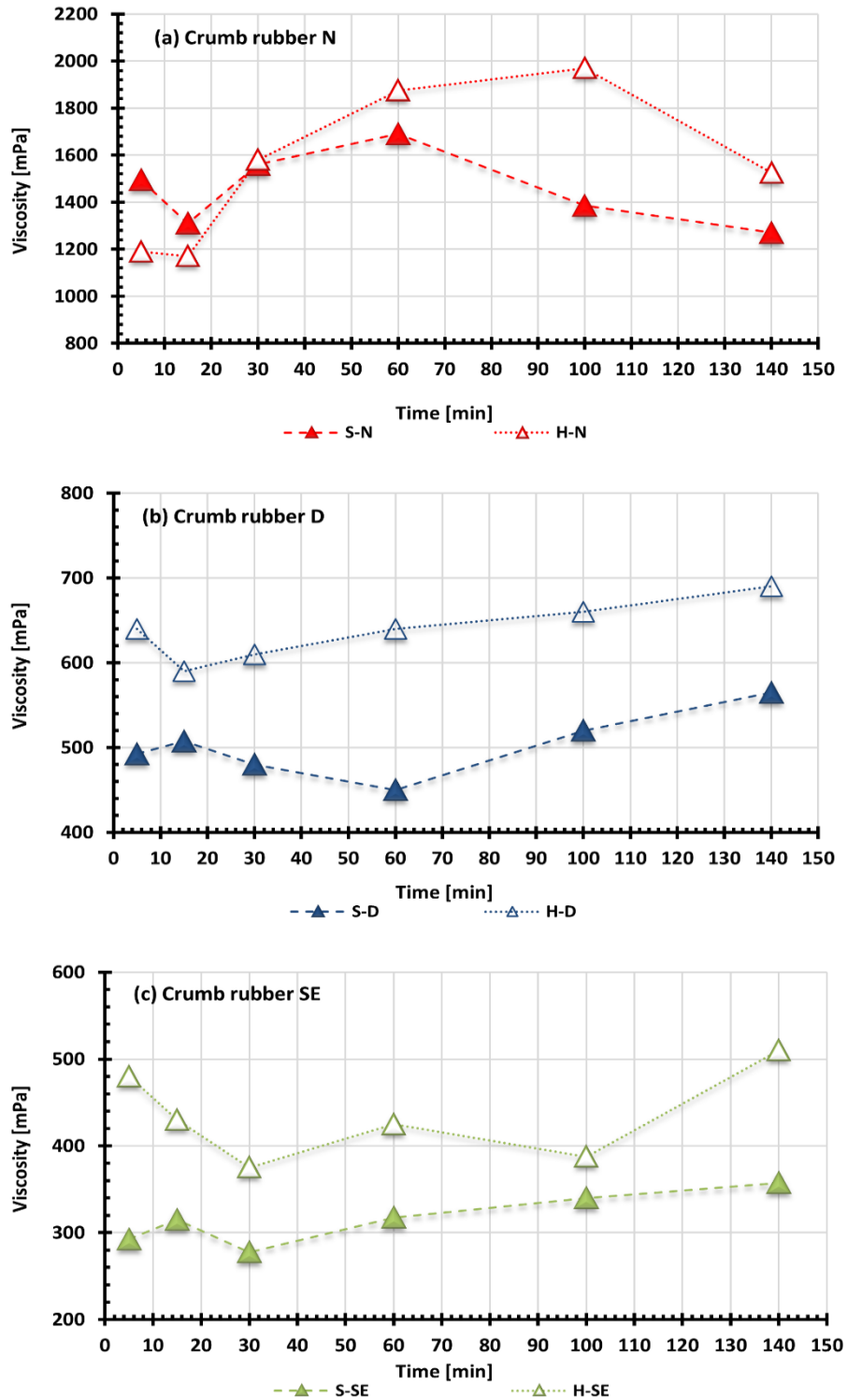


Figure 4.2: High-temperature viscosity development measured at 180°C

4.4 Multiple Stress Creep and Recovery (MSCR)

Multiple Stress Creep Recovery (MSCR) tests were conducted to provide a more satisfactory understanding of the effect of blending time. In this case, the materials were collected at different blending times (30, 60, 100 and 140 min) to determine which will be the optimum one. Figure 4.3 shows the results of the average non-recoverable compliance for the 10 creep and recovery cycles (for two replicates) over a wide range of stresses at a test temperature of 60°C. The previous results of MSCR in Chapter 3 of binders produced using crumb rubber D showed that varying the processing conditions follows the same trend regardless of the base bitumen. Thus and for brevity, the binder H-D was not included for MSCR tests and consider only S-D binder. It can be seen that varying the blending time resulted in significant variation in J_{nr} values. However, the trend of varying the blending time on J_{nr} is different for binders produced using the pre-treated crumb rubbers (D and SE) from those produced using the standard crumb rubber N. For materials produced using crumb rubber N, increasing the blending time up to 100 min was enough to complete the swelling and gave the minimum J_{nr} values. After that, the J_{nr} values increased at a blending time of 140 min due to the possible degradation of the rubber network in the blend. On the other hand, it seems that binders produced using crumb rubbers D and SE never completed the swelling process within 140 min of blending. Thus, their J_{nr} values decreased as the blending time increased. However, there was a marginal difference in J_{nr} between materials collected at blending times of 100 min and 140 min. In terms of the effect of base bitumen, varying the blending times changed the materials in the same trend regardless of base bitumen. But, the effect of crumb rubber type was dominant on the trend of altering the J_{nr} with respect to blending times.

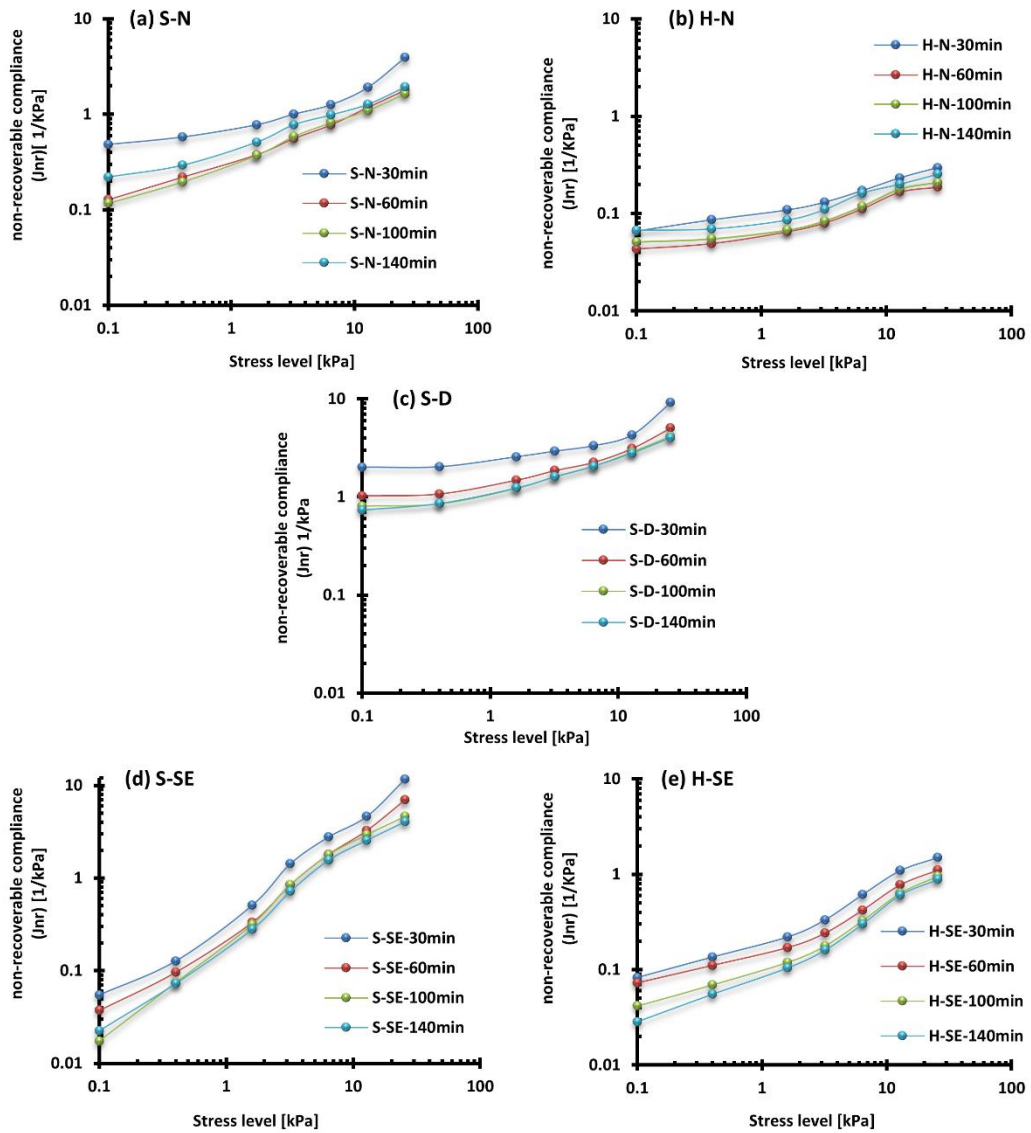


Figure 4.3 J_{nr} at $60^{\circ}C$ of RTR-MBs collected at different blending time

To obtain more information about the effect of blending time on the creep and recovery properties of binders, the accumulated strain consisting of 10 cycles of creep and recovery over three different stresses (0.1, 3.2 and 6.4 kPa) for a total of 300s test duration are presented in Figure 4.4. The results indicate that blending time for 30 min exhibited the highest accumulated strain for all materials tested. This suggests that 30 min blending time was not sufficient to establish a robust polymer network in the blend. The optimum blending time based on accumulated strain was 60 min for binders produced using crumb N while longer blending time ~ 140 min was needed to keep the accumulated strain at its minimum for binders produced using crumb rubbers D and SE. The modification with crumb rubber N showed the minimum accumulated strain for all blending times and hence superior rutting

resistance compared to the modification of D and SE crumb rubber. However, the worst high-temperature properties were associated with binders modified by crumb rubber D.

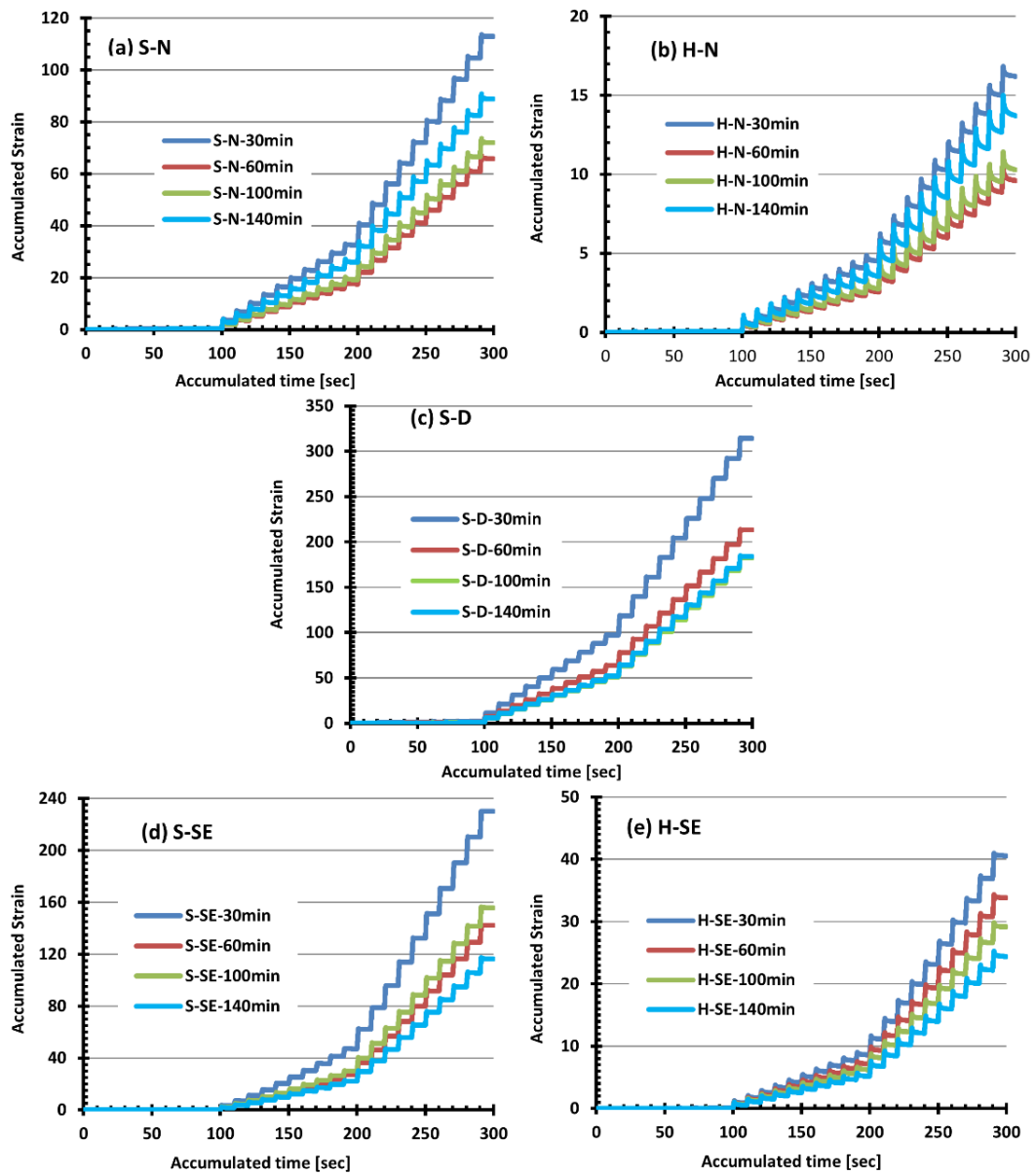


Figure 4.4 Total accumulated strain of RTR-MBs produced at different blending times

Figure 4.5 shows the average percentage recovery of 10 cycles at three stress levels (0.1, 3.2 and 6.4 kPa). The error bars are used to denote the standard deviation of the 10 cycles. It can be seen that the effect of blending times on recovery percentage followed a similar ranking to J_{nr} and accumulated strain. However, the only difference was with binders produced using crumb rubber N where the blending time at 100 min showed slightly higher recoveries than blending time at 60 min. Based on the MSCR results, the optimum blending times that will be used to manufacture the RTR-MBs for future testing are:

1. (90 min) for binders produced using crumb rubber N
2. (140 min) for binders produced using crumb rubber D and SE

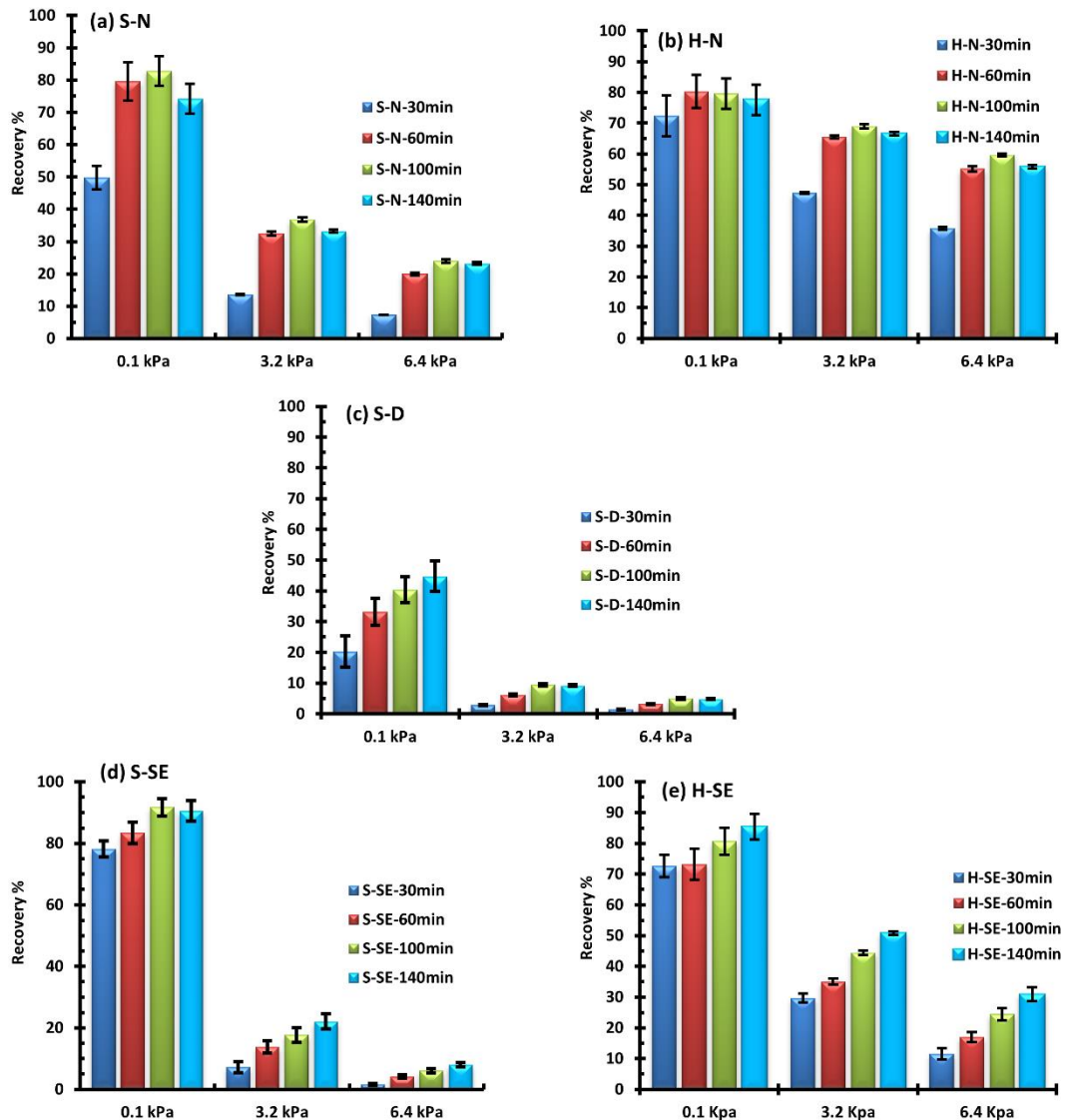


Figure 4.5 Recovery percentage of RTR-MBs produced at different blending time

4.5 Storage Stability of RTR-MBs

It is well known that RTR-MBs are heterogeneous blends and tend to experience phase separation between rubber particles and the base bitumen during hot storage. Therefore, it is important to characterise the phase separation of RTR-MBs and investigate the effect of using different crumb rubber modifiers. The binders produced at the optimum blending times were evaluated after being stored vertically in aluminium tubes at 180°C for 6 and 24 hours. Table 4.1 shows the results of softening point of samples taken from the top and bottom of the tube. The difference between the softening points of the top and bottom samples gives an indication of the extent of separation. It is clear from the difference in softening point that

all RTR-MBs underwent significant phase separation. For binders produced using crumb rubber N, the rubber particles tended to float at the top of the tube rather than settle down as in the case of crumb rubber D and SE. This indicates that the density of crumb rubber N had been reduced after the interaction process (swelling and digestion) with base bitumen to a degree less than the density of base bitumen. The change in rubber particle density after interaction with base bitumen was studied by Memon (2011) and he showed that a reduction in rubber density of up to 19% could occur after the rubber-bitumen interaction. The results also show that binders produced using crumb N were relatively more stable after 6 hours of static storing than binders produced using crumb D and SE. However, the differences in softening points for binders produced using crumb rubber N become considerable after 24 hours of static storing, they become higher than the differences of binders produced using crumb rubber D and SE.

Table 4.1: The softening point of RTR-MBs after static storing at high temperature

Material	Softening point @ 6hr [°C]			Softening point @ 24hr [°C]		
	Top	Bottom	Diff.	Top	Bottom	Diff.
S-N	65	58	7	64.4	50	14.4
S-D	48.4	59.2	-10.8	44.4	58.2	-13.8
S-SE	77	85.8	-8.8	73.4	82	-8.6
H-N	73.6	69	4.6	77.6	61.4	16.2
H-D	58.2	67.8	-9.6	56	68.8	-12.8
H-SE	74	83	-9	75	84.6	-9.6

The rheological changes of rubberised bitumens associated with static storing were also studied using G^* master curves and black diagrams. Figures 4.6 to 4.8 show the G^* master curves and black diagrams of samples taken from the top and bottom of the tube after 6 hours and 24 hours of storage.

The complex modulus master curves of binders produced using crumb rubber N in Figure 4.6 show a significant increase in G^* at high frequencies as the storing time increases for samples taken from the bottom. This may have been the result of accumulation of high molecular weight fractions at the bottom after being separated from the rubber particles that had been swollen by light fractions. On the other hand, the increase in G^* at low frequencies for samples taken from the top is attributed to the high percentage of floating rubber particles. Despite the fact that the binders tested from the top and bottom after 6 hours of storing have

higher G^* , at low frequencies, than the material tested from the top after 24 hours, this does not mean that S-N-24hr (Top) and H-N-24hr (Top) have lower rubber percentage. This was probably due to release of some light fractions which had been absorbed by rubber particles and/or the descent of some high molecular weight fractions into the bottom of the tube. Support for this assumption can be found in the black diagrams. Black diagrams are sensitive to the presence of rubber structure in the binders and this is revealed by a clear shift of black diagram curves towards lower phase angles. Obviously, the findings of black diagrams in Figure 4.6 (d), suggest that there is more rubber concentration accumulation at the top of the tube after 24 hours of storing, as indicated by the decrease in phase angles at low G^* values.

The complex modulus master curves and black diagrams of binders produced using crumb rubber D and SE in Figures 4.7 and 4.8 show an opposite trend to crumb rubber N. Figure 4.7 shows a marked increase in G^* master curves for binders taken from the bottom, and a marked decrease in G^* master curves for binders taken from the top, at low frequencies. This trend reverses at high frequencies, but the difference is not as marked as at low frequencies. The black diagrams show a clear shift towards lower phase angles for binders taken from the bottom and a clear shift towards higher phase angles for binders taken from the top.

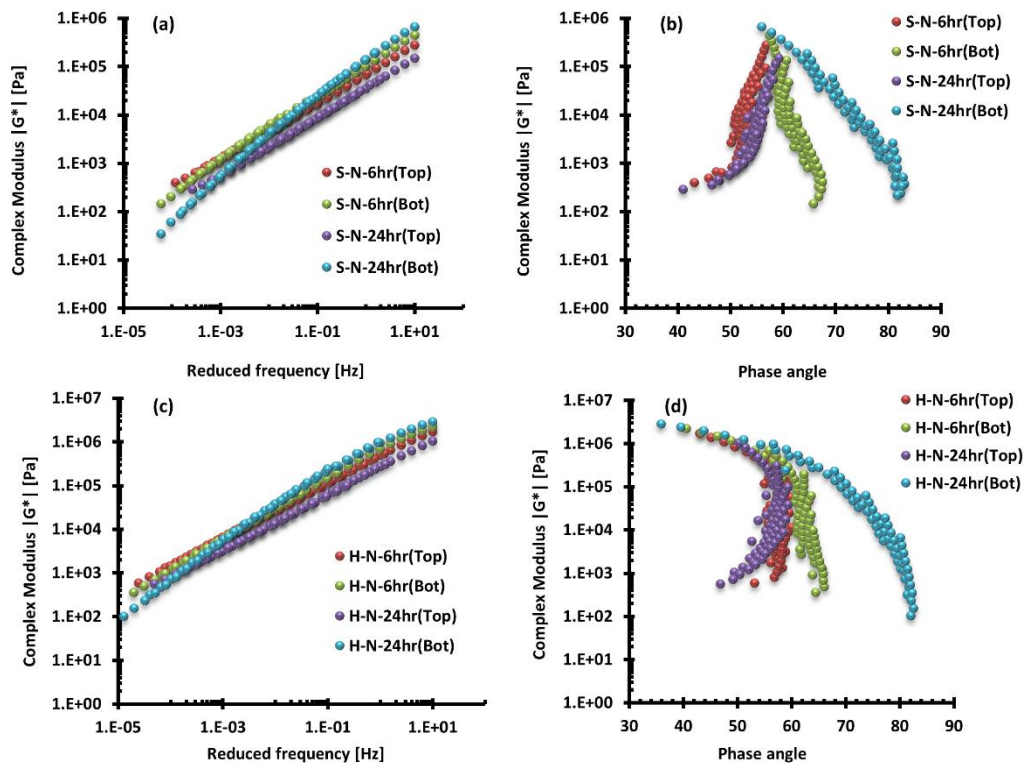


Figure 4.6: Master curves at 30 °C reference temperature and black diagrams for (a) G^* master curves for S-N binders, (b) Black diagrams for S-N binders, (c) G^* master curves for H-N binders and (d) black diagrams for H-N binders

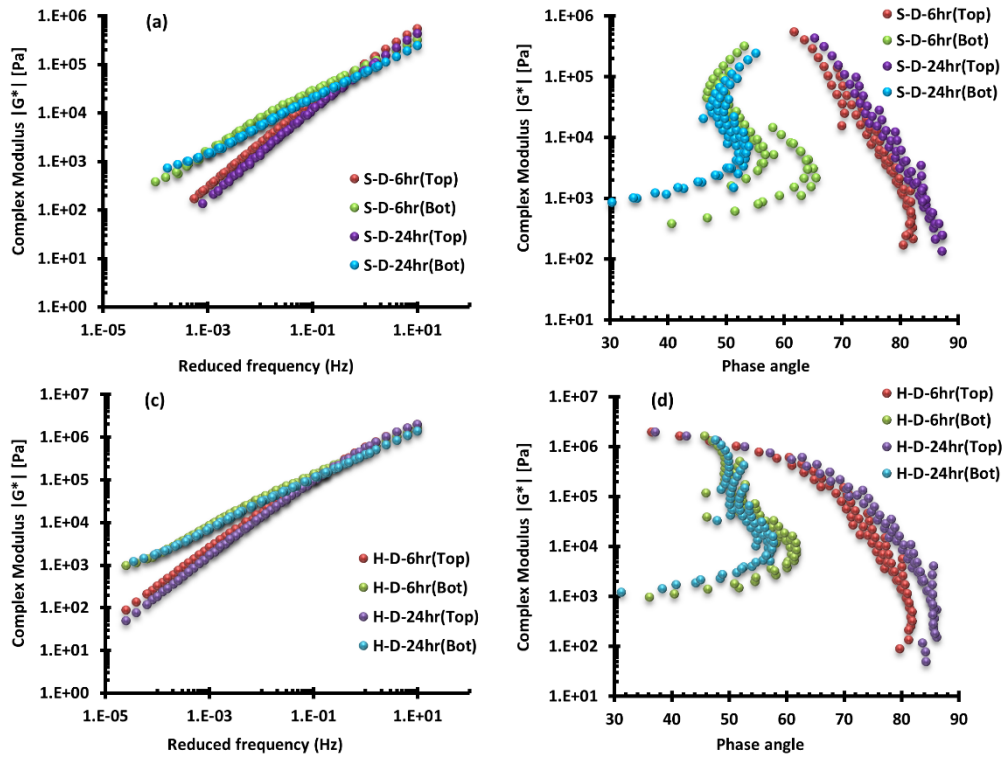


Figure 4.7: Master curves at 30 °C reference temperature and black diagrams for (a) G^* master curves for S-D binders, (b) Black diagrams for S-D binders, (c) G^* master curves for H-D binders and (d) black diagrams for H-D binders

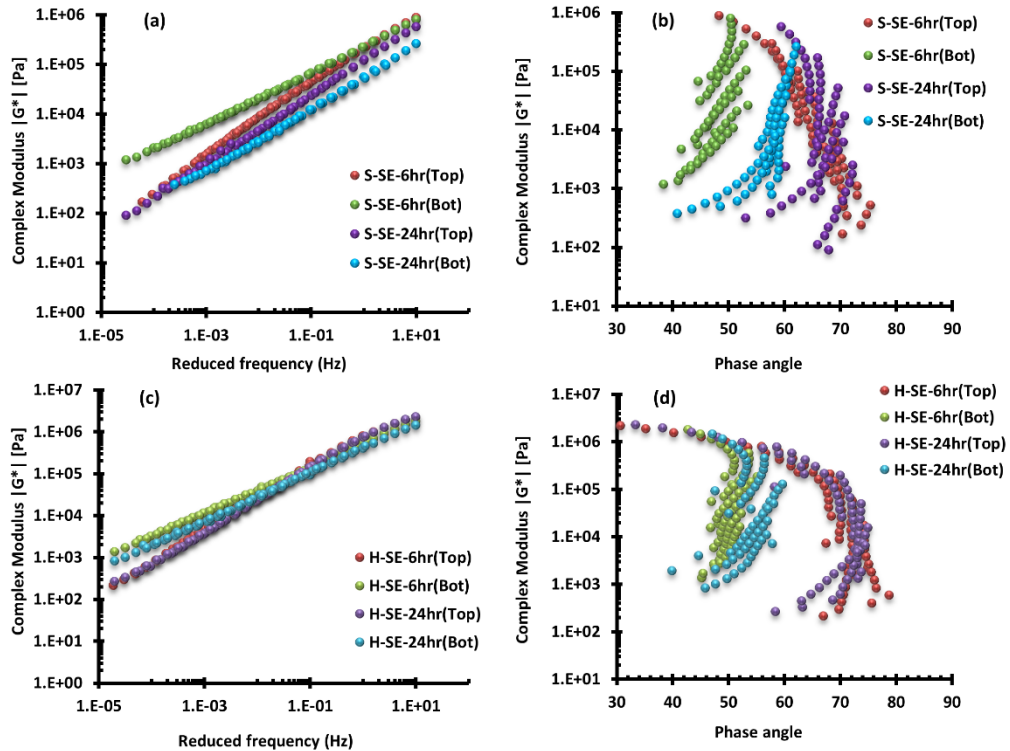


Figure 4.8: Master curves, at 30 °C reference temperature, and black diagrams for (a) G^* master curves for S-SE binders, (b) Black diagrams for S-SE binders, (c) G^* master curves for H-SE binders and (d) black diagrams for H-SE binders

The complex modulus master curves in Figure 4.8 (a) show a rather unexpected trend for binders taken after 24 hours of static storing. It can be seen that the difference in G^* master curves, at low frequencies, between the top and bottom for binders taken after 24 hours, is smaller than the difference between the top and bottom for binders taken after 6 hours. The explanation for this could be due to the effect of FT-wax segregation degree which may have occurred after 24 of static storing. The density of FT-wax, (0.59 to 0.62 g/cm^3), is significantly smaller than that of the base bitumen ($\sim 1.03g/cm^3$); therefore, there could be a probability that some waxes migrated to the top of the tube (Jamshidi, Hamzah et al. 2013). This could compensate the difference in G^* master curves between the top and bottom samples. On the other hand, the results of G^* master curves in Figure 4.8 (c) seem to suggest that the segregation degree was not dominant between FT-wax and the hard bitumen H.

4.6 The effect of artificial ageing

The DMA was conducted before and after artificial ageing in order to understand the physical changes that occur due to ageing for different RTR-MBs. The G^* master curves and black diagrams for the base bitumens, and their RTR-MBs, before and after ageing are presented in Figures 4.9 to 4.12. It should be mentioned that the ageing mechanism of RTR-MBs are complex and that the applicability of the accelerated artificial ageing (TFOT and PAV) used in this study, has only been proven for neat bitumens. However, it is still reasonable to adopt these available procedure to have a general idea about the effect of artificial ageing on RTR-MBs.

For the base bitumens shown in Figure 4.9, the effect of ageing on the G^* master curves is associated with an increase in G^* , particularly at low frequencies and/or high temperatures. The physical change in G^* after PAV ageing is considerably greater than after TFOT ageing due to the severe ageing conditions in the PAV. The effect of ageing on the black diagrams of base bitumens, as shown in Figure 4.9 (b and d), is to shift the curves towards lower phase angles, indicating a higher elastic response. Therefore, the general effect of ageing on rheological properties for the base bitumens S and H is an increase in G^* and a decrease in phase angle. However, the only difference between those base bitumens is that the effect of ageing on G^* master curves at high frequencies and/or low temperatures, is clearly marked for base bitumen S, while this effect almost disappears for base bitumen H. This may be attributed to the high amount light fractions that are available in bitumen S; they are more susceptible to oxidative ageing.

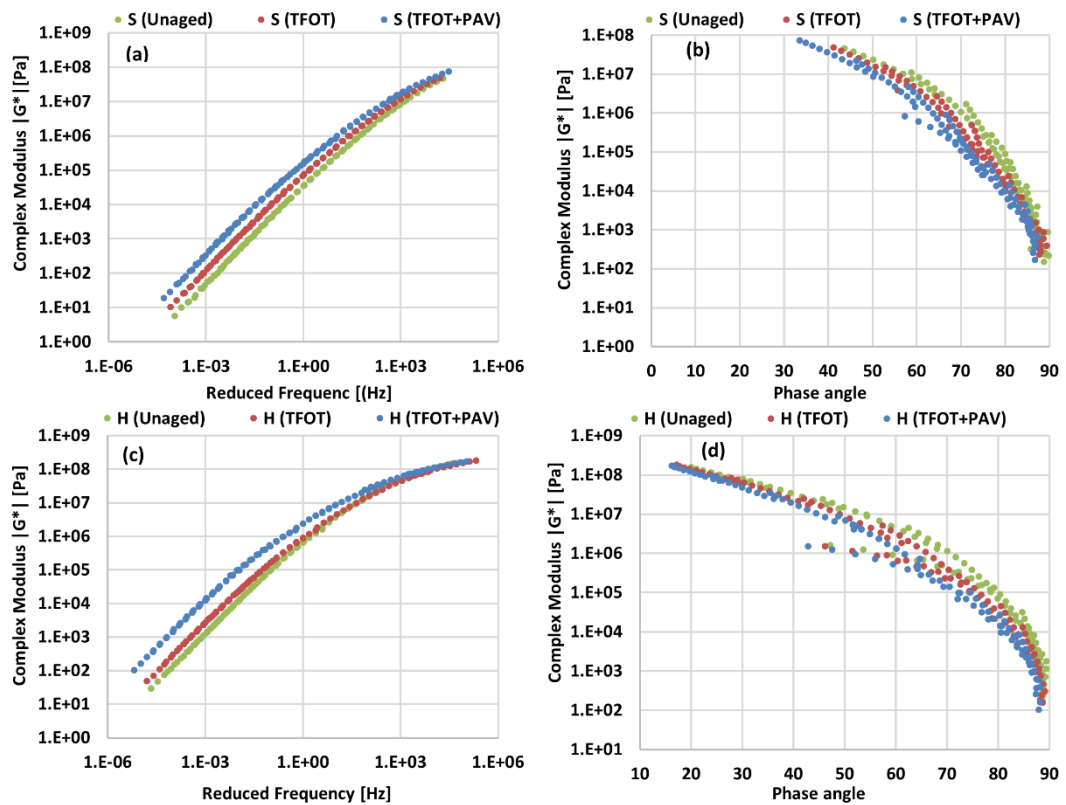


Figure 4.9: Master curves, at 30 °C reference temperature, and Black diagrams for the base bitumens

For RTR-MBs produced using crumb rubber N, as shown in Figure 4.10, it can be seen that the effect of ageing on G^* master curves has a similar trend to that found in the base bitumens, except that the relative increase in G^* after ageing is significantly reduced over the frequency domain and there is a slight decrease in G^* master curve at high frequencies after PAV ageing as seen in Figure 4.10 (c). The black diagrams, in Figures 4.10 (b and d), show a considerable difference from that found in the base bitumens. It can be seen that the curves are disentangled after ageing, particularly after PAV ageing for H-N material. There is also an increase in the phase angles towards more viscous behaviour after ageing when G^* becomes below 10^4 Pa. This confirms the hypothesis that crumb rubber particles could have undergone some degradation by the means of devulcanisation /depolymerisation during the ageing process.

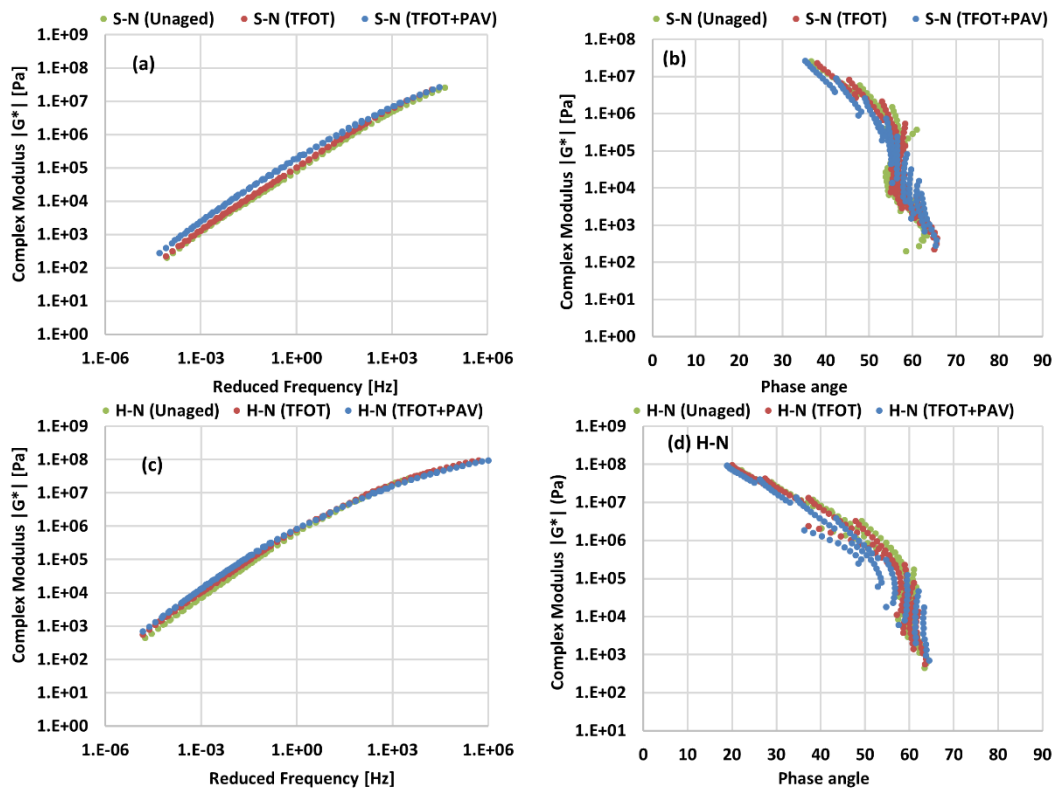


Figure 4.10: Master curves, at 30 °C reference temperature, and black diagrams for RTR-MBs produced using crumb rubber N

For RTR-MBs produced using crumb rubber D, as shown in Figures 4.11, the G^* master curves show exactly the same trend as base bitumens. Figure 4.11 (a) shows that the relative increase in G^* after ageing over the frequency domain is even higher than that seen in base bitumen S. The effect of ageing on the black diagrams as seen in Figure 4.11 (b and d) is different from all other materials and depends on the ageing condition and the base bitumen. For example, in Figure 4.11 (b), there is a slight shift towards lower phase angles after TFOT ageing for G^* values greater than 10^6 Pa, and there is a clear shift towards higher phase angles for G^* values lower than 10^3 Pa. The explanation for the decrease in phase angle at lower G^* may be the dissolution of the pre-devulcanised rubber particles (about 20% of total rubber added, see section 3.2.1) into the base bitumen. The black diagram for the unaged and aged H-D binders, in Figure 4.11 (d), has the same trend as the black diagram of base bitumens, a decrease in phase angle with ageing. The marked change in phase angle after PAV ageing can be seen in Figure 4.11 (b), the black diagram shifts significantly towards lower phase angle and higher G^* ; this is particularly evident at low G^* values. The possible explanation that could be given for this difference is that crumb rubber D may have undergone swelling during PAV ageing and formed a 3D polymer network in the modified binder. The observations in this Chapter and the previous one with regard to the effect of

processing condition on crumb rubber D, show that crumb rubber D has never reached complete swelling. Therefore, the swelling process might have occurred under the severe conditions of PAV ageing.

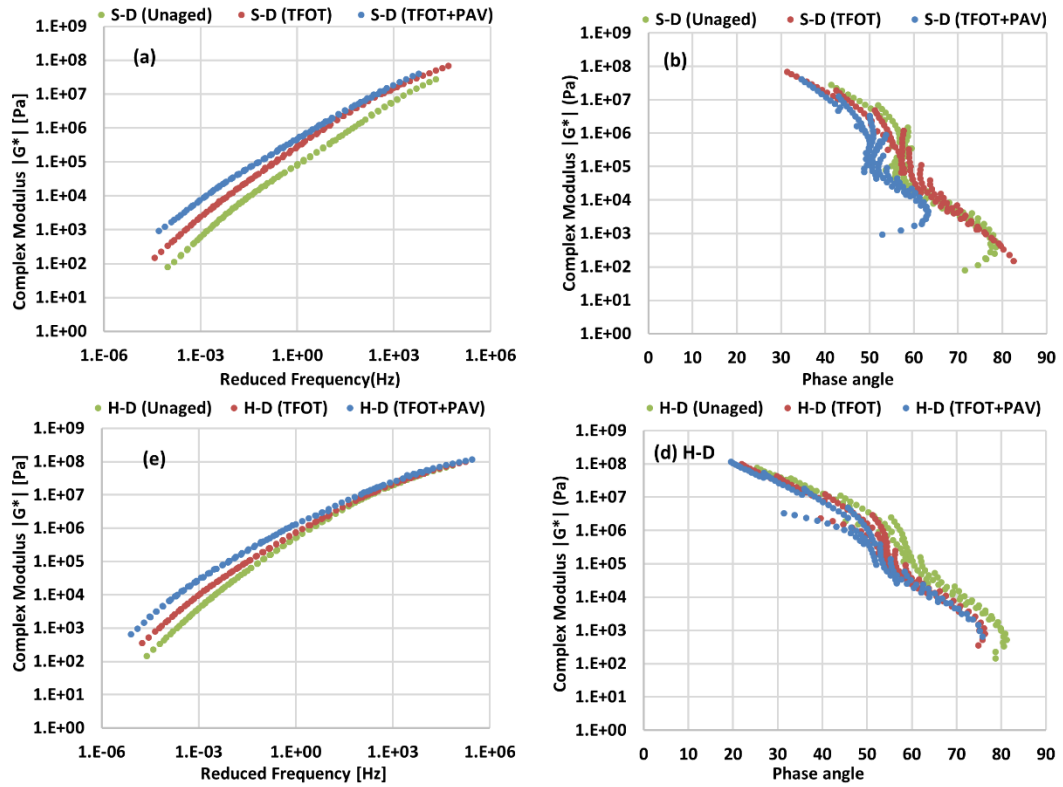


Figure 4.11: Master curves, at 30 °C reference temperature, and Black diagrams for RTR-MBs produced using crumb rubber D

For RTR-MBs produced using crumb rubber SE, shown in Figure 4.12, the changes in G^* master curves and black diagram after ageing resemble more those seen in RTR-MBs produced using crumb rubber N. However, the change in G^* master curves in Figure 4.12 (a), at reduced frequencies lower than 10^{-3} Hz, is reversed to a reduction in G^* rather than an increase after PAV ageing. Also, in Figures 4.12 (b and d), the relative increase in phase angle after PAV ageing, at low G^* values ($<10^4$ Pa), is significantly greater than those found in S-N and H-N groups as found in Figure 4.10 (b and d). These findings seem to suggest that the polymer network in S-SE and H-SE groups was more susceptible to disintegrate during PAV ageing.

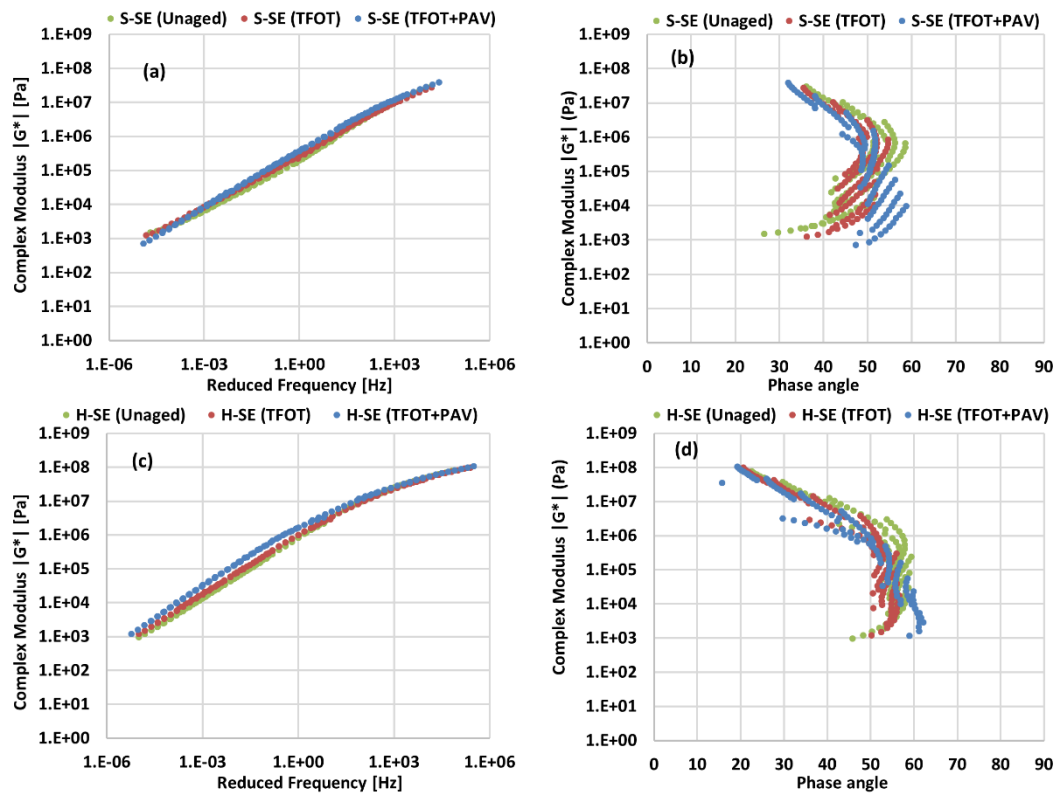


Figure 4.12: Master curves, at 30 °C reference temperature, and Black diagrams for RTR-MBs produced using crumb rubber SE

In order to understand more the effect of ageing on pavement performance with regard to intermediate temperature cracking resistance and high temperature rutting resistance, the SHRP fatigue and rutting parameters were determined before and after ageing to produce the ageing indices, as shown in Figures 4.13 and 4.14. The ageing indices for TFOT and TFOT+PAV aged materials indicate that RTR-MBs produced using crumb rubbers N and SE have generally lower ageing indices than the base bitumens. This is particularly apparent when softer bitumen is used as seen in Figure 4.13. The rubber modification is, therefore, important to compensate the hardening in the rheological properties due to oxidative ageing. Consequently, the RTR-MBs can possibly result in having aged pavement material with superior performance in terms of cracking resistance. However, it can be seen that the ageing indices for RTR-MBs produced using crumb rubber D differ considerably from those produced using crumb rubbers N and SE. They exhibit unexpectedly high ageing indices; this is particularly evident after TFOT ageing as seen in Figure 4.13 (a), where they are even greater than the ageing indices of base bitumens.

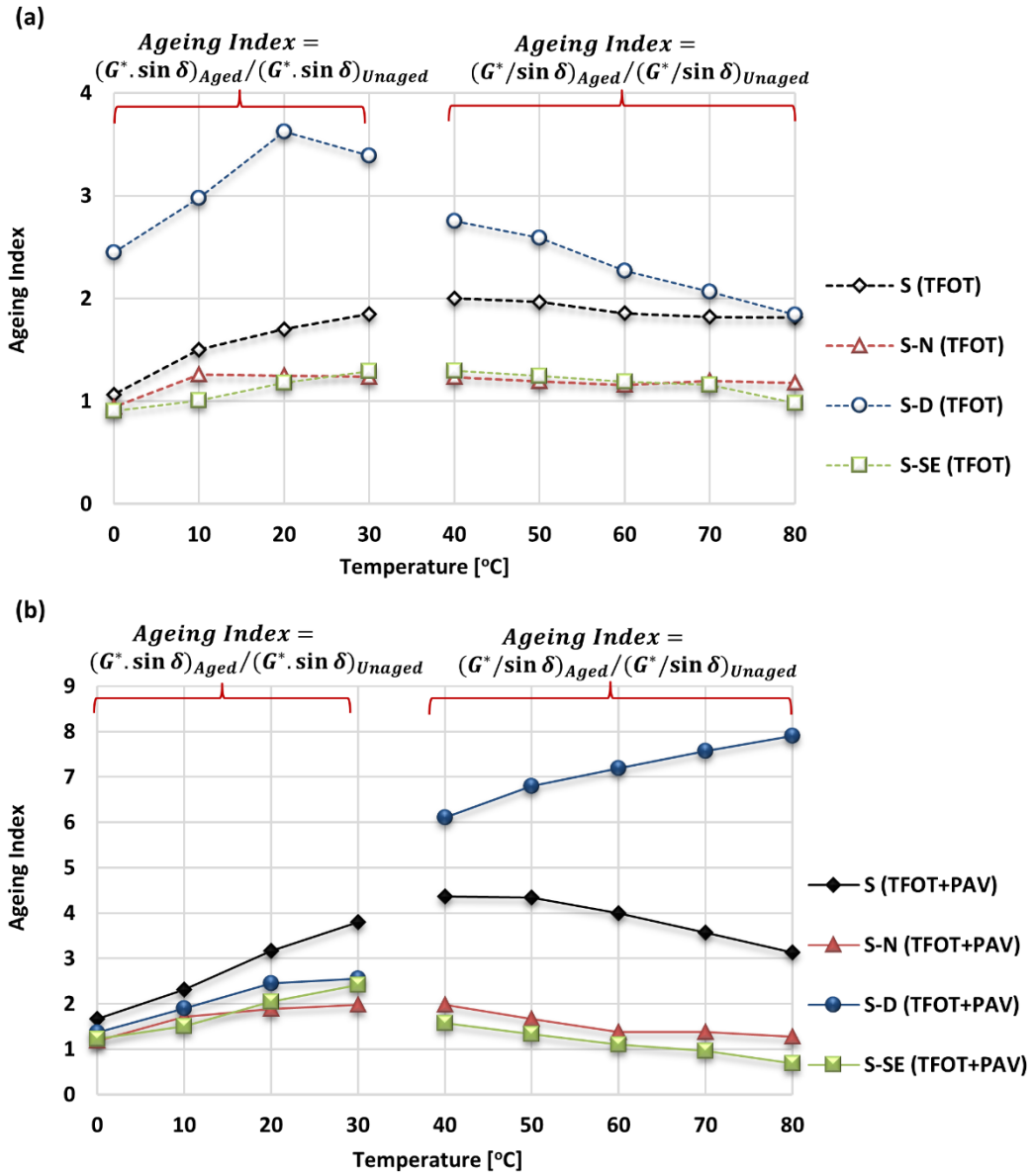


Figure 4.13: The ageing indices for base bitumen S and its RTR-MBs

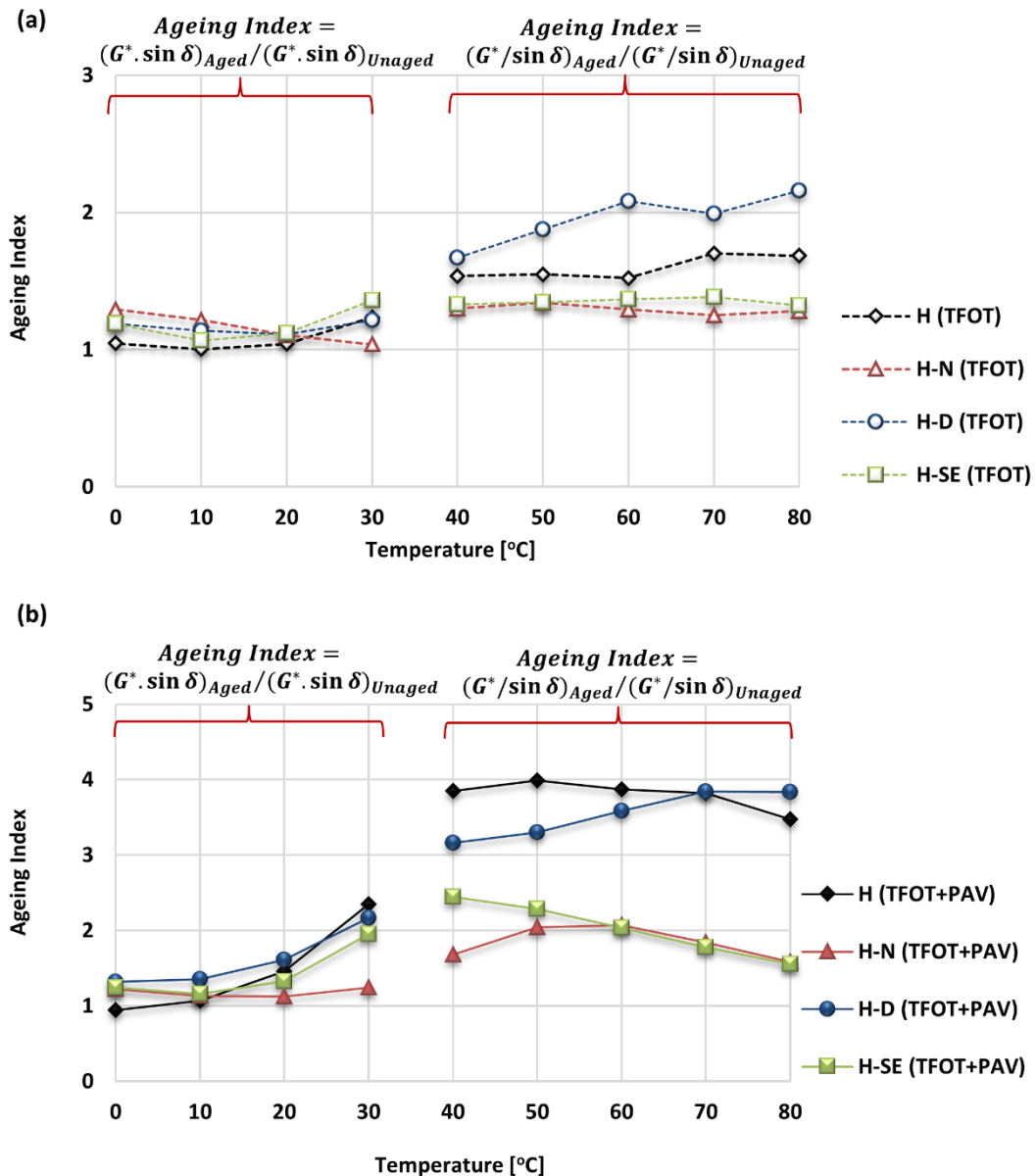


Figure 4.14: The ageing indices for base bitumen H and its RTR-MBs

4.7 Summary and conclusions

The Silverson L4RT High Shear Mixer was utilised to blend different combinations of RTR-MBs. The combinations consisted of blending two base bitumens together with three different sources of crumb rubber modifiers. The effect of blending time on the mechanical properties of RTR-MBs was investigated by the means of High-Temperature Viscosity HTV and MSCR test. The optimum blending time that gave the most desirable mechanical properties based on the MSCR results was then identified. The storage stability and the effect of ageing were also investigated for RTR-MBs produced at the optimum blending time. In view of the results offered in this chapter, the following summary and conclusions are warranted:

- (1) The effect of using different sources of crumb rubber modifiers can result in a considerable difference in rheological behaviour of RTR-MBs, even though they are blended with the same base bitumen.
- (2) Using the pre-treated crumb rubbers (D and SE) significantly reduces the HTV of RTR-MBs which is important for better handling, wetting the aggregate and to reduce mixing and compaction temperatures.
- (3) Varying the blending time can result in significant differences in the creep and recovery properties of RTR-MBs. The HTV was unable to provide a complete characterisation for these differences. Therefore, it can be concluded that, although the HTV was able to satisfactorily identify the swelling/digestion state of RTR-MBs produced using the straight crumb rubber N, it was unable to effectively differentiate between the RTR-MBs collected at different blending times for crumb rubbers D and SE
- (4) Based on MSCR analysis of RTR-MBs produced using crumb rubber N, a blending time of 90 min can result in developing binders with optimum performance. The findings of the MSCR for binders produced using crumb rubbers D and SE indicated that a blending time of 140 min offered the most desirable properties for those materials.
- (5) The findings of the storage stability tests have shown that RTR-MBs are heterogeneous unstable binders when stored statically at high temperature. Therefore, a continuous agitation is required to prevent phase separation. These findings have also revealed that crumb rubber particles are not only separated by settling down to the bottom but also separated by floating to the top of the storage container. Floating the rubber particles to the top of the storage container is attributed to the reduction in rubber density due to the interaction process, i.e. swelling and digestion. This phenomenon can also result in slowing down the separation rate of RTR-MBs. On the other hand, the crumb rubbers that have minimum interaction with the base bitumen, as found in crumb rubber D, are more prone to rapid separation during hot storage.
- (6) The incorporation of crumb rubber into the bitumen can alter the mechanism through which the binder is being aged. The DMA analysis for crumb rubbers N and SE shows that artificial ageing can partly disintegrate and dissolve the rubber particles, particularly after PAV ageing, resulting in softening the modified binders. This, in turn, has reduced the hardening susceptibility of binders after ageing. Although this

likely would adversely affect the rutting resistance of materials, this is important to enhance the resistance of materials for intermediate and low temperature cracking, since the ageing of a pavement is mainly considered as a cracking related problem. It can, therefore, be concluded that RTR-MBs can be expected to provide enhanced ageing characteristics, and hence, a durable pavement.

Chapter 5 RTR-MB Asphalt Mixtures

5.1 Introduction

The laboratory investigations of asphalt mixtures are important to understanding and then predicting reliably the performance of RTR-MB mixtures in full-scale field applications. RTR-MBs have been successfully used in hot mix asphalt HMA in addition to other applications such as chip seal binders and SAMIs (Stress Absorbing Membrane Interlayers). In terms of HMA, RTR-MBs have been incorporated by various highway agencies and researchers in different mixture designs such as dense graded, open graded and gap graded (Khalid and Artamendi 2004, Liu, Han et al. 2012, Haiping, Sri et al. 2014). Due to the high content of RTR (18% by weight of bitumen), a gap graded mixture is selected in this study. These mixtures can adequately accommodate the thicker film thickness of RTR-MBs. A typical stone mastic gradation (10mm) suitable for surface courses is selected from the British specification BS EN 13108-5/ PD 6691:2007 for designing RTR-MBs mixtures. RTR-MBs produced at the optimum blending time (based on the findings of Chapter 4), in addition to the base bitumen H, will be used to manufacture HMA mixtures. With the aim of investigating only the effect of different binders on the asphalt mixture properties, the aggregate type and gradation have been kept constant for all mixture combinations. This chapter aims to present a brief description of materials and the mixture design procedure associated with manufacturing HMA samples. The current chapter also investigates the mixture's volumetric properties, stiffness and moisture susceptibility. It should be mentioned that only two types of RTRs (N and SE) will be considered in the mixture testing. RTR-MBs

produced using crumb rubber D are excluded from mixture testing as their properties were poor in comparison to N and SE.

5.2 Materials selection

5.2.1 Binders, selection and content

Three different RTR-MBs, in addition to a control bitumen, are selected to manufacture the HMA mixtures. The RTR-MBs selected are; H-N, H-SE and S-N. The base bitumen H is selected for the control mixture. The physical properties of those binders were presented in the previous chapter. The bitumen content of the control mixture is specified as 6.2% by mass of the total mixture as recommended in the British specification. However, in the case of RTR-MB mixtures, the binder content is normally increased in order to take into account the reduced amount of actual bitumen in the binder due to the rubber content. The binder increase would also help in restoring the mobility of the binder which is important to effectively coat the aggregate, as the mobile lighter components of bitumen are reduced by rubber absorption. Therefore, the design binder content for RTR-MBs should be determined so that an optimum asphalt mixture performance is ensured. The RTR-MB content is generally decided by keeping the same actual amount of bitumen as in the control mixture (Khalid and Artamendi 2004, Shen, Amirghanian et al. 2006, Lee, Amirghanian et al. 2008, Memon 2011). This means that the rubber particles are treated as inert filler, and the RTR-MBs are also treated as two separated phases, i.e. bitumen and rubber particles. However, an interaction between rubber particles and bitumen does exist as seen in Chapter 3. There is also a significant amount of rubber particles being dissolved into the bitumen by means of devulcanisation and depolymerisation. Therefore, the bitumen content of RTR-MBs should be investigated to understand its effect on the performance of asphalt mixture. In this study, three different binder contents of RTR-MBs are selected, each selected binder content represents a special hypothesis as shown below. In this chapter, the effect of binder content on the volumetric properties, elemental stiffness and moisture damage is investigated. The binder content will also be evaluated in terms of its effect on fatigue and rutting resistance in Chapter 6 and Chapter 7, respectively. The three binder contents represent different cases as follows:

Case (A): binder content of 6.2% which is the same as the binder content of the control mixture. In this case, the RTR-MBs are considered to act as single homogenised binders and the existence of rubber particles as inert filler is ignored.

Case (B): binder content of 6.8%, it is assumed in this case that about 50% of the added rubber interacts and/or is dissolved into the bitumen. Therefore, the binder content is increased to compensate the reduction in the actual bitumen due to other rubber particles that would keep their physical shape and are not dissolved into the bitumen.

Case (C): binder content of 7.4%; in this case, a similar amount of actual bitumen as in the control mixtures, is provided. All added rubber particles are treated as solid fillers. The diffusion of lighter fractions from bitumen by rubber absorption is also compensated here.

5.2.2 Aggregate

The coarse and fine aggregate fractions used in this study consisted of Granite aggregate obtained from Bardon Hill, UK. The filler was a limestone obtained from Foster Yeoman (Torr Works Quarry, Somerset, UK). The specific gravity for the coarse and fine aggregate, filler, bitumen and rubber fractions of the mixtures are presented in Table 5.1. The SMA gradations used in this study for both control and RTR-MBs are shown in Figure 5.1. As the recycled tyre rubber in the modified binders can occupy some space in the mixtures, the gradations of RTR-MBs mixtures were slightly amended to keep the same gradation for both control and RTR-MBs mixtures as seen in Figure 5.1.

Table 5.1: Aggregate, rubber and bitumen properties

Component	Type	Specific gravity
Coarse aggregate	Granite	2.81
Fine aggregate	Granite	2.82
Filler	Limestone	2.72
Rubber	N and SE	1.15
Bitumen	H and S	1.03

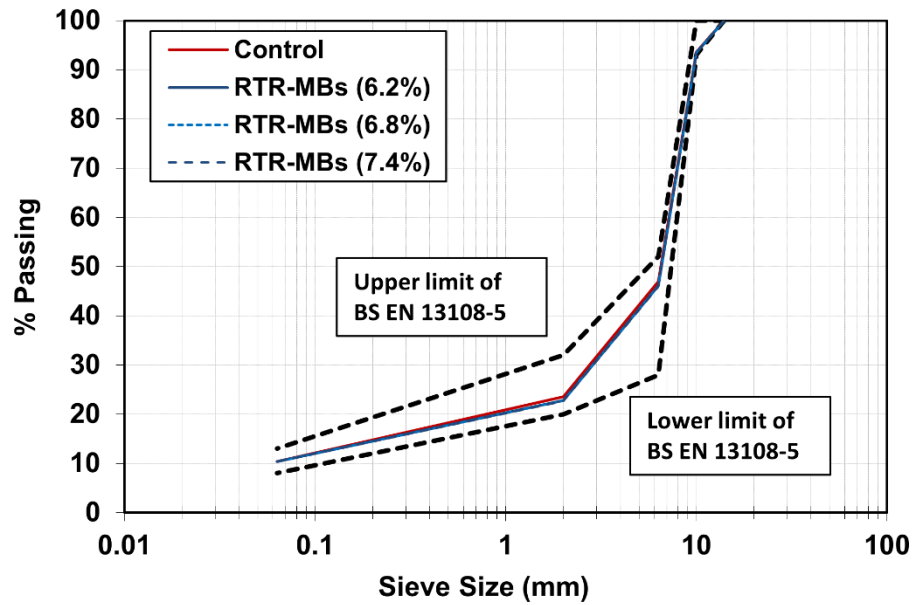


Figure 5.1: The 10mm SMA gradations for control and RTR-MBs mixtures according to BS EN 13108-5/ PD 6691:2007

5.3 Specimen production

The required quantities of aggregate and binder for mixing were pre-heated at the specified mixing temperature, at least 8 hours for aggregate, 3 hours for the binder, to distribute heat uniformly. The aggregate and filler were placed and mixed in a mechanical asphalt mixer, as shown in Figure 5.2 (a), at the specified mixing temperature, the pre-heated binder was then added to the mixture and the mixing continued for three minutes. The mixture was then placed in a preheated slab mould (306 x 306mm) and compacted by a smooth steel roller, as shown in Figure 5.2 (b), according to BS EN 12697-33:2003, until the desired final height of the slab (~60mm), was achieved. The mixing and compaction temperatures of bituminous mixtures are normally specified based on their binder viscosities. For example, the selected mixing and compaction temperatures should be corresponding to binder viscosity of 170 ± 20 mPa.s and 280 ± 30 mPa.s, respectively (Asphalt Institute 2003). However, this criterion is not always possible to apply to RTR-MBs because unreasonably high mixing and compaction temperatures are predicted with this method. For instance, the mixing and compaction temperatures associated with the mentioned viscosities would be higher than 220°C . This higher temperature is not acceptable, it raises concerns about workers' health due to possible hazardous fumes in addition to possible thermal separation and oxidation. Therefore, the mixing and compaction temperatures were selected so that the aggregate fractions could be sufficiently coated by the binder and practically compacted to the prescribed voids contents. The mixing and compaction temperatures were specified for

RTR-MBs produced with H-N binder as 190 ± 5 °C and 170 ± 5 °C, respectively. For control mixtures, and RTR-MBs produced with H-SE and S-N, the mixing and compaction temperatures were specified as 170 ± 5 °C and 150 ± 5 °C, respectively. A stabiliser is normally added to the SMA mixtures to prevent draindown of the bitumen. Thus, cellulose fibres at 0.3% of the bitumen were included in the control mixtures. Cellulose fibres were not included into the RTR-MB mixtures. The experimental design of this study involved seven different asphalt mixture combinations, as shown in Table 5.2. Three slabs were manufactured for each mixture, and five specimens with 100 mm diameter were cored from each slab. The cores were then trimmed from each end to produce cylindrical samples of 100mm diameter and 40mm thickness suitable for indirect tensile and RLAT tests.

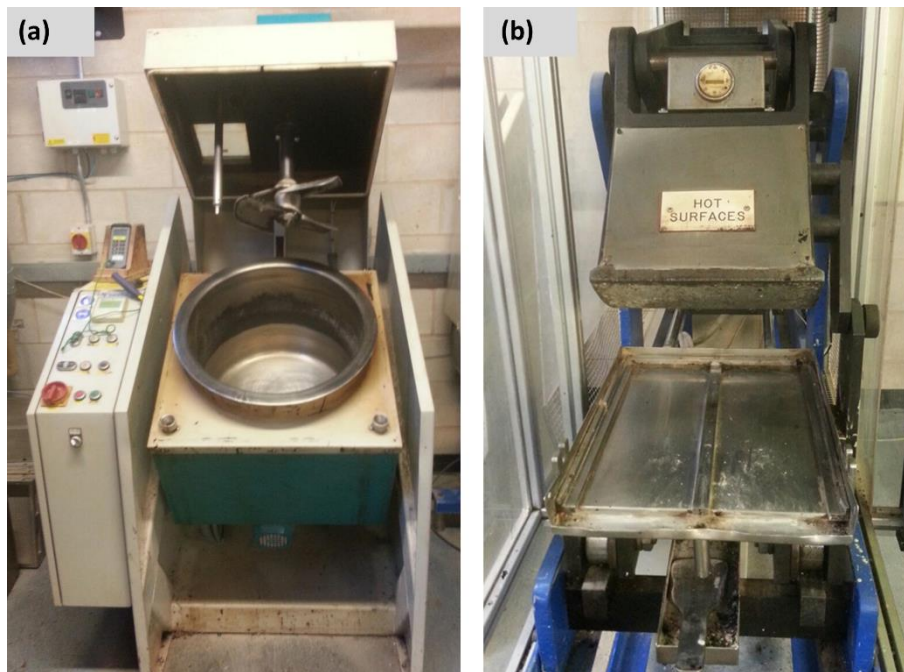


Figure 5.2: (a) the mechanical mixer, and (b) steel roller, that used for asphalt mixture production

Table 5.2: The main parameters associated with the production of SMA mixtures

Mixture	Bitumen type in the mixture	Binder content	Mixing temperature °C	Compaction temperature °C	Designed air void	Added cellulose fibres
Control H (6.2%)	base bitumen H	6.20%	170±5	150±5	4%	0.3% of bitumen
H-N (6.2%)	RTR-MB (H-N)	6.20%	190±5	170±5	4%	N/A
H-N (6.8%)	RTR-MB (H-N)	6.80%	190±5	170±5	4%	N/A
H-N (7.4%)	RTR-MB (H-N)	7.40%	190±5	170±5	4%	N/A
H-SE (6.2%)	RTR-MB (H-SE)	6.20%	170±5	150±5	4%	N/A
H-SE (7.4%)	RTR-MB (H-SE)	7.40%	170±5	150±5	4%	N/A
S-N (6.2%)	RTR-MB (S-N)	6.20%	170±5	150±5	4%	N/A

5.4 Volumetric properties of SMA mixtures

The maximum densities of the asphalt mixtures were calculated from the densities of their constituent materials (coarse aggregate, fine aggregate, filler, rubber and bitumen); according to BS EN 12697-5:2009 standards; mathematical procedure. The maximum density of each mixture was obtained using the following mathematical equation:

$$\rho_m = \frac{100}{\left(\frac{p_{coarse}}{\rho_{coarse}} + \frac{p_{fine}}{\rho_{fine}} + \frac{p_{filler}}{\rho_{filler}} + \frac{p_{rubber}}{\rho_{rubber}} + \frac{p_{bitumen}}{\rho_{bitumen}}\right)} \quad \text{Equation 5.1}$$

where;

ρ_m is the maximum density of the mixture, (kg/m³)

p_{coarse} is the proportion of coarse aggregate in the mixture

ρ_{coarse} is the apparent density of the coarse aggregate (kg/m³)

p_{fine} is the proportion of fine aggregate in the mixture

ρ_{fine} is the apparent density of the fine aggregate (kg/m³)

p_{filler} is the proportion of the filler in the mixture

ρ_{filler} is the apparent density of the filler (kg/m³)

p_{rubber} is the proportion of the rubber particles in the mixture

ρ_{rubber} is the apparent density of the rubber particles (kg/m³)

$p_{bitumen}$ is the proportion of the bitumen in the mixture

$\rho_{bitumen}$ is the apparent density of the bitumen (kg/m³)

Using the above equation, the theoretical bulk densities of the different mixtures are calculated using the following equation:

$$\rho_{bulk} = \rho_m (1 - v_v) \quad \text{Equation 5.2}$$

where;

ρ_{bulk} is the bulk density of the mixture (kg/m³)

v_v is the air voids in the mixture (for theoretical bulk density, the air voids is specified as 0.04)

The theoretical mass and volumetric proportions of the compositions of asphalt mixtures are presented in Figure 5.3 (a) and (b). Figure 5.3 shows a consistent decrease in the densities of mixtures as the aggregate proportion decreased, this is due to the higher specific gravity of aggregate compared to the binder. It can also be seen that the densities of RTR-MB (6.2%) mixture are slightly higher than the densities of the Control (6.2%) mixture; this is due to the slightly higher density of RTR-MB compared to the Control base bitumen.

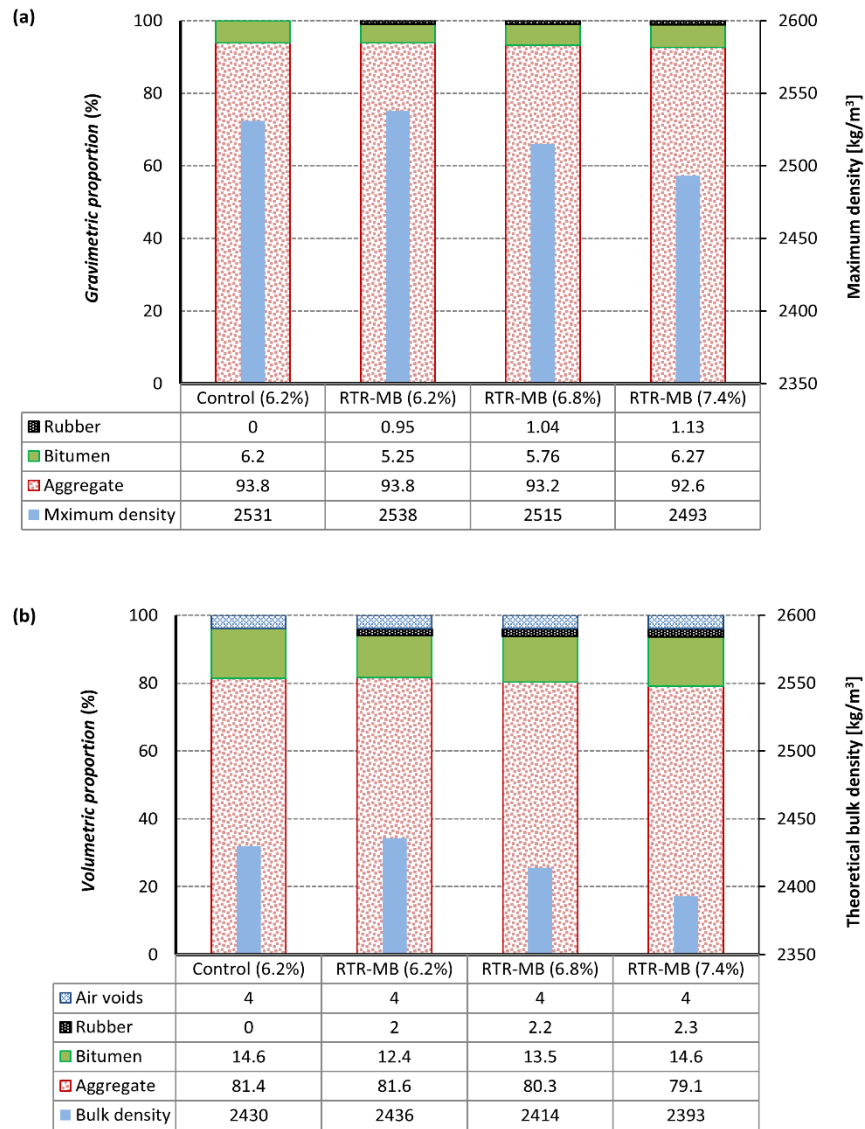


Figure 5.3: (a) Gravimetric proportions and maximum densities of the different mixtures; (b) volumetric proportions and the theoretical bulk densities of the different mixtures with designed air voids of 4%

Figure 5.4 shows the measured bulk densities and air voids for the different asphalt mixture combinations. The bulk densities test method was performed in accordance with the BS EN 12697-6:2012, using the Bulk density-dry procedure, as follows:

$$\rho_{bulk-dry} = \frac{m_1}{m_1 - m_2} x \rho_w \quad \text{Equation 5.3}$$

where;

$\rho_{bulk-dry}$ is the bulk density of the mixture (kg/m³)

m_1 is the mass of the dry specimen in gram (g)

m_2 is the mass of the specimen in water, in gram (g)

ρ_w is the density of the water at the test temperature

The measured air voids for each specimen was then calculated from the following equation;

$$v_v = \frac{\rho_m - \rho_{bulk-dry}}{\rho_m} \times 100\% \quad \text{Equation 5.4}$$

The findings shown in Figure 5.4, represent the average values of 15 sample for each mixture. The range bars represent the maximum and minimum values of bulk density and air voids for the 15 samples. The results of air voids and bulk densities agree with the theoretical one, although there is a variation between the minimum and maximum values. This variation could be attributed to the distribution of air voids and the orientation of aggregate within the slab. However, this range is still within the allowable limit ($v_{min 1,5}$; $v_{max 5}$) in accordance with BS EN 13108-5/ PD 6691:2007. It can be seen that the mixtures with higher binder content resulted in relatively lower air voids. The better compactability of those mixtures could be responsible for this decrease. Although the mixtures produced using H-SE binders were mixed and compacted at temperatures 20°C lower than the mixing and compaction temperatures of other RTR-MB mixtures, the H-SE mixtures showed much better workability and handling. Where the required sample height was achieved by applying less compaction energy (275 kPa) compared to (380 to 480 kPa) for RTR-MBs produced using H-N binder. The FT-wax component indeed contributed to significantly improve the workability and compactability.

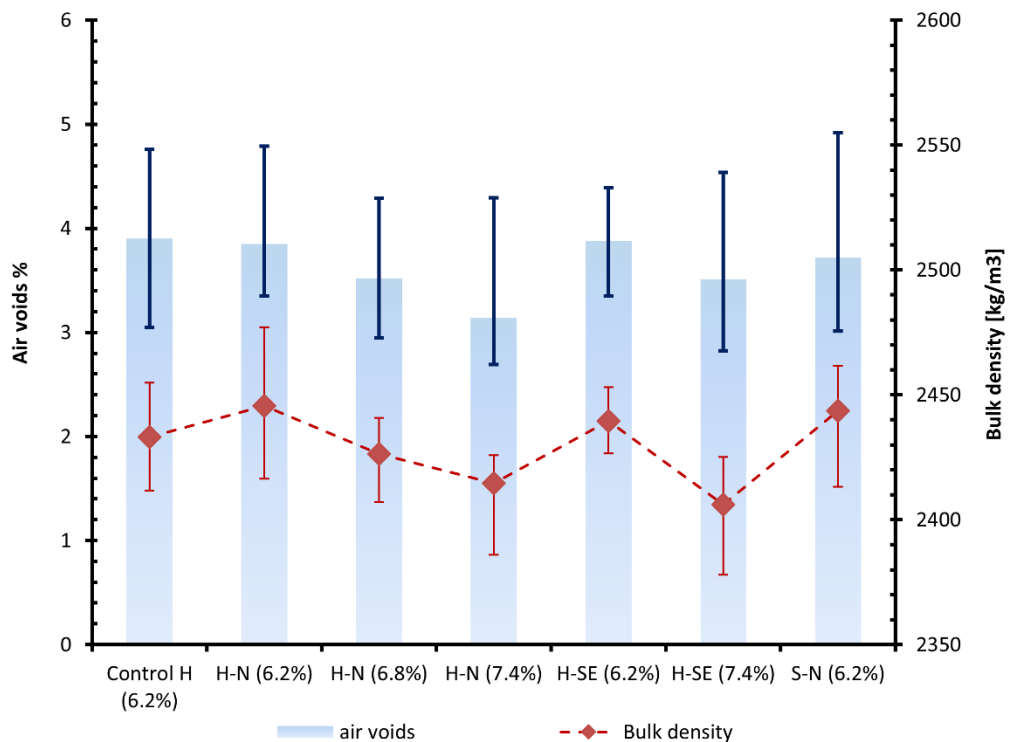


Figure 5.4: The measured air voids and bulk densities of the different mixtures

5.5 Indirect Tensile Stiffness Modulus (ITSM)

The stiffness modulus is an important indicator for asphalt mixtures, and it is considered the main input property to determine the required layer thickness in mechanistic pavement design. The stiffness of bituminous materials reflects the capability of material to spread the traffic loading over an area in a pavement. For example, stiffer materials can spread the traffic loading over a wider area, and vice versa.

The Nottingham Asphalt Tester (NAT), a picture of the configuration of which is shown in Figure 5.5, was used for testing samples in the indirect tensile mode, for stiffness determination. The test is conducted by applying a pulsating load vertically across the diameter of the cylindrical specimen, the resultant tensile horizontal deformation is measured using two linear variable differential transformers (LVDT), as seen in Figure 5.5, which are fixed diametrically opposite each other in a rigid frame clamped to the sample.

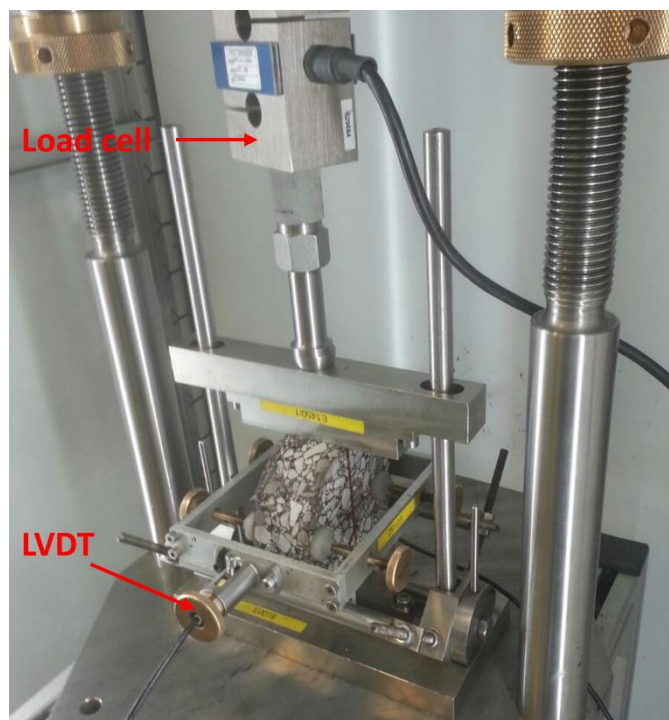


Figure 5.5: ITSM testing configuration in the NAT

The ITSM is calculated from the following equation by applying an impulse loading to induce small horizontal strains of $5 \pm 2 \mu\text{m}$.

$$ITSM = \frac{P(0.273 + \nu)}{\delta t} \quad \text{Equation 5.5}$$

where; P = applied load, t = specimen thickness, δ =horizontal deformation and ν = Poisson's ratio. The following test parameters were applied in ITSM testing according to BS EN 12697-26:2004:

Rise time (milliseconds) = 125 ± 10

Deflection requirements = $5 \pm 2 \mu\text{m}$

Pulse duration = 3s

Number of conditioning pulses = 10

Number of test pulses = 5

Test temperature = 20 ± 0.5

Poisson's ratio = 0.35

Rotation of sample = $90^\circ \pm 10^\circ$

Time to reach equilibrium > 4hrs

The ITSM is taken as the mean of two measurements on one specimen by rotating $90^\circ \pm 10^\circ$ about its horizontal axis. Figure 5.6 shows the ITSM results for Control and RTR-MBs mixtures. The average value of 15 sample for each mixture is presented in Figure 5.6, and the range bars represent the maximum and minimum of values of ITSM.

It can be seen that for asphalt mixtures produced using binders, H, H-N and H-SE, sharing the same binder content of 6.2%, there is no significant difference among the ITSM values of those mixtures. This indicates that the size of the mineral aggregate skeleton in the mixture has a dominant effect on the ITSM. In the case where the size of the mineral aggregate skeleton is reduced by increasing the binder content, there is a clear reduction in the ITSM values. This is expected as part of the aggregate skeleton is replaced by the highly flexible binder. On the other hand, the ITSM values of the mixture produced using the binder S-N, are considerably affected by the binder. In order to obtain a better understanding of the effect of binder on the ITSM, the magnitude of the complex modulus of binders measured at approximately similar conditions (temperature and loading frequency) of ITSM testing, are included in Table 5.3. Although the complex moduli of binders H-N and H-SE are about half of the complex modulus of binder H, these differences are not clearly revealed in the ITSM of asphalt mixtures. However, the effect of binder in the case of S-N is substantial on the ITSM where the ITSM values of S-N mixtures are about half the ITSM values of other mixtures. This is not surprising, as the complex modulus of binder S-N is about seven times smaller than the minimum value of the complex modulus among other binders.

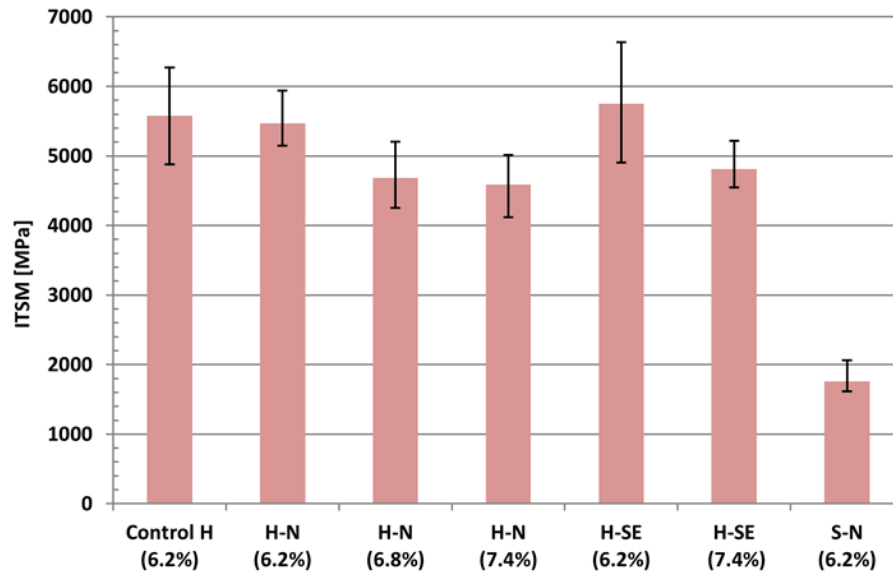


Figure 5.6: ITSM results for the different mixtures

Table 5.3: The complex modulus of the control binder and RTR-MBs

Binders	G* , [kPa], @20 °C and 8 Hz	
	Unaged	TFOT
H	23358	23717
H-N	11306	12493
H-SE	12218	13728
S-N	1337	1642

5.6 Water damage susceptibility

Because the SMA mixtures considered in this study are designed for surfacing and there is a concern about inadequate coating for aggregate by the thicker RTR-MB, therefore, it is important to evaluate the water sensitivity of the mixtures. Water damage generally deteriorates the structural integrity of bituminous materials through loss of cohesion of bitumen or through the failure of the adhesive bond between the bitumen and aggregate (Kennedy 1985, Airey and Choi 2002, Huang, Shu et al. 2010). The water sensitivity of asphalt mixtures is normally investigated by the change in a mechanical property after immersion in water. The indirect tensile stiffness and/or indirect tensile strength are the mechanical properties that are traditionally measured before and after immersion in water (Airey and Choi 2002). The moisture susceptibility of the control and RTR-MB mixtures with different binder content was evaluated based on determining the ratio of conditioned to unconditioned indirect tensile stiffness modulus values measured using the NAT, and the ratio of conditioned to unconditioned indirect tensile strength measured using the INSTRON

(hydraulic loading frame with a maximum load capacity of ± 100 kN) test equipment. The following procedure has been developed specifically for the assessment of thin surfacing systems by the Highways Agency Product Approval Scheme (HAPAS) to protect against water damage. The testing procedure involves measuring the non-destructive ITSM in the dry condition, designated as $ITSM_U$, and subsequently the same samples having undergone a water immersion regime as follows:

- (1) Three specimens were selected for each mixture
- (2) Saturation under a partial vacuum of 510 mm Hg at 20°C for 30 minutes
- (3) The samples are then transferred to a preheated water bath at 60°C under atmospheric pressure for 6 hours and moved to another water bath at atmospheric pressure at 5°C for 16 hours. The samples are finally conditioned under water at 20°C (atmospheric pressure) for 2 hours prior to stiffness testing
- (4) The conditioned ITSM at a test temperature of 20°C for the first conditioning cycle is determined. This is labelled as $ITSM_{c1}$
- (5) The steps (2) and (3) are repeated, and the conditioned ITSM of the specimen is determined for the successive conditioning cycles, these are labelled as $ITSM_{ci}$; $i = 1, 2, 3, \dots 6$
- (6) The ITSM ratio for each specimen is calculated for each conditioning cycle as follows: $ITSM_{ratio,ci} = \frac{ITSM_{ci}}{ITSM_U}$

Table 5.4: The ITSM before and after successive cycles of water immersion

Mixture	ITSM _u [MPa]	Conditioned stiffness [MPa]					
		ITSM _{c1}	ITSM _{c2}	ITSM _{c3}	ITSM _{c4}	ITSM _{c5}	ITSM _{c6}
Control H (6.2%)	5576	5742	6205	5936	5591	5425	5225
H-N (6.2%)	5415	5595	5878	6114	----	----	5139
H-N (6.8%)	4621	4680	4737	5352	----	----	4243
H-N (7.4%)	4705	5189	4828	4943	----	----	4650
H-SE (6.2%)	5936	6939	6940	6414	6820	----	6188
S-N (6.2%)	1782	1823	1822	1747.5	1859	----	1821

Table 5.4 shows the ITSM values for the Control and RTR-MB mixtures before and after being exposed to successive water immersion cycles. The average value of ITSM for three specimens is reported in Table 5.4. The results in Table 5.4 indicate that the immersion regime after three cycles led to an increase in ITSM compared to its dry value for all mixtures, except that the S-N mixture exhibited a slight reduction. It should be mentioned

that the number of conditioning cycles is specified as three cycles in HAPAS Certification Procedure; however, the number of conditioning cycles has been doubled to six, because the retained ITSM after three conditioning cycles had not exhibited any reduction. The increase in stiffness value after water immersion could be attributed to the binder ageing during conditioning. The effect of binder ageing on ITSM was possibly dominant over the water damage. However, all mixtures showed a reduction in the retained ITSM after six cycles of water immersion. The retained ITSM ratio versus the number of water immersion cycles is presented in Figure 5.7 for the different mixtures. A minimum retained stiffness ratio of 80% has been set to safeguard against stripping (Lottman 1978). It can be seen that all mixtures passed the minimum limit indicating excellent moisture damage resistance. With respect to the effect of binder content, increasing the binder content for H-N (7.4%) mixture compared to H-N (6.2%), led to a reduction in moisture damage after six cycles of water immersion. Also, the specimens made with binders H-SE and S-N, are less susceptible to water damage in comparison to other mixtures. This indicates that the pre-treatment with WMA for H-SE binder, and using softer base bitumen for S-N binder, resulted in a better aggregate coating, and consequently less water was allowed to penetrate into the mixture matrix and affect the structure integrity.

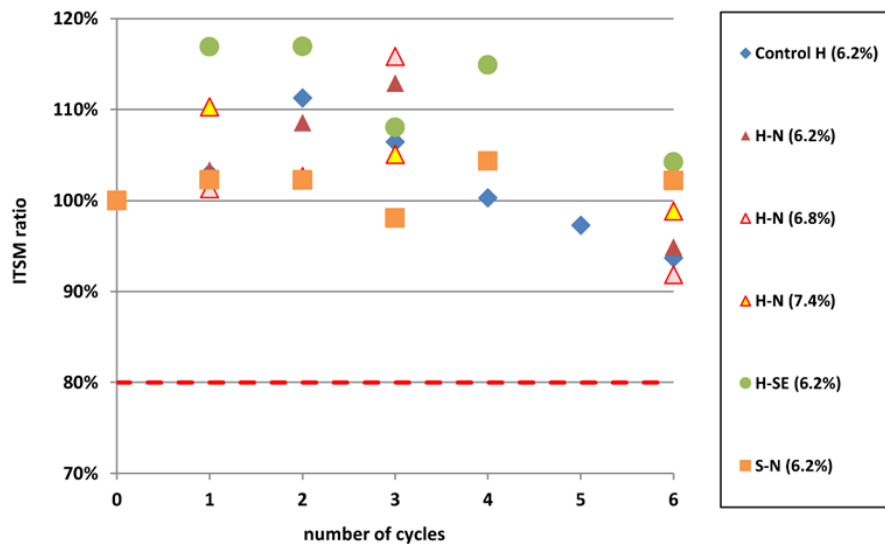


Figure 5.7: ITSM ratio for the mixtures after several water immersion cycles

Finally, the specimens that had undergone six water immersion cycles were tested destructively for their indirect tensile strength (ITS) values at 20°C test temperature. The ITS test is conducted by applying diametrically a load at 50 mm/min displacement speed to a

cylindrical specimen until breaks. The test is conducted in accordance with BS EN 12697-23. The ITS is calculated according to the following formula:

$$ITS = \frac{2P}{\pi.D.H} \quad \text{Equation 5.6}$$

where;

ITS: indirect tensile strength (MPa)

P: peak load (N)

D: diameter of the specimen (mm)

H: height of the specimen (mm)

The average ITS value for the three conditioned samples is compared with the average ITS value for three other dry samples, as shown in Figure 5.8, with the range bars representing the minimum and maximum values. In most cases, the results of the conditioned ITS values, are similar or slightly lower than the unconditioned ones. It can be seen that the H-N (7.4%) mixture has a conditioned ITS value even higher than the unconditioned one. This demonstrates that a higher binder content is beneficial to the moisture resistance of asphalt mixtures.

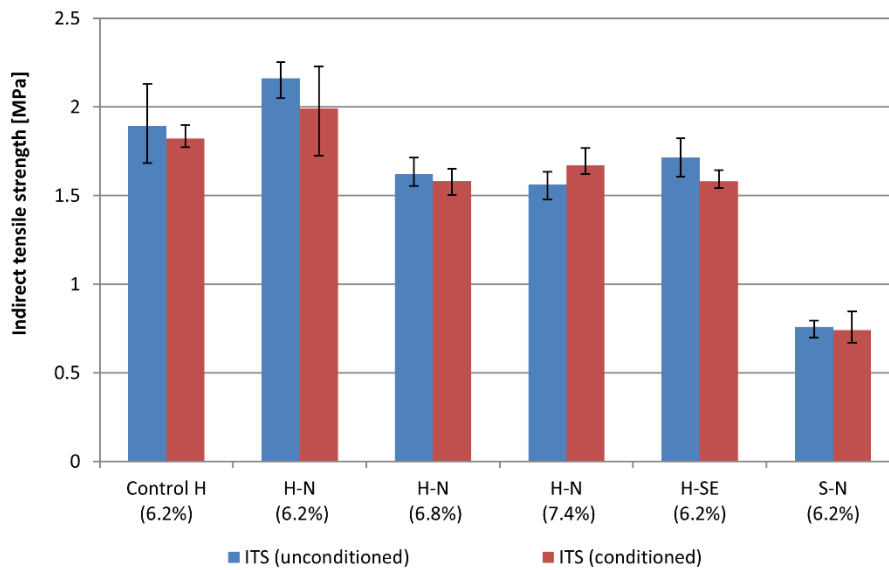


Figure 5.8: ITS values for the conditioned and unconditioned specimens

5.7 Summary and Conclusions

In this chapter, a brief description of the materials used in the production of asphalt mixtures, mixture design procedure and specimen preparation, have been presented. A typical stone mastic gradation (10mm) was selected from the British specification BS EN 13108-5/ PD

6691:2007 for manufacturing the RTR-MB mixtures and the control one. The mixing and compaction process of RTR-MBs mixtures were reasonably accomplished by considering higher mixing and compaction temperature. On the other hand, the pre-treatment with WMA, in the case of H-SE binder, provided a significantly improved workability and compactability for RTR-MB mixtures. The tests on evaluating the water sensitivity of RTR-MB mixtures have revealed that those mixtures exhibit as excellent water damage resistance as the control one. It can, therefore, be concluded that the aggregate can be adequately coated by the thicker RTR-MBs, even though the actual bitumen content is reduced. In the next two chapters, a detailed investigation on binders (H, H-N, H-SE and S-N) and their mixtures, to assess their main performance parameters in terms of fatigue cracking and rutting, will be presented.

Chapter 6 Fatigue Cracking in Binders and Mixtures

6.1 Introduction

Fatigue cracking can lead to a significant reduction in the lifespan of flexible pavements. It is a very complicated distress mode and no single asphalt mixture property has been found to reliably predict and control the fatigue of a flexible pavement (Roque, Birgisson et al. 2004). However, the fatigue life of hot-mix asphalt (HMA) has been recognised to be highly sensitive to the properties of the binder and fatigue cracking normally initiates and propagates within the binder, binder-filler mastic or bitumen-aggregate interface. Although, many studies have shown that mixtures with RTR-MBs possess superior fatigue characteristics, very limited studies have considered characterising their binders. It is well appreciated that there is a challenge to find a representative binder test and parameter that can accurately describe the binder contribution to fatigue damage resistance. Many studies have suggested that characterising the binders at small strains within only the linear viscoelastic region as the case with the SHRP fatigue parameter $G^*\sin\delta$ does not necessarily reflect the true binder performance related to asphalt mixture or pavement performance. Therefore, a large number of research groups have attempted to identify testing procedures and fundamental parameters that can accurately reflect the contribution of the binders' properties on the fatigue resistance of asphalt mixtures and subsequently pavement performance (Bahia, Zhai et al. 1999, Chen and Tsai 1999, Bahia, Hanson et al. 2001, Andriescu, Hesp et al. 2004, Planche, Anderson et al. 2004, Baaj, Di Benedetto et al. 2005, Tsai and Monismith 2005, Johnson, Bahia et al. 2007, Zhou, Mogawer et al. 2012).

The Time Sweep Repeated Cyclic Loading (TSRCL) test has been successfully used to evaluate the fatigue properties of binders (Anderson, Hir et al. 2001, Bahia, Hanson et al. 2001, Planche, Anderson et al. 2004). It allows simulating of the fatigue phenomenon and monitoring directly of the damage behaviour of binders through the change in their viscoelastic properties, i.e. modulus of stiffness and phase angle. Moreover, researchers at Queen's University proposed the double-edged notched tension (DENT) test which is based on the concept of essential work of fracture (EWF) of materials under the ductile state for characterising the fracture properties of binders (Andriescu, Hesp et al. 2004).

In this study, the binders (H, H-N, H-SE and S-N) developed in Chapter 4 are evaluated in detail for their fatigue and fracture performance. TSRCL and DENT tests are adopted to study the binders' resistance to fatigue and fracture. The fatigue data of the TSRCL test are analysed using the dissipated energy approach in addition to traditional fatigue analysis. In order to evaluate the healing potential for the binders, different rest periods are introduced among the continuous loading sequence in the TSRCL test. This chapter also provides a review and critical evaluation of different approaches used to define the fatigue failure to assess accurately the fatigue damage resistance. A new and simple approach is also suggested in this chapter to determine a reliable plateau value PV. The new method is applied successfully on both base bitumen and RTR-MBs. In terms of mixture testing, the different mixtures produced in Chapter 5 are characterised using the ITFT and the Superpave indirect tensile IDT tests.

6.2 Testing Programme

6.2.1 Binder Testing Protocol

Time Sweep Repeated Cyclic Load (TSRCL)

The TSRCL test was performed using a Kinexus Model Dynamic Shear Rheometer (DSR) supplied by Malvern Instruments Ltd. This model of DSR uses a Peltier system to control the temperature in which the air is used as the cooling/heating medium, unlike other DSRs that use a water bath which could have side effects on the fatigue process. Most of the fatigue tests were carried out under controlled stress conditions with one set of data being produced under controlled strain conditions in order to examine the effect of loading mode. All tests were conducted at a single frequency of 10Hz using a 2mm gap with the 8 mm plate-plate testing geometry. Different testing temperatures were selected for H group binders and for binder S-N to ensure high initial complex modulus $|G^*|$ (higher than 15 MPa) so that edge

effects or plastic flow can be eliminated and the binders fail due to “true” fatigue damage rather than “instability flow” (Anderson, Hir et al. 2001). Various stress levels were applied on the different binders to induce different initial strains. Table 6.1 shows test conditions and parameters applied in this study. To investigate the impact of rest period duration on bitumen fatigue, an intermittent loading sequence was used by introducing different short rest times (10 and 20 seconds) after every 500 load pulses. The intermittent loading sequence is believed to provide a better simulation of field loading conditions compared with other loading sequences in which a single long stop period is used (Shen, Chiu et al. 2010). All tests were carried out on unaged binders.

Table 6.1: Test conditions and parameters

Material	Temperature [°C]	Stress-control [kPa]	Strain-control [%]	Rest period RP [sec]	Initial stiffness [MPa]
H	10	900, 1000, 1100, 1200, 1300, 1400, 1500	n/a	0	82
	10	900, 1000, 1100, 1200, 1300, 1400, 1500	n/a	10	82
	10	900, 1000, 1100, 1200, 1300, 1400, 1500	n/a	20	82
	10	n/a	1.25, 1.5, 1.75, 2	0	82
	20	200, 250, 300, 350, 400, 500	n/a	0	21
	20	200, 250, 300, 350, 400, 500	n/a	20	21
H-N	10	400, 450, 500, 550, 600, 650, 700, 800	n/a	0	33
	10	400, 450, 500, 550, 600, 650, 700, 800	n/a	20	33
	20	125, 150, 200, 250, 300	n/a	0	11
H-SE	10	400, 450, 500, 550, 600, 650, 700, 800	n/a	0	40
	10	400, 450, 500, 550, 600, 650, 700, 800	n/a	20	40
	20	125, 150, 200, 250, 300	n/a	0	13
S-N	0	250, 300, 350, 400, 450	n/a	0	28
	0	250, 300, 350, 400, 450	n/a	20	28

Double Edged Notched Tension (DENT)

The double edged notched tension (DENT) test was conducted in a force-ductility apparatus installed in a ductilometer. The elastic recovery specimen mould was modified by manufacturing new DENT inserts from a 360 brass to have a space between the matching pair of notches equal to the three different ligament lengths of 5, 10, and 15 mm, when fitted with the end pieces of a standard mould, as shown in Figure 6.1. The test was performed according to the following protocol:

- Specification: LS-299 (method of test for the determination of asphalt cement’s resistance to ductile failure using double edge notched tension test (DENT))
- Temperature: 10°C and 0°C for binder S-N, the H group binders were tested at 10 °C and 20 °C
- Displacement rate of 50 mm/min
- Two replicates for each observation

- The ageing effect was evaluated in this study, the tests were conducted on unaged samples, TFOT samples and TFOT+PAV samples.

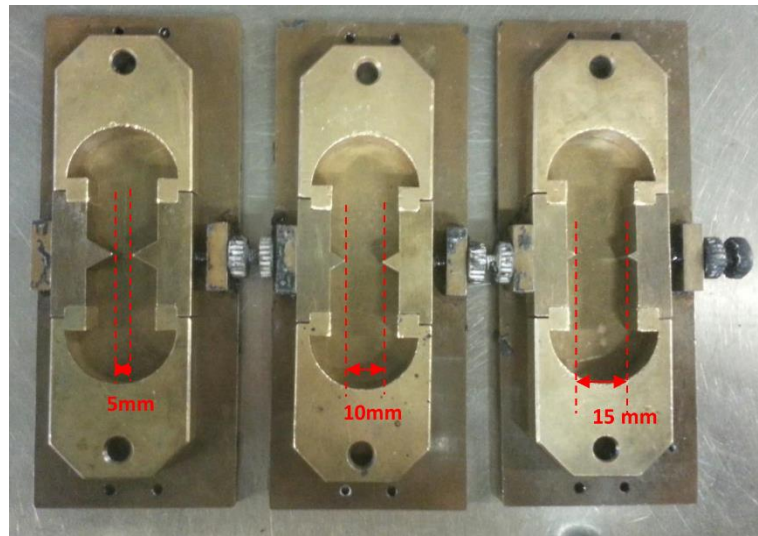


Figure 6.1: DENT test moulds

6.2.2 Mixture Testing Protocol

Indirect Tensile Fatigue Test (ITFT)

The ITFT is the most widely used in the United Kingdom to evaluate the fatigue properties of bituminous mixtures. The mixtures are investigated under repeated load applications with a constant load mode using the NAT machine. The test is implemented according to EN 12697-24:2012 (E) using the following test parameters:

- Test temperature: 20°C
- Loading condition: Controlled-stress
- Loading rise-time: 0.1 sec loading time and 0.4 sec rest time
- Poisson's ratio : 0.35
- Failure condition: the fatigue life is determined as the total number of load applications that cause a complete fracture of the specimen

During the fatigue test, a haversine load signal is applied to the vertical diametric plane which causes a tensile stress along the vertical diametric plane perpendicular to the load direction. The resultant horizontal deformation is measured and monitored continually through two linear LVDTs fixed on steel strips as shown in Figure 6.2. The tensile strain at the centre of the specimen is calculated as follows:

$$\varepsilon_o = \frac{2\delta(1+3\nu)}{d(4+\pi\nu-\pi)} \quad \text{Equation 6.1}$$

where; ε_o = the tensile strain, δ = the horizontal deformation (mm), ν = the Poisson's ratio and d = the specimen diameter (mm). If $\nu = 0.35$, then

$$\varepsilon_o = \frac{2.1\delta}{d} \quad \text{Equation 6.2}$$

The initial tensile strain is an important parameter for determining the fatigue life of different mixtures. Therefore, the fatigue life of bituminous mixtures can be represented by the following equation:

$$N_f = k \left[\frac{1}{\varepsilon_o} \right]^n \quad \text{Equation 6.3}$$

where; N_f = the fatigue life, k and n = material constants and ε_o = the initial tensile strain at the centre of the specimen calculated according to Equation 6.3.

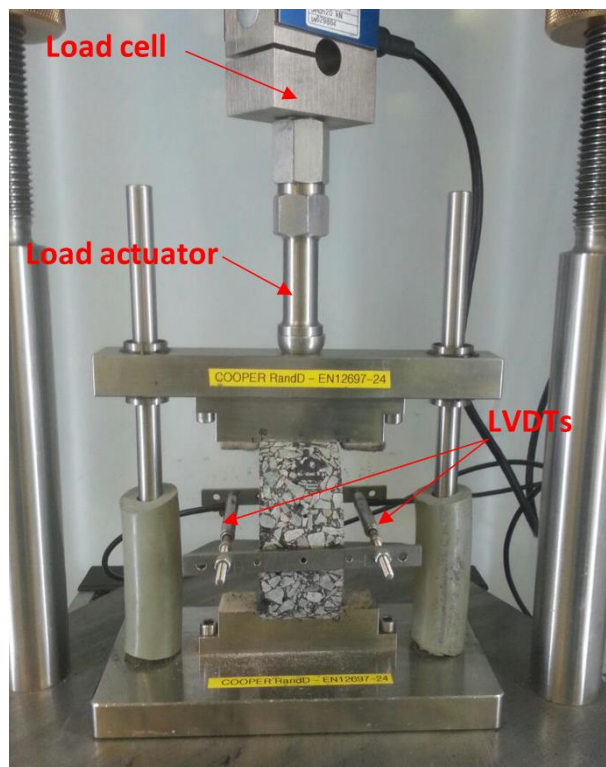


Figure 6.2: ITFT testing configuration in NAT

SuperPave Indirect Tensile Test (IDT)

Three types of test are performed with the Superpave IDT on each specimen: resilient modulus (non-destructive test), creep compliance (non-destructive test), and tensile strength (destructive test). The tests are performed at 20°C using the INSTRON (hydraulic loading frame with a maximum load capacity of ± 100 kN) test equipment. Three replicate specimens

were tested at each temperature. The effect of binder content, for H-N and H-SE mixtures, is investigated in this test. To obtain accurate measurements for vertical and horizontal strains, 90° 2-element cross polyester wire strain gauges were used. The vertical and horizontal strain measurements are taken from the strain gauges through a data acquisition box. The load measurements are also taken from the data acquisition box and the latter receives the load signals through the Digital Controller of the INSTRON, as shown in Figure 6.3. The details about specimen preparation, test settings, and connections can be found in Appendix A. Three consecutive tests are conducted as follows:

- The resilient modulus test: The resilient modulus test was conducted in load control mode by applying a repeated haversine waveform load to the specimen for a 0.1 s followed by a 0.9 s rest period. In order to keep the specimen undamaged and maintain the linearity of the material response, the load was selected to generate a horizontal strain between 100 and 300 microstrain during the test
- The creep test: After finishing the resilient modulus test, 5 min is given to allow the specimen to re-stabilize. Then, a static load is imposed along a diametric axis for 1000s. The creep compliance test is non-destructive; therefore, the constant load should be selected such that the generated horizontal deformation does not exceed the upper linear-elastic boundary. Also, the horizontal deformation should be high enough to minimise the noise effect in the data acquisition process. Buttlar and Roque suggested that a load that induces horizontal strains within 40 and 120 microstrains at t=30 s is appropriate, and the test should be stopped if strains exceed these limits (Buttlar and Roque 1994).
- The tensile strength test: The indirect tensile strength test is a destructive test and performed by applying a load at a constant rate (50mm/min) with vertical ram movement until the specimens fail. The vertical and horizontal strains in addition to the load, are recorded and the maximum load is identified as the occurrence of a tensile failure.

It should be mentioned that, in this study, almost the same testing procedure as that suggested by Roque and Buttlar was used but with the following differences:

- (1) The sample diameter used in this study is 100mm, not 150mm which is normally used with Superpave IDT

- (2) Using 60mm length strain gauge which is not equal to one-quarter of the specimen diameter as suggested by Roque and Buttlar
- (3) The cross strain gauge was placed only on one face. In the Roque and Buttlar procedure, the LVDTs or strain gauges are placed on both flat faces
- (4) Using the simple average over three replicates, instead of the trimmed mean used in the AASHTO procedure

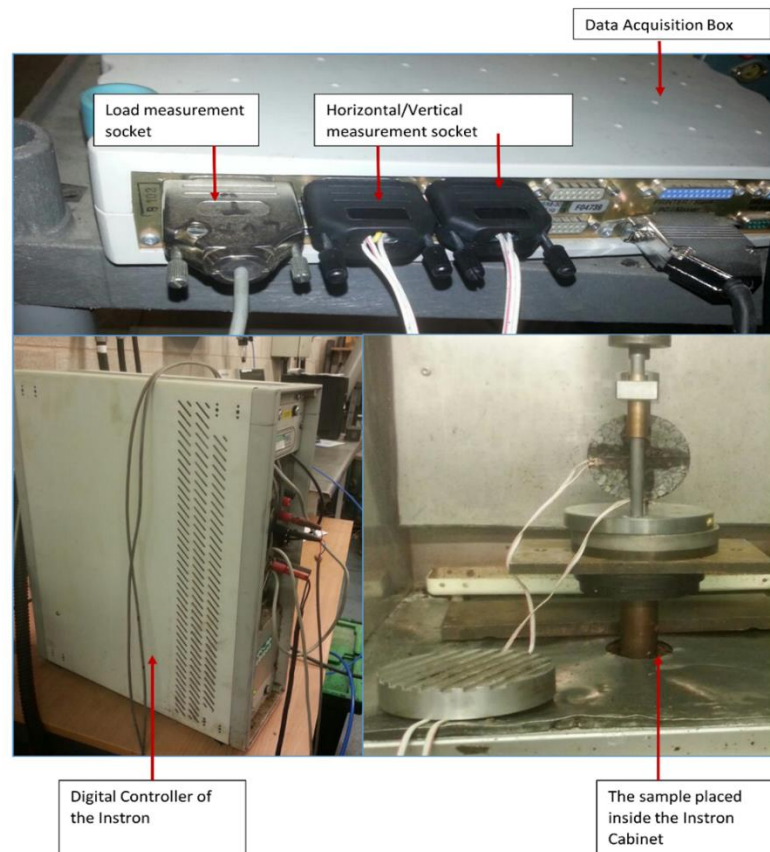


Figure 6.3: The IDT configuration in the INSTRON

6.3 Time Sweep Repeated Cyclic Load (TSRCL)

6.3.1 Definition of fatigue failure

The different failure criteria; 50% decrease in the initial stiffness, DER and Black diagram approaches were compared to see if there is a significant difference between them that could affect the fatigue analysis. Figure 6.4 shows the evolution of the complex modulus as a function of load cycles for all the binders during a fatigue test with no rest periods. The 50% reduction in stiffness was applied on the initial stiffness as taken from the raw data and on the initial stiffness obtained by extrapolation which is conducted by fitting a third order polynomial relationship to the data as shown in Figure 6.4. The extrapolated initial stiffness

is often used as the rapid decrease at the beginning of a fatigue test is thought to be due to other artefact effects such as heating and thixotropy and not only fatigue (Di Benedetto, De La Roche et al. 2004, Di Benedetto, Nguyen et al. 2011).

Previous studies have shown that the distinction between crack initiation and crack propagation could be defined by focusing on the rate of change in the material's response with load applications, dG^*/dN (Little, Lytton et al. 1998, Roque, Sankar et al. 1999). When the rate of change of dG^*/dN is constant (linear), the materials can be considered to be undergoing crack initiation. When the rate of change of dG^*/dN is no longer linear, then the material can be considered to be experiencing crack propagation. Therefore, the transition zone between crack initiation and crack propagation can be considered to lie between the two dashed lines shown in Figure 6.4. It can be seen that the failure points based on the 50% classical approach for the H-N and S-N binders were not totally in agreement with the estimated transition zone or with the other failure criteria. If a fatigue comparison was made based on the classical failure criterion between binders H-N and S-N on the one hand, and between binders H and H-SE on the other, the fatigue analysis would be biased and misleading as the difference in their viscoelastic properties and deterioration path would not have been considered. The viscoelastic properties of binders H-N and S-N allow larger strains to be sustained before the material is fractured and thus larger continuous decreases in stiffness (more than 50%) would still be within the fatigue lifespan. Conversely, the binders H and H-SE were less strain tolerant and hence do not allow larger continuous decreases in stiffness. Other failure criteria, i.e. DER and Black diagram, cannot be taken as arbitrary and indeed they have been shown to correspond to a particular stage of fatigue damage. As the results show that the fatigue failure points based on the Black diagram is the closest to the transition zone, it has been taken as the failure criterion for fatigue analysis in this study.

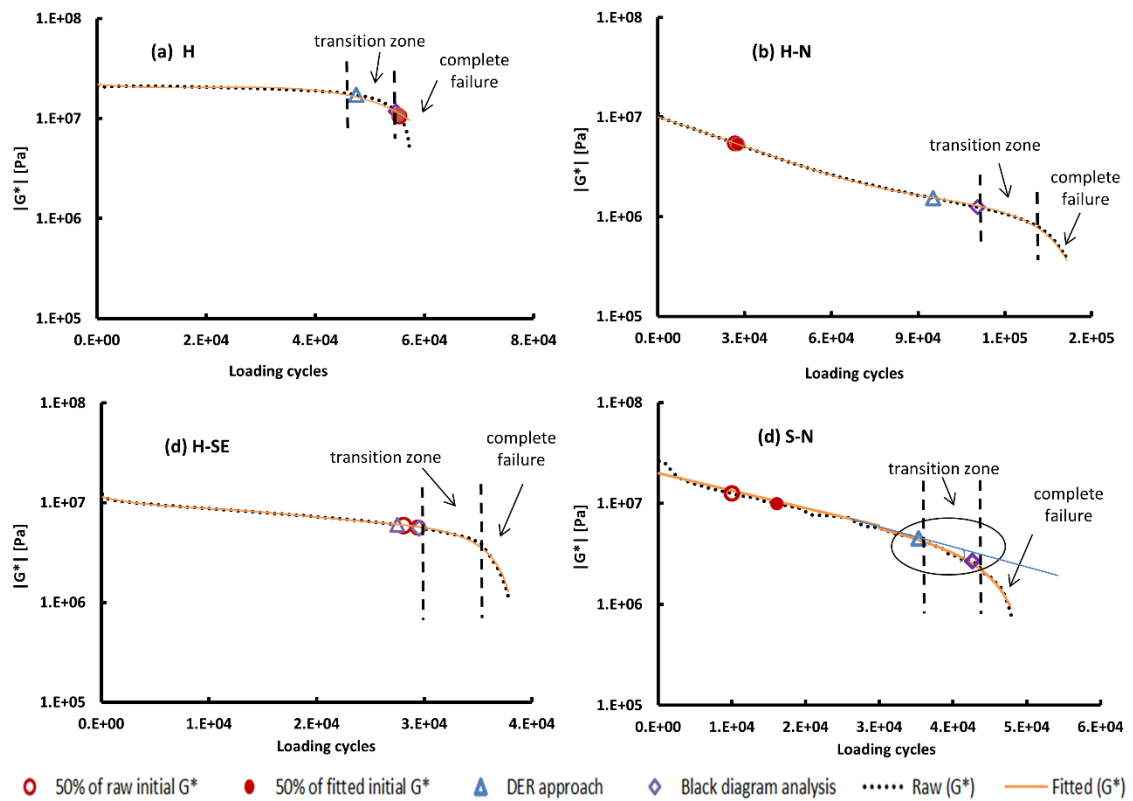


Figure 6.4: The failure points identified by different methods located at the evolution of $|G^*|$ vs. load cycles during fatigue tests for all binders

6.3.2 Traditional fatigue analysis

It has been noticed that the initial strain has the most significant effect on fatigue life, therefore, the average strain during the first 1000 cycles from the stress-controlled tests was selected as an independent variable. The fatigue test results under different conditions are graphically presented by the classical “WÖHLER” curve, in Figure 6.5. These curves show the relation between the fatigue life N_f and initial strain and are expressed using a power fatigue law as follows:

$$N_f = a (\epsilon_0)^b \quad \text{Equation 6.4}$$

where N_f = number of cycles to failure from black diagram analysis, ϵ_0 = initial strain, a and b are experimentally determined constants.

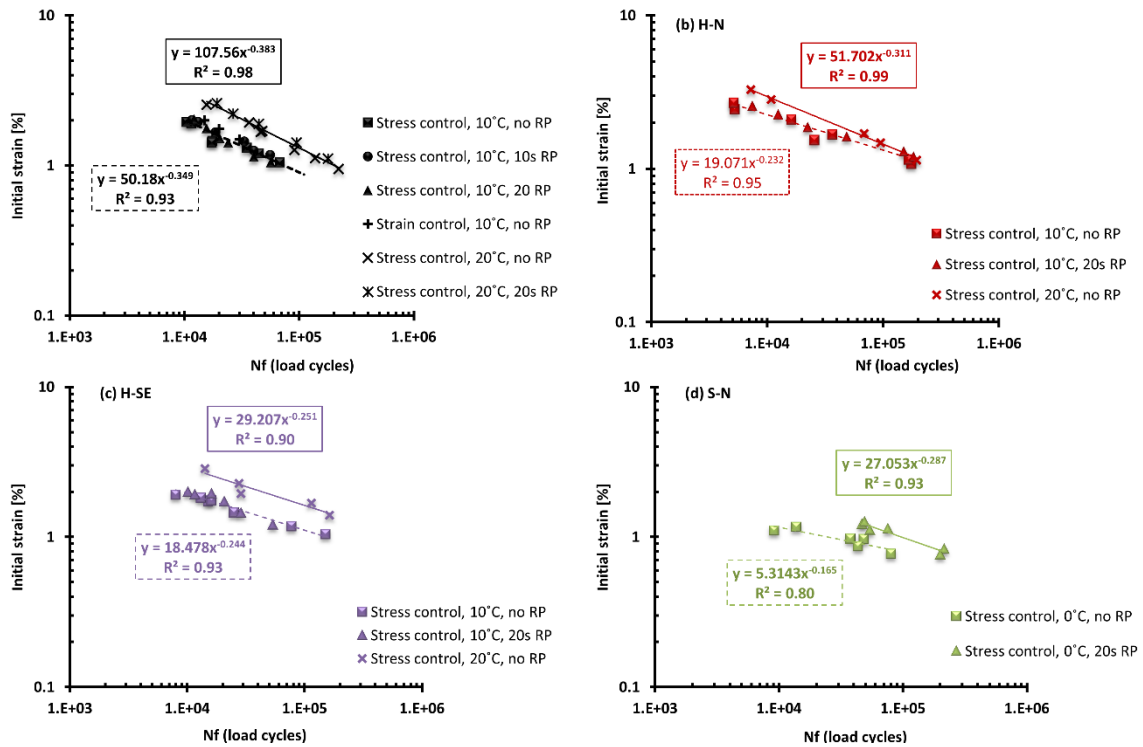


Figure 6.5: Traditional fatigue curves “WÖHLER” for all binders

The traditional fatigue curves for binders H, H-N and H-SE, in Figure 6.5 a, b and c, show that fatigue curves are clearly dependent on test temperature, with an increase in fatigue life when those binders are tested at 20°C compared to 10°C. In accordance with some findings in the literature, the fatigue life of stiffer materials is normally longer than the fatigue life of softer materials when tested under controlled-stress loading (Baaj, Di Benedetto et al. 2005, Wu, Huang et al. 2013). This means that the binders tested at a higher temperature (stiffness decreased) should have a shorter fatigue life. However, the effect of stiffness on fatigue life in those curves has been minimised as the fatigue law is plotted as a function of the initial strain and not as a function of stress level. In this regard, it is logical to have materials with longer fatigue life at a higher temperature, because they become more capable of sustaining larger strains before fatigue failure than stiffer materials. It can be seen that the inclusion of rest periods (for binders H, H-N and H-SE) and the change of loading mode (for binder H), do not have a significant effect on the fatigue law, and the fatigue curves can be grouped into a single one with an acceptable regression coefficient (R^2). On the other hand, the inclusion of rest periods has considerably increased the fatigue life for binder S-N, as shown in Figure 6.5c, and there is a clear difference between the two fatigue curves. This is attributed to the characteristics of the base bitumen that had been used to produce the binder S-N. The binder S-N is made with a very soft bitumen that has higher content of low

molecular weight fractions. A number of researchers have indicated that soft bitumen has higher healing and recovery capability than hard bitumen (Kim, Little et al. 2003, García, Norambuena-Contreras et al. 2014, Ayar, Moreno-Navarro et al. 2015). In addition, increasing the light fractions can make the bitumen more susceptible to other reversible phenomena such as thixotropy that happen together with microcracking during the fatigue test. Thus, introducing rest periods during cyclic loading could reduce significantly the influence of those phenomena and hence increase the fatigue life for binder S-N.

6.3.3 Cumulative dissipated energy

The total dissipated energy until failure was computed for all materials. As mentioned previously, there is a strong relationship between cumulative total energy and number of cycles at fatigue failure.

$$W_{fat} = A.N_{fat}^z \quad \text{Equation 6.5}$$

This relationship should be independent of the mode of loading, frequency and temperature and depends only on material properties. However, the results, in Figure 6.6a, show that this relationship is temperature dependent for binder H. For the other binders, a unique intrinsic relation between the cumulative dissipated energy and number of cycles to failure exists irrespective of different temperature and rest periods. According to the conceptual hypothesis of the accumulated dissipated energy with fatigue life, a material with a higher magnitude of total dissipated energy until failure indicates better fatigue resistance (Bhasin, Castelo Branco et al. 2009). In this regard, the fatigue curves, shown in Figure 6.6a, demonstrate that the binder H has a better fatigue resistance when tested at a lower temperature. This is contrary to the fatigue analysis based on the traditional approach, as shown in Figure 6.5a, in the previous section. One possible explanation for this inconsistency is the relatively higher stiffness for binder H at a temperature of 10°C that required applying higher stresses, as shown in Table 6.1. This generated significantly larger viscoelastic energy dissipation for each cycle in comparison to the viscoelastic energy dissipation generated at a temperature of 20°C. This again emphasises the concern about this approach that the sum of dissipated energy includes energies that are not responsible for fatigue damage, and thus, it could be misleading to rank the fatigue resistance of different materials based on this approach. Therefore, the Ratio of Dissipated Energy Change (RDEC) from which the Plateau Value (PV) is derived will be applied in detail in the next section in order to minimise

the side effect of those energies, and provide a solid foundation to rank reliably the fatigue cracking performance of the different binders.

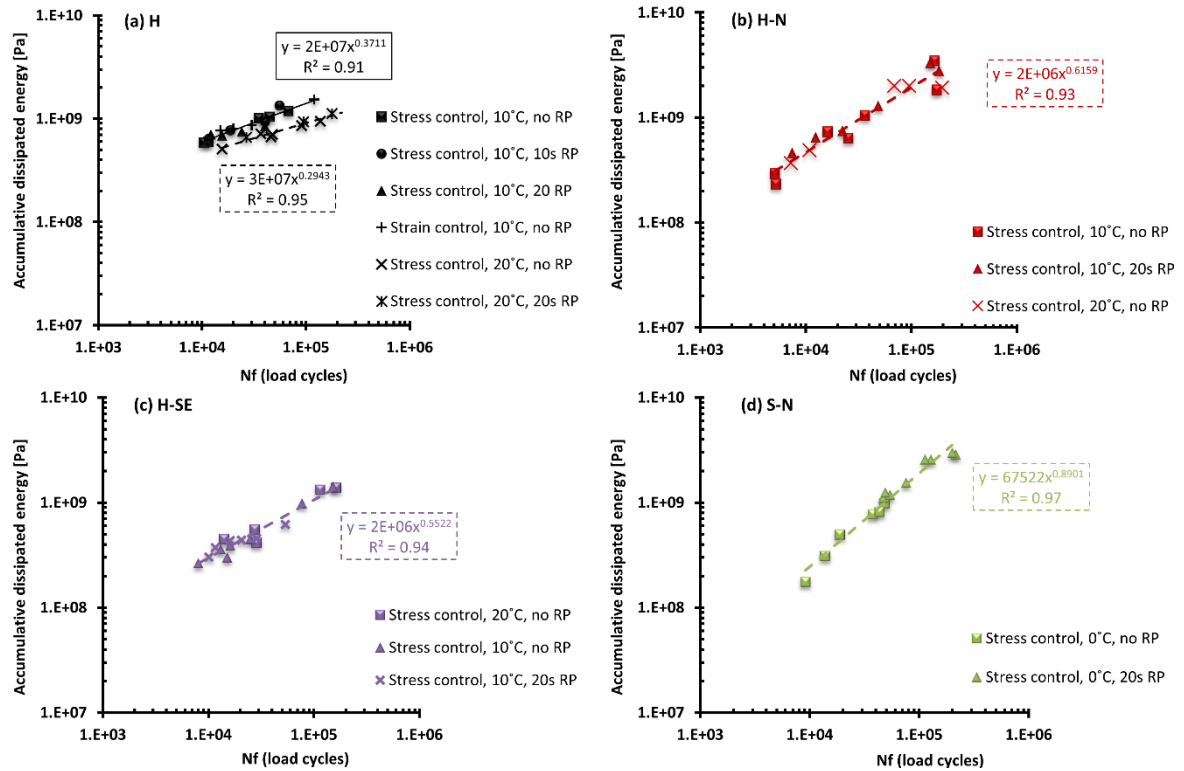


Figure 6.6: Total accumulative dissipated energy vs. N_f for all binders

6.3.4 Ratio of Dissipated Energy Change (RDEC)

Although the RDEC and PV concept is fundamental and has a direct relation to damage accumulation, the determination of a consistent PV is not a straightforward exercise and needs special calculations. Figure 6.7 shows an example of the RDEC evolution calculated directly from the raw data based on Equation 6.6 versus the number of load cycles.

$$RDEC_i = \frac{(w_i - w_j)}{w_i \cdot (i - j)} \quad \text{Equation 6.6}$$

where $RDEC_i$ = ratio of dissipated energy change value at cycle i ; w_i and w_j = dissipated energies at cycles i and j .

It can be seen that obtaining a direct representative PV is not possible due to the amount of scattering in the measured data. Shen and Carpenter (2006) proposed a simplified approach to calculate the PV. The approach is based on obtaining the best fit regression equation for dissipated energy, w_i , versus the number of load cycles which generally follows a power law relationship ($A \cdot x^k$). The exponential slope of the curve, k , is then used with the defined failure point, N_f , to calculate the PV using the following equation:

$$PV = \frac{1 - \left(1 + \frac{100}{N_f}\right)^k}{100}$$

Equation 6.7

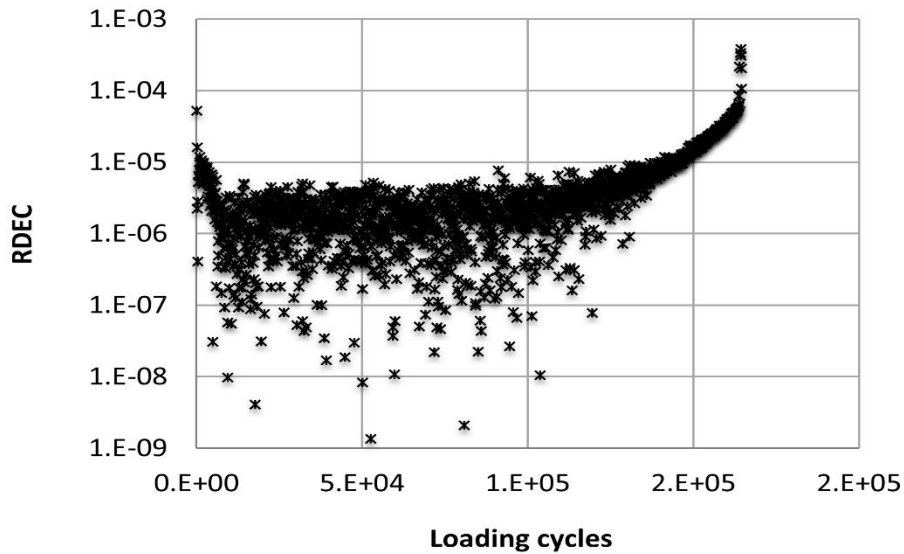


Figure 6.7: RDEC evolution vs. the number of load cycles for H binder tested under stress control mode, 20 °C and no RP

In this study, obtaining a consistent power law model was not possible due to the complicated shape of the dissipated energy vs. number of load cycles plot, as shown in Figure 6.8. In addition, when skipping the data in Phase I and Phase III and keeping only the data in Phase II (the steady-state damage development phase) to make the curve shape simpler, the best fit is still poor. Table 6.2 shows R^2 and k values obtained when considering either the entire data or data within Phase II. It can be seen that the best fit regression gives significantly different exponential slopes, k , for the complete w_i vs load cycles curve versus the values obtained when only considering Phase II. This results in differences in the intrinsic PV fatigue law once calculated as shown in Figure 6.9. It should be mentioned that high variability and difficulties in obtaining a “correct” PV were also reported in other studies (Bhasin, Castelo Branco et al. 2009, Pais, Pereira et al. 2009, Boudabbous, Millien et al. 2013).

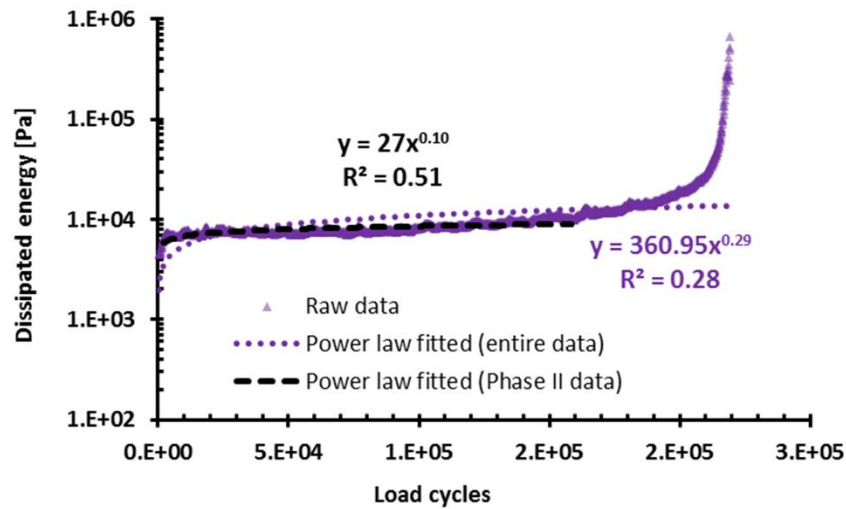


Figure 6.8: Shape of dissipated energy vs. number of load cycles and the best-fit regression of different segments

Table 6.2: Calculated PV based on Equation 6.6 for H binder tested under stress control mode, 20 °C and no RP

Stress level	Nf	Entire data fitting			Phase II fitting		
		k	R ²	PV	K	R ²	PV
200	221300	0.08	0.16	3.61E-07	0.02	0.31	9.04E-08
250	137300	0.14	0.24	1.02E-06	0.06	0.71	4.37E-07
300	90700	0.14	0.25	1.54E-06	0.073	0.71	8.04E-07
350	47500	0.12	0.2	2.52E-06	0.07	0.6	1.47E-06
400	36600	0.09	0.14	2.46E-06	0.06	0.67	1.64E-06
500	15600	0.12	0.2	7.66E-06	0.075	0.65	4.79E-06

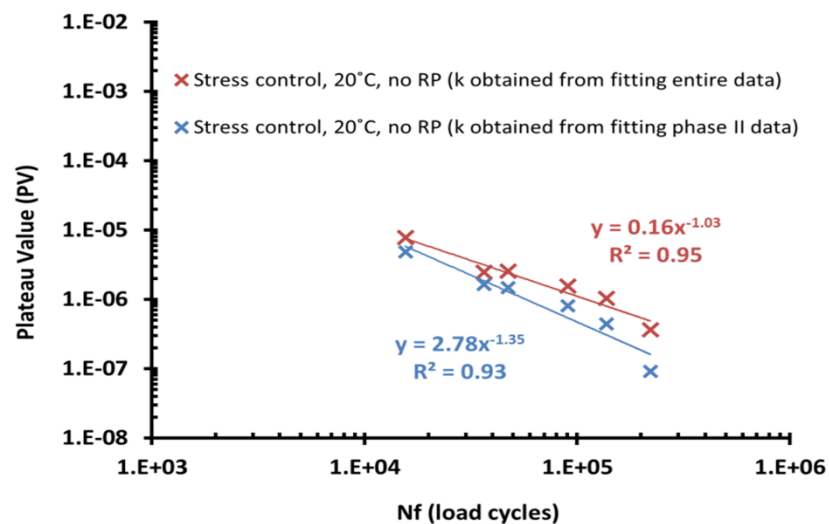


Figure 6.9: PV fatigue curves based on Equation 6.6 for H binder tested under stress control mode, 20 °C and no RP

To minimise the ambiguity in calculating the plateau value, an alternative approach has been proposed to compute the PV based on the direct linear slope of the steady-state phase and also based on the fundamental definition of RDEC. In Equation 6.6 the term $\frac{(w_i-w_j)}{(i-j)}$ represents the linear slope of a small segment in Phase II of the dissipated energy w_i vs. load cycles curve. To overcome experimental data noise and optimise the best fit regression process, the linear slope of Phase II was defined from the raw data of dissipated energy as follows:

$$\mu = \frac{(\dot{w}_f - \dot{w}_a)}{(N_f - a)} \quad \text{Equation 6.8}$$

where μ = the linear slope of Phase II; \dot{w}_f = the dissipated energy at the defined failure point; \dot{w}_a = the dissipated energy at the end of Phase I; N_f = the number of load cycles to the defined failure and a = the number of cycles at the end of Phase I (it can be estimated graphically from the w_i vs. load cycles curve). The PV is then calculated by dividing μ by the initial value of dissipated energy, w_o .

$$PV = \frac{\mu}{w_o} \quad \text{Equation 6.9}$$

Figure 7 illustrates graphically the procedure for calculating PV. This approach provides a consistent method to obtain a realistic PV and produces an intrinsic fatigue law. Applying the proposed approach, the plateau value was computed for all the binders in the study under different testing conditions (stress levels, temperature and rest periods).

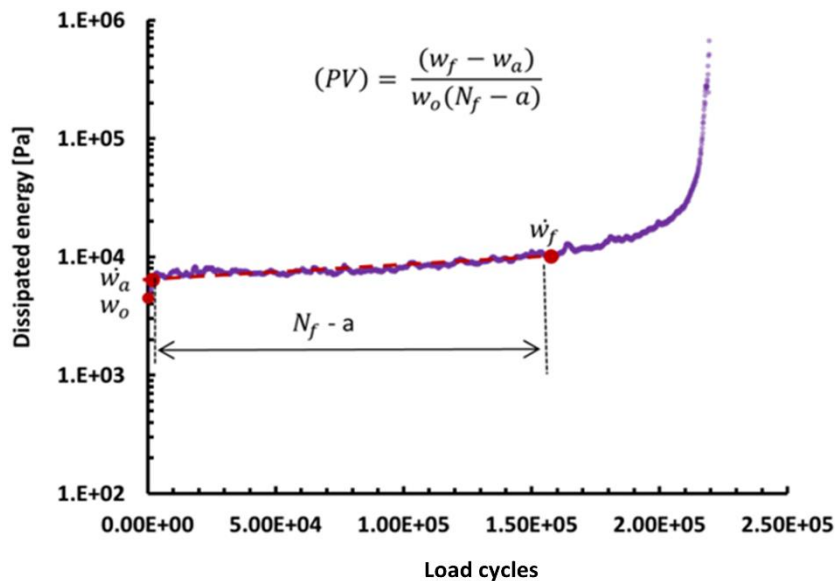


Figure 6.10: Graphical illustration of determining PV according to the proposed approach

The PVs are then plotted against the defined failure point N_f , as shown in Figure 6.11. The results show that there is a unique power-law relationship between PV and N_f with acceptable $R^2 \approx 0.95$, regardless of loading mode, temperature or rest periods, for binder H, and regardless of temperature or rest periods, for binder H-N, and regardless of rest periods, for binders H-SE and S-N. However, the power law relationship was strongly dependent on material type. These PV- N_f curves are contradictory to other fatigue findings presented by Shen and her co-workers (Shen and Carpenter 2005, Shen, Airey et al. 2006, Shen and Carpenter 2006, Shen, Chiu et al. 2010). They showed that this relationship is unique regardless of mixture type. However, considering the results of this study and comparing other fatigue studies conducted by other researchers (Shen and Carpenter 2005, Shen, Airey et al. 2006, Bhasin, Castelo Branco et al. 2009, Pais, Pereira et al. 2009, Shen, Chiu et al. 2010, Boudabbous, Millien et al. 2013) it can be concluded that the PV- N_f relationship cannot always be considered to be independent of material type. Figure 6.12 shows a comparison of different PV- N_f curves (asphalt mixtures and binders) adopted from the aforementioned studies. The results in Figure 6.12 clearly show that the PV- N_f relationship is dependent on material type.

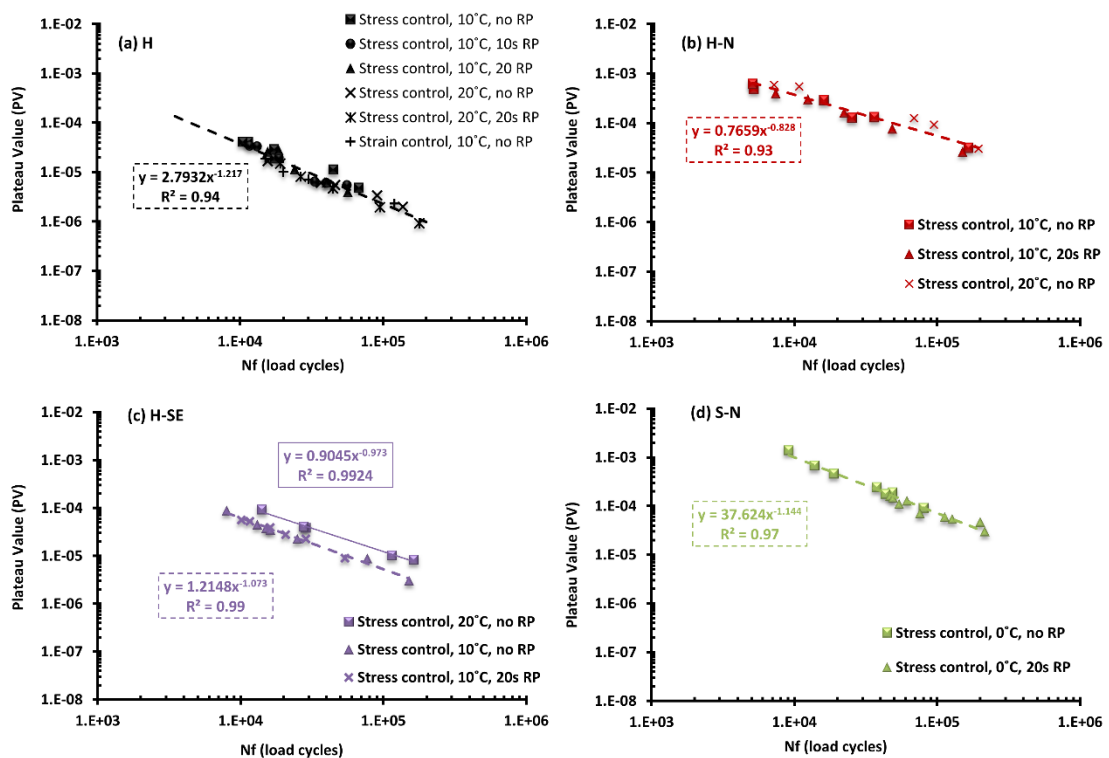


Figure 6.11: PV vs. N_f computed by the proposed approach

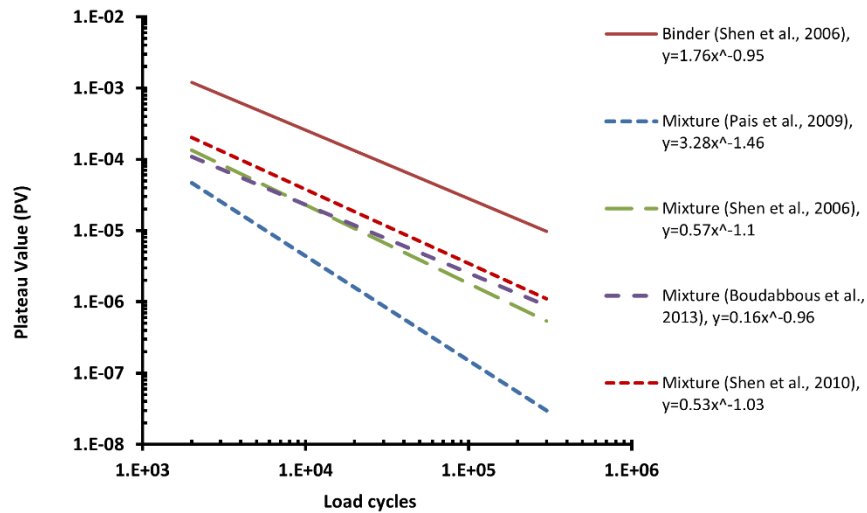


Figure 6.12: Comparison of different PV-N_f curves (asphalt mixtures and binders) adopted from various research studies

Thus, the fatigue resistance of different asphalt mixtures or binders can be evaluated on the basis of the PV-N_f curve. In that sense, the material with desirable fatigue properties is the material that has a higher number of fatigue cycles at a certain amount of relative dissipative energy, PV. The PV-N_f curves in Figure 6.13 show that the addition of rubber, for binders H-N, H-SE and S-N, can result in better fatigue performance compared to unmodified bitumen. It can also be seen that the binder S-N outperforms other binders, follows by H-N, H-SE and H. This is logical since the S-N is a highly flexible binder that allows sustaining higher damage input during fatigue evolution. The absence of an intrinsic PV-N_f fatigue curve, in the case of binder H-SE, might have been caused by the complex modification of rubber and waxes that resulted in a considerable alteration in the rheological properties of this binder. However, the PV-N_f curves for binder H-SE are consistent with the general effect of temperature on fatigue characteristics, and with the traditional fatigue analysis that shows the binder H-SE has a better fatigue life at a higher temperature.

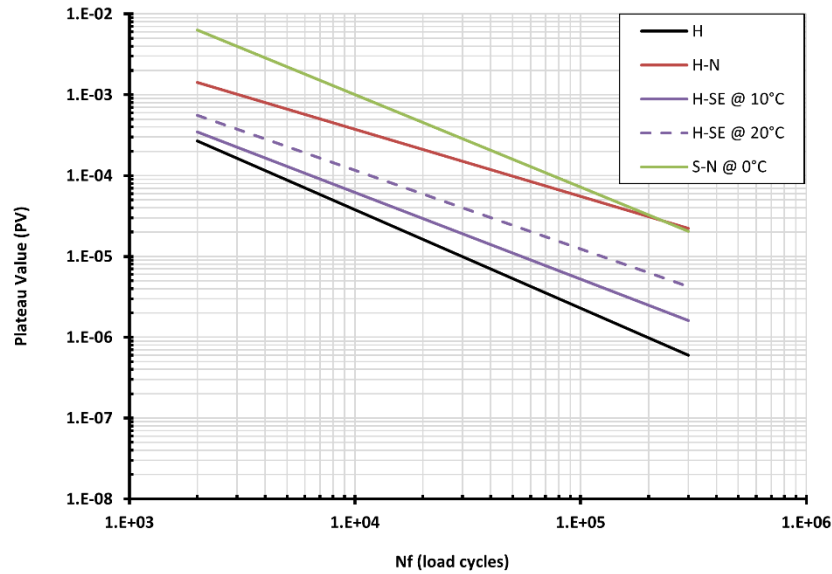


Figure 6.13: Comparison of different PV-Nf curves of the current binders

6.4 The Essential Work of Fracture and CTOD

The fracture characterisations of binders in the ductile state were studied by means of the essential work of fracture (EWF) needed to generate new surfaces using the DENT test. This test allows evaluating the materials resistance to fracturing on notched samples under high levels of strain, yielding and fracture processes. Figure 6.14 shows the typical force–displacement curves obtained from the DENT tests for all materials and at different ligament lengths. The repeatability of the test is excellent and all ligament lengths have the same force-displacement curve but each binder has its unique failure mechanism. All binders have a clear maximum point which corresponds to the yielding around the ligament area. However, the rubberized binders produced with N crumb rubber show two yielding points. A behaviour known as strain-hardening which is found in some polymers could be responsible for the two yielding points. Researchers working on asphalt materials stated that strain-hardening can also be found in polymer modified bitumens (Johnson, Bahia et al. 2009, Zoorob, Castro-Gomes et al. 2012). It happens due to the crosslinked network in the rubber which acts as a two-phase system when subjected to stretching to high strains. Johnson, Bahia et al. (2009) suggested that this phenomenon may explain the superior fatigue performance of SBS-modified pavements when tested under the Accelerated Loading Facility (ALF) as stiffening the binder under higher strains can prevent extra damage. The two yielding points are very clear in S-N binder where the second yield point is even higher than the first. The very soft properties of the base bitumen S may explain why the second yield point prevailed over the first point while it is lower in H-N. The effect of

rubber modification on total fracture energy is clear when a comparison of the force-displacement curves is made between the base bitumens and RTR-MBs. Obviously, the addition of recycled tyre rubber resulted in toughening of the materials, i.e. it made them stronger and more flexible which can be translated into better fracture properties. It can be seen from Figure 6.14c that binder H-SE is stronger but less able to stretch than the base bitumen H. The pre-treatment by waxes can make the binders less flexible due to the crystal lattice structure of waxes that prevents the movement of molecules in the modified binder (Jamshidi, Hamzah et al. 2013).

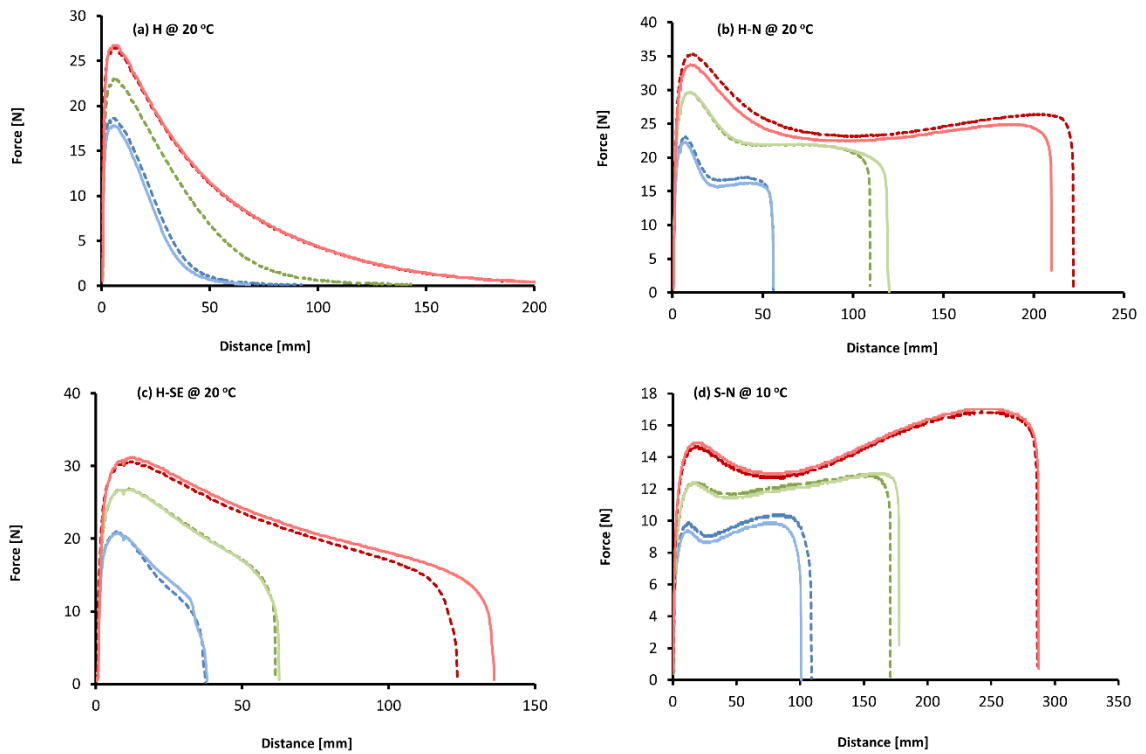


Figure 6.14: The typical force-displacement curves for all unaged binders

Figure 6.15 shows the net section stress as a function of the ligament length. As the net section stress decreases with the increase in ligament length, it can be concluded that all binders were tested under plane-stress/plane-strain mixed mode. As all binders had undergone the same mixed mode stress conditions, therefore, the determined fracture parameters in the next sections should identify reliably the differences in their fracture properties.

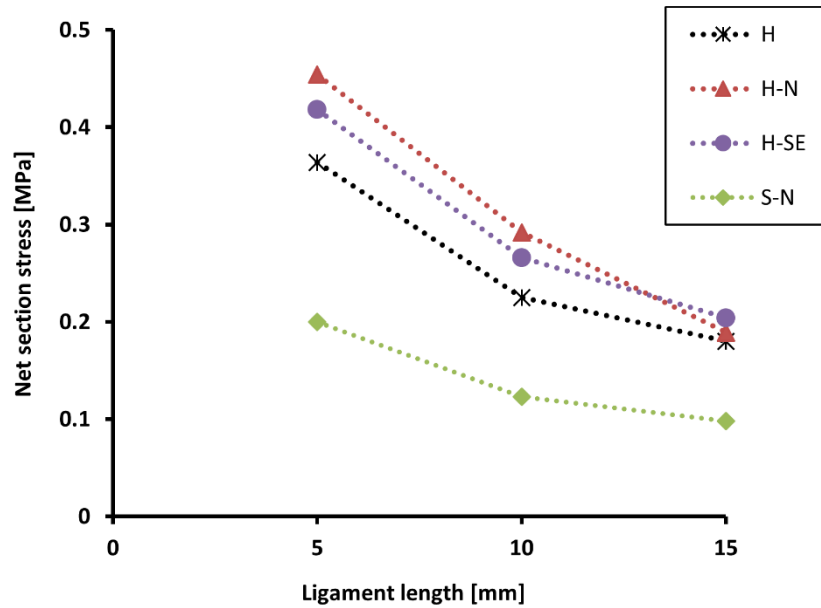


Figure 6.15: Net section stress as a function of the ligament length, for unaged binders, for H, H-N and H-SE @ 20 °C and for S-N @ 10 °C

Having the total fracture energy under the force-displacement curves determined and divided by ligament cross-sectional area ($L \times B$), the w_t is obtained and plotted against the ligament length as shown in Figures 6.16. By using a linear fitting procedure the specific essential work, w_e , and the plastic work of fracture term, βw_p , are determined from the intercept and from the slope of the line, respectively. The linear regression of data points in Figure 6.16 demonstrates an acceptable fitting procedure indicating that the assumptions of the EWF approach are successfully met. Figure 6.16 clearly shows that the plastic work of fracture term, βw_p , in the base bitumen H is significantly smaller than in the case of the modified binders, H-N, H-SE and S-N.

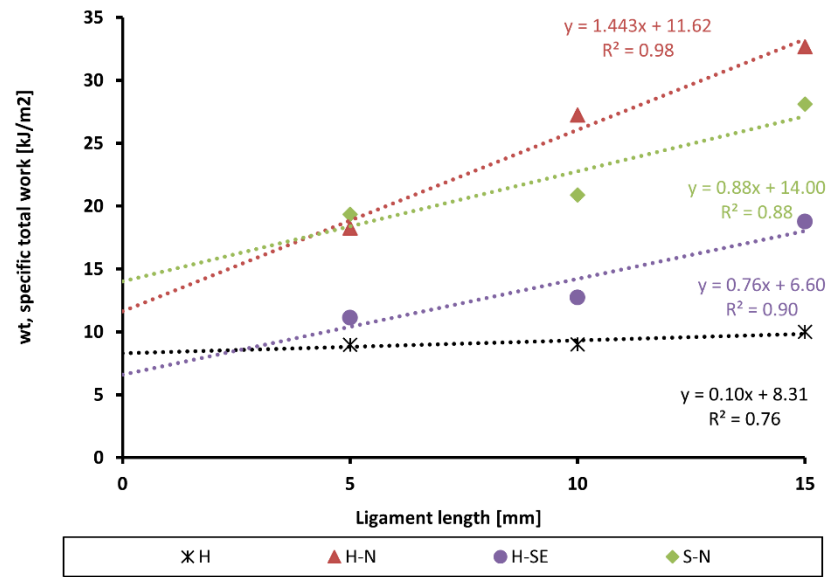


Figure 6.16: Determination of the essential and plastic works of fracture, for unaged binders, for H, H-N and H-SE @ 20 °C and for S-N @ 10 °C

Figure 6.17 shows both the essential work of fracture, w_e , and Crack Tip Opening Displacement (CTOD) values for all binders and at different temperatures. The data of bitumen H at 10°C is missing because it was not possible to fulfil a ductile state failure, i.e. the base bitumen H tended to fail in a brittle state without yielding the ligament section.

It can be seen that both w_e and CTOD have been improved by the modification of crumb rubber N. On the other hand, it seems that the fracture properties of H-SE, were probably compromised by the wax pre-treatment as their fracture properties were inferior in comparison to base bitumen H. However, the fracture properties of H-SE at low temperatures may be considered better than its base bitumen H as the later was too brittle to be tested at 10 °C.

Temperature decrease, as seen Figure 6.17, is accompanied by an increase in w_e and a decrease in CTOD. Temperature decrease makes the binders stiffer but less able to stretch; therefore, the relative effect between them (load and displacement) was different with respect to w_e and CTOD. The ductile fracture results, in Figure 6.17, also verify the superior fracture characteristics of binder S-N in comparison to other binders, though it is tested at lower temperatures.

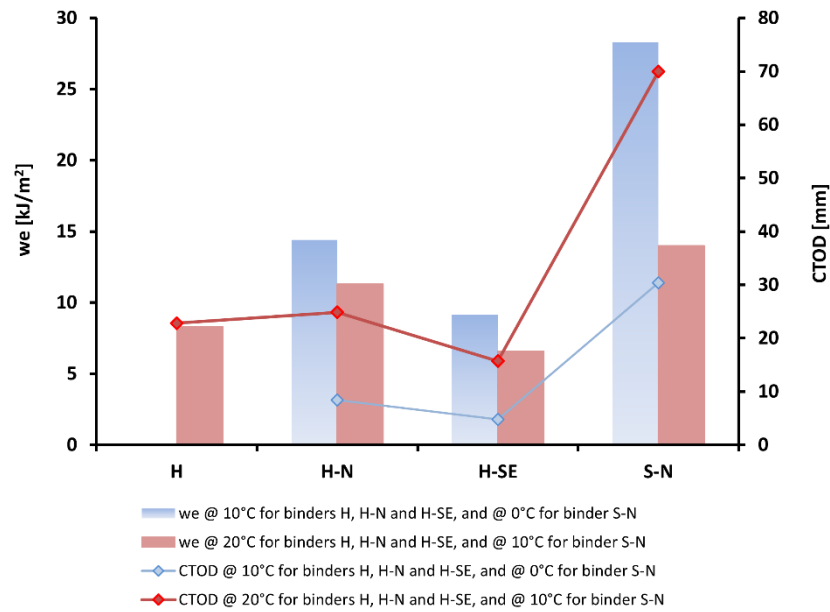


Figure 6.17: The essential work of fracture w_e and CTOD values for unaged binders

As has been mentioned, in the literature Chapter, applying energy partitioning may also be useful in determining reliable fracture parameters. It allows evaluating the resistance of materials to prevent “existing” cracking from being further propagated. Figure 6.18 shows the linear fitting of w_t calculated from the force-displacement curves at the maximum load against ligament length. The results in Figures 6.18 show that fracture energies dissipated during the first stage (yielding) are much smaller (30 to 15% of total essential work) and the rest was used in the second stage (necking and tearing). Also, the plastic work of fracture term, βw_p , is almost negligible in the initiation first stage (3 to 5% total plastic work) which indicates that most of the plastic constraints are occurring during the necking, propagating and tearing stage. The results of essential work of fracture w_{ei} and $CTOD_i$ that are necessary for yielding are shown in Figure 6.19. In that sense, $CTOD_i$ represents here the ability of materials to elongate before existing cracks start propagating while the former CTOD represents the total elongation that materials can sustain after cracks have already propagated. It can be seen that the fracture parameters of H-SE at 20°C were the worst among other binders when the fracture energy is taken globally; however, it changes to be better than H and H-N binders when the energy partitioning concept is applied. The results show that H-SE could be more resistant to the onset of crack propagation, but, less resistant to post-yield fracture. From the viewpoint of pavement designers, ideal asphalt materials should resist better both crack initiation and crack propagation. Thus, the binder S-N can be considered the best to resist the ductile fracture cracking among other binders.

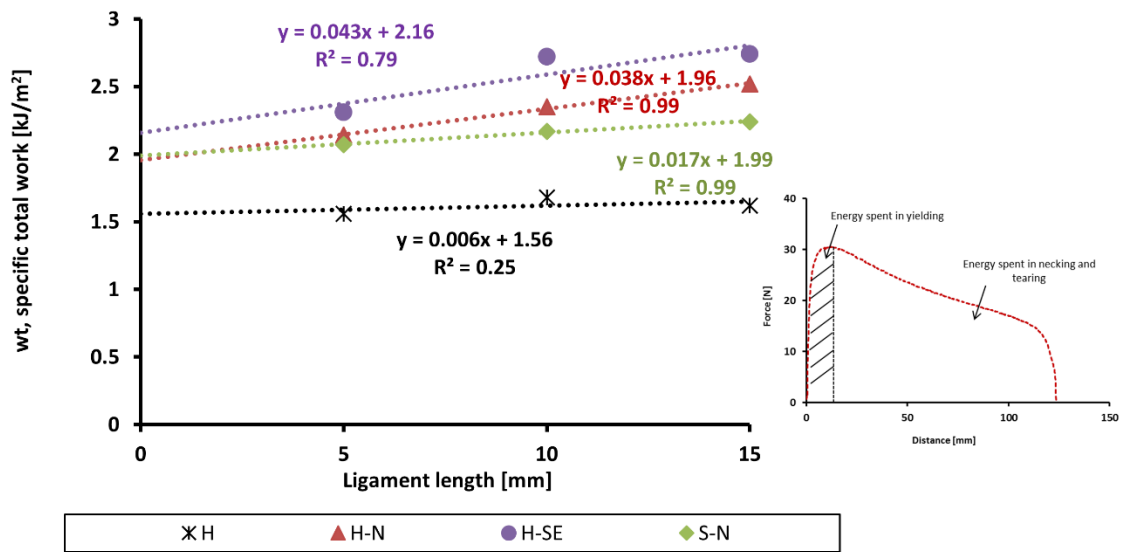


Figure 6.18: The essential and plastic works of fracture analysis based on partitioning concept, for unaged binders, for H, H-N and H-SE @ 20 °C and for S-N @ 10 °C

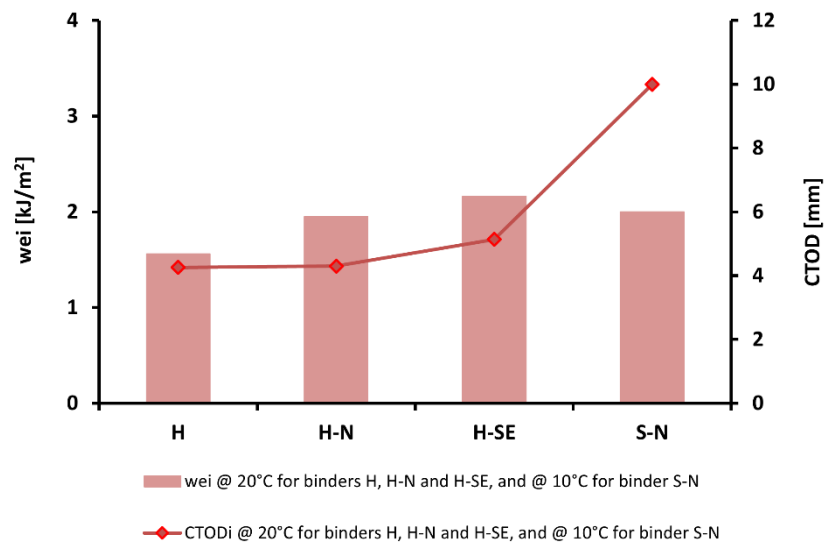


Figure 6.19: The essential work of fracture, w_{ei} , and CTOD_i values that are necessary for yielding, for unaged binders

The resistance of a pavement to fatigue cracking is age dependent. Therefore, it is important to evaluate the effect of ageing on the fracture properties of materials. The laboratory tests used to simulate the hardening development of the bitumen in an accelerated way are the thin film oven test (TFOT) and pressure ageing vessel (PAV) for short-term ageing and long-term ageing, respectively. Figure 6.20 shows that the effect of ageing on the w_e , for H and

H-N binders, is quite similar to the effect of temperature decrease; the w_e increases with ageing. For H-SE and S-N binders, the effect of ageing on the w_e displays a totally opposite trend. These differences can probably be related to the different extent of rubber disintegration, and to the different extent of bitumen oxidation and volatilisation, during the artificial ageing.

Generally, the fatigue performance is expected to deteriorate with ageing (for a typical pavement structure and loading conditions). However, the values of w_e increase with ageing, which may be interpreted as fatigue improvement with more ageing. This trend would have been considered true if the test was done at equi-stiffness-temperature. Since the stiffness of aged materials is much higher than unaged materials, and since the fracture energy depends significantly on stiffness, the values of w_e can then be expected to increase with ageing. On the other hand, the CTOD values seem to be more consistent with ageing and fatigue performance. As can be seen in Figure 6.20, and for all binders, the CTOD values decrease with ageing, and that is in accordance with the general effect of ageing on fatigue cracking performance. It should be mentioned that CTOD is not only a single property but rather it contains information about the tensile fracture energy represented in w_e which is altered by the tensile yield stress, σ_{net} .

When the effects of different base binders are compared in Figure 6.20, it can be seen that the fracture properties of S-N binder were generally more susceptible to ageing than other binders processed using bitumen H. This could be attributed to the larger amount of free aromatic and light fractions content that are available in the soft bitumen S. The results in Figure 6.20 also show that the w_e of H-N binder, is less sensitive to ageing in comparison to the others, i.e. the relative increase or decrease in w_e with ageing is smaller in H-N than in other binders.

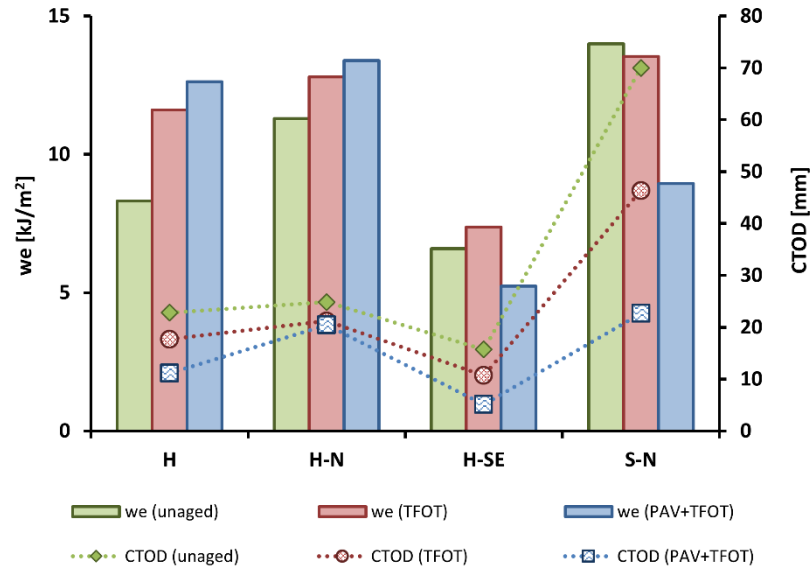


Figure 6.20: The essential work of fracture, w_e , and CTOD values under different ageing condition, for H, H-N and H-SE @ 20 °C and for S-N @ 10 °C

6.5 Fatigue Properties of Asphalt Mixtures

6.5.1 ITFT Results

Results of ITFT for each mixture are shown in Figures 6.21 to 6.23, in terms of the relationship between stress, or tensile strain, and fatigue life (N_f) on logarithmic scales. It can be seen that the rank orders and fatigue lives of the different mixtures, strongly depend on how to identify the independent variable, i.e. stress, or initial strain, or resilient strain. Figure 6.21 presents the fatigue curves as a function of the applied stress. These results indicate that the control mixture H has higher fatigue lives, in comparison with S-N and H-SE mixtures, and in comparison with H-N mixture at a stress level above 450 kPa. It is expected to find the mixture made with binder S-N to have considerably lower fatigue lives due to the lower stiffness modulus. The fatigue results, in Figure 6.21, are however contrary to the fatigue and fracture properties of the binders which demonstrated superior fatigue performance for the RTR-MBs. However, the fatigue data for asphalt mixtures is generally recommended to be plotted against the strain criterion (Airey, Liao et al. 2006).

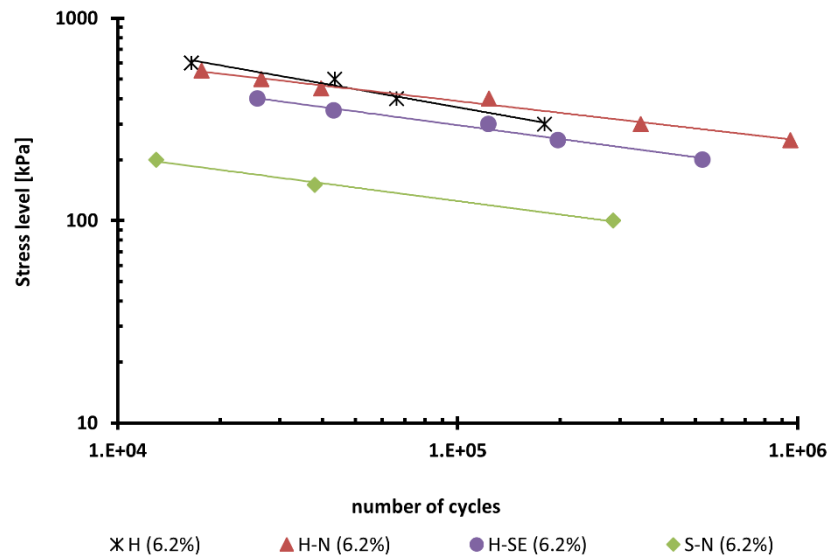


Figure 6.21: ITFT fatigue lives versus stress for control and RTR-MBs mixtures.

The comparison of fatigue curves based on the strain criterion seems to be more reliable than the stress criterion, and the effect of the differences in stiffness among the mixtures on fatigue lives, particularly for S-N mixture, can be eliminated. In addition, the strain is the main parameter used in the analytical design of flexible pavements. Figures 6.22 and 6.23 depict the fatigue lives plotted against strains defined by two different methods, based on EN 12697-24: 2004 and EN 12697-24: 2012 standards, respectively. According to EN 12697-24: 2004, the initial strain is determined from the difference between the average of the maximum strains of 5 load cycles from 98 to 102 and the average of minimum strains of 5 load cycles from 60 to 64. The resilient strain based on EN 12697-24: 2012, presented in Figure 6.23, is the recoverable strain at the 100th load application.

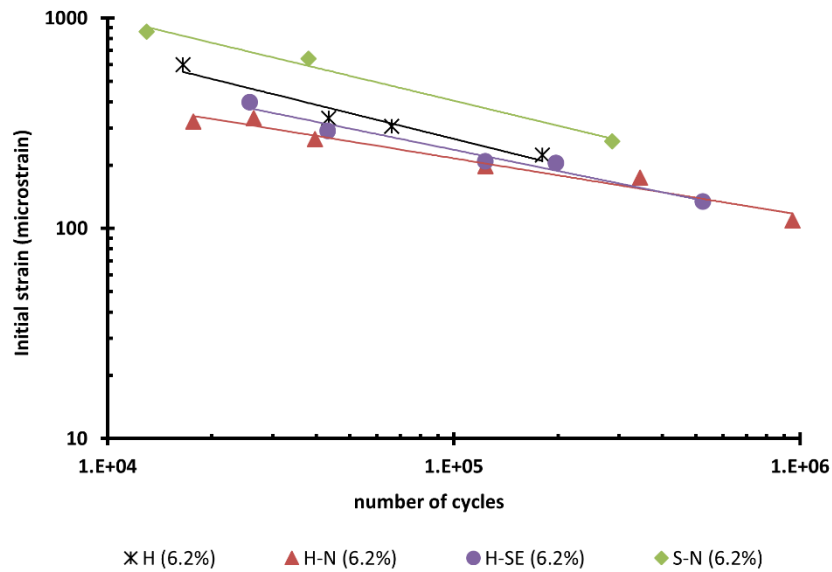


Figure 6.22: ITFT fatigue lives versus strain obtained according to EN 12697-24: 2004 for the control and RTR-MBs mixtures.

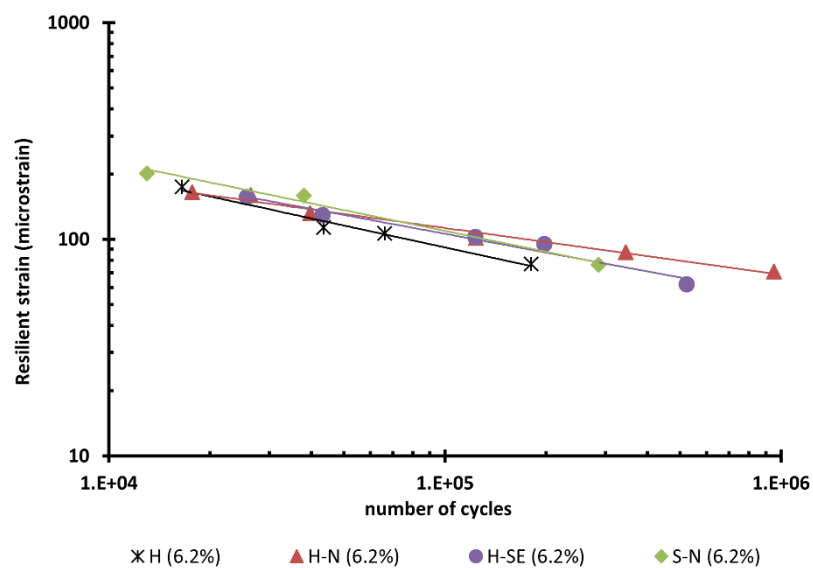


Figure 6.23: ITFT fatigue lives versus strain obtained according to EN 12697-24: 2012 for the control and RTR-MBs mixtures

It can be seen that the mixture made with S-N binder has the best fatigue lives according to the EN 12697-24: 2004 method, as seen in Figure 6.22. The control mixture H, in Figure 6.22, outperformed other RTR-MBs mixtures made with binders H-N and H-SE, at initial strains above 200 $\mu\epsilon$. It should be mentioned that the initial strain calculated from EN 12697-24: 2004, is largely influenced by the susceptibility of materials to permanent deformation. Asphalt mixtures which are more susceptible to permanent deformation during fatigue

evolution would reveal significantly higher initial strain, and consequently, indicate falsely better fatigue properties, when the EN 12697-24: 2004 is considered. Figure 6.24 depicts the results of the horizontal strains against load cycles during the first 105 load pulses, for the control H mixture, and H-N mixture, tested at 300 kPa stress level.

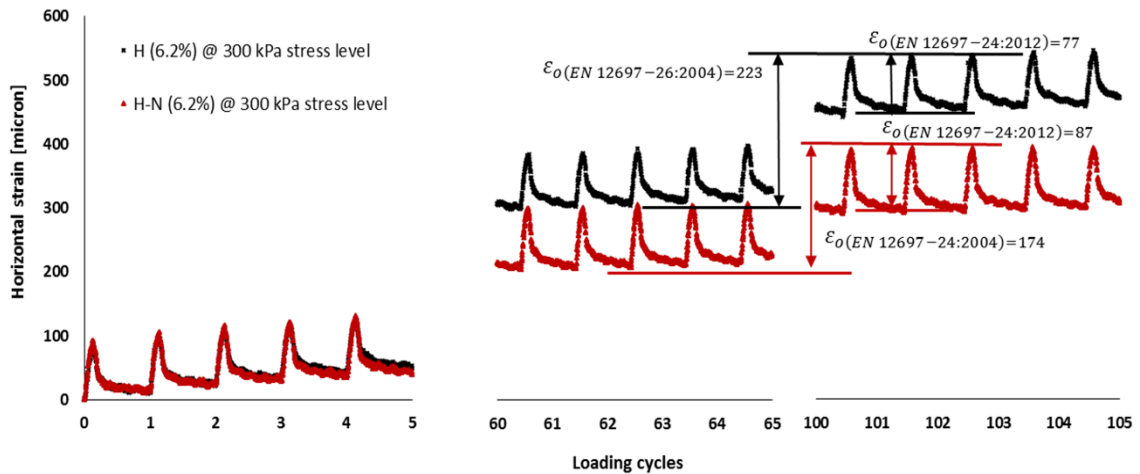


Figure 6.24: The horizontal strain evolution during the first 105 load applications for H mixture and H-N mixture.

The results, in Figure 6.24, show that the definition of strain criterion can play a significant role in fatigue analysis. Although, both mixtures have relatively the same strain amplitude during the first 5 load cycles; however, the difference in the total strains between the two mixtures becomes considerable after 60 load cycles. Therefore, the initial strain obtained from EN 12697-24: 2004, for H mixture, is significantly higher than the initial strain for H-N mixture; hence, the fatigue resistance of H mixture appears to be better than H-N mixture. The accumulation of permanent deformation can, however, make the pavement more prone to cracking due to the strain hardening phenomenon which changes the viscoelastic properties of materials into more brittle and rigid behaviour (Moreno-Navarro and Rubio-Gómez 2016). Consequently, the fatigue analysis based on EN 12697-24: 2004 standard can be biased and lead to misleading judgement. On the other hand, the resilient strain obtained from EN 12697-24: 2012, does not account for the effect permanent deformation and provides more reliable and unbiased comparison between the fatigue properties of different mixtures. Figure 6.23 demonstrates that the RTR-MBs mixtures have better fatigue lives than the control, and that is particularly evident at low strain levels. The H-N mixture appears clearly to be the most fatigue resistant at strain levels below $100 \mu\epsilon$. It should be mentioned that the possible strain levels to be experienced in a flexible pavement are below $200 \mu\epsilon$ (Brown and Needham 2000). The equations of the fatigue regression curves shown in Figure

6.23, between the fatigue lives and the resilient strain, are presented in Table 6.3. The high R^2 indicates that a strong relationship between fatigue lives and the resilient strains can be confidently established. The equations shown in Table 6.3, are used to predict the fatigue life for $100 \mu\epsilon$, as presented in Figure 6.25. The predicted fatigue lives, presented in Figure 6.25, demonstrate that RTR-MB mixtures have higher fatigue life in comparison to the control mixture H, with H-N mixture having the highest fatigue life.

Table 6.3: Fatigue equations versus resilient strain for the control and RTR-MBs asphalt mixtures

Mixture	Fatigue equation	Regression coefficient (R^2)
H (6.2%)	$N_f = 5 \times 10^{10} \epsilon^{-2.91}$	0.98
H-N (6.2%)	$N_f = 2 \times 10^{14} \epsilon^{-4.55}$	0.98
H-SE (6.2%)	$N_f = 7 \times 10^{11} \epsilon^{-3.37}$	0.97
S-N (6.2%)	$N_f = 2 \times 10^{11} \epsilon^{-3.08}$	0.99

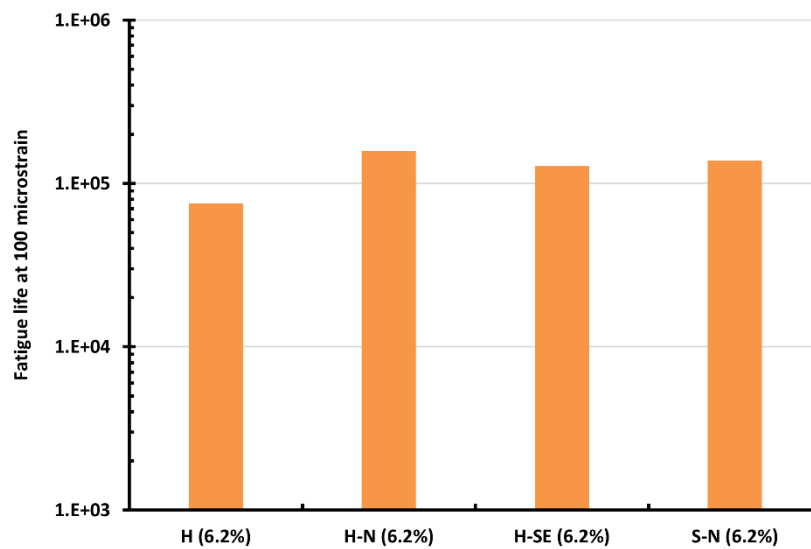


Figure 6.25: Fatigue lives at 100 με for the control and RTR-MBs asphalt mixtures

6.5.2 Superpave Indirect Tensile Test (IDT) Results

The fracture energy ratio (ER) is the main parameter obtained from IDT. The ability of the ER parameter to reliably evaluate the cracking performance of different asphalt mixtures has been proven by several studies (Roque, Birgisson et al. 2004, Shu, Huang et al. 2008, Timm, Sholar et al. 2009, Zou, Roque et al. 2013). The ER is based on the fact that each asphalt mixture, has the ability to resist the initiation of cracking, if its fundamental dissipated creep strain energy threshold $DCSE_f$ is larger than its minimum dissipated creep strain energy

$DCSE_{min}$. Therefore, an asphalt mixture with a larger ER value is desirable and should have better fatigue performance in comparison to an asphalt mixture with a lower ER value.

The creep compliance progression with time from of IDT results are shown in Figure 6.26, and the power parameters of the creep compliance curve, D1 and m-value, in addition to the IDT strength and resilient modulus, are shown in Table 6.4, for each mixture. It can be seen from Figure 6.26 that the modification by recycled tyre rubber has decreased significantly the increase rate of creep compliance with time. This, in turn, would lead to a retarding of the rate of damage accumulation, thereby enhancing the ability of the mixture to resist the initiation of cracking. The results of resilient modulus, presented in Table 6.4, are slightly different from the ITSM results, which is not surprising given that the definition of strain in the Resilient Modulus is somewhat different from that in the ITSM. The total strain is used in the calculation of the ITSM, while the recoverable or resilient strain is used in the calculation of the Resilient Modulus. However, the amount of elastic energy EE which is a function of the Resilient Modulus is marginal with respect to the total fracture energy FE. Thus, these differences would not make a significant change in the $DCSE_f$ values.

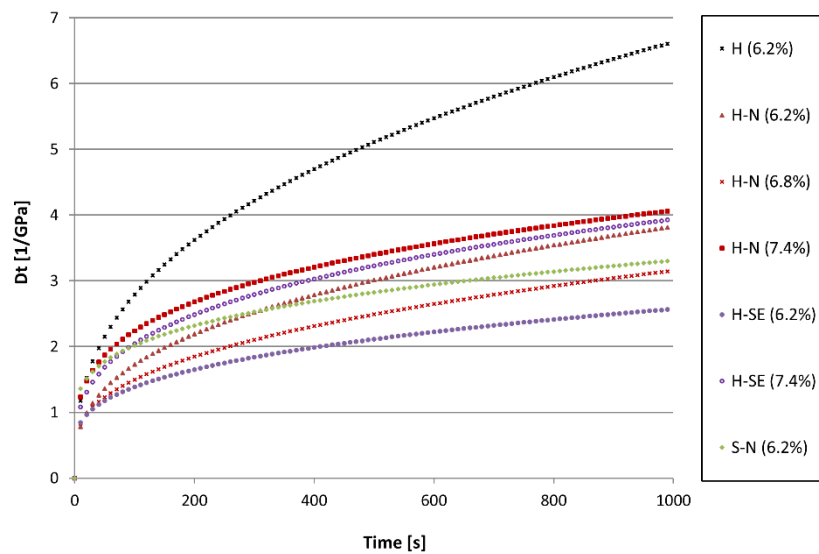


Figure 6.26: Creep compliance curves evolution with time for the different mixtures

Table 6.4: The IDT results for the different mixtures

Mixture	Resilient Modulus [MPa]	Creep Compliance		IDT strength [MPa]
		D1	m-value	
H (6.2%)	6221	0.71	0.33	2.00
H-N (6.2%)	5398	0.31	0.31	1.98
H-N (6.8%)	5459	0.33	0.35	1.67
H-N (7.4%)	5330	0.68	0.25	1.70
H-SE (6.2%)	6150	0.41	0.25	1.94
H-SE (7.4%)	5220	0.41	0.32	1.85
S-N (6.2%)	2080	0.81	0.25	0.82

Figure 6.27 depicts the stress–strain curves, from the IDT strength test, for the different mixtures. The stress-strain curves are important to evaluate the fracture resistance of materials by determining their failure parameters, including the IDT strength, the tensile failure strain ε_f , and $DCSE_f$. It can be seen that the mixtures made with H-N and S-N binders exhibit much higher failure strains than mixtures made with binders H and H-SE. This explains that the modification with crumb rubber N, can also increase the strain tolerance of mixtures in addition to the binders, as has been shown in TSRCL and DENT tests. The mixture made with the soft binder, S-N, experiences the largest failure strain; this compensates its fracture energy due to its lower IDT strength. On the other hand, the modification with crumb rubber SE, has slightly reduced the failure strains compared to the control; once again the crystal lattice structure of waxes in the SE could be responsible for that.

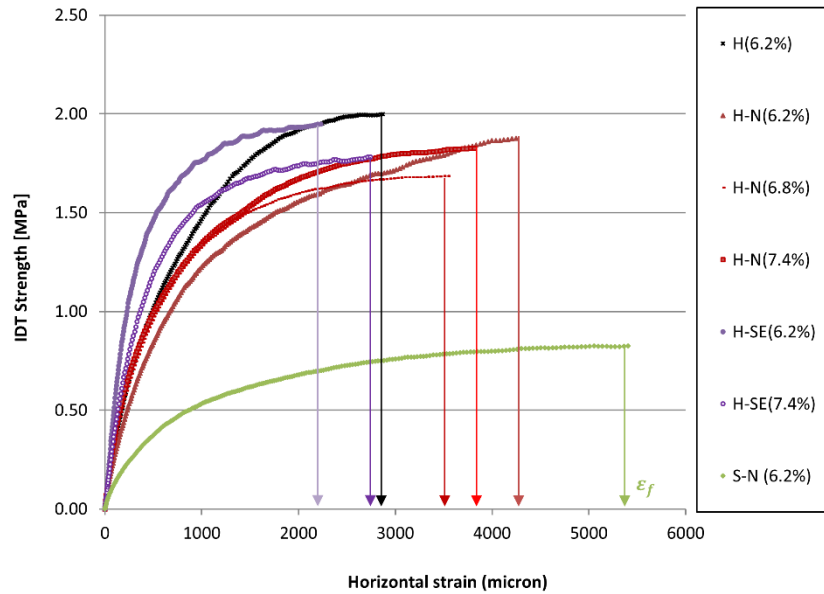


Figure 6.27: Stress-Strain curve from the indirect tensile strength test for the different mixtures

By analysing the data of creep and strength tests, the $DCSE_f$ and $DCSE_{min}$ are determined and presented in Figure 6.28. The range bars represent the maximum and minimum of values of replicates. It can be observed that the addition of crumb rubber has a clear effect on decreasing the $DCSE_{min}$ compared to the control mixture. This is beneficial for having materials with superior cracking resistance. On the other hand, the $DCSE_f$ seems to be less affected by the rubber modification than the $DCSE_{min}$. Although there is an increase in $DCSE_f$ for mixtures made with binder H-N in comparison to the control mixture, the results show a significant amount of variation that makes it difficult to draw a clear conclusion, as seen from the range bars. In terms of the effect of using different binder content, for mixtures made with H-N and H-SE binders, there is a different trend between the two binders. Increasing the binder content for H-N mixture leads to a consistent decrease in $DCSE_{min}$ and unclear slight changes in $DCSE_f$, while there is a slight increase in the $DCSE_f$ and $DCSE_{min}$ when increasing the binder content for mixtures made with H-SE binder. Figure 6.29 shows the ER values for all mixtures. The results also demonstrate the superior cracking performance for mixtures made with RTR-MBs. The results in Figure 6.29 indicate that increasing the binder content to 6.8%, for H-N binder, resulted in a modest change in ER, while increasing the binder content to 7.4% resulted in higher ER. Increasing the binder content from 6.2% to 7.4% for H-SE mixtures seems to have a less pronounced effect on the ER compared to H-N group. The higher deformability of the S-N binder can provide superior cracking performance for asphalt mixtures, and that is reflected in its ER value.

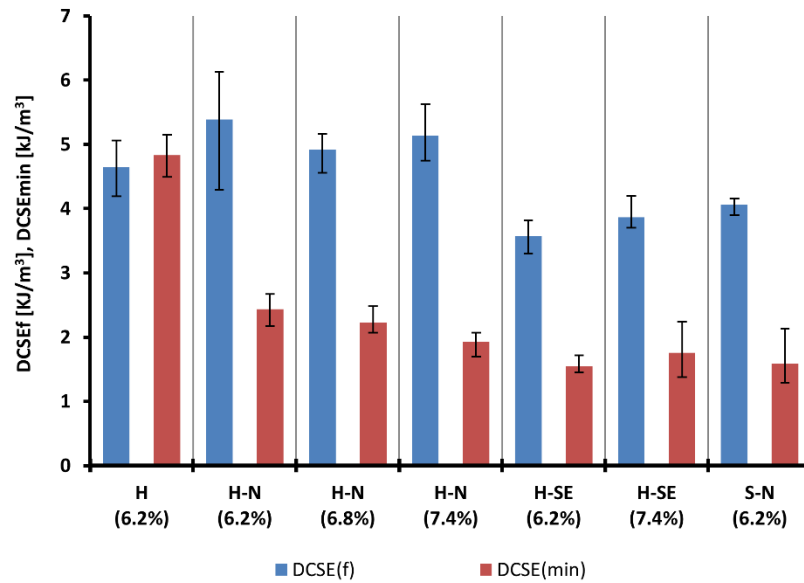


Figure 6.28: DCSE_f and DCSE_{min} for the different mixtures

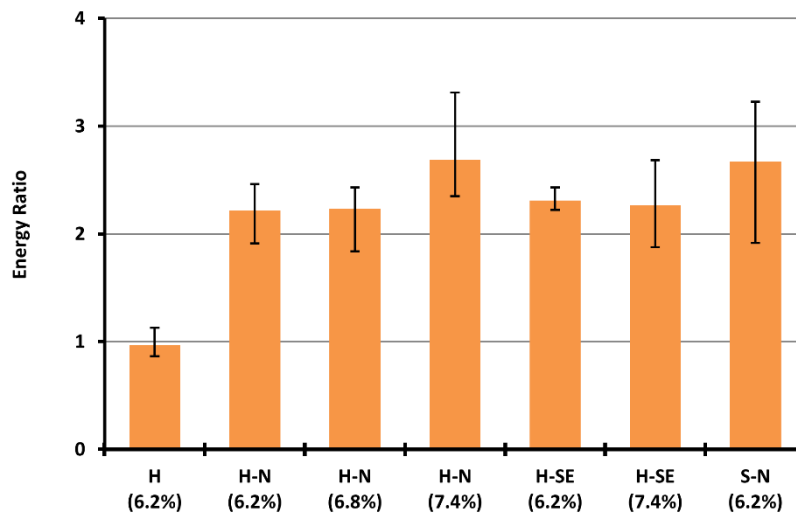


Figure 6.29: ER for the different mixtures

6.6 Summary and Conclusions

In this chapter, the fatigue properties of binders in addition to their mixtures were studied by different test methods and parameters. The fatigue performance testing of binders has involved time sweep repeated cyclic loading (TSRCL) tests using the DSR, and fracture testing by means of DENT. Different energy methods in addition to the traditional fatigue analysis “WÖHLER” curve have been applied for analysing the data of the TSRCL test. These energy methods are the cumulative dissipated energy and the Ratio of Dissipated Energy Change (RDEC) approach. The fatigue life failure point has been assessed by different methods, including 50% decrease in the initial stiffness of the material, DER

approach and Black diagram failure criterion in order to define the fatigue life appropriately. The study has proposed a promising methodology for determining a consistent and reliable PV which was able to generate a unique fatigue law. The effect of the artificial ageing (TFOT and PAV) on the fracture parameters of binders (w_e and CTOD), has also been evaluated. The cracking resistance of the different asphalt mixtures, considered in this study, has been evaluated using the ITFT and the Superpave indirect tensile IDT tests. Based on the discussion and analysis described in this chapter, the following conclusions and findings can be drawn:

- (1) It is crucial to evaluate and then appropriately identify the fatigue failure point before commencing the fatigue analysis. The classical approach of 50% decrease in the initial stiffness is an arbitrary definition and can lead to incorrect analyses. Therefore more fundamental approaches should be considered to provide a more realistic definition of fatigue failure
- (2) The traditional fatigue analysis has shown that the fatigue lives of H group binders are temperature dependent while the inclusion of rest periods and the change of loading mode have not changed the fatigue lines. Unlike H group binders, the inclusion of rest periods has revealed a significant effect on extending the fatigue life for S-N binder. Thus, it is important to investigate the healing mechanism of different binders in addition to their fatigue properties for an appropriate material selection
- (3) Although a unique fatigue law could be produced from the fatigue analysis based on accumulated dissipated energy, this approach generates in some cases a misleading fatigue curve due to encompassing viscoelastic energies that are not responsible for fatigue damage
- (4) The PV obtained by the proposed method has been able to distinguish between the fatigue resistances of different binders, and thus it can be used as a reliable fatigue parameter. The results of this study and some other similar studies found in the literature show that the PV-Nf relationship is material dependant and there was limited evidence to accept that this relationship is unique regardless of material type
- (5) The DENT test offers a simple test method with reproducible data to characterise the fracture properties of bituminous binders under ductile condition. CTOD obtained from the DENT test has been reliably sensitive to the effect of temperature and ageing, and can be considered a good discriminating parameter to quantify the fatigue

performance of binders. The concept of partitioning the total fracture work of energy has been successfully applied on bituminous binders; it enables determining and separating the resistance of materials to fracture initiation in addition to fracture propagation resistance. The DENT has caught the detrimental effect of FT-waxes on fatigue properties, for H-SE binder. Several studies have indicated that Sasobit® could make the bituminous binders fragile at low temperatures and hence more susceptible to cracking (Goh and You 2009, Arega, Bhasin et al. 2011, Liu and Li 2011, Medeiros Jr, Daniel et al. 2012, Jamshidi, Hamzah et al. 2013). However, despite the H-SE binder appearing to have poorer fatigue resistance than the base bitumen H when the fracture energy is taken globally, its ability to resist the propagation of existing cracking was better than other binders when the fracture parameters were obtained from the energy partitioning concept

- (6) The ITFT fatigue results, based on EN 12697-24: 2004, have shown that the permanent deformation can change falsely the rank order of materials. While the fatigue analysis based on the resilient strain obtained from EN 12697-24: 2012, has been shown to provide a more reliable rank order that is in agreement with the fatigue properties of binders
- (7) The results of SuperPave IDT have shown that the addition of rubber can significantly decelerate the rate of damage accumulation which, in turn, leads to enhanced cracking resistance of mixtures. Indeed, the ER values have revealed that RTR-MBs mixtures have superior cracking resistance to the control mixture.
- (8) The rubber modification for a very soft base bitumen (200 dmm penetration), as in the case of S-N binder, can produce binder with excellent fracture and cracking properties, as indicated by the CTOD parameter and PV. The excellent strain tolerance of S-N binder has been reflected in the mixture through the failure strain ε_f and subsequently through the ER parameter. Thus, the PV and CTOD are recommended to evaluate reliably the fatigue properties of binders, and the ER parameter to evaluate the cracking resistance of mixtures.
- (9) All test methods and parameters, for binders and mixtures, have proven that the addition of rubber can improve the fatigue properties of materials

Chapter 7 Permanent Deformation in Binders and Mixtures

7.1 Introduction

Rutting or permanent deformation is one of the most common forms of load-associated distress in flexible pavements. Although, aggregate skeleton interlocking has a direct influence on the permanent deformation resistance of bituminous mixture, the viscoelastic properties of the binder at high temperatures also play a key role in determining the surface ruts in a flexible pavement. Consequently, it is important to understand the mechanical characteristics that can determine the actual contribution of binders to the permanent deformation of mixtures. Despite the fact that there have been many comprehensive reviews investigating those characteristics for unmodified bitumens, there has been still limited studies conducted on modified bitumens, and particularly for RTR-MBs. For unmodified bitumens, a correlation between the linear viscous component of a bitumen's behaviour and pavement rutting performance, has been well established (Hofstra and Klopm 1972, Morris, Haas et al. 1974, Anderson, Christensen et al. 1991, Phillips and Robertus 1996, Shenoy 2001, Morea, Agnusdei et al. 2011). However, this correlation has tended to break down with modified bitumens. It is believed that the considerable sensitivity of modified binders to different stress/strain levels and rate is behind this lack of correlation (D'Angelo 2009, Wasage, Stastna et al. 2011, Zoorob, Castro-Gomes et al. 2012). It is, therefore, necessary to characterise the deformation behaviour of RTR-MBs using testing methods and parameters associated with different damage mechanisms. In response to that, this chapter is

concerned with providing an improved understanding of the rutting behaviour of RTR-MBs by measuring both their linear and nonlinear viscoelastic properties. The binders (H, H-N, H-SE and S-N) developed in Chapter 4 are further characterised by their permanent deformation behaviour. Also, the mixtures that were designed in Chapter 5 are used in this Chapter. As a first step towards establishing a better relation between binder properties and their mixtures, the permanent deformation properties of binders using the SHRP rutting parameter, Shenoy rutting parameter, ZSV and MSCR tests are investigated. The next step is to investigate the deformation behaviour of mixtures using the Repeated Load Axial Test (RLAT). The possible correlations between the different rutting parameters of binders and the deformation behaviour of the mixtures are presented. Finally, a more fundamental analysis is suggested to provide a closer assessment of the realistic conditions that binder films would experience in the mixtures.

7.2 Testing Programme

7.2.1 Binder Testing

In order to make a clear relationship between binder properties and mixture performance, the binder testing conditions should match the mixture conditions. Therefore, the binder testing is performed on the TFOT residues to take into account the short-term ageing that occurs during mixture production. The following test methods and parameters are used to characterise the high-temperature properties of binders.

SHRP Rutting Parameter

The SHRP rutting parameter ($|G^*|/\sin \delta$) of the TFOT aged residues was determined at 50°C and 60°C, and at 1.59 Hz, from the oscillatory raw data of Chapter 4.

Shenoy Rutting Parameter

The Shenoy rutting parameter $|G^*|/(1-(1/\sin\delta \tan\delta))$ was also determined from the oscillatory raw data of Chapter 4. The parameter was calculated, at 50°C and 60°C, and at 0.1 Hz.

Zero Shear Viscosity ZSV

The oscillatory raw data of the complex viscosity at test temperatures of 50°C and 60°C was used for the ZSV calculations. The simplified three parameters of the Cross model are used to fit the data and extrapolate the complex viscosity to very low or zero frequency as demonstrated in the following equation.

$$\eta^* = \frac{ZSV}{1 + (K\omega)^m} \quad \text{Equation 7.1}$$

where η^* is complex viscosity; ZSV is zero shear viscosity; ω is frequency (rad/s), K and m are constants. The three parameters (ZSV, K and m) of the Cross model are solved with the aid of the Solver function in a Microsoft Excel Spreadsheet. This function is used to fit the experimental data into a model using an iteration process. The Solver function finds the optimum values of the parameters by minimising the sum of the differences between the experimental data values and the model values.

Multiple Stress Creep and Recovery (MSCR)

The MSCR test was conducted on the TFOT residues under the same testing protocol presented in Chapter 4. The TFOT residues of RTR-MBs and base bitumen were tested at testing temperatures of 50°C and 60°C.

7.2.2 Mixture Testing Using Repeated Load Axial Test

The Repeated Load Axial Test (RLAT) is the most widely used in the United Kingdom to characterise the permanent deformation behaviour of bituminous mixtures. The test is performed according to BS DD 226 using the Nottingham Asphalt Tester (NAT) machine. In this test, a load pulse consisting of a square wave with a frequency of 0.5 Hz (one second loading followed by one second rest period), is applied by an actuator. The actuator is controlled by compressed air with the aid of a solenoid valve. The load is applied vertically to the specimen whose two faces are coated with a thin layer of silicone grease and graphite powder. Figure 6.1 shows the configuration of the RLAT inside the NAT machine. The resultant strain during the cycling load is measured along the same axis as the applied stress, using two linear variable displacement transformers (LVDTs).

The following test parameters were applied in RLAT testing:

- Test temperature: 50°C
- Test duration: 7200 seconds (3600 cycles)
- Axial stress: 100 kPa
- Conditioning stress: 10 kPa for 600 seconds
- All test specimens were subjected to at least 4 hours conditioning at the test temperature prior to testing
- Three specimens for each mixture were tested, and the average values are reported.

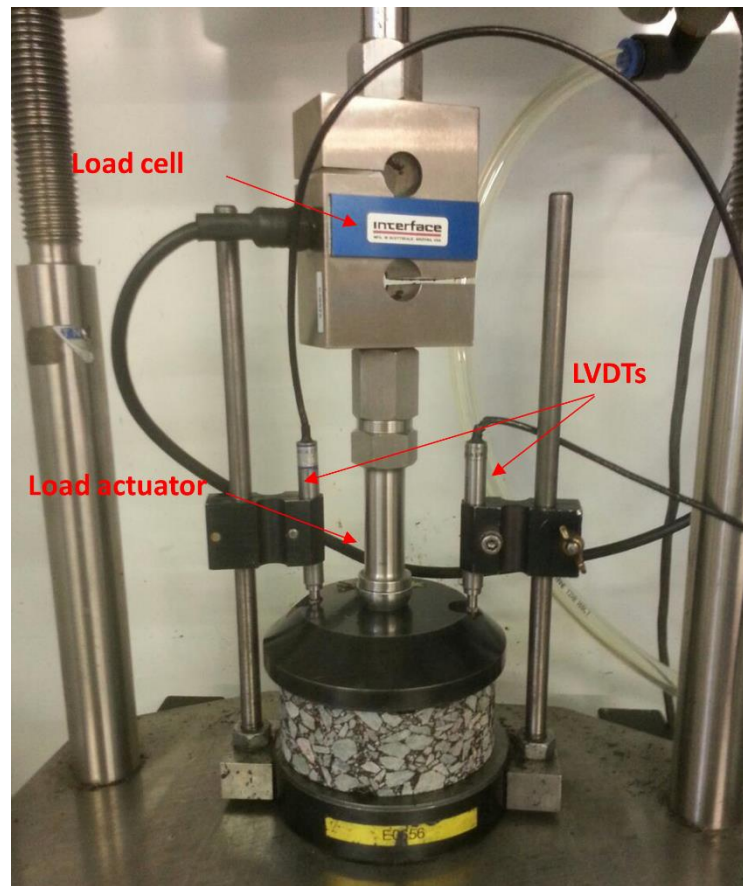


Figure 7.1: RLAT testing configuration in NAT

7.3 Rutting Resistance of Binders

SHRP Rutting Parameter

The SHRP parameter was derived from the definition of the loss compliance ($J'' = \sin\delta/|G^*|$) to measure the contribution of binder to rutting performance (Shenoy 2001). It is, therefore, necessary to select a binder with a reduced (J'') to minimise the unrecovered strain (γ_{unr}) to control the rutting. Figure 7.2 shows the $|G^*|/\sin\delta$ values for temperatures of 50°C and 60°C at a constant frequency of 1.59 Hz. It is clear that the addition of the recycled tyre rubber into the base bitumen H has resulted in a significant improvement in the rutting resistance of binders H-N and H-SE. Although the H-SE has the smallest HTV compared to the other modified binders, as shown in Chapter 4/ section 4.3, the findings in Figure 7.2 show that H-SE has the largest SHRP rutting parameter at both temperatures. This highlights the desirable contribution of the FT-wax in H-SE. Reducing the HTV of RTR-MBs by FT-wax is important to ensure the binder can be easily pumped and mixed with aggregates. In addition, the FT-wax can improve the rutting resistance of binders due to its crystal lattice structure. It can be seen that S-N has the smallest SHRP parameter at both temperatures.

This is expected as this binder was produced using very soft base bitumen. However, the difference in SHRP parameter between S-N and H becomes marginal at a temperature 60°C. This confirms that the RTR-MBs have an improved temperature susceptibility, as shown in Chapter 3/ section 3.5.3. The ranking for the four binders according to the SHRP parameter at a temperature 50°C should be;

H-SE > H-N > H > S-N

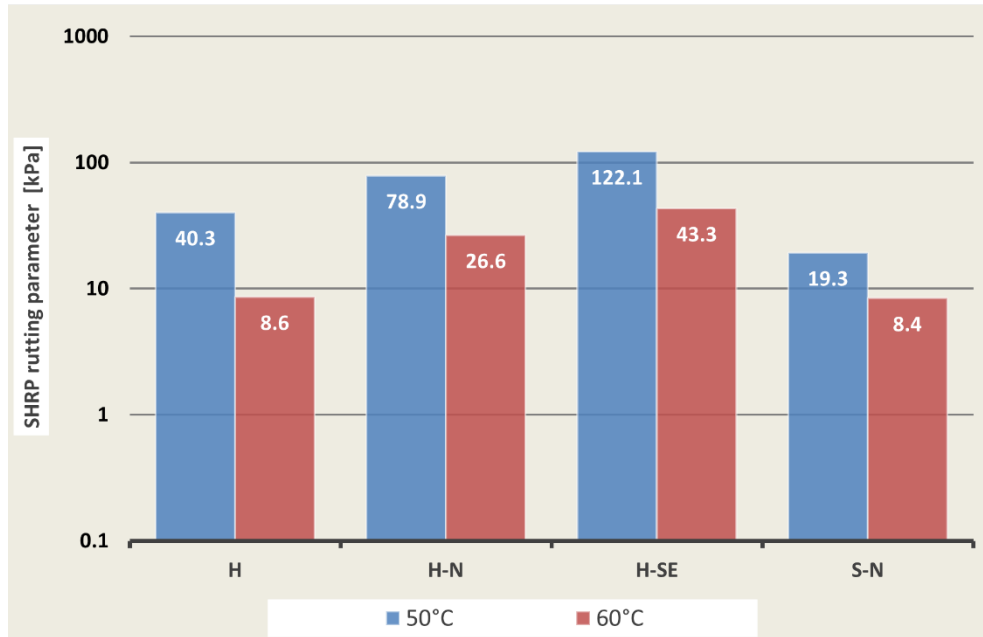


Figure 7.2: SHRP rutting parameters for different binders

Shenoy Rutting Parameter

This parameter was proposed as a refinement to the SHRP parameter (Shenoy 2001). The parameter is more sensitive to the phase angle than the SHRP parameter, therefore, it would better explain the changes in elastic properties when adding the polymeric modifiers. The results of the Shenoy rutting parameter for the different binders are presented in Figure 7.3. The same general trend as for the SHRP parameter is observed here, with the exception that the binder S-N becomes more rutting resistant than binder H, at both temperatures. Also, the results show that the relative difference between Shenoy parameter for H-SE and other binders is much larger in comparison to the SHRP parameter. This is due to the relative decrease in phase angle measurements (more elastic response) for H-SE compared to other binders, and that is significantly reflected in the Shenoy parameter. The ranking for the four binders according to Shenoy parameter at temperature 50°C should be;

H-SE > H-N > S-N > H

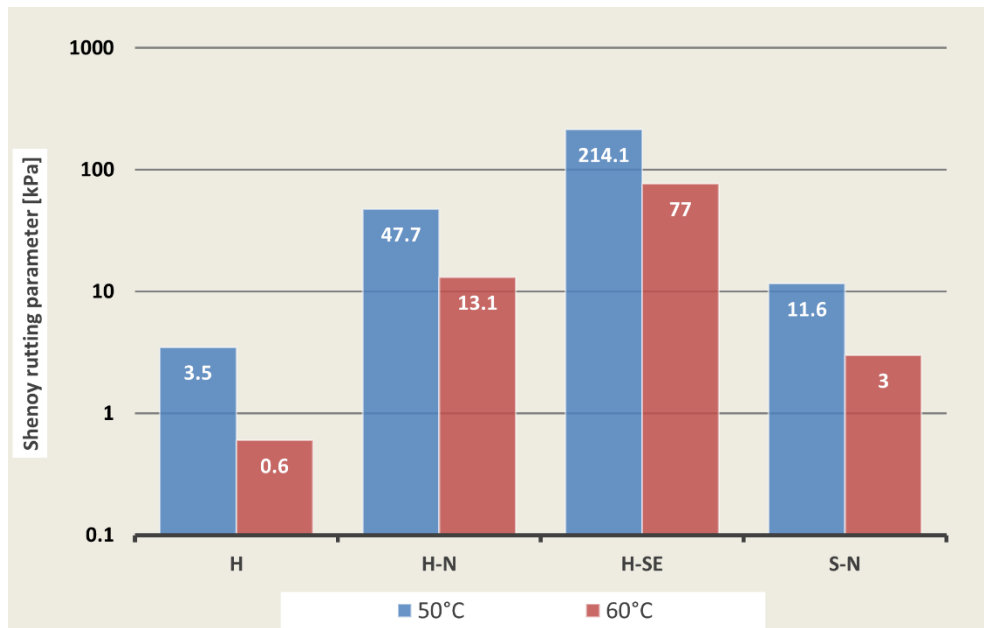


Figure 7.3: Shenoy rutting parameters for different binders

Zero Shear Viscosity ZSV

ZSV is determined by utilising cyclic oscillatory tests within the linear viscoelastic regime. Figures 7.4 (a) and (b) show the results of complex viscosities for the different binders with their Cross Model. It is clear that the low or zero shear viscosity is increased by the addition of recycled tyre rubber which can be translated into improving the rutting resistance of a pavement. It can be seen that the behaviour of the base bitumen H is independent of the applied frequency (Newtonian fluid like behaviour), and the ZSV can be readily identified by the asymptote. In contrast, the RTR-MB combinations are sensitive to the frequency and exhibit Non-Newtonian behaviour (shear thinning). The values of the complex viscosity for binder S-N are lower than the values of the complex viscosity for the base bitumen H at high frequencies; however, these values increase as the frequencies decrease for binder S-N due to the complex response of modified binders to the shear rate. Therefore, the extrapolated ZSV of binder S-N becomes higher than the ZSV of the base bitumen H at both temperatures. The different binders are ranked similarly to the Shenoy rutting parameter;

$$H-SE > H-N > S-N > H$$

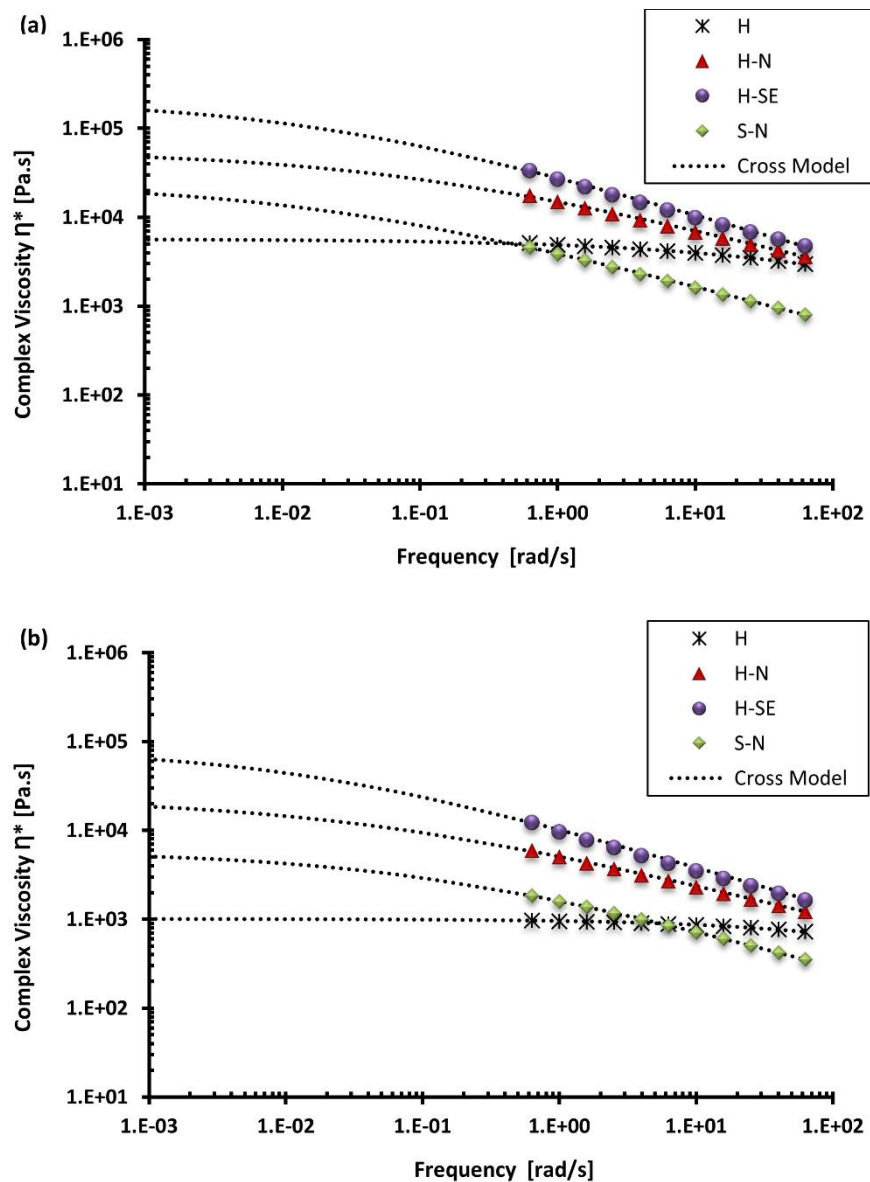


Figure 7.4: Complex viscosity of different binders tested at (a) 50°C and (b) 60°C

Multiple Stress Creep and Recovery (MSCR)

The non-recoverable creep compliance (J_{nr}) has been recommended as an alternative to the current SHRP parameter $|G^*|/\sin\delta$ when assessing the permanent deformation performance of different bitumens (D'Angelo, Kluttz et al. 2007). J_{nr} is more sensitive to the stress dependency of modified binders making it suitable for specification purposes for both neat and modified bitumen (D'Angelo 2009, Tabatabaee and Tabatabaee 2010). Also, measuring the J_{nr} of binders at high stresses and outside the linear viscoelastic region is conceivably more appropriate, as the strains in binder films on aggregate surfaces can be several hundred times greater than the overall average strain of the mixture. Figure 7.5 (a) and (b) shows the results of J_{nr} over a wide range of stresses between 0.1 kPa and 25.6 kPa at test temperatures

of 50°C and 60°C. The average percentage of recovery of 10 cycles over a wide range of stresses is also presented in Figures 7.6 (a) and (b). The results in Figures 7.5 (a) and (b) clearly indicate that all the RTR-MBs experience shear thinning (increasing J_{nr} with the applied shear stress) while the base bitumen H exhibits Newtonian behaviour (maintains the same J_{nr} with the applied stress). The results also indicate that the binders are ranked differently from the rutting parameters obtained by the dynamic oscillatory test. This is not surprising, as many factors associated with the two tests are not equal. For example, the degree of stress sensitivity, delayed elasticity, relaxation times and nonlinearity, can all play a significant role in having a different response for materials tested under dynamic oscillatory, or, under creep and recovery conditions. The results of percentage recovery demonstrate that the RTR-MBs are considerably more capable of recovering the induced strains than the base bitumen H. This is very apparent for the binder H-N which maintains excellent recovery response over the wide range of stresses. The binders are ranked based on J_{nr} at a test temperature of 50°C as follows;

$$H-N > H-SE > S-N \geq H$$

It seems that the binders are ranked differently under different binder tests and parameters. In order to identify the binder rutting test that can rank the binders most reliably, the rutting resistance of mixtures produced using those binders is evaluated and presented in the following section.

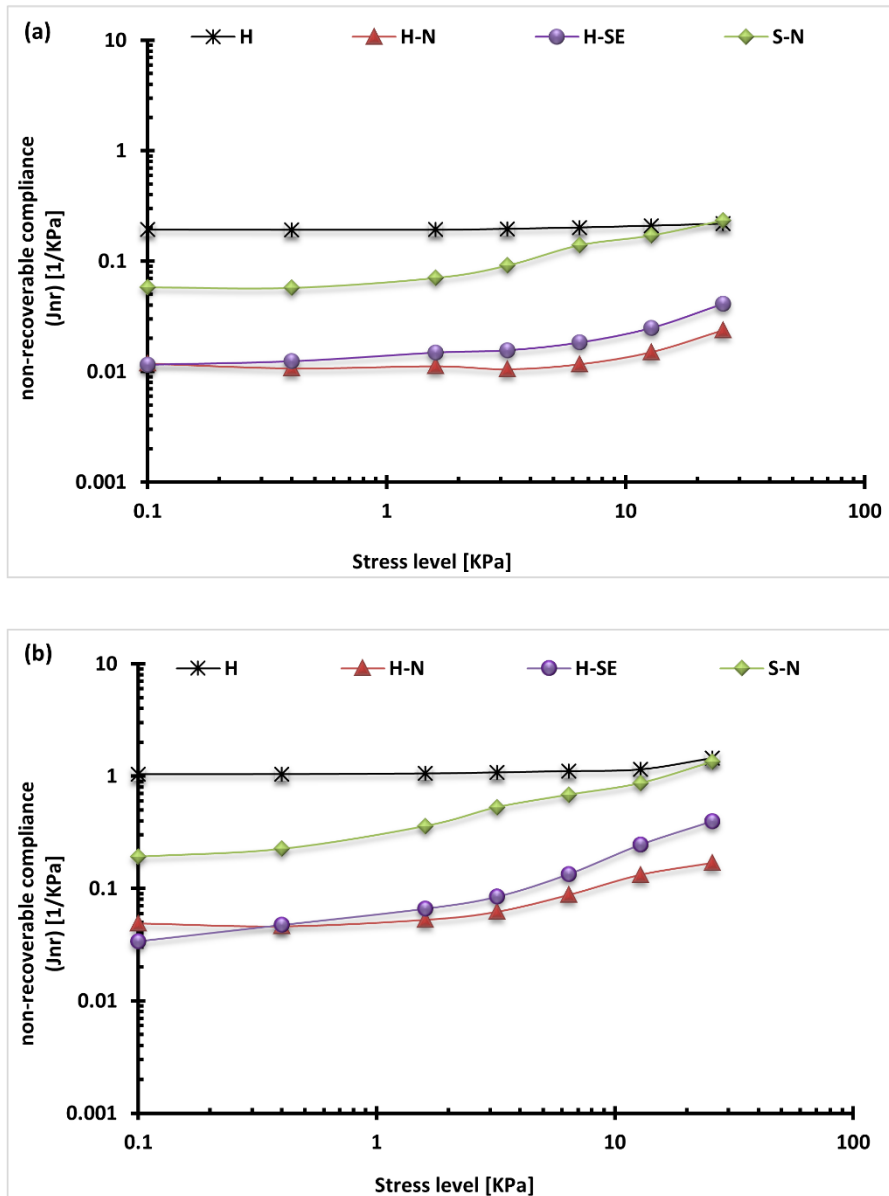


Figure 7.5: J_{nr} of binders at (a) 50°C and (b) 60°C

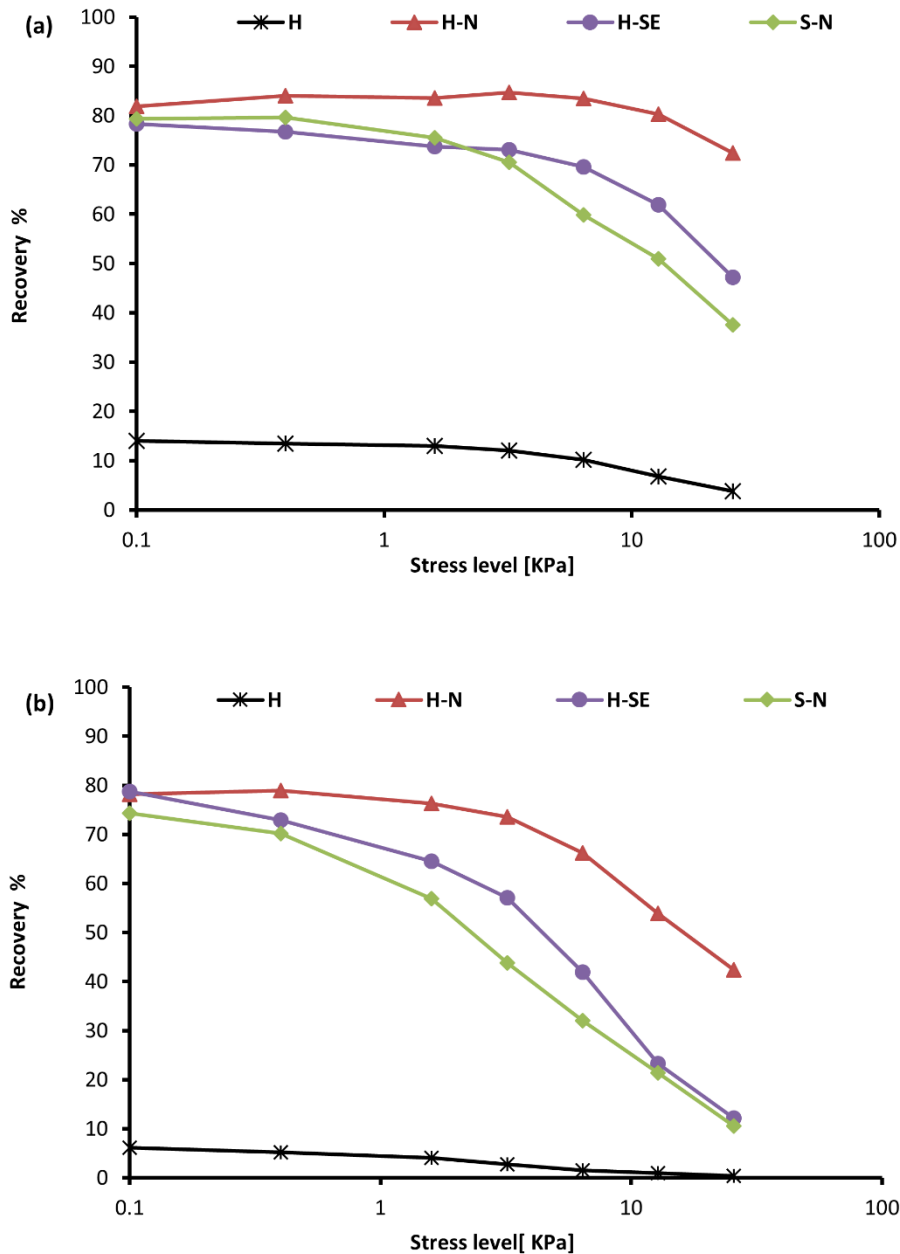


Figure 7.6: Recovery percentage of binders at (a) 50°C and (b) 60°C

7.4 Rutting Resistance of Mixtures

The typical results obtained from the RLAT at a test temperature of 50°C for the different mixtures are shown in Figure 7.7, where permanent axial strain is plotted against load cycles. This kind of plot generally gives three distinctive phases of the material. In the first or primary phase, the accumulation of vertical strain increases rapidly due to a combination of adjustment of loading platens and material densification. However, the permanent deformation rate gradually decreases. The secondary phase takes place when the strain rate reaches approximately a steady state response, and the strain increases approximately in proportion to the load cycles. The tertiary phase starts when the rate of deformation increases

rapidly indicating specimen failure; however, none of the mixtures considered in this study reached the tertiary phase. The cumulative axial strain at the end of the 3600 load pulses or at the initiation of tertiary phase, and/or, the slope of the steady state phase, have been used to distinguish between better performing materials.

In this study, the slope of the steady state phase is determined from a segment between 1500 to 3000 pulses as follows;

$$\text{Minimum strain rate } \left[\frac{\mu\epsilon}{\text{cycle}} \right] = \frac{\epsilon_{3000} - \epsilon_{1500}}{1500} \times 10^{-6} \quad \text{Equation 7.2}$$

where;

ϵ_{3000} = accumulated strain at 3000 pulses

ϵ_{1500} = accumulated strain at 1500 pulses

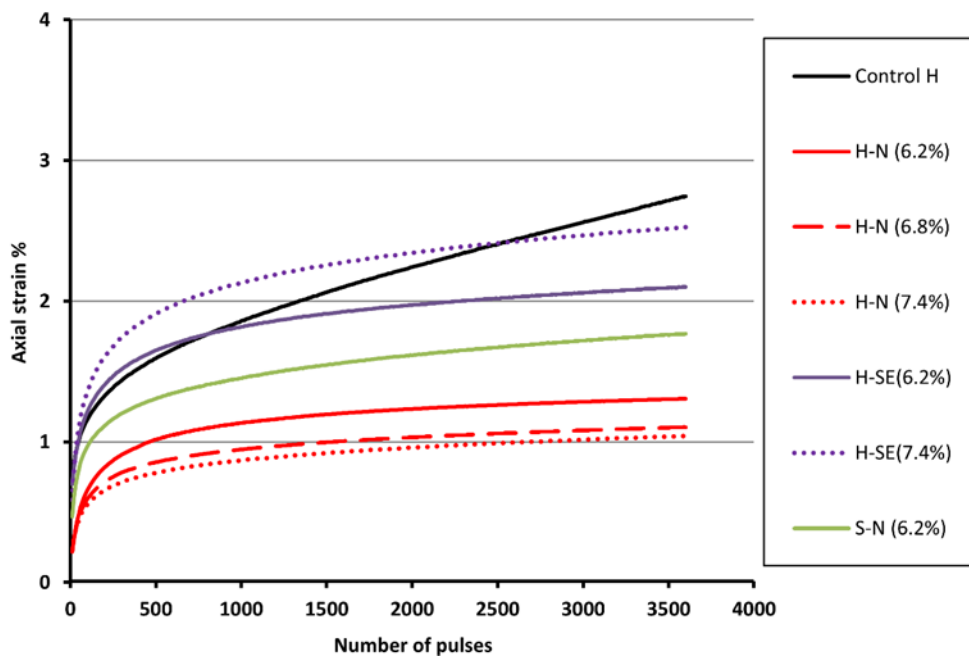


Figure 7.7: RLAT results of different mixtures tested at 100kPa stress and at 50°C temperature

The permanent deformation results in terms of the total accumulated strain at the end of 3600 pulses, and in terms of the minimum strain rate, are presented in Figure 7.8. The range bars represent the maximum and minimum values for replicates. The results in Figure 7.8 clearly confirm the enhanced rutting performance of RTR-MBs in comparison to the base bitumen H. In particular, the mixtures made with binder H-N at the three binder contents show the best rutting properties among other mixtures. The influence of binder content on permanent

deformation performance for mixtures made with H-N binder shows an unexpected trend. It can be seen that increasing the binder content has resulted in a slight reduction in the total strain and an insignificant change in the minimum strain rate for H-N groups. Increasing the binder content can make the asphalt mixtures more susceptible to permanent deformation as the binder film becomes thicker between aggregate particles (Khanzada 2000, Tayfur, Ozen et al. 2007). It is the high-performance recovery of binder H-N that might have contributed to making the rutting resistance for mixtures with higher binder content, less affected by the thicker binder film. In other words, the reduction in rutting resistance for mixtures with higher binder content is compensated by the recovery improvement due to the relative increase of rubber content in the mixture. In contrast to the H-N groups, increasing the binder content for mixtures made with H-SE binder has led to increasing the total accumulated strain and the minimum strain rate. These findings are in agreement with the general effect of binder content as higher binder content can increase the plastic flow susceptibility. Despite the fact that the binder S-N and the mixtures made with this binder are much softer than the control H, the results in Figure 7.8 indicate that the mixtures of binder S-N are less susceptible to high-temperature deformation than the control mixtures. This again seems to emphasise the high-performance ability of rubber modified binders to recover the induced strain in comparison to unmodified binders. Figure 7.9 demonstrates graphically how the binder S-N can have a comparable non-recoverable strain with bitumen H even though the total strain of binder S-N is considerably larger than the total strain of bitumen H.

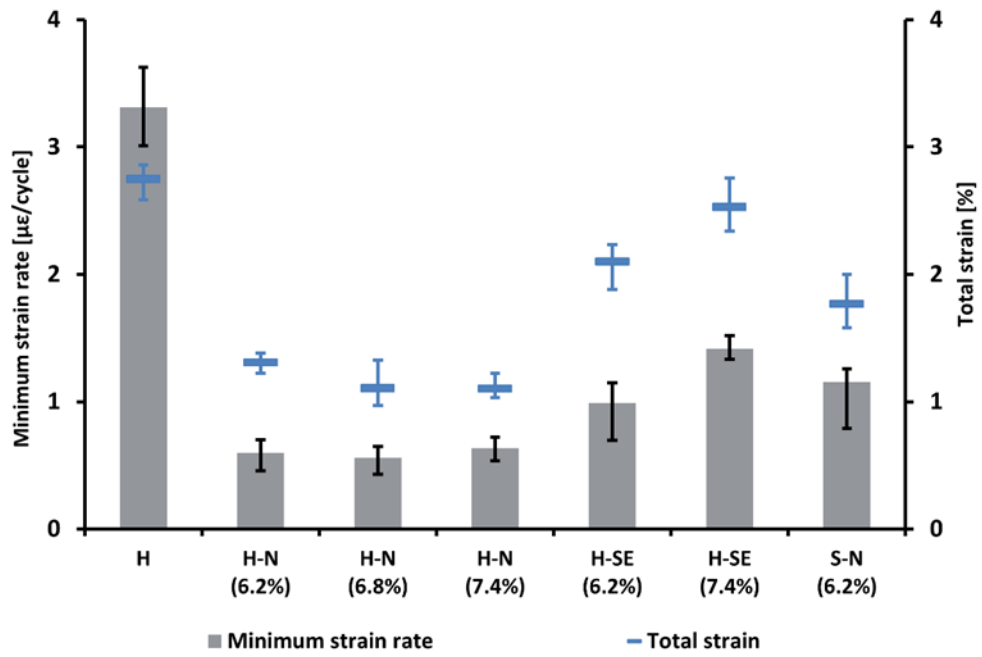


Figure 7.8: RLAT results in terms of the minimum strain rate and total strain

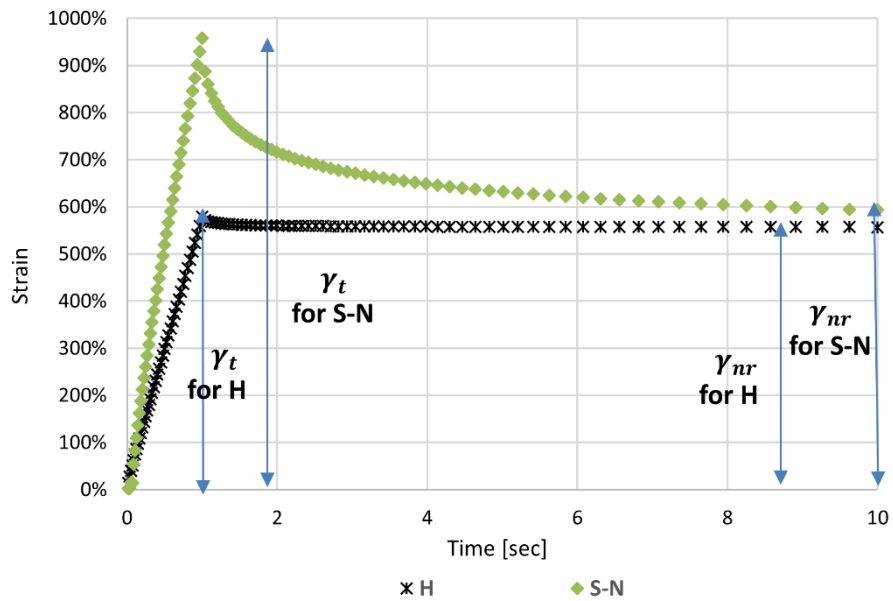


Figure 7.9: One cycle results of MSCR test for binders S-N and H, at stress level of 25.6 kPa, and at temperature of 50 °C

7.5 Rutting susceptibility: From binders to mixtures

7.5.1 Correlation between binder rutting parameters and RLAT

The different test parameters used to characterise the high-temperature properties of binders have ranked the binders differently. Therefore, it is important to identify the best binder parameter that can predict correctly the binder contribution in the rutting performance of mixtures. The rutting performance of different mixtures produced with a binder content of 6.2% only is considered for comparison in this section. The total strain is largely affected by the initial strain at the beginning of the test. And, the initial strain is more sensitive to the initial conditioning of the test apparatus as well as the different orientation of the aggregate within the mixtures, for different specimens, while the minimum strain rate is considered more fundamental to reliably characterise the rutting resistance of mixtures. Also, the effect of using different binder is clearly revealed in the minimum strain rate. For these reasons and to establish a relationship between binder properties and mixtures, the different rutting parameters of binders are correlated with the minimum strain rate of mixtures. Based on the results in Figure 7.8, the overall ranking of the different mixtures, in terms of minimum strain rate, is

$$\text{H-N (6.2\%)} > \text{H-SE (6.2\%)} > \text{S-N (6.2\%)} > \text{H (6.2\%)}$$

Amongst the different binder testing parameters, only the MSCR has been able to rank the binders correctly in terms of rutting performance. On the other hand, the SHRP parameter has totally failed to rank the binders correctly, while the ranking of binders based on the ZSV and Shenoy parameters, is much closer to predicting correctly the rutting performance of mixtures. In order to evaluate statistically how these parameters are associated with the rutting resistance of mixtures, a simple linear regression analysis is applied to the values of different binder parameters and the minimum strain rate of mixtures, as shown in Figures 7.10 (a to f). It can be seen that the rutting parameters obtained from the dynamic oscillatory test, as shown in Figures 7.10 (a, b, and c), have a very poor correlation with the mixture rutting property characterised by the minimum strain rate. On the other hand, the J_{nr} parameter obtained from MSCR, at stress levels of 0.1 kPa and 3.2 kPa, as shown in Figures 7.10 (d and e), has the best correlation. However, a lower correlation coefficient ($R^2= 0.42$) can be seen in Figure 7.10 (f), for the J_{nr} tested at a high stress level of 25.6 kPa. However, it can be seen that the correlation improves significantly with a correlation coefficient ($R^2= 0.99$), as shown in Figure 7.11, after omitting the S-N point. This fall is mainly caused by

the significant increase of J_{nr} for binder S-N at high stress. The binder S-N was processed using very soft bitumen, and under high-stress levels, the physical linkages between rubber and base bitumen are not strong enough to sustain high strains and act as a single phase in a very soft medium (Subhy, Lo Presti et al. 2015). Consequently, the resistance of modified binders to deformation would be greatly affected, and it would derive mainly from the base bitumen. It should be mentioned that because of the binder S-N is much softer than others, the stress level of 25.6 kPa induced considerably high strain $\sim 960\%$. Although, the binder films in a mixture may undergo very high strains, this high strain seems unlikely to happen under the RLAT conditions. The following analysis is introduced to understand better the effect of strain levels on the high-temperature performance of materials.

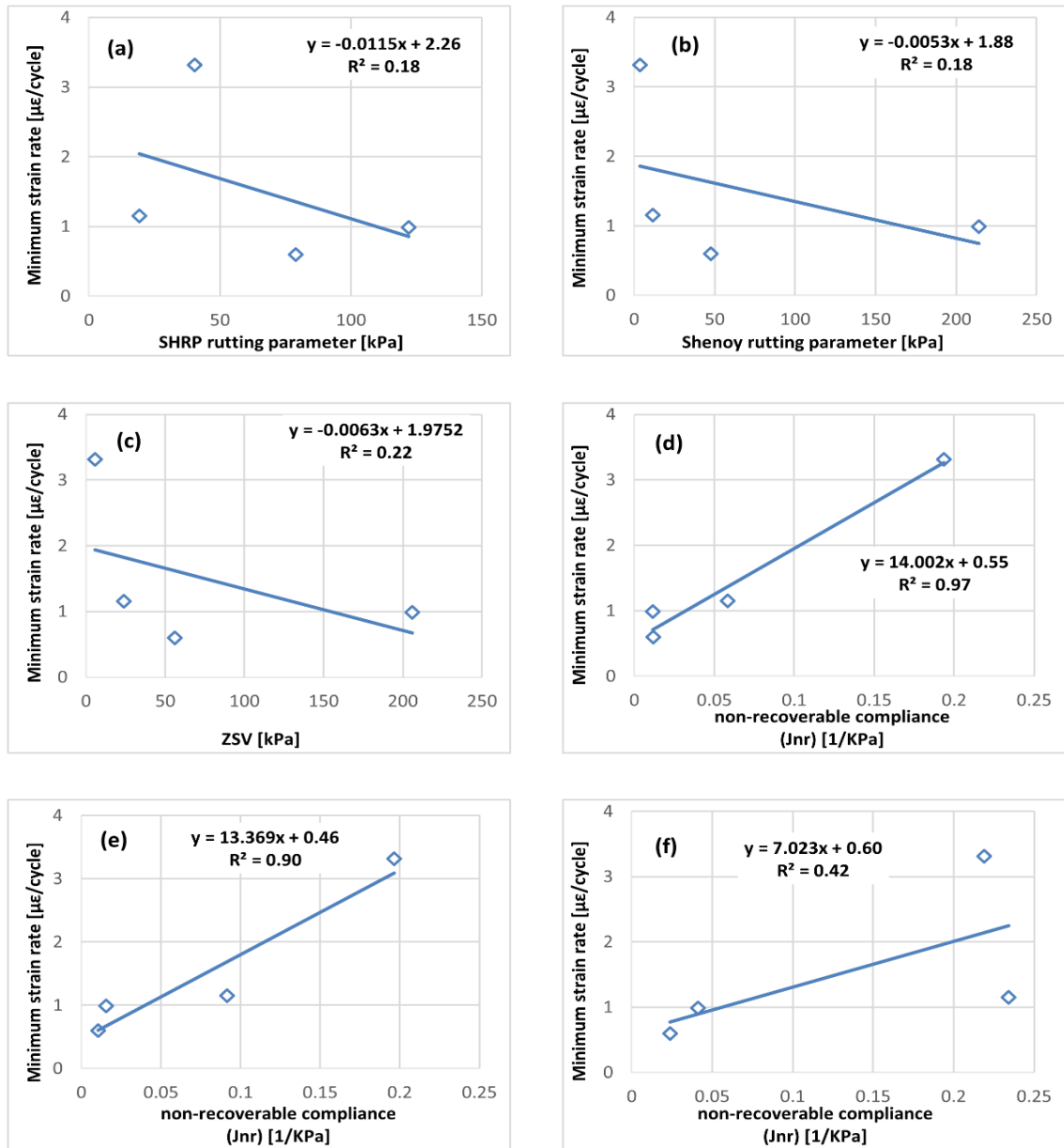


Figure 7.10: Correlation between different rutting parameters with the minimum strain rate of mixtures; (a) SHRP, (b) Shenoy, (c) ZSV, (d) J_{nr} @ 0.10 kPa stress level, (e) J_{nr} @ 3.2 kPa stress and (f) J_{nr} @ 25.6 kPa stress

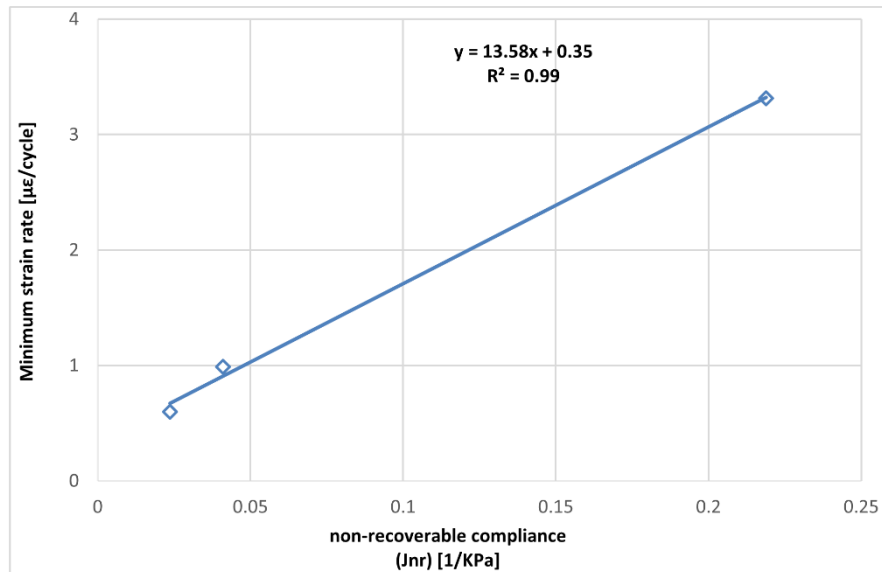


Figure 7.11: Correlation between J_{nr} @ 25.6 kPa stress with the minimum strain rate for only three mixtures

7.5.2 Establishing a more fundamental relationship between binders and mixtures

Binders within the mixture undergo a wide range of strain distribution depending on the volumetric properties of mixtures, and constituent material properties (Bahia, Zhai et al. 1999, Masad and Somadevan 2002). Bahia, Zhai et al. (1999) demonstrated that strains within the binder films, based on finite-element analysis, can be realistically assumed to be between 10 and 100 times the bulk strains of the total mixture. In order to establish a reliable relationship between the binder properties and mixtures, it is important to consider the realistic strains that binders experience in the mixtures. Therefore, an approximation of the average strains that binders may undergo in the mixtures is estimated and compared with the binder strains that occur in the MSCR. Table 7.1 shows the estimated strains in a binder for each mixture, and the strains obtained from MSCR test at different stress level. The estimated strains in the binder are calculated by multiplying the total accumulated strain from RLAT results by the median value (55) of the aforementioned Bahia's assumption. The strain values in Table 7.1, for the MSCR test, represent the average total strains of 10 cycles for each stress level. The shaded values denote the strains for the MSCR test that are close to the estimated binder strains under the RLAT conditions.

Table 7.1: The estimated binder strains under the RLAT conditions, and MSCR strains, for the different binders

	H	H-N	H-SE	S-N
Estimated strain%	151.03	71.83	115.54	97.17
Stress level [kPa]	MSCR strains %			
0.10	2.25	0.65	0.53	2.82
0.40	8.91	2.68	2.14	11.30
1.60	35.48	10.89	9.08	46.08
3.20	71.51	21.94	18.58	99.25
6.40	143.94	45.06	38.65	222.49
12.80	288.09	97.43	83.43	446.26
25.60	582.32	220.15	198.91	959.64

It can be seen that for binder S-N the stress level of 3.20 kPa induced approximately the same strain that would happen under the RLAT conditions. For the control bitumen H, the stress level of 6.4 kPa is close enough to produce the same strain as in the RLAT. For binders H-N and H-SE, their corresponding strain values have to be extrapolated between two stress levels, as shown in Table 7.1. Having obtained the J_{nr} for each binder at a stress level that matches the mixture conditions, a linear fitting is used to correlate those J_{nr} values with the minimum strain rate of mixtures, as can be found in Figure 7.12. The J_{nr} obtained at stress levels that resemble the strains condition of binders in the RLAT correlates very well with the minimum strain rate of mixtures with R^2 of 0.93. It can be seen that the correlation at a stress level of 0.1 kPa, as shown in Figure 7.10 (d), provides a better correlation coefficient ($R^2= 0.97$) than in Figure 7.12 ($R^2= 0.93$). However, the J_{nr} at 0.1 kPa stress level is almost the same for binders H-N and H-SE, but there is a large difference between the rutting properties for mixtures made using those binders. The J_{nr} determined in Figure 7.12 is able to distinguish between the rutting properties for all mixtures. Therefore, it can be concluded that considering the realistic strain conditions, as in the case of Figure 7.12, is more appropriate to relate binder properties to mixture properties.

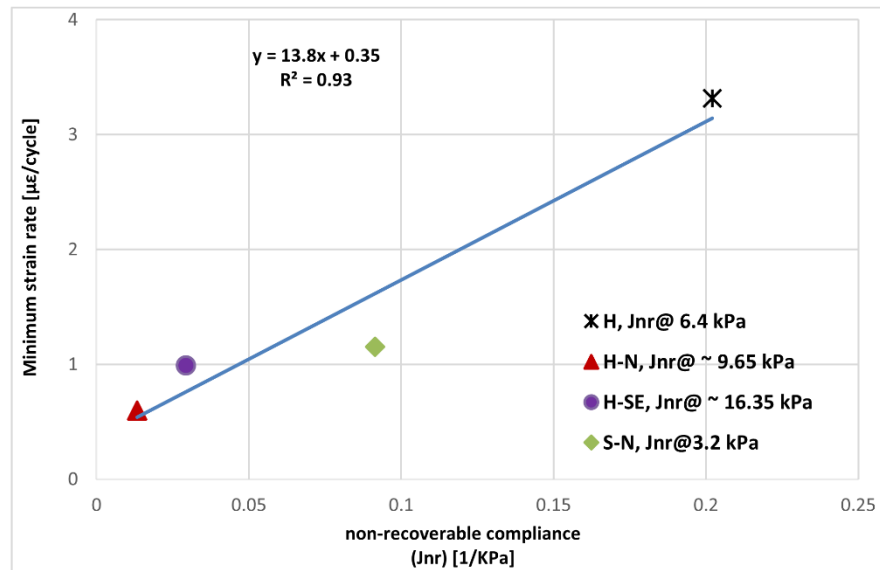


Figure 7.12: Correlation between J_{nr} obtained at different stress level with the minimum strain rate

7.6 Summary and Conclusions

The permanent deformation resistance at high temperatures for binders and their mixtures has been evaluated in this chapter. The rutting performance of binders has been investigated using two different types of tests in the DSR. The first test is based on the dynamic oscillatory test, while the second is based on the MSCR test. Different rutting parameters were obtained from the first test to evaluate the high-temperature properties of binders. Those parameters are; SHRP rutting parameter, Shenoy rutting parameter and ZSV. The J_{nr} is used as a rutting parameter from MSCR. The rutting resistance of mixtures has been evaluated by the RLAT. The following conclusions can be drawn from this chapter:

- (1) In general, the addition of rubber can produce bituminous materials with enhanced rutting characteristics. This is especially evident for binder S-N. This binder was manufactured using very soft base bitumen (200 dmm penetration). However, the results of RLAT reveal that the mixtures made with binder S-N were even more rut resistant than mixtures made with bitumen H (40 dmm penetration). Such results suggest that binder S-N can be a very effective option for pavements that are prone to both low temperature cracking and to permanent deformation
- (2) All the rutting parameters obtained from the dynamic oscillatory test were inadequate to characterise the rutting properties of RTR-MBs. On the contrary, the MSCR test was able to capture the rutting properties of binders that were reflected correctly into the rutting resistance of mixtures

- (3) The results have shown that the mixtures made with binder H-N are the most rut resistant followed by H-SE then S-N and H
- (4) Taking into account the realistic strain conditions that binder films experience in the mixtures, under certain laboratory test conditions or field conditions, would provide a more fundamental approach to relating binder properties to mixture properties. Thanks to the MSCR test, it allows characterising the binders at multiple stress conditions, and then select the effective stress condition that induces approximately similar strains as in the mixture conditions
- (5) The influence of increasing the binder content on the rutting properties, in the case of mixtures made with binder H-N, has shown an unexpected trend. In general, higher binder content leads to higher permanent deformation. However, the findings of this study reveal that the rutting resistance of mixtures made with binder H-N is not negatively affected by increasing the binder content. This confirms that binder H-N possesses superior anti-rutting peculiarities that contribute to the stabilisation of aggregates

Chapter 8 **Conclusions and Recommendations**

8.1 Conclusions

The primary aim of this research was to characterise and develop rubberised bituminous materials with enhanced performance-related characteristics. Incorporating recycled tyre rubber into flexible pavement applications by the means of Recycled Tyre Rubber-Modified Bitumen (RTR-MBs) would solve a serious waste problem, save energy and materials, and enhance pavement life and performance. On the other hand, the excessively high viscosity of rubberised binders imposes handling difficulties during the mixing and compaction process. Therefore, producing rubberised binders with acceptable high-temperature viscosity, and also having desirable mechanical properties that are truly reflected in asphalt mixtures, would significantly improve the workability of rubberised bitumen and make it industrially more acceptable.

The results indicate that pre-treatment of the recycled rubber can significantly reduce the high-temperature viscosity; however, the fracture properties of binders are compromised, i.e. the bituminous binders become fragile and hence more susceptible to cracking. In general, the addition of rubber can produce bituminous materials with enhanced rutting and fatigue characteristics. This is especially evident for rubberised bitumen manufactured using very soft base bitumen (200 dmm penetration). The results of RLAT testing have revealed that the mixtures made with this binder were even more rut resistant than mixtures made with the hard base bitumen H (40 dmm penetration). Such results suggest that rubberised bitumens produced with a very soft base bitumen can be a very effective option for pavements that are prone to both low temperature cracking and to permanent

deformation. All tests methods and parameters, for binders and mixtures, have proven that the addition of rubber can improve the fatigue and rutting properties of materials.

One of the main outcomes of this research is the effect of binder content for rubberised asphalt mixtures on the fatigue and rutting properties. The results have shown that the same binder content as in the control mixtures can also be used for the rubberised asphalt mixtures. The laboratory testing results have indicated that an increase in the binder content for rubberised bitumen mixtures has not significantly enhanced the performance-related properties. Indeed, the RTR-MBs can be treated as a single modified binder and, thus, the same binder content as for the control can be used. In terms of the mixture design procedure, the existence of rubber particles as inert filler can, therefore, be ignored. This can result in a cost reduction for rubberised bitumen alternative.

In the following sections, a detailed review of the main findings and conclusions are presented after an in-depth investigation and analysis conducted in this study.

8.1.1 The Mechanical Characteristics of RTR-MBs

Based on the rheological and mechanical investigation for RTR-MBs undertaken in this research, the following conclusions and findings can be drawn:

- (1) The RTR-MBs' properties are largely dependent on their manufacturing conditions; therefore, carefully assessing these variables is essential to develop better materials. The results have shown that processing the RTR-MBs at low temperature $\sim 160^{\circ}\text{C}$ was not appropriate for developing high-performance binders.
- (2) Selecting higher mixing temperature (200°C) can significantly reduce the time needed to reach the maximum swelling extent for binders produced using a straight non-pre-treatment recycled rubber. This can also develop superior rheological properties and potential saving in energy consumption.
- (3) The results have also highlighted that selecting materials based only on the linear viscoelastic region properties is not sufficient and in some cases might be misleading. Optimising the blending variables based only on the highest viscosity does not always guarantee the best performance of materials. Using rheological testing within and outside the LVE region would help increase understanding of the material and hence optimise effectively the processing conditions. Therefore, characterising the

non-linear behaviour in addition to linear is essential for an appropriate materials selection

- (4) Using different sources for crumb rubber modifiers can result in a considerable difference in rheological behaviour of RTR-MBs, even though they are blended with the same base bitumen
- (5) The findings of the storage stability tests have shown that the RTR-MBs are heterogeneous unstable binders when stored statically at high temperature. Therefore, a continuous agitation is required to prevent phase separation. These findings have also revealed that crumb rubber particles are not only separated by settling down to the bottom but also separated by floating to the top of the storage container
- (6) The addition of recycled tyre rubber into the bitumen can alter the mechanism by which the binder is aged. The DMA analysis has shown that artificial ageing can partly disintegrate and dissolve the rubber particles, particularly after PAV ageing, resulting in softening of the modified binders. This, in turn, reduced the hardening susceptibility of binders after ageing. Although it is likely to adversely affect the rutting resistance of materials, it provides important enhancement to the resistance of materials for intermediate and low-temperature cracking. Since the ageing of a pavement is mainly considered to result in a cracking related problem, it can, therefore, be concluded that RTR-MBs can be expected to provide enhanced ageing characteristics, and hence, a durable pavement.

8.1.2 The Performance-Related Properties of RTR-MBs

The main conclusions and finding that can be drawn based on the results obtained from the investigations into the fatigue and rutting properties of binders are:

- (1) Rubber modification of a very soft base bitumen (200 dmm penetration) can produce binder with excellent fracture and cracking properties, as indicated by the CTOD parameter and PV
- (2) The DENT has caught the detrimental effect of FT-waxes on fatigue properties, for the RTR-MBs produced using the rubber pre-treated with Sasobit[®]. However, despite this binder appearing to have poorer fatigue resistance than the base bitumen when the fracture energy is taken globally, its ability to resist the propagation of existing cracking was better than other binders when the fracture parameters were obtained from the energy partitioning concept

- (3) The traditional fatigue analysis (initial strain Vs Nf) has shown that the fatigue lives of H group binders are temperature dependent while the inclusion of rest periods and the change of loading mode do not change the fatigue lines. Unlike H group binders, the inclusion of rest periods revealed a significant effect on extending the fatigue life for RTR-MBs produced using the soft base bitumen. Thus, it is important to investigate the healing mechanism of different binders in addition to their fatigue properties for an appropriate material selection
- (4) Although a unique fatigue law could be produced from the fatigue analysis based on accumulated dissipated energy, this approach generates in some cases misleading fatigue curves due to encompassing viscoelastic energies that are not responsible for fatigue damage
- (5) The PV obtained by the proposed method has been able to distinguish between the fatigue resistances of different binders, and thus it can be used as a reliable fatigue parameter. The results of this study and some other similar studies found in the literature show that the PV-Nf relationship is material dependant but there was limited evidence to accept that this relationship is unique regardless of material type
- (6) The addition of rubber can produce bituminous materials with enhanced rutting characteristics. This is especially evident for binder S-N, this binder was manufactured using very soft base bitumen (200 dmm penetration) but the rubber modification significantly enhanced its rutting resistance
- (7) The addition of rubber can significantly increase the high-performance ability of binders to recover induced strain in comparison to unmodified binders. This, in turn, improves the rutting resistance of bituminous materials

8.1.3 The Relations between Different Test Binder Methods and Asphalt Mixtures

The main conclusions that could be drawn based on the laboratory investigations for binders and asphalt mixtures in this study are:

- (1) The ITFT fatigue results, based on EN 12697-24: 2004, have shown that the permanent deformation can give a fake indication of the rank order of materials, while the fatigue analysis based on the resilient strain obtained from EN 12697-24: 2012, has been shown to provide a more reliable rank order that is in agreement with the fatigue properties of binders
- (2) It is crucial to evaluate and then appropriately identify the fatigue failure point before commencing the fatigue analysis. The classical approach of a 50% decrease in the

initial stiffness is an arbitrary definition and can lead to incorrect analyses. Therefore more fundamental approaches should be considered to provide a more realistic definition of fatigue failure

- (3) The DENT test offers a simple test method with reproducible data to characterise the fracture properties of bituminous binders under ductile condition. CTOD obtained from the DENT test has been found to be reliably sensitive to the effect of temperature and ageing, and can be considered a good discriminating parameter to quantify the fatigue performance of binders. The concept of partitioning the total fracture work of energy has been successfully applied on bituminous binders; it enables determining and separating the resistance of materials to fracture initiation in addition to fracture propagation resistance
- (4) The results of SuperPave IDT have shown that the addition of rubber can significantly decelerate the rate of damage accumulation which, in turn, leads to enhanced cracking resistance of mixtures. Indeed, the ER values have revealed that RTR-MB mixtures have superior cracking resistance to the control mixture. The excellent strain tolerance of RTR-MBs produced using the soft base bitumen and a straight non-pre-treatment recycled rubber has been reflected in the mixture through the failure strain and subsequently through the ER parameter. Thus, the PV and CTOD are recommended to evaluate reliably the fatigue properties of binders, and the ER parameter to evaluate the cracking resistance of mixtures
- (5) All the rutting parameters obtained from the dynamic oscillatory test were inadequate to characterise the rutting properties of RTR-MBs. In contrast, the MSCR test was able to capture the rutting properties of binders that were reflected correctly by the rutting resistance of mixtures
- (6) Taking into account the realistic strain conditions that binder films experience in the mixtures, under certain laboratory test conditions or field conditions, would provide a more fundamental approach to relating binder properties to mixture properties. The MSCR test enables characterisation of binders at multiple stress conditions, and then selection of the effective stress condition that induces approximately similar strains as in the mixture

8.2 Recommendations for Future Research

In this section, a list of recommendations and suggestions are presented for work that was not included in the current study due to the lack of time and resources. These recommendations are important to understand better the behaviour of rubberised bituminous materials in order to accurately predict their performance.

- (1) The study was limited to using only one rubber percentage (18% by bitumen weight which is equal to 15.25% by weight of the total blend). Although many studies have addressed the effect of rubber percentage, it is still necessary to study this variable based on the testing procedures used in this study, which included testing the materials under different damage circumstances. The manufacture method protocol developed in this study using the Brookfield rotational viscometer and a modified impeller (Dual Helical Impeller (DHI)) would give an excellent opportunity to effectively investigate this variable in addition to the other many variables associated with the manufacturing of RTR-MBs using minimum material consumption for laboratory needs
- (2) The study has covered the characterisation of materials from binder to mixture. However, it would be of great interest to extend this to full-scale pavement trials. This will enrich the understanding of the behaviour of rubberised asphalt materials and to maximise their performance based on full-scale pavement trials
- (3) Asphalt mixture properties were evaluated using a single type of aggregate and a typical job formula. It is important for future research to study the effect of aggregate type and gradation on the performance characteristics
- (4) The effect of artificial ageing, in the current work, was only studied on binders. It is recommended for future studies to investigate the effect of ageing on asphalt mixtures produced using the rubberised binders
- (5) The investigated performance-related characteristics in this study were limited to fatigue cracking and rutting. Future researchers are encouraged to further extend that to evaluate low temperature cracking
- (6) The effect of using different base bitumens was studied based on their physical properties. It is important to also consider the chemistry of base bitumen in order to evaluate and establish a relationship between the chemical properties of base bitumen and the rheological properties of the rubberised binders

- (7) The current study included a wide range of laboratory results in terms of mechanical and performance-related properties for asphalt mixtures. However, it would be of great interest for future research to perform a theoretical analytical study to investigate the relative influence of adopting the rubberised binder technology on pavement life and the thickness of pavement structural layers
- (8) The PV obtained by the proposed method in this study was able to distinguish between the fatigue resistances of different materials, and thus it can be used as a reliable fatigue parameter. It is recommended that the PV calculation method proposed in this study be further evaluated on asphalt mastics or asphalt mixtures
- (9) The current study considered neat unmodified bituminous materials as a reference for performance comparison. However, polymer modified bitumen (PMB) is considered the most accepted modification for road pavement applications and widely used by many transport agencies. Future research should, therefore, concentrate on comparing the rubberised binders with PMB. A Life-Cycle Cost Analysis (LCCA) can be used to evaluate the long-term performance of the alternatives and provide a rational cost comparison to transport agencies for those competing pavement alternatives
- (10) The inclusion of WMA (FT-Sasobit®) in the rubberised binder technology is a promising combination, since it can produce materials with a reduced high temperature viscosity and enhanced rutting characteristics. However, the fracture properties of binders were affected because of the waxes. There are many other WMA additives types, i.e. Zeolite, Evotherm, and WAM Foam that need to be investigated and their effect on the rubberised binders evaluated in future research
- (11) The SuperPave IDT enables evaluation of the fracture properties and the cracking performance of different asphalt mixtures. The test was carried out in this study using strain gauges. Although strain gauges can accurately measure the induced strains, they are expensive and cannot be re-used. On the other hand, linear variable displacement transformers (LVDTs) offer reliable strain measurements and they are designed for frequent use. Due to the lack of time, it was not possible to manufacture the miscellaneous parts needed for installing the LVDTs on the specimen. It is, therefore, recommended for future research to develop this test using LVDTs

References

AASHTO "Multiple Stress Creep Recovery Test of Asphalt Binder Using a Dynamic Shear Rheometer (MSCR), TP70-12, 2012."

Abdelrahman, M. (2006). "Controlling performance of crumb rubber-modified binders through addition of polymer modifiers." Transportation Research Record: Journal of the Transportation Research Board **1962**(1): 64-70.

Abdelrahman, M. (2006). "Controlling performance of crumb rubber-modified binders through addition of polymer modifiers." Transportation Research Record: Journal of the Transportation Research Board(1962): 64-70.

Abdelrahman, M. and S. Carpenter (1999). "Mechanism of interaction of asphalt cement with crumb rubber modifier." Transportation Research Record: Journal of the Transportation Research Board(1661): 106-113.

Airey, G. (2003). "State of the art report on ageing test methods for bituminous pavement materials." International Journal of Pavement Engineering **4**(3): 165-176.

Airey, G., et al. (2006). Fatigue behaviour of bitumen-filler mastics. 10TH INTERNATIONAL CONFERENCE ON ASPHALT PAVEMENTS-AUGUST 12 TO 17, 2006, QUEBEC CITY, CANADA.

Airey, G., et al. (2002). "Properties of polymer modified bitumen after rubber-bitumen interaction." Journal of materials in civil engineering **14**(4): 344-354.

Airey, G. D. (1997). Rheological characteristics of polymer modified and aged bitumens, University of Nottingham.

Airey, G. D. (2002). "Use of black diagrams to identify inconsistencies in rheological data." Road Materials and Pavement Design **3**(4): 403-424.

Airey, G. D. (2004). "Fundamental binder and practical mixture evaluation of polymer modified bituminous materials." International Journal of Pavement Engineering **5**(3): 137-151.

Airey, G. D. and S. F. Brown (1998). "Rheological performance of aged polymer modified bitumens." Journal of the Association of Asphalt Paving Technologists **67**.

Airey, G. D. and Y.-K. Choi (2002). "State of the art report on moisture sensitivity test methods for bituminous pavement materials." Road Materials and Pavement Design **3**(4): 355-372.

Airey, G. D. and B. Rahimzadeh (2004). "Combined bituminous binder and mixture linear rheological properties." Construction and Building Materials **18**(7): 535-548.

Al-Mansob, R. A., et al. (2016). "Rheological characteristics of unaged and aged epoxidised natural rubber modified asphalt." Construction and Building Materials **102**: 190-199.

Anderson, D. A., et al. (1991). "Physical properties of asphalt cement and the development of performance-related specifications." Journal of the Association of Asphalt Paving Technologists **60**.

Anderson, D. A., et al. (1994). "Binder characterization and evaluation, volume 3: Physical characterization." Strategic Highway Research Program, National Research Council, Report No. SHRP-A-369.

Anderson, D. A., et al. (2001). "Evaluation of fatigue criteria for asphalt binders." Transportation Research Record: Journal of the Transportation Research Board **1766**(1): 48-56.

Anderson, D. A., et al. (2002). "Zero shear viscosity of asphalt binders." Transportation Research Record: Journal of the Transportation Research Board **1810**(1): 54-62.

Andriescu, A., et al. (2004). "Essential and plastic works of ductile fracture in asphalt binders." Transportation Research Record: Journal of the Transportation Research Board(1875): 1-7.

Andriescu, A. and S. A. Hesp (2009). "Time-temperature superposition in rheology and ductile failure of asphalt binders." International Journal of Pavement Engineering **10**(4): 229-240.

Andriescu, A., et al. (2004). "Essential and plastic works of ductile fracture in asphalt binders." Transportation Research Record: Journal of the Transportation Research Board **1875**(1): 1-7.

Arega, Z., et al. (2011). "Influence of warm-mix additives and reduced aging on the rheology of asphalt binders with different natural wax contents." Journal of materials in civil engineering **23**(10): 1453-1459.

Asphalt Institute (2003). "Superpave Mix Design " Superpave Series No. 2 (SP-2), Lexington, KY.

Attia, M. and M. Abdelrahman (2009). "Enhancing the performance of crumb rubber-modified binders through varying the interaction conditions." International Journal of Pavement Engineering **10**(6): 423-434.

Ayar, P., et al. (2015). "The healing capability of asphalt pavements: a state of the art review." Journal of Cleaner Production.

- Baaj, H., et al. (2005). "Effect of binder characteristics on fatigue of asphalt pavement using an intrinsic damage approach." Road Materials and Pavement Design **6**(2): 147-174.
- Bahia, H. U. and R. Davies (1994). "Effect of crumb rubber modifiers (CRM) on performance related properties of asphalt binders." Asphalt paving technology **63**: 414-414.
- Bahia, H. U., et al. (2001). Characterization of modified asphalt binders in superpave mix design.
- Bahia, H. U., et al. (1999). "Non-linear viscoelastic and fatigue properties of asphalt binders." Journal of the Association of Asphalt Paving Technologists **68**: 1-34.
- Bárány, T., et al. (2010). "Application of the essential work of fracture (EWF) concept for polymers, related blends and composites: a review." Progress in Polymer Science **35**(10): 1257-1287.
- Barany, T., et al. (2005). "In-plane and out-of-plane fracture toughness of physically aged polyesters as assessed by the essential work of fracture (EWF) method." International journal of fracture **135**(1-4): 251-265.
- Bhasin, A., et al. (2009). "Quantitative comparison of energy methods to characterize fatigue in asphalt materials." Journal of materials in civil engineering **21**(2): 83-92.
- Billiter, T., et al. (1997). "Investigation of the curing variables of asphalt-rubber binder." Petroleum Science and Technology **15**(5-6): 445-469.
- Billiter, T., et al. (1997). "Production of asphalt-rubber binders by high-cure conditions." Transportation Research Record: Journal of the Transportation Research Board(1586): 50-56.
- Bonnetti, K. S., et al. (2002). "Measuring and defining fatigue behavior of asphalt binders." Transportation Research Record: Journal of the Transportation Research Board **1810**(1): 33-43.
- Boudabbous, M., et al. (2013). "Shear test to evaluate the fatigue of asphalt materials." Road Materials and Pavement Design **14**(sup1): 86-104.
- Brown, S. and D. Needham (2000). "A study of cement modified bitumen emulsion mixtures." Asphalt paving technology **69**: 92-121.
- Buttlar, W. G. and R. Roque (1994). "Development and evaluation of the strategic highway research program measurement and analysis system for indirect tensile testing at low temperatures." Transportation Research Record(1454).

Carpenter, S. H. and S. Shen (2006). "Dissipated energy approach to study hot-mix asphalt healing in fatigue." Transportation Research Record: Journal of the Transportation Research Board **1970**(1): 178-185.

Celauro, B., et al. (2012). "Definition of a laboratory optimization protocol for road bitumen improved with recycled tire rubber." Construction and Building Materials **37**: 562-572.

Celauro, B., et al. (2012). "Definition of a laboratory optimization protocol for road bitumen improved with recycled tire rubber." Construction and Building Materials **37**: 562-572.

Chen, J.-S. and C.-J. Tsai (1999). "How good are linear viscoelastic properties of asphalt binder to predict rutting and fatigue cracking?" Journal of materials engineering and performance **8**(4): 443-449.

Cheng, G., et al. (2011). "A study on the performance and storage stability of crumb rubber-modified asphalts." Petroleum Science and Technology **29**(2): 192-200.

Chippis, J. F., et al. (2001). "A model for oxidative aging of rubber-modified asphalts and implications to performance analysis." Energy & fuels **15**(3): 637-647.

CLEMSON-UNIVERSITY (2013). "Wet Grind Tire Processing System." from <http://www.clemson.edu/ces/arts/wetgrind.html>.

Collop, A., et al. (1995). "Viscoelastic approach to rutting in flexible pavements." Journal of Transportation Engineering **121**(1): 82-93.

CWC (1998). "Best Practices in Scrap Tires & Rubber Recycling-Ambient Versus Cryogenic Grinding; BP-T2-03-04.doc." from http://www.cwc.org/tire_bp/t_bp_pdf/2-03-04.pdf.

D'Angelo, J., et al. (2006). Evaluation of repeated creep and recovery test method as an alternative to SHRP+ requirements for polymer modified asphalt binders. Fifty-First Annual Conference of the Canadian Technical Asphalt Association (CTAA).

D'Angelo, J., et al. (2007). "Revision of the superpave high temperature binder specification: The multiple stress creep recovery test (with discussion)." Journal of the Association of Asphalt Paving Technologists **76**.

D'Angelo, J. A. (2009). "The relationship of the MSCR test to rutting." Road Materials and Pavement Design **10**(sup1): 61-80.

De Visscher, J. and A. Vanelstraete (2004). "Practical test methods for measuring the zero shear viscosity of bituminous binders." Materials and Structures **37**(5): 360-364.

Department for Transport Statistics (2016). Road traffic (vehicle miles) by vehicle type in Great Britain, <https://www.gov.uk/government/statistical-data-sets/tra01-traffic-by-road-class-and-region-miles>.

Di Benedetto, H., et al. (2004). "Fatigue of bituminous mixtures." Materials and Structures **37**(3): 202-216.

Di Benedetto, H., et al. (2011). "Nonlinearity, heating, fatigue and thixotropy during cyclic loading of asphalt mixtures." Road Materials and Pavement Design **12**(1): 129-158.

Dong, R., et al. (2011). "Laboratory evaluation of pre-devulcanized crumb rubber-modified asphalt as a binder in hot-mix asphalt." Journal of materials in civil engineering **23**(8): 1138-1144.

Dongré, R., et al. (2003). New developments in refinement of the superpave high temperature specification parameter. 40th annual meeting of the Petersen asphalt research conference, Laramie, WY.

Emery, J. (1995). "Evaluation of rubber modified asphalt demonstration projects." Transportation Research Record **1515**: 37-46.

Epps, J. A. (1994). Uses of recycled rubber tires in highways, Transportation Research Board.

Flory, P. J. and J. Rehner Jr (1943). "Statistical mechanics of cross-linked polymer networks II. Swelling." The Journal of Chemical Physics **11**(11): 521-526.

Galooyak, S. S., et al. (2010). "Rheological properties and storage stability of bitumen/SBS/montmorillonite composites." Construction and Building Materials **24**(3): 300-307.

García, A., et al. (2014). "Single and multiple healing of porous and dense asphalt concrete." Journal of Intelligent Material Systems and Structures: 1045389X14529029.

Gent, A. N. (2012). Engineering with rubber: how to design rubber components, Carl Hanser Verlag GmbH Co KG.

Ghaly, N. (2008). "Effect of sulfur on the storage stability of tire rubber modified asphalt." World Journal of Chemistry **3**(2): 42-50.

Ghavibazoo, A. and M. Abdelrahman (2012). "Composition analysis of crumb rubber during interaction with asphalt and effect on properties of binder." International Journal of Pavement Engineering: 1-14.

Ghavibazoo, A. and M. Abdelrahman (2013). "Composition analysis of crumb rubber during interaction with asphalt and effect on properties of binder." International Journal of Pavement Engineering **14**(5): 517-530.

Ghavibazoo, A. and M. Abdelrahman (2014). "Effect of Crumb Rubber Dissolution on Low-Temperature Performance and Aging of Asphalt-Rubber Binder." Transportation Research Record: Journal of the Transportation Research Board(2445): 47-55.

Ghuzlan, K. A. and S. H. Carpenter (2000). "Energy-derived, damage-based failure criterion for fatigue testing." Transportation Research Record: Journal of the Transportation Research Board **1723**(1): 141-149.

Gibson, N., et al. (2010). "Full-scale accelerated performance testing for superpave and structural validation." Final Report FHWA-RD-xx-xxxx, Federal Highway Administration: August.

Gibson, N., et al. (2011). "Full-scale accelerated performance testing for superpave and structural validation." Final Rep. FHWA-RT-01946, Federal Highway Administration, Washington, DC.

Gibson, N., et al. (2012). Performance testing for Superpave and structural validation.

Glover, C. J., et al. (2000). A Comprehensive Laboratory and Field Study of High-Cure Crumb-Rubber Modified Asphalt Materials.

Goh, S. W. and Z. You (2009). Warm mix asphalt using sasobit in cold region. Proceedings of the 14th Conference on Cold Regions Engineering.

González, O., et al. (2006). "Bitumen/polyethylene blends: using m-LLDPEs to improve stability and viscoelastic properties." Rheologica acta **45**(5): 603-610.

González, V., et al. (2012). "A study into the processing of bitumen modified with tire crumb rubber and polymeric additives." Fuel Processing Technology **95**: 137-143.

Green, E. and W. J. Tolonen (1977). THE CHEMICAL AND PHYSICAL PROPERTIES OF ASPHALT RUBBER MIXTURES. PART I. BASIC MATERIAL BEHAVIOR.

Green, E. and W. J. Tolonen (1977). The chemical and physical properties of asphalt rubber mixtures. Part I. basic material behaviour.

Haiping, Z., et al. (2014). "Caltrans use of scrap tires in asphalt rubber products: a comprehensive review." Journal of Traffic and Transportation Engineering (English Edition) **1**(1): 39-48.

Hamed, G. R. (1992). "Materials and compounds." Engineering with Rubber: How to Design Rubber Components **2**: 11.

Hanson, D. I. and G. M. Duncan (1995). "Characterization of crumb rubber-modified binder using strategic highway research program technology." Transportation Research Record(1488): 21-31.

Hashemi, S. (1993). "Plane-stress fracture of polycarbonate films." Journal of materials science **28**(22): 6178-6184.

Heitzman, M. (1992). Design and construction of asphalt paving materials with crumb rubber modifier.

Hesami, E., et al. (2012). "An empirical framework for determining asphalt mastic viscosity as a function of mineral filler concentration." Construction and Building Materials **35**: 23-29.

Hill, R. t. (1952). "On discontinuous plastic states, with special reference to localized necking in thin sheets." Journal of the Mechanics and Physics of Solids **1**(1): 19-30.

Hintz, C., et al. (2011). "Modification and Validation of Linear Amplitude Sweep Test for Binder Fatigue Specification." Transportation Research Record: Journal of the Transportation Research Board **2207**(1): 99-106.

Hofstra, A. and A. Klop (1972). Permanent deformation of flexible pavements under simulated road traffic conditions. Presented at the Third International Conference on the Structural Design of Asphalt Pavements, Grosvenor House, Park Lane, London, England, Sept. 11-15, 1972.

Huang, B., et al. (2010). "Laboratory evaluation of moisture susceptibility of hot-mix asphalt containing cementitious fillers." Journal of materials in civil engineering **22**(7): 667-673.

Huang, S.-C. (2008). "Rubber concentrations on rheology of aged asphalt binders." Journal of materials in civil engineering **20**(3): 221-229.

Huang, S.-C. and A. T. Pauli (2008). "Particle size effect of crumb rubber on rheology and morphology of asphalt binders with long-term aging." Road Materials and Pavement Design **9**(1): 73-95.

Jamshidi, A., et al. (2013). "Performance of warm mix asphalt containing Sasobit®: state-of-the-art." Construction and Building Materials **38**: 530-553.

JLLC (2008). "Scientific and industrial group "Ecological Alternative". Retrieved 13/05/2016, from http://www.recycle.by/en/production/oborudovanie_dlia_pererabotki_shin/.

Johnson, C., et al. (2009). "Practical application of viscoelastic continuum damage theory to asphalt binder fatigue characterization." Asphalt Paving Technology- Proceedings **28**: 597.

Johnson, C. and H. U. Bahia (2010). "Evaluation of an accelerated procedure for fatigue characterization of asphalt binders." Submitted for publication in Road Materials and Pavement Design.

Johnson, C. M., et al. (2007). Evaluation of strain-controlled asphalt binder fatigue testing in the dynamic shear rheometer. 4th Int. Siiv Congress.

Jung, J.-S., et al. (2002). "Life Cycle Cost Analysis: Conventional Versus Asphalt-Rubber Pavements." Rubber Pavements Association.

Kandhal, P. S. (1992). Waste Materials in Hot Mix Asphalt: An Overview, National Center for Asphalt Technology.

Karger-Kocsis, J. and D. Ferrer-Balas (2001). "On the plane-strain essential work of fracture of polymer sheets." Polymer Bulletin **46**(6): 507-512.

Kennedy, T. W. (1985). Prevention of water damage in asphalt mixtures. Evaluation and Prevention of Water Damage to Asphalt Pavement Materials, ASTM International.

Kennedy, T. W., et al. (1994). "SHR-A-410 Superior Performing Asphalt Pavements (Superpave)'. The Product of the SHRP Asphalt Research Program."

Khalid, H. and I. Artamendi (2004). Mechanical properties of used-tyre rubber. Proceedings of the Institution of Civil Engineers-Engineering Sustainability, Thomas Telford Ltd.

Khazada, S. (2000). Permanent deformation in bituminous mixtures, University of Nottingham.

Kim, Y.-R., et al. (2003). "Fatigue and healing characterization of asphalt mixtures." Journal of materials in civil engineering **15**(1): 75-83.

Lee, S.-J., et al. (2008). "The effect of crumb rubber modifier (CRM) on the performance properties of rubberized binders in HMA pavements." Construction and Building Materials **22**(7): 1368-1376.

Lee, S.-J., et al. (2008). "The effects of compaction temperature on CRM mixtures made with the SGC and the Marshall compactor." Construction and Building Materials **22**(6): 1122-1128.

Lee, S.-J., et al. (2007). "Laboratory study of the effects of compaction on the volumetric and rutting properties of CRM asphalt mixtures." Journal of materials in civil engineering **19**(12): 1079-1089.

Leite, L. F. M., et al. (2001). "Rheological studies of asphalt with ground tire rubber." Road Materials and Pavement Design **2**(2): 125-139.

Liang, Z.-Z. (1999). Bituminous compositions prepared with process treated vulcanized rubbers, Google Patents.

Little, D. N., et al. (1998). "AN ANALYSIS OF THE MECHANISM OF MICRODAMAGE HEALING BASED ON THE APPLICATION OF MICROMECHANICS FIRST PRINCIPLES OF FRACTURE AND HEALING."

Liu, J. and P. Li (2011). "Low temperature performance of sasobit-modified warm-mix asphalt." Journal of materials in civil engineering **24**(1): 57-63.

Liu, M., et al. (1998). "Oxygen uptake as correlated to carbonyl growth in aged asphalts and asphalt Corbett fractions." Industrial & engineering chemistry research **37**(12): 4669-4674.

Liu, Y., et al. (2012). "Design and evaluation of gap-graded asphalt rubber mixtures." Materials & Design **35**: 873-877.

Lo Presti, D. (2011). RHEOLOGY AND CURING OF TYRE RUBBER MODIFIED BITUMENS.

Lo Presti, D. (2013). "Recycled tyre rubber modified bitumens for road asphalt mixtures: a literature review." Construction and Building Materials **49**: 863-881.

Lo Presti, D. and G. Airey (2013). "Tyre rubber-modified bitumens development: the effect of varying processing conditions." Road Materials and Pavement Design **14**(4): 888-900.

Lo Presti, D., et al. (2014). "Toward more realistic viscosity measurements of tyre rubber-bitumen blends." Construction and Building Materials.

Lottman, R. P. (1978). PREDICTING MOISTURE--INDUCED DAMAGE TO ASPHALTIC CONCRETE.

Lundstrom, R., et al. (2004). "Influence of asphalt mixture stiffness on fatigue failure." Journal of materials in civil engineering **16**(6): 516-525.

Martinez, A., et al. (2009). "The essential work of fracture (EWF) method--analyzing the post-yielding fracture mechanics of polymers." Engineering Failure Analysis **16**(8): 2604-2617.

Masad, E. and N. Somadevan (2002). "Microstructural finite-element analysis of influence of localized strain distribution on asphalt mix properties." Journal of Engineering Mechanics **128**(10): 1105-1114.

Medeiros Jr, M. S., et al. (2012). "Evaluation of moisture and low-temperature cracking susceptibility of warm-mixture asphalt." International Journal of Pavement Engineering **13**(5): 395-400.

Memon, M. (1999). Activated method for treating crumb rubber particles, Google Patents.

Memon, N. (2011). "Characterisation of conventional and chemically dispersed crumb rubber modified bitumen and mixtures." University of Nottingham. Nottingham, UK: sn PhD thesis.

Mohammad, L., et al. (2000). "Accelerated loading performance and laboratory characterization of crumb rubber asphalt pavements." Road Materials and Pavement Design **1**(4).

Morea, F., et al. (2010). "Comparison of methods for measuring zero shear viscosity in asphalts." Materials and Structures **43**(4): 499-507.

Morea, F., et al. (2011). "The use of asphalt low shear viscosity to predict permanent deformation performance of asphalt concrete." Materials and Structures **44**(7): 1241-1248.

Morea, F., et al. (2012). "Rheological properties of asphalt binders with chemical tensoactive additives used in warm mix asphalts (WMAs)." Construction and Building Materials **29**: 135-141.

Moreno-Navarro, F. and M. Rubio-Gámez (2016). "A review of fatigue damage in bituminous mixtures: Understanding the phenomenon from a new perspective." Construction and Building Materials **113**: 927-938.

Morris, J., et al. (1974). Permanent deformation in asphalt pavements can be predicted. Proc. AAPT.

Navarro, F., et al. (2005). "Influence of crumb rubber concentration on the rheological behavior of a crumb rubber modified bitumen." Energy & fuels **19**(5): 1984-1990.

Navarro, F., et al. (2004). "Thermo-rheological behaviour and storage stability of ground tire rubber-modified bitumens." Fuel **83**(14): 2041-2049.

Navarro, F., et al. (2007). "Influence of processing conditions on the rheological behavior of crumb tire rubber-modified bitumen." Journal of Applied Polymer Science **104**(3): 1683-1691.

Nejad, F. M., et al. (2012). "Investigating the properties of crumb rubber modified bitumen using classic and SHRP testing methods." Construction and Building Materials **26**(1): 481-489.

Nelson Gibson, X. Q., Aroon Shenoy, Ghazi Al-Khateeb,, et al. (2012). Performance Testing for Superpave and Structural Validation.

Pais, J. C., et al. (2009). "Application of plateau value to predict fatigue life."

Paliukaite, M., et al. (2015). "Double-edge-notched tension testing of asphalt cement for the control of cracking in flexible asphalt pavements." Bituminous Mixtures and Pavements VI: 13.

Peralta, E. J. F. (2009). "Study of the Interaction between Bitumen and Rubber."

Pérez-Lepe, A., et al. (2007). "High temperature stability of different polymer-modified bitumens: A rheological evaluation." Journal of Applied Polymer Science **103**(2): 1166-1174.

Phillips, M. and C. Robertus (1996). Binder rheology and asphaltic pavement permanent deformation; the zero-shear-viscosity. EURASPHALT & EUROBITUME CONGRESS, STRASBOURG, 7-10 MAY 1996. VOLUME 3. PAPER E&E. 5.134.

Planche, J.-P., et al. (2004). "Evaluation of fatigue properties of bituminous binders." Materials and Structures **37**(5): 356-359.

Planche, J.-P., et al. (2004). "Evaluation of fatigue properties of bituminous binders." Materials and Structures **37**(5): 356-359.

Pronk, A. and P. Hopman (1991). Energy dissipation: the leading factor of fatigue.

Putman, B. J. and S. N. Amirkhanian (2006). Crumb rubber modification of binders: interaction and particle effects. Proceedings of the Asphalt Rubber 2006 Conference.

Ragab, M., et al. (2013). "Performance Enhancement of Crumb Rubber-Modified Asphalts Through Control of the Developed Internal Network Structure." Transportation Research Record: Journal of the Transportation Research Board(2371): 96-104.

Rahman, M. (2004). Characterisation of dry process crumb rubber modified asphalt mixtures, University of Nottingham.

Read, J. and D. Whiteoak (2003). The shell bitumen handbook, Thomas Telford.

Reschner, K. (2008). "Scrap tire recycling; a summary of prevalent disposal and recycling methods." Waste Management World.

Roberts, F. L., et al. (1991). "Hot mix asphalt materials, mixture design and construction."

Romberg, J., et al. (1959). "Some Chemical Aspects of the Components of Asphalt." Journal of Chemical and Engineering Data **4**(2): 159-161.

Roque, R., et al. (2004). "Development and field evaluation of energy-based criteria for top-down cracking performance of hot mix asphalt (with discussion)." Journal of the Association of Asphalt Paving Technologists **73**.

Roque, R. and W. G. Buttlar (1992). "The development of a measurement and analysis system to accurately determine asphalt concrete properties using the indirect tensile mode (with discussion)." Journal of the Association of Asphalt Paving Technologists **61**.

Roque, R., et al. (1999). "Determination of Crack Growth Rate Parameters Of Asphalt Mixtures Using the Superpave IOT."

Ruan, Y., et al. (2003). "Oxidation and viscosity hardening of polymer-modified asphalts." Energy & fuels **17**(4): 991-998.

Shatanawi, K., et al. (2009). "Effects of water activation of crumb rubber on the properties of crumb rubber-modified binders." International Journal of Pavement Engineering **10**(4): 289-297.

Shen, J. and S. Amirkhanian (2005). "The influence of crumb rubber modifier (CRM) microstructures on the high temperature properties of CRM binders." The International Journal of Pavement Engineering **6**(4): 265-271.

Shen, J., et al. (2006). "Recycling of laboratory-prepared reclaimed asphalt pavement mixtures containing crumb rubber-modified binders in hot-mix asphalt." Transportation Research Record: Journal of the Transportation Research Board(1962): 71-78.

Shen, J., et al. (2009). "Influence of surface area and size of crumb rubber on high temperature properties of crumb rubber modified binders." Construction and Building Materials **23**(1): 304-310.

Shen, S., et al. (2006). "A dissipated energy approach to fatigue evaluation." Road Materials and Pavement Design **7**(1): 47-69.

Shen, S. and S. Carpenter (2005). "Application of the dissipated energy concept in fatigue endurance limit testing." Transportation Research Record: Journal of the Transportation Research Board(1929): 165-173.

Shen, S. and S. H. Carpenter (2005). "Application of the dissipated energy concept in fatigue endurance limit testing." Transportation Research Record: Journal of the Transportation Research Board **1929**(1): 165-173.

Shen, S. and S. H. Carpenter (2006). Dissipated energy concepts for HMA performance: Fatigue and healing. **67**.

Shen, S., et al. (2010). "Characterization of fatigue and healing in asphalt binders." Journal of materials in civil engineering **22**(9): 846-852.

Shenoy, A. (2001). "Refinement of the Superpave specification parameter for performance grading of asphalt." Journal of transportation engineering **127**(5): 357-362.

Shenoy, A. (2003). "High temperature performance grading of asphalts through a specification criterion that could capture field performance." Journal of Transportation Engineering **130**(1): 132-137.

Shu, X., et al. (2008). "Laboratory evaluation of fatigue characteristics of recycled asphalt mixture." Construction and Building Materials **22**(7): 1323-1330.

Shulman, V. L. (2000). "Tyre recycling after 2000: status and options."

Subhy, A., et al. (2015). "An investigation on using pre-treated tyre rubber as a replacement of synthetic polymers for bitumen modification." Road Materials and Pavement Design **16**(sup1): 245-264.

Subhy, A., et al. (2015). "Rubberised bitumen manufacturing assisted by rheological measurements." Road Materials and Pavement Design: 1-21.

Sybilski, D. (1996). "Zero-shear viscosity of bituminous binder and its relation to bituminous mixture's rutting resistance." Transportation Research Record: Journal of the Transportation Research Board **1535**(1): 15-21.

Tabatabaee, N. and H. Tabatabaee (2010). "Multiple stress creep and recovery and time sweep fatigue tests: Crumb rubber modified binder and mixture performance." Transportation Research Record: Journal of the Transportation Research Board(2180): 67-74.

Tabatabaee, N. and H. A. Tabatabaee (2010). "Multiple Stress Creep and Recovery and Time Sweep Fatigue Tests." Transportation Research Record: Journal of the Transportation Research Board **2180**(1): 67-74.

Takallou, H. and R. G. Hicks (1988). Development of improved mix and construction guidelines for rubber-modified asphalt pavements.

Tapsoba, N., et al. (2012). "Analysis of fatigue test for bituminous mixtures." Journal of materials in civil engineering **25**(6): 701-710.

Tayfur, S., et al. (2007). "Investigation of rutting performance of asphalt mixtures containing polymer modifiers." Construction and Building Materials **21**(2): 328-337.

Thives, L. P., et al. (2013). "Assessment of the digestion time of asphalt rubber binder based on microscopy analysis." Construction and Building Materials **47**: 431-440.

Thodesen, C., et al. (2009). "Effect of crumb rubber characteristics on crumb rubber modified (CRM) binder viscosity." Construction and Building Materials **23**(1): 295-303.

Thom, N. (2008). "Principles of pavement engineering."

Timm, D., et al. (2009). "Forensic investigation and validation of energy ratio concept." Transportation Research Record: Journal of the Transportation Research Board(2127): 43-51.

Tsai, B.-W. and C. Monismith (2005). "Influence of Asphalt Binder Properties on the Fatigue Performance of Asphalt Concrete Pavements (With Discussion)." Journal of the Association of Asphalt Paving Technologists **74**.

Tsai, B.-W., et al. (2005). "Influence of asphalt binder properties on the fatigue performance of asphalt concrete pavements." Journal of the Association of Asphalt Paving Technologists **74**: 733-790.

TUT (2013). "Tampere University of Technology." Retrieved 25/10/2013, from https://www.tut.fi/ms/muo/tyreschool/moduulit/moduuli_7/hypertext/1/1_10.html.

Van Dijk, W. (1975). "Practical fatigue characterization of bituminous mixes." Journal of the Association of Asphalt Paving Technologists **44**: 38-72.

Van Dijk, W., et al. (1972). The fatigue of bitumen and bituminous mixes. Presented at the Third International Conference on the Structural Design of Asphalt Pavements, Grosvenor House, Park Lane, London, England, Sept. 11-15, 1972.

Van Dijk, W. and W. Visser (1977). Energy Approach to Fatigue for Pavement Design. Association of Asphalt Paving Technologists Proc.

Wang, H., et al. (2012). "Laboratory evaluation on high temperature viscosity and low temperature stiffness of asphalt binder with high percent scrap tire rubber." Construction and Building Materials **26**(1): 583-590.

Wang, S., et al. (2015). "Thermooxidative aging mechanism of crumb-rubber-modified asphalt." Journal of Applied Polymer Science.

Wasage, T., et al. (2011). "Rheological analysis of multi-stress creep recovery (MSCR) test." International Journal of Pavement Engineering **12**(6): 561-568.

Wong, C. C. and W.-g. Wong (2007). "Effect of crumb rubber modifiers on high temperature susceptibility of wearing course mixtures." Construction and Building Materials **21**(8): 1741-1745.

Wu, H., et al. (2013). "Characterizing fatigue behavior of asphalt mixtures utilizing loaded wheel tester." Journal of materials in civil engineering **26**(1): 152-159.

Wu, J. and Y. W. Mai (1996). "The essential fracture work concept for toughness measurement of ductile polymers." Polymer Engineering & Science **36**(18): 2275-2288.

Xiao-qing, Z., et al. (2009). "Rheological property of bitumen modified by the mixture of the mechanochemically devulcanized tire rubber powder and SBS." Journal of materials in civil engineering **21**(11): 699-705.

Zanzotto, L. and G. Kennepohl (1996). "Development of rubber and asphalt binders by depolymerization and devulcanization of scrap tires in asphalt." Transportation Research Record: Journal of the Transportation Research Board(1530): 51-58.

Zhou, F., et al. (2012). "Evaluation of fatigue tests for characterizing asphalt binders." Journal of materials in civil engineering **25**(5): 610-617.

Zoorob, S., et al. (2012). "Investigating the multiple stress creep recovery bitumen characterisation test." Construction and Building Materials **30**: 734-745.

Zoorob, S., et al. (2012). "Investigating the multiple stress creep recovery bitumen characterisation test." Construction and Building Materials **30**: 734-745.

Zou, J., et al. (2013). "Long-term field evaluation and analysis of top-down cracking for Superpave projects." Road Materials and Pavement Design **14**(4): 831-846.

Appendix A - Specimen fabrication and testing procedure of the Superpave IDT Tests

To obtain accurate measurements for vertical and horizontal strains, a 90° 2-element cross polyester wire strain gauge was used. This type of gauge strain is mainly used for measurement on concrete, mortar or rock materials. The properties (provided by the manufacturer) of strain gauges used in this study are presented in the table below. The following steps were taken in order to bond the strain gauge on one flat face of specimen:

1. Polish with sandpaper the strain gauge bonding area, the polished area should be considerably wider than the strain gage size.



2. Equal quantity of hardener and resin are mixed properly together and then enough quantity of the adhesive are applied to the polished area of the specimen. Any holes along the vertical and horizontal axes of the specimen should be filled with the adhesive product



3. Place the strain gauge along the vertical and horizontal axes of the specimen with the intersection point of the strain gauge being exactly above the centre point of the specimen. Quickly cover the strain gauge with accessory polyethylene sheet and strongly press the strain gauge over the sheet with a thumb for about 1 min



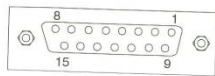
4. When the adhesive is cured, small connecting terminals are glued near to each end of the strain gauge. These Terminals provide convenient junction points to connect strain gauges to instrumentation leads.



5. Leave the specimens overnight at the room temperature.
6. Connect the leadwire using three-wire connection (Quarter Bridge Connection Mode) to 15-pin socket, see Figure x. Figure x shows the specimens with the strain gauges.

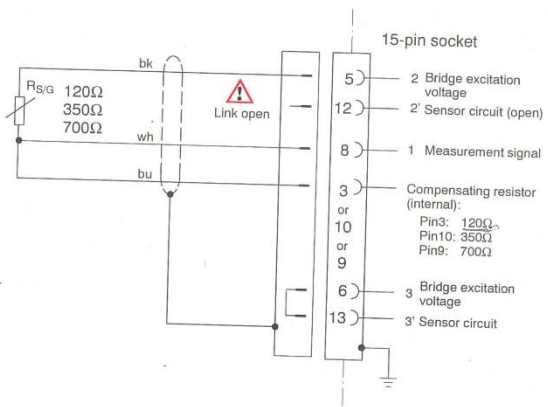


Connection to carrier-frequency module SR30



15-pin socket

3.1.4 Single S/G using three-wire connection



Mode for this connection: **quarter bridge**.

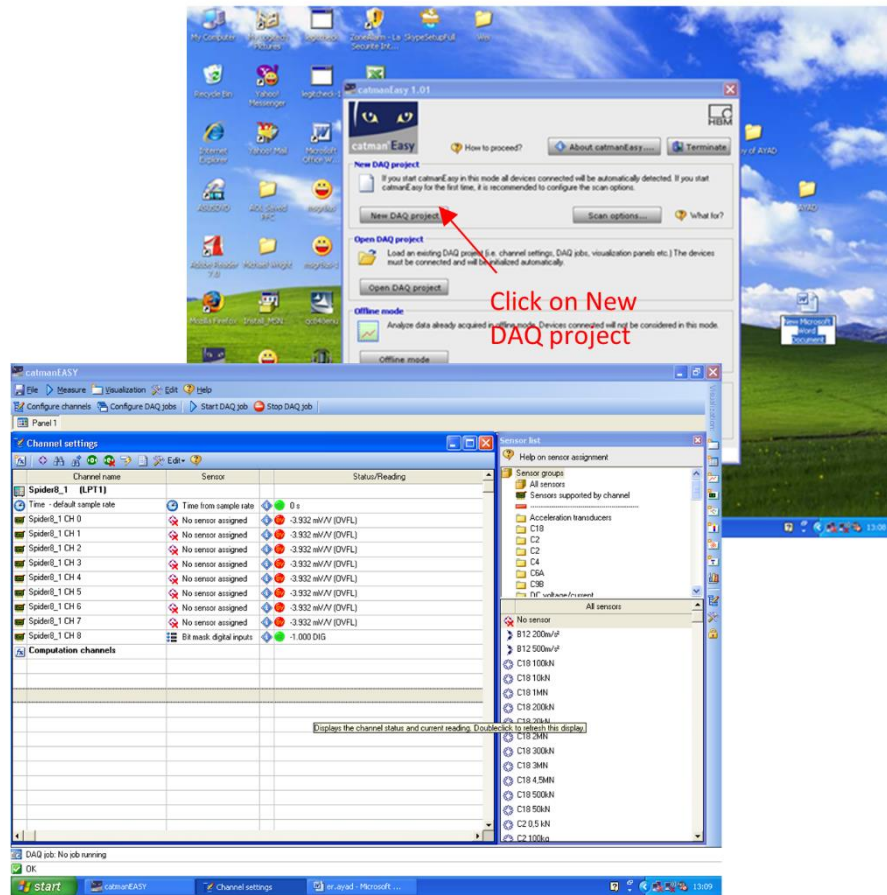
Gauge pattern	Gauge size mm		Backing size mm		Resistance Ω	Remarks
	Lengt h	Width	Lengt h	Width		

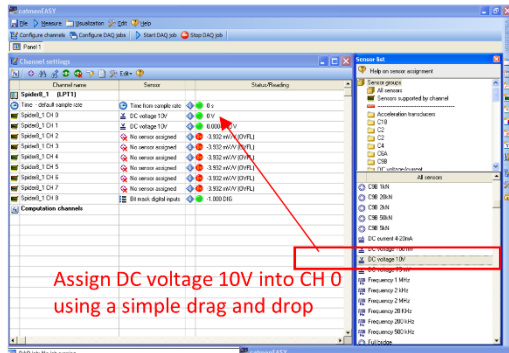
90° 2-element cross PLC-60-11	60	1	74	8	120	Operational temperature -20~+80°C Temperature compensation range +10~+80°C Quarter bridge with 3-wire system is usable to avoid an unexpected effect of resistance change with temperature
-------------------------------	----	---	----	---	-----	---

- Place the specimen inside the Instron cabinet and plug the 15-pin sockets (For horizontal and vertical strain gauges) into any of channels of the data acquisition box. Also, plug the load socket which connected through the Digital Controller of the Instron into the data acquisition box. In this study, CH 0 assigned for load measurement, CH4 and CH 6 assigned for horizontal and vertical strain measurement, respectively.

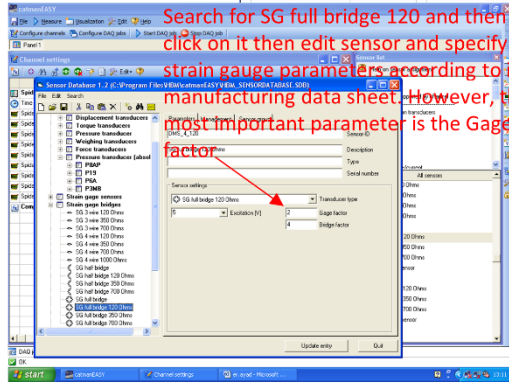
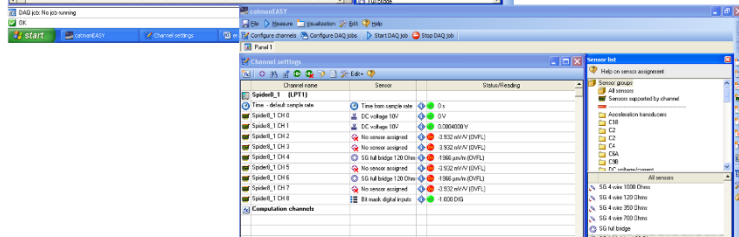


- Open the CatmanEASY software (on the laptop that connected with the data acquisition box) and follow the below instructions:



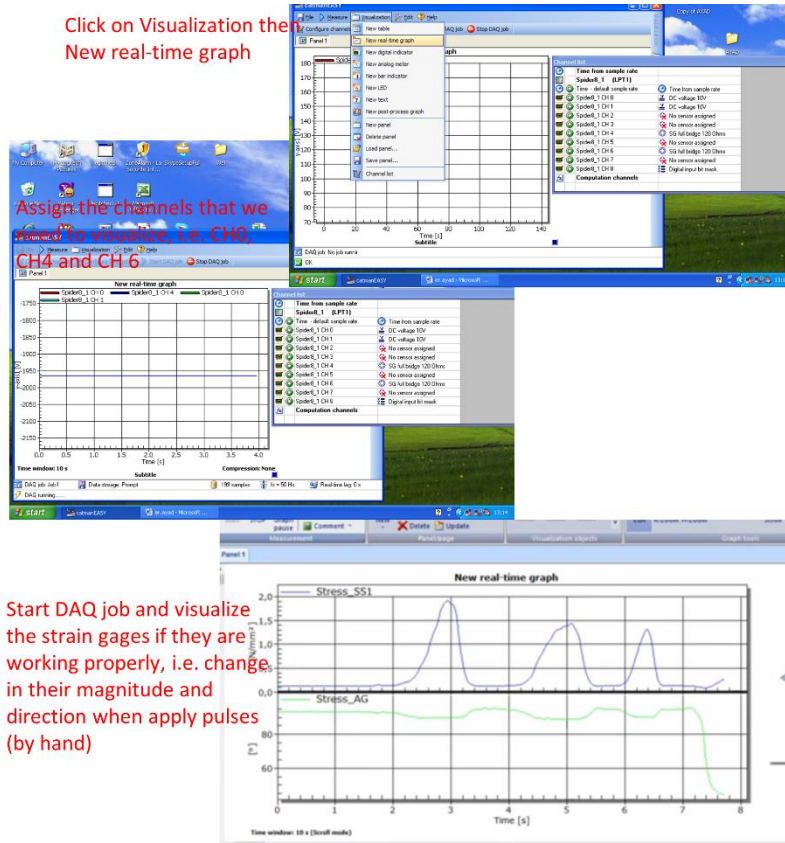


Assign DC voltage 10V into CH 0 using a simple drag and drop



Search for SG full bridge 120 and then right click on it then edit sensor and specify strain gauge parameters according to its manufacturing data sheet. However, the most important parameter is the Gage factor

Update entry



9. Open the software of the Instron (Rubicon) in order to conduct the Superpave IDT Tests:



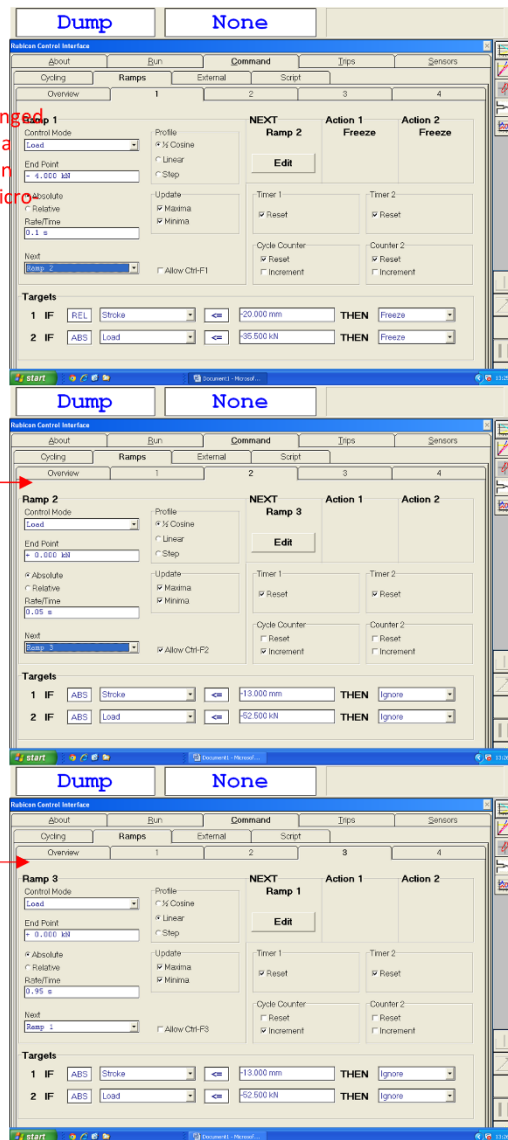
- a. The resilient modulus test: The resilient modulus test was conducted in load control mode by applying a repeated haversine waveform load to the specimen for a 0.1 s followed by a 0.9 s rest period. In order to keep the specimen undamaged and maintain the linearity of the material response

the load was selected to generate horizontal strain between 100 and 300 micro-strain during the test. The ramps for this test were specified as following:

Ramp 1: The load was ranged from (1 to 5 KN) to have a generate horizontal strain between 100 and 300 micro-strain during the test

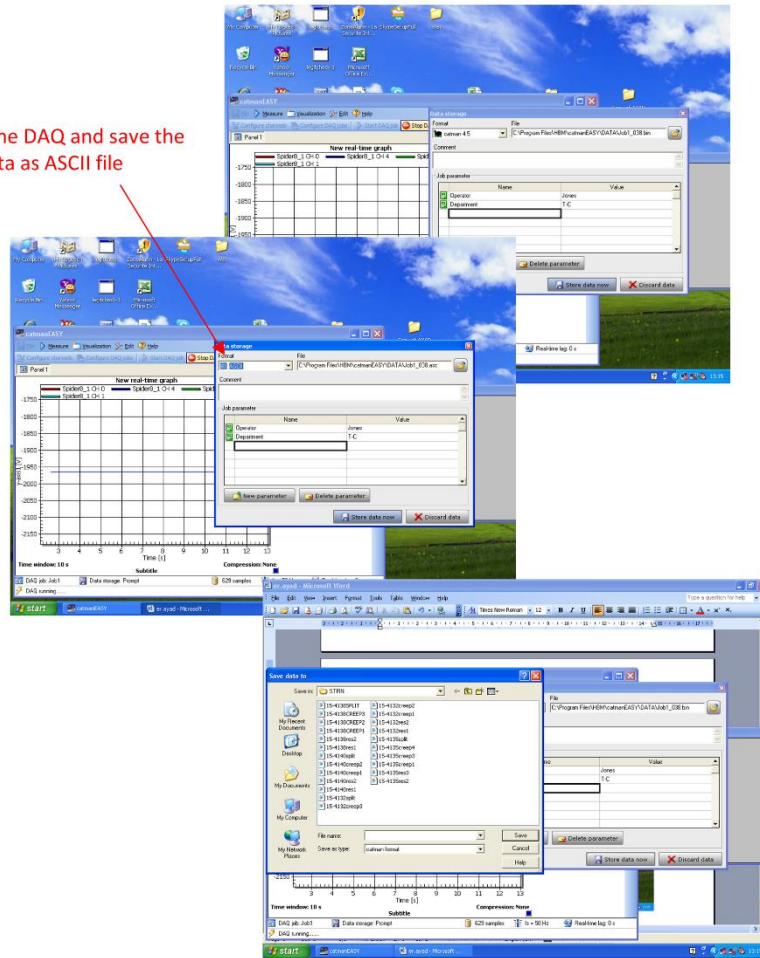
Ramp 2

Ramp 3

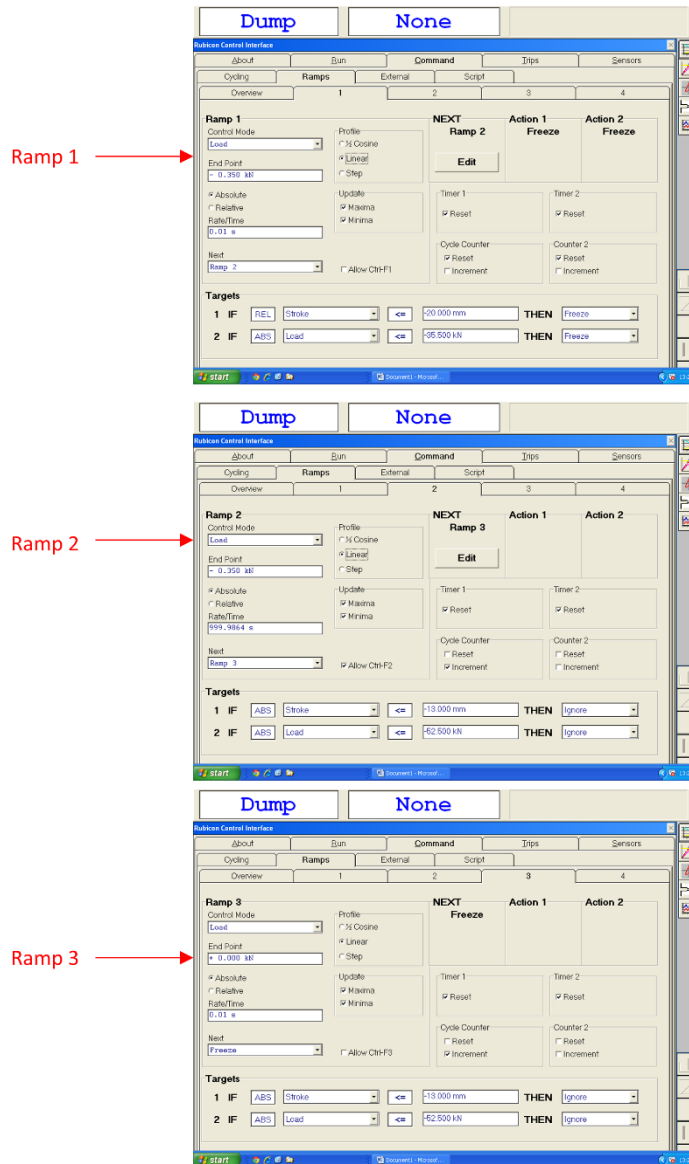


- b. Start the DAQ job as real-time graph in CatmanEASY together with actual test, check the horizontal strain if it is within the specified range (100 to 300 micro-strain). If not, you need to change the applied load accordingly. It is important to begin with low load and increase it gradually to keep the sample undamaged.

Stop the DAQ and save the file data as ASCII file

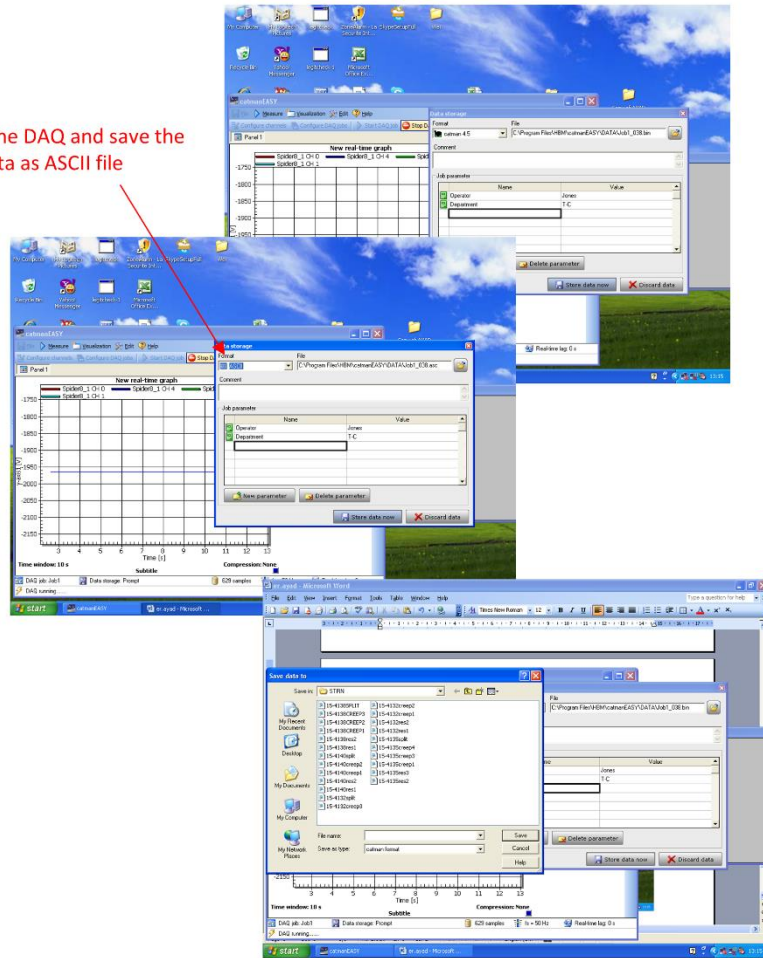


- c. The creep test: After finishing the resilient modulus test, a 5 min is given to allow the specimen to re-stabilize. Then, a static load is imposed along a diametral axis for 1000 s. The creep compliance test is non-destructive; therefore, the constant load should be selected such that the generated horizontal deformation is not exceeding the upper linear-elastic boundary i.e. within 40 and 120 microstrains at $t=30$ s should be used, and the test should be stopped if strains exceed these limits.

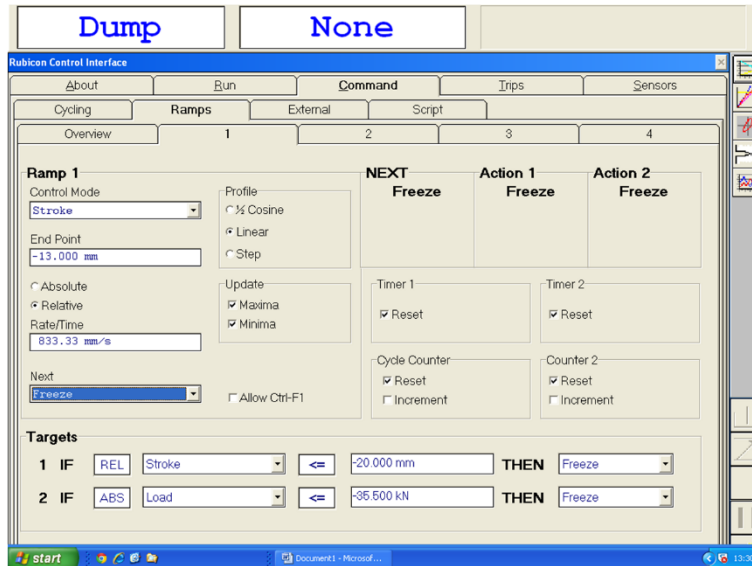


- d. Start the DAQ job as real-time graph in CatmanEASY together with actual test, check the horizontal strain if it is within 40 and 120 microstrains at $t=30$ s. If not, you need to stop the test and change the applied load accordingly

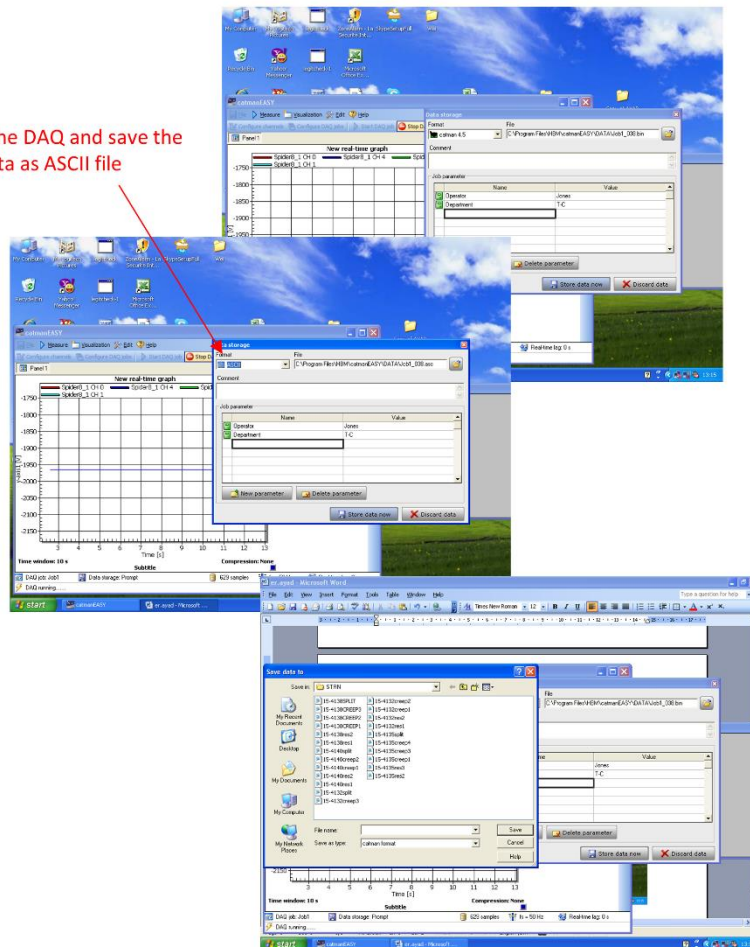
Stop the DAQ and save the file data as ASCII file



- e. The tensile strength test: The indirect tensile strength test is a destructive test and was performed by applying a load to the specimen at a constant rate of vertical ram movement 50 mm/min until the specimens failed.



Stop the DAQ and save the file data as ASCII file



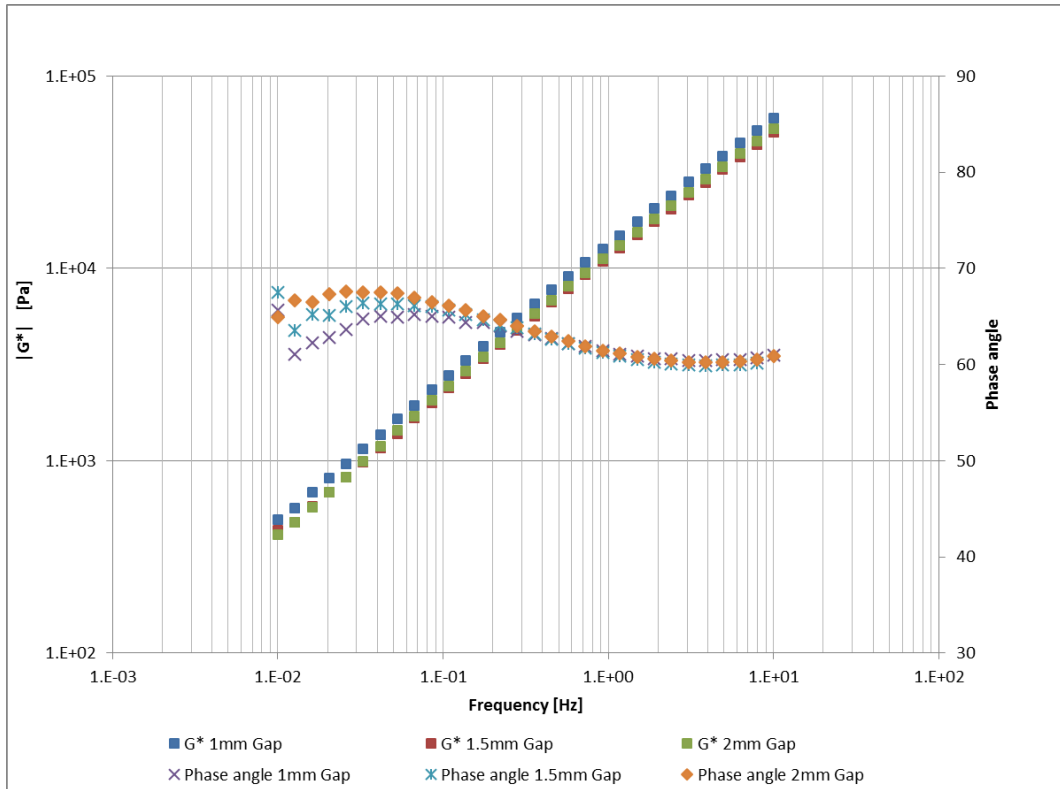
Appendix B- Gap setting investigation

G* and phase angle δ at 60 °C (Hard bitumen H blending with recycled tyre rubber N)

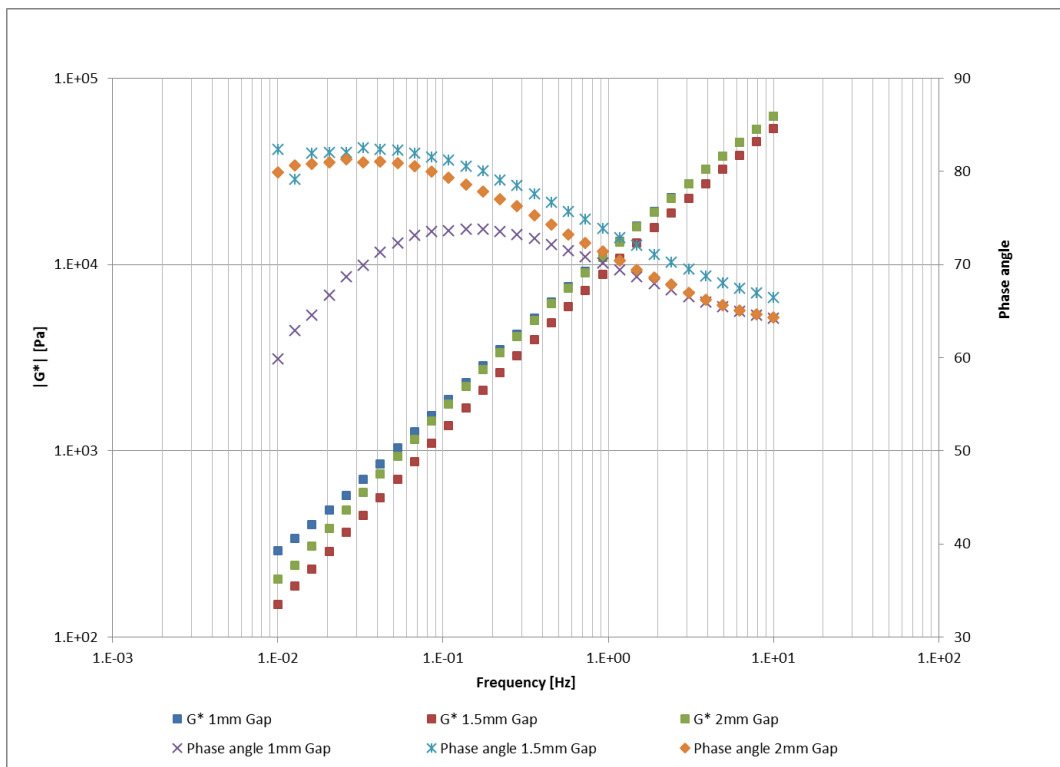
Frequency	G*			Phase angle		
	1 mm	1.5 mm	2 mm	1 mm	1.5 mm	2 mm
0.01	495.2	436.3	412.5	65.71	67.55	64.96
0.01269	570.1	478.1	477.6	61.11	63.53	66.7
0.0161	684.1	576.8	571.8	62.3	65.25	66.48
0.02043	814.9	686.9	688.1	62.87	65.13	67.3
0.02593	965.4	820.3	824.1	63.69	66	67.64
0.03291	1154	983.8	991.3	64.77	66.44	67.48
0.04175	1373	1169	1191	65	66.28	67.47
0.05298	1646	1388	1438	64.92	66.32	67.39
0.06723	1943	1675	1710	65.21	66.09	66.96
0.08532	2333	1997	2055	65.02	66.04	66.47
0.1083	2777	2392	2448	64.91	65.72	66.17
0.1374	3315	2845	2929	64.42	65.17	65.66
0.1744	3941	3395	3475	64.37	64.65	65.07
0.2212	4658	4026	4122	63.99	64.11	64.62
0.2809	5531	4771	4899	63.49	63.82	64
0.3563	6532	5651	5797	63.07	63.19	63.43
0.4525	7736	6663	6853	62.69	62.68	62.93
0.5747	9119	7848	8084	62.18	62.21	62.49
0.7282	10740	9239	9527	61.9	61.71	61.87
0.9259	12630	10890	11210	61.4	61.26	61.48
1.176	14830	12760	13150	61.12	60.89	61.16
1.493	17430	14970	15440	60.88	60.56	60.83
1.899	20480	17560	18110	60.64	60.29	60.6
2.4	23910	20420	21110	60.59	60.08	60.45
3.061	28070	23940	24730	60.45	59.98	60.25
3.896	32890	28020	28980	60.47	59.9	60.22
4.918	38250	32580	33830	60.5	59.95	60.27
6.25	44710	38030	39440	60.56	60.02	60.37
7.895	52030	44190	45840	60.71	60.17	60.56
10	60460	51220	53190	60.99	60.45	60.86

G* and phase angle δ at 60 °C (Hard bitumen H blending with recycled tyre rubber D)

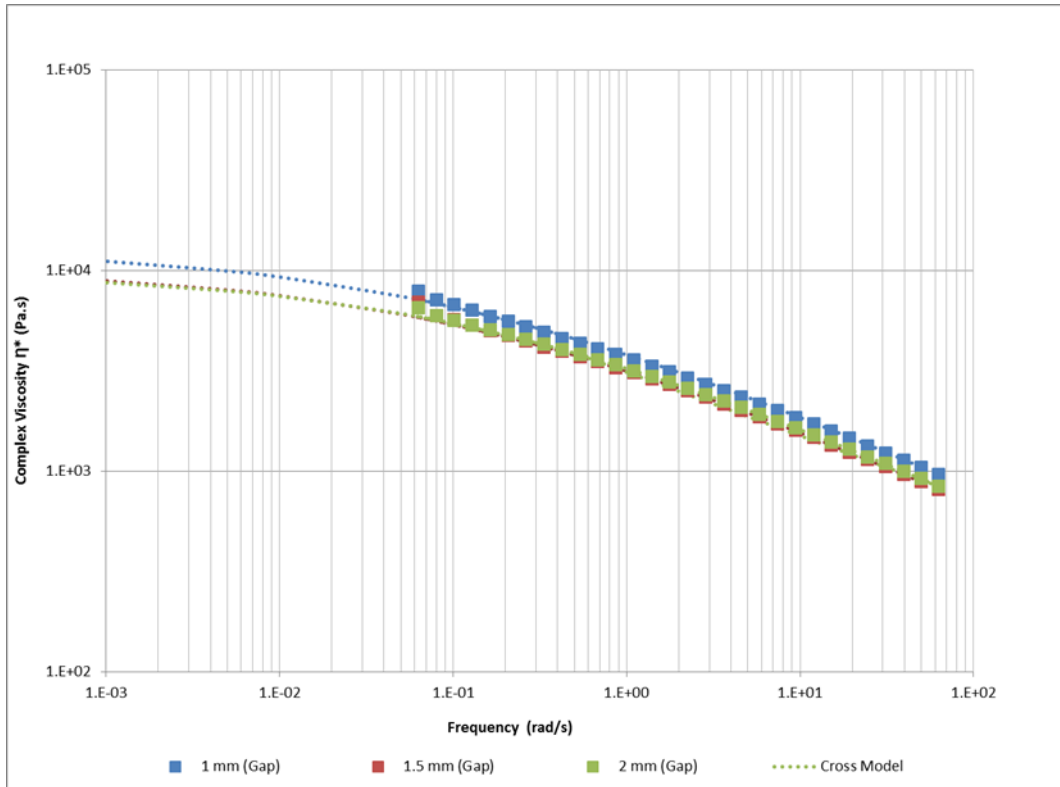
Frequency	G*			Phase angle		
	1 mm	1.5 mm	2 mm	1 mm	1.5 mm	2 mm
0.01	291.7	150.3	204.3	59.9	82.34	79.92
0.01269	338.5	188.2	243.4	62.97	79.2	80.64
0.0161	400.3	231.4	307.2	64.59	82	80.81
0.02043	480.1	288.3	383.9	66.69	82.02	80.98
0.02593	577.9	364	479.4	68.71	82.04	81.33
0.03291	700.5	451.4	597.7	69.95	82.54	80.98
0.04175	848.6	561.9	749.7	71.32	82.38	81.04
0.05298	1035	703	932.4	72.34	82.31	80.89
0.06723	1269	877.5	1155	73.16	81.96	80.57
0.08532	1553	1095	1442	73.56	81.56	79.99
0.1083	1894	1365	1785	73.68	81.23	79.3
0.1374	2319	1698	2208	73.84	80.58	78.56
0.1744	2851	2111	2719	73.83	80.04	77.82
0.2212	3479	2618	3353	73.57	79.1	77.04
0.2809	4229	3229	4119	73.24	78.51	76.24
0.3563	5164	3972	5023	72.8	77.58	75.28
0.4525	6297	4876	6155	72.16	76.68	74.33
0.5747	7616	5966	7483	71.51	75.69	73.24
0.7282	9178	7267	9048	70.88	74.85	72.35
0.9259	11090	8889	10950	70.16	73.92	71.44
1.176	13360	10800	13220	69.41	72.94	70.43
1.493	16030	13080	15920	68.72	72.06	69.48
1.899	19220	15770	19100	67.98	71.11	68.63
2.4	22800	18850	22670	67.28	70.27	67.84
3.061	27250	22730	27150	66.58	69.49	66.97
3.896	32390	27240	32380	65.99	68.75	66.26
4.918	38220	32420	38190	65.49	68.07	65.68
6.25	45330	38570	45180	64.97	67.46	65.1
7.895	53300	45700	53130	64.59	66.95	64.69
10	62580	53910	62250	64.28	66.48	64.31



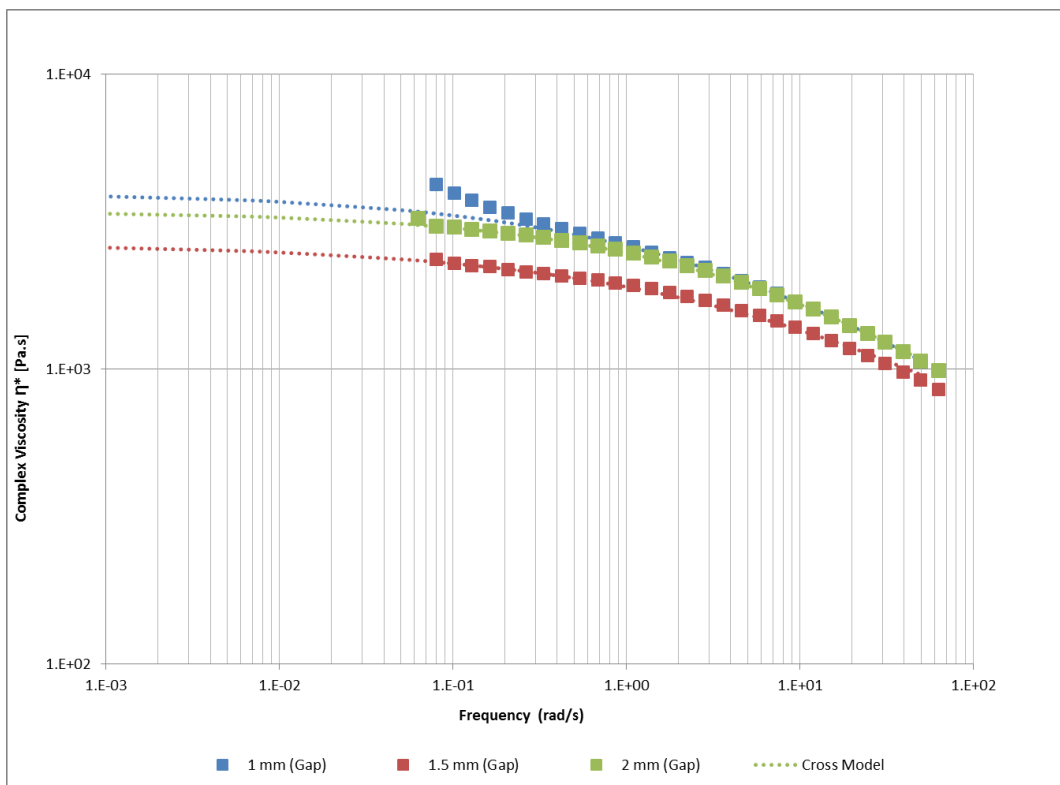
G^* and phase angle δ at 60 °C (Hard bitumen H blending with recycled tyre rubber N)



G^* and phase angle δ at 60 °C (Hard bitumen H blending with recycled tyre rubber D)



ZSV at 60 °C (Hard bitumen H blending with recycled tyre rubber N)



ZSV at 60 °C (Hard bitumen H blending with recycled tyre rubber D)

Appendix C- Results

Files related to the test results of this study can be obtained from Professor Gordon Airey by email at gordon.airey@nottingham.ac.uk

The files include the following results:

- 1. The DMA using the DSR for low shear development stage**
- 2. The MSCR using the DSR for the low shear development stage**
- 3. The DMA using the DSR for high shear development stage**
- 4. The MSCR using the DSR for the high shear development stage**
- 5. The TSRCL results**
- 6. The DENT test results**
- 7. ITSM Test Results**
- 8. ITFT Test Results**
- 9. RLAT Test Results**
- 10. The SuperPave IDT results**